TYMOTEUSZ BĄKOWSKI*

AIR-SHAFTS IN THE INTERWAR PERIOD BUILDINGS AS A PROTOTYPE IDEA OF THE GROUND HEAT EXCHANGER

SZYBY WENTYLACYJNE W BUDYNKACH MIĘDZYWOJENNYCH JAKO PROTOTYP IDEI GRUNTOWEGO WYMIENNIKA CIEPŁA

Abstract

In was common practice in the inter-war years of the twentieth century, for special large cross-section ducts to be included in residential buildings, in addition to the common ventilation and plumbing shafts, as well as, in the chimneys. In residential houses, such shafts were fitted with small windows that could be opened for inspection and access. These technical features provide identical physical and thermal dynamics and effects to the core principles of a high-tech ground heat exchanger, as used in today's modern passive houses. Ventilation shaft windows located in the individual apartments in these earlier buildings were designed to provide cool air flow in the hot summer season and warm air throughout the winter months.

Keywords: air-shafts, ground heat exchanger, passive houses

Streszczenie

W okresie dwudziestolecia międzywojennego ubiegłego wieku w budynkach mieszkalnych, oprócz pionów wentylacyjnych, kominowych i instalacyjnych, dość często projektowano szyby wentylacyjne o znacznym przekroju. W mieszkaniach szyby te zaopatrywano w nieduże otwieralne okna. Zapomniane rozwiązanie techniczne wykorzystywało te same zjawiska fizyczno--termiczne, które stanęły u podstaw współczesnej zaawansowanej technologii gruntowego wymiennika ciepła, stosowanego w domach pasywnych. Okna szybów wentylacyjnych znajdujące się w mieszkaniach miały za zadanie dostarczać chłodne powietrze w sezonie upalnym, a cieplejsze z otoczenia w okresie chłodów.

Słowa kluczowe: szyby wentylacyjne, gruntowy wymiennik ciepła, domy pasywne

---

* Ph.D. student Tymoteusz Bąkowski, Faculty of Architecture, Cracow University of Technology.

1. Introduction

In the last few decades of the twentieth century, scientists and the industry became increasingly aware of the importance of the need for energy economizing, as a result of the world's dwindling natural resources, the increase in demand and the consequent higher costs of power generation and supply. This work is ongoing. It covers all areas of human activity, including the construction industry. This paper deals with one aspect of the construction process: steps to reduce energy consumption by, at the same time, maintaining stable temperature conditions in residential premises. In view of the extensive range of materials used for the fabric and insulation of the building, etc., this paper takes a narrower focus on the question of obtaining savings on heating and cooling units.

In tracing the recent history of the development of house building, we note that the latest techniques used in the construction of a passive house, rely (consciously or unconsciously) on historically-proven methods which are largely overlooked in the technical literature of today. An article by Tadeusz Niedzielski[1] in a 1914 edition of Architect Magazine [2], a monthly magazine for professionals, examined the construction of new buildings and attitudes towards the art and design of the time, and stated that the advances made in terms of knowledge and safety around the globe had led to a realization that: "health and hygiene had a psychological, as well as, a physical dimension. (...) This provides us with a fresh perspective of the Construction Act, and an important new principle: maximum sunlight and air (...) The provision of proper ventilation and modern lighting provides for most of what is known as the rear building line to a distance equal to half the height of the building, (...) In addition, we should ask whether there should be a minimum volume of air in homes. The minimum volume for an adult should not fall below 16 cubic meters. For a child under 14 years, the amount is 12 cubic meters. (...) The Progressive Building Act is a legal guide to sanitation and construction standards, and should be regarded as an ABC guide to building use by all and sundry. Such an example is provided by the London Act, which runs to some 300 pages including a number of pictures. The equivalent statute for New York is a technical masterpiece, and even small townships have extensive and comprehensive local laws restricting the licensing of contractors in the sanitation and construction industries (...).Wrote Tadeusz Niedzielski[2]. Therefore, this paper compares the cost-effectiveness and efficiency of a typical ventilation shaft, coupled with vent risers and used in the buildings of the interwar period, with the output of a modern geothermal heat exchanger, as used in passive houses and increasingly deployed in other less sophisticated buildings, in which the same physical and thermal dynamics are present.

A ground heat exchanger, also known as a ground air heat exchanger, is a system that uses the natural or artificially-controlled temperature of the ground to assist in maintaining a steady and constant temperature in the building (so that it provides a cooling effect in the summer and a heating effect in winter). This system is mainly formed of pipes made of PVC, sunk a minimum 20 cm below the frost penetration level (underneath the building), in which air circulates after being heated or cooled by a process of ground temperature absorption and storage. Polish law requires that air intake should occur not lower than 2 meters above

---

[1] *Braki i niedomagania naszych ustaw budowlanych*, [w:] Architekt, r. XV, kwiecień 1914, z. 4, s. 55-66.

[2] *Ibidem*, s. 55-66.

ground level. The combined use of the solar chimney (which has been known for centuries in ancient Rome and the Middle East [3, 4]) should guarantee no additional energy needs. The solar chimney works by a process of air convection and should be made of a material that absorbs solar radiation in a vacuum. It should be located on a south-facing wall and should extend above the roof level.

2. What is an air vent and how is it defined?

The Minister of Infrastructure issued a Regulation dated 12 April 2002 [5] concerning the technical requirements for buildings and also for locations. Part IV of the Regulation (as amended) addresses technical equipment to be installed in buildings. Section 6 sets out the conditions and standards to be met by ventilation and air conditioning systems. The current regulations and standards do not define the parameters of ventilation shafts. These only give details on what calculations are required for installation. The flow rate and other factors determine the dimensions for the cross-sectional area of the tube (or funnel) for manmade exhaust and (in the case of mechanical ventilation of air conditioning). The 1928 Building Regulation [6] required further protection against moisture and the negative effects of weathering and obliged builders to make provision for reasonable facilities for heating, ventilation and airing of all living units designed to accommodate people, as well as kitchen areas, servants' quarters and toilets. It was common practice to construct ventilation shafts to meet this statutory duty[3]. Thus, the ventilation shaft can be defined as a "functional interior space in a residential building that meets the statutory requirements for heating, ventilation and aeration."

3. Shafts in residential buildings in the early twentieth century

In addition to the flue ducts and pipes to expel exhaust gases, flues from gas boilers and coal furnaces were often fitted before windows were installed, and function as the equivalent of modern day "air-conditioning". These provided a natural means of regulating the temperature inside the building, offered a constant supply of fresh air into the room (isolated from the internal partition walls which housed the exterior windows) and, to a lesser extent, controlled the temperature in the living quarters.

The number of ventilation shafts required for these purposes depends on the number of living units on each floor in a typical residential building, as well as the number of multi-

---

[3] Rozp. Prez. Rp. z dn. 16.02.1928 r. o prawie budowlanem i zabud. osiedli, Rozdz. 10, Art. 241.

(1) Premises designed to accommodate people, particularly living rooms, dining areas, servants' rooms, classrooms, kitchens, offices, commercial premises, premises for meetings, etc., should be effectively protected from the negative effects of moisture and pollutants and have the proper equipment for heating and ventilation.

(2) These properties should be provided with a sufficient number of windows for interior open spaces and to ensure an adequate supply of lighting and proper ventilation of the rooms in question.

(3) In rooms designed to accommodate people, the total surface area of the windows should be at least one-tenth of the floorspace area, except in cases which are detailed in Art. 325.

storey buildings in the vicinity. In the twentieth century, much of this construction work in Krakow took place in the 1930s on both sides of the natural/urban belt that delineates the Second Ring Road, together with the Slovacki, Mickiewicz and Krasinski Avenues [1]. These buildings were typically between 3–4 storeys, except at certain locations, such as road junctions where buildings overlooking intersections were built to a different size and scale. Here, the priority in terms of the urban design was given over to the junction. In the larger triple storey houses, rooms were located away from the street along a dark and unlit corridor, with access halfway down the rear passage facing an interior courtyard enclosed block. Typically, various ancillary rooms were adjacent to the corridors running the length of the boundary walls, notably: a small service room, illuminated fanlights, a walker economy kitchen overlooking the courtyard, and sanitary facilities, designed either with the first modern-era toilet, or a bathroom with a cast iron bath. Pantries and small storage units were fitted adjacent in the rear.

4. The location and construction of ventilation shafts in the structure of a residential building

The ventilation shaft was placed so that it was accessible through a small glass window (Fig. 1). Possible locations were the kitchen, bathroom and storage room. It was normal for two inspection windows to be fitted in, and one inspection window in a smaller spaced room lacking a pantry. Different types of shafts and ducts were installed in these buildings partly because of limited opportunities for ventilation. There was no other method of providing rapid exchange or air to keep the air fresh inside the property, and to maintain a ground temperature of around 8–10°C – given the Polish climate.

Fig. 1. Interior apartment view
of the window

One house located in Szlak street 14B in Krowodrza district provides us with a working example. In 2005, a study was conducted into the technical infrastructure of this property, which by twenty-first century standards is well preserved. In addition to the ventilation and chimney stacks, three vertical shafts were installed each with a surface area of 0.50 m²,

covered by a skylight on top of the roof. These conduits provided an important source of ventilation for the bathroom, toilet and maid's room and also enabled natural light emanating from the kitchen window to illuminate the property. Subsequent repair works resulted in the removal of several windows, which may be evident of a desire on the part of the owners to extend the living space. Over time, smaller windows were bricked up, reducing the prospect of additional ventilation into more secluded rooms. This work may have allowed for additional installations to be fitted. The ground floor plan of the larger residential building units shows of the presence of two shafts (Fig. 2A, B) and a service shaft located in the corner of the courtyard balcony to bring coal from the basement up to the kitchen. We also note that there is one window in the kitchen in the smaller two-bedroom apartments.
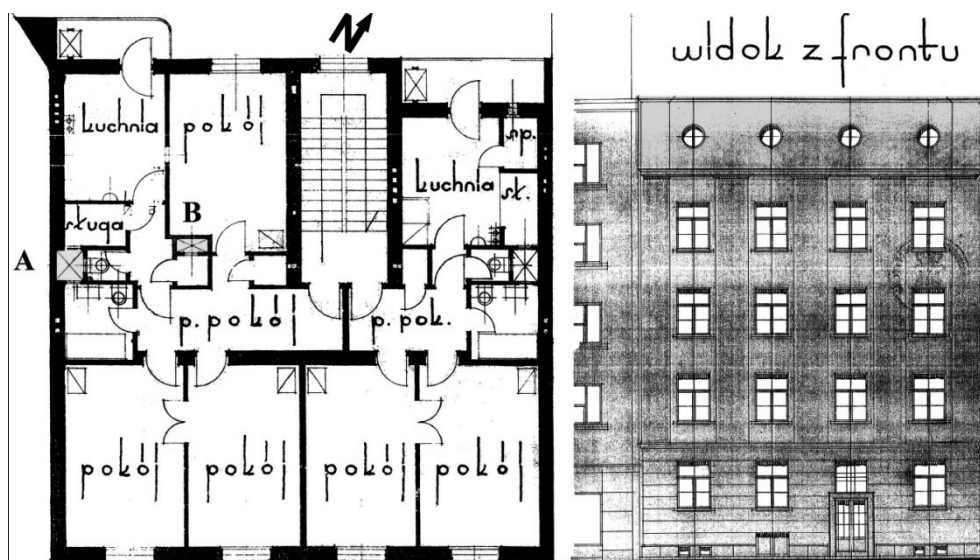
Fig. 2. Location of the air-shafts in the selected town house, 14B Szlak Street, Kraków

Shaft A, located in the western boundary wall, has three small rectangular single- framed windows opening into the bathroom, toilet and a small maid's room adjacent to the kitchen. These provide additional temperature control and ventilation capacity, as well as illumination into an otherwise dark room which has no windows in the exterior wall of the building.

Shaft B is located in the central part of the property and is serviced by two small single-rectangular windows. One of these vents is located in a small hallway connecting the kitchen to a more spacious internal central corridor. The second vent is designed to enable cool air to flow from the basement to keep the pantry at a stable temperature. The pantry is accessed from the hallway adjacent to the kitchen and the living room at the rear of the property.

Any removal of the remaining access ducts for the kitchen, bathroom and pantry by current users or buyers would be detrimental to the property. Refurbishment work was carried out and some of the original ventilation ducts were dismantled which could undermine the building.

In the process of renovating the apartment on the ground floor, builders removed the excellent and cost-effective ventilation windows, cutting the rooftop units from the apartment

with the result that functionality was lost. Ventilation was reduced in bathrooms, and the lack of sufficient natural ventilation pipes in the chimney shafts of the perimeter wall caused a gradual build up of moisture in the bathrooms, toilet, maid's rooms, kitchen, pantry and hallways on all floors of the residential property. The effect is the same whether or not the shaft is plastered or is left as an exposed masonry brick wall (Fig. 3).

Fig. 3. Interior view of the air-shafts

Extensive plaster on the surface of the normative[4] is visible from the foundation level, although a hole may have been drilled in the ceiling of the basement. If so, it was located about 1 metre above the apex of the side window aperture, covered by a rooftile or glass skylight.

5. Conclusions

The inter-war construction of these shafts can now be regarded as a precursor and as a prototype for today's ground heat exchangers. This conclusion follows a comparison of operating principles, purposes and economic considerations. The shafts were sunk into the ground, using techniques and materials whose capabilities were well-known before the outbreak of World War II. The system fulfilled a similar role to the previous practice of drawing air at ground-level temperatures from the basement and into the building, but without the need for advanced technologies and materials. This simple air conditioning system was, and still remains, safe and reliable. The construction industry of today still drills wells into the ground which can be an affordable practical solution to the problem of ventilating and heating low-cost social housing, especially as the alternatives can be costly.

Air conditioning or mechanical air cooling in residential buildings occurred sporadically across Poland before 1989. This was a result of economic backwardness and the high cost of such devices. After the fall of Communism and the re-modelling of the economy, despite

---

[4] Rozp. Prez. Rp. z dn. 16 .02.1928 r. o prawie budowlanem i zabud. osiedli, Rozdz. 8, Art. 217-218.
Art. 217. Premises not intended to accommodate people like pantry, hall, corridors, stairs, passages rinsed with water and the like, can also be lit by skylights.
Art. 218. (1) Horizontal cross-section of the skylight, where the skylight is not intended to illuminate steps should be at least 4 square meters, and the distance of opposite walls – at least 2 meters.

the rapid progress in catching up to more economically-developed countries, improvements in the standards of living did not result in modern air conditioning systems becoming as widespread as might be expected. For example, we can compare two cities with similar climate conditions: Chicago in the U.S.A. and Kraków in Poland. In Chicago, it is common for simple air conditioners to be fitted in properties in poorer neighbourhoods. In Kraków, this is rarer. The reason is the price of electricity in each country: it is twice as expensive in Poland than in the U.S.A.

If financial resources are scarce, the use of ventilation shafts presents a more affordable alternative to modern energy-intensive systems. Many people currently occupying the inter-war apartment blocks in Poland may not be aware of the purpose and benefits of the shafts. In the best case scenario, the windows were simply bricked up. In the worst case scenario, the walls were demolished and less efficient glass ceilings were installed in an attempt to gain extra living space. This practice not only led to the other occupants of the building being denied the benefits of additional ventilation from the shafts but, in the worst case scenario, exposed them to the risk of a weakened construction (eg cracking walls above the ceilings, which became evident as a result of widespread scratching scraping of the ceiling).

In view of the fact that this practice was carried out on a large scale, it is important that we remind administrators and officials that before any permissions are granted for conversion or renovation works to buildings where there is no information presented about shafts in walls rather than in partitions, checks and surveys should be carried out to analyse the impact of proposed work on the safety of the building.

R e f e r e n c e s

[1] *Dzieje Krakowa. Kraków w latach 1918–1939*, red. J. Bieniarzówna, J.M. Małecki, Tom IV, Wydawnictwo Literackie, Kraków 1997.

[2] Niedzielski T., *Braki i niedomagania naszych ustaw budowlanych*, [w:] Architekt, r. XV, kwiecień z. 4, Kraków 1914, 55-66.

[3] Zimny J., *Odnawialne źródła energii w budownictwie niskoenergetycznym*, wyd. I, PGA, AGH Wydawnictwa Naukowo-Techniczne, Kraków 2010.

[4] Zębala K., *Nowe technologie energooszczędne w aspekcie ich kosztorysowania*, [w:] Czasopismo Techniczne, Wydawnictwo Politechniki Krakowskiej, Kraków 2011, 221-228.

[5] Rozporządzenie Ministra Infrastruktury z dnia 12 kwietnia 2002 r. w sprawie warunków technicznych, jakim powinny odpowiadać budynki i ich usytuowanie (z późniejszymi zmianami), Dz.U. Nr 75, poz. 690.

[6] Rozporządzenie Prezydenta Rzeczypospolitej z dnia 16 lutego 1928 r. o prawie budowlanem i zabudowie osiedli, Rozdz. 10, Art. 241, Dz.U. Nr 34, poz. 216.

WACŁAW BRACHACZEK, PAULINA LISZKA, SZYMON FRYC, ŁUKASZ DZIDA[*]

EFFECT OF REDISPERSIBLE RESINS ON THE MECHANICAL STRENGHT AND CAPILLARY RISING OF HARDENED CEMENT MORTARSWPŁYW ŻYWIC REDYSPERGOWALNYCH

WPŁYW ŻYWIC REDYSPERGOWALNYCH NA WYTRZYMAŁOŚĆ MECHANICZNĄ I PODCIĄGANIE KAPILARNE STWARDNIAŁYCH ZAPRAW CEMENTOWYCH

Abstract

This paper shows the results of impact that polymer additives with different chemical composition have on physical and mechanical properties of solidified mortar. During the research, modern polymer redispersed admixtures were used. An analysis of the changes was carried out using statistical methods and linear regression. It was found that the analyzed polymer admixtures affect the analyzed parameters with varying degrees of intensity.

Keywords: redispersible polymers, the strength of the cement-based mortars on compression, bending strength, capillary rising

Streszczenie

W pracy przedstawiono wyniki badań wpływu domieszek polimerówych o zróżnicowanym składzie chemicznym na właściwości fizyczne i mechaniczne utwardzonych zapraw cementowych. W badaniach wykorzystano nowoczesne domieszki polimerów redyspergowalnych w postaci: kopolimeru octan winylu/wersenian winylu, kopolimeru octan winylu, wersenian winylu, etylen i akrylan butylu oraz kopolimer ester kwasu akrylowego/styren. Analizę zachodzących zmian przeprowadzono z wykorzystaniem metod statystycznych, posiłkując się regresją liniową. Stwierdzono, że analizowane domieszki polimerowe z różnym natężeniem oddziałują na analizowane parametry.

Słowa kluczowe: polimery redyspergowalne, wytrzymałość zapraw cementowych na ściskanie, wytrzymałość zapraw na zginanie, podciąganie kapilarne

[*] Ph.D. Eng. Wacław Brachaczek, Paulina Liszka, student, Szymon Fryc, student, Łukasz Dzida, student, Faculty of Materials and Environmental Sciences, University of Bielsko-Biala.

Designation

Rc – compressive strength [MPa]
R_G – tensile strength in bending R_G [MPa]
w/c – water-to-cement ratio
H – capillary rising [mm]
R – correlation coefficients
p – computer level of significance
F – the value of statistics F Fisher-Snedecor

1. Introduction

The addition of polymer resins creates new possibilities for modifying the properties of mortars. Factors affecting them positively include: increase flexibility, increase in hydrophobicity, and improving adhesion and mechanical strength. Resin binders bind during mortar hardening in which they are distributed by means of coalescence. As a result of the evaporation of water, "rolls" of polymer chains get close to each other, binding irreversibly. In the bound form, the polymer creates thin layers of high flexibility (so called "polymer film") which are covering the grain mixes. The tightness of such coating, the continuity of the "film" in the volume of hardened material, the viscosity, and the formed microstructure, all depend on the type and quantity of the polymer present in the mortar.

In construction mortars, the addition of polymer resins does not exceed 2% of all the constituents of the recipe. Higher amounts of polymer can adversely affect the workability of the mortar. The most commonly used polymer resins contain polyvinyl acetate vinyl or acrylic acid esters. Research of the influence of these polymers on the properties of hardened mortar have been well documented in the literature. It was found that, while the addition of these polymers improves the physical properties of the mortar (absorption, adhesion, flexibility, etc.), the mechanical properties – especially compressive strength – are lowered. New, innovative redispersible resins are usually copolymers containing within their main chain – in addition to the previously mentioned – other compounds and this way one can better influence the change of mechanical properties of hardened mortars.

This paper presents *the results of research of the dependence of mortar cement's compressive strength R_C* [MPa], tensile strength in bending R_G [MPa], and capillary rising H [mm] based on the share of polymers of diverse chemical structure, forming the modern technological solutions in the production of redispersed polymer resins. In the interpretation of the results, statistical methods based on linear regression model were used.

2. The experimental part

2.1. Materials used

The research was conducted on cuboidal samples made in laboratory-scale from the formulas containing: cement CEM I 42.5 R (140 kg/t), cellulose texture agent (1 kg/t), a super

white lime (50 kg/t) and silica sand with a particle size of 0.00–0.5 mm. Three series of samples were prepared, where during the individual tests conducted within each of the series, one of the tested resins was added in the amounts of C_{PR} = 0.0, 5.0, 10.0, 15.0, 20.0 kg/t (C_{PR}– polymer share). Three redispersible powders were chosen for the purpose of research: 1 – copolymer vinyl acetate/vinyl versatate; 2 – copolymer vinyl acetate, vinyl versatate, ethylene and butyl acrylate, 3 – acrylic acid ester-styrene. Each change in weight, resulting from varying amounts of the individual components, was replenished up to 100% with quartz sand. The study was conducted at constant ratio *w/c* ratio of 2.5.

2.2. Preparation of samples

First, dry ingredients weighed on a laboratory scales to the nearest 0.01 g had been mixed. A prepared dry mix was mixed with water in a standardized stirrer according to the standard: PN-EN 196-1: 2006 [7]. Then rectangular forms with dimensions of 40 mm × 40 mm × 160 mm were filled with the mortar, in two equal layers; each of the layers was compacted by 25 rammer impacts. Prepared samples had been seasoned for 7 days in a polyethylene bag, and later on, after stripping, for another 21 days in relative humidity conditions of 65% +/–5%.

The strength test was performed on the Tecnotest testing machine. First tensile strength test was carried out by applying the load with the steady increase in the force until the destruction of the sample caused by a break.

One half of each of the broken bars was allocated to the compressive strength test and the second one to the capillary rising test. The result of each of these tests was a value destroying the sample. The samples intended for capillary rising study were weighed and placed in the dryer in a temperature of 60°C until a constant mass was achieved.

Dry samples were coated with wax mass on the surface, perpendicular to the mirror of water, in which they were submerged during the test.

After 24 hours the samples were weighed, and then cut along the longer axis thus specifying the height of the capillary rising and the weight absorbability

One result was an average measurement of three tests.

2.3. The study of the mechanical properties

Table 1 presents the results of compressive strength research R_C [MPa], and tensile strength in bending R_G [MPa] of the hardened mortar samples, containing polymeric additives which are: 1 – copolymer of vinyl acetate/vinyl versatate, 2 – redispersible binder based on a copolymer of vinyl acetate, vinyl versatate, 3 – copolymer of acrylic acid ester/styrene. The amount of dopants in the individual samples were varied and were, respectively at a level of: C_{PR} = 0, 5, 10, 15 and 20 kg/t. For each quantity of a particular polymer admixtures three samples were made.

The visual evaluation of the scatter plot (Fig. 1–2) shows that the relationship is linear and for all of the tested polymer additives, along with increasing participation of polymer additives, compressive strength and tensile strenght of hardened mortars is increased.

Correlation coefficients (R) in each case are high and are, respectively for R_{C1}: 0.9122 for R_{C2}: 0.87 and R_{C3}: 0.948, so in each case, there is a strong dependence of compressive strength on the quantity of polymer additives. Because F is high and $p < 0.0000$ – linearity is important.

The results of the summary statistics for compressive strength and bending strength

Statistics	Summary statistics, the dependent variable					
	R_{C1}	R_{C2}	R_{C3}	R_{G1}	R_{G2}	R_{G3}
R	0.9122	0.87	0.9482	0.99197	0.97144	0.98017
R^2	0.8321	0.758	0.8992	0.98399	0.94370	0.96073
$R2$	0.8192	0.739	0.8914	0.97866	0.92494	0.94765
$F(1,3)$	64.46	40.78	115.98	184.471	50.289	73.413
p	< 0.0000	< 0.0000	< 0.0000	< 0.0008	< 0.0057	< 0.0033
Standard error of estimation	0.75	0.34	0.59	1.15	2.16	1.80
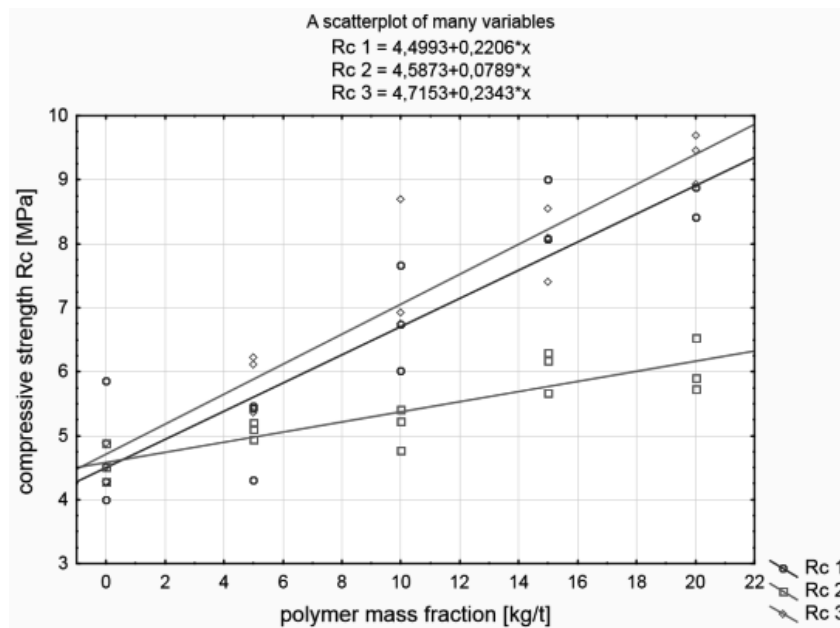
Fig. 1. Scatterplot, along with a selection of linear regression function at compression strength and at tensile strength. Markings on the chart correspond to the 1 – copolymer of vinyl acetate, vinyl versatate, 2 – redispersible binder based on a copolymer of vinyl acetate, vinyl versatate, ethylene and butyl acrylate,
3 – copolymer of ester acrylic acid – styrene
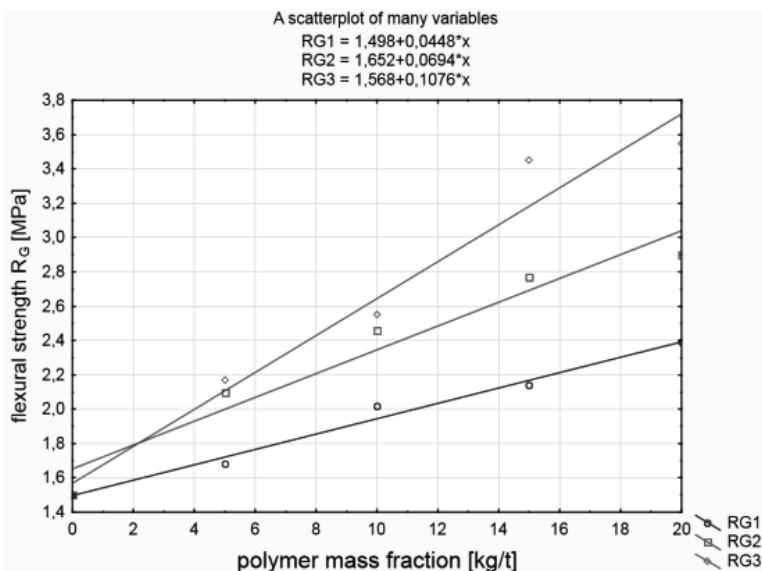
Fig. 2. Scatterplot, along with a selection of linear regression function at
compression at tensile strength. Markings on the chart correspond to the
1 – copolymer of vinyl acetate, vinyl versatate, 2 – redispersible binder based
on a copolymer of vinyl acetate, vinyl versatate, ethylene and butyl acrylate,
3 – copolymer of ester acrylic acid – styrene

The dependence of compressive strength on the quantity of the analyzed polymer additives
can be described with the following equations:

$$R_{C1} = 4.4993 + 0.2206 \cdot C_{PR1} \pm 0.75 \tag{1}$$

$$R_{C2} = 4.5873 + 0.0789 \cdot C_{PR2} \pm 0.34 \tag{2}$$

$$R_{C3} = 4.715 + 0.2343 \cdot C_{PR3} \pm 0.59 \tag{3}$$

where:

R_C – compressive strength on the quantity of the analyzed polymer additives,
C_{PR} – polymer share of the analyzed polymer additives.

This means that the largest increase in compressive strength is associated with an increase
in the participation of copolymer No. 1 (polymer increase by 1 kg, increases R_{C1} by 0.22 MPa),
and copolymer No. 3 (increase of the polymer by 1 kg increases R_{C3} 0.2343 MPa). In this
case, the addition of admixtures of these polymers to the mortar recipe in an amount of
20 kg/t has increased the compressive strength approx. by 5 MPa compared to the samples that
did not contain polymer admixtures. For copolymer No. 2, lower increases in compressive
strength – R_{C2} were observed (polymer increase by 1 kg increases R_{C2} by 0.0789 MPa). The
polymer additive in an amount of 20 kg/t caused a rise of R_C approx. by 1 MPa.

The results of the measurement of tensile strength in bending of the samples were given a similar statistical analysis. The parameters R, R^2, $R2$, $F(1.3)$, p, have been assessed as in the previous case. Also, in this case, a strong dependence of bending strength on the quantity of polymer additives was observed.

The dependence of tensile strength in bending on the amount of polymer additives can be described with the following equations:

$$R_{G1} = 1.498 + 0.0448 \cdot C_{PR1} \pm 1.15 \tag{4}$$

$$R_{G2} = 1.652 + 0.0694 \cdot C_{PR2} \pm 2.16 \tag{5}$$

$$R_{G3} = 1.568 + 0.1076 \cdot C_{PR3} \pm 1.80 \tag{6}$$

where:

R_G – tensile strength in bending on the quantity of the analyzed polymer additives,
C_{PR} – polymer share of the analyzed polymer additives.

This means that the largest increase in tensile strength in bending is associated with an increase in the participation of copolymer No. 3 (increase by 1 kg increases R_{G3} by 0.1076 MPa). In this case, the addition of polymer admixture to the mortar recipe in an amount of 20 kg/t has increased the compressive strength approx. by 3 MPa compared to the samples that did not contain polymer admixtures. Then in case of copolymer No. 2 (polymer increase by 1 kg increases R_{G2} by 0.069 MPa), the addition of polymer admixture in an amount of 20 kg/t has increased R_{G2} approx. by 1.5 MPa. For copolymer No. 1 lower increase in the R_{G1} strength was observed (polymer increase by 1 kg increases R_{G1} by 0.0448 MPa), the addition of polymer admixture in an amount of 20 kg/t has increased R_{G1} approx. by 1.0 MPa

Table 2

Results of summary statistics for the capillary rise test

Statistics	Summary statistics, the dependent variable		
	$H1$	$H2$	$H3$
R	0.99154	0.98226	0.97036
R^2	0.98315	0.96483	0.94161
$R2$	0.97754	0.95311	0.92214
$F(1, 3)$	175.146	82.317	48.379
P	< 0.0009	< 0.0028	< 0.0060
Standard error of estimation	1.18	1.71	2.20

Regression summary is presented in Fig. 3:
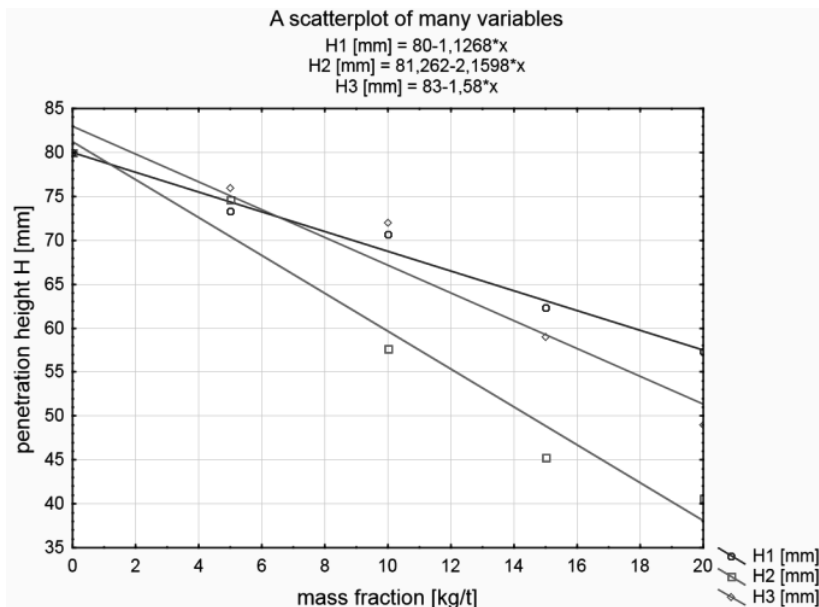
Fig. 3. Scatterplot, along with a selection of linear regression function. Markings on the chart correspond to the 1 – copolymer of vinyl acetate, vinyl versatate, 2 – redispersible binder based on a copolymer of vinyl acetate, vinyl versatate, ethylene and butyl acrylate, 3 – copolymer of ester acrylic acid – styrene

The relationship of capillary rising water on the amount of polymer additives in the recipe of mortar can be described by the following equations:

$$H1 = 80 - 1.1268 \cdot C_{PR1} \pm 1.18 \tag{7}$$

$$H2 = 81.262 - 2.1598 \cdot C_{PR2} \pm 1.71 \tag{8}$$

$$H3 = 83 - 1.58 \cdot C_{PR3} \pm 2.20 \tag{9}$$

where:
H – capillary rising water [mm],
C_{PR} – polymer share of the analyzed polymer additives.

The visual evaluation of the scatter plot (Fig. 3) shows that the relationship is linear, and for all studied polymer additives, together with the increase in participation of polymer additives, the height of capillary rise was getting smaller. The lowest values of capillary rising were determined for samples containing polymer No. 2 (redispersible binder based on a copolymer of vinyl acetate, vinyl versatate, ethylene and butyl acrylate). the addition of polymer admixture in an amount of 20 kg/t to all the components of dry mortar mix reduces the height of capillary rising by 40 mm.

3. Conclusions

The aim of this study was to investigate the effect of polymer additives on mechanical and physical properties of hardened mortars. These additives have a positive impact on studied properties in the mortar's recipes. It may be noted, however, that despite the great innovation that has been made in terms of redispersible resins production, there is none that would improve all mechanical and physical properties of mortars. Vinyl acetate/vinyl versatate copolymer shows reinforcing properties in terms of compressive strength, the additive: copolymer of vinyl acetate, vinyl versatate ethylene and butyl acrylate significantly increases the bending strength and capillary rising of the hardened mortars, copolymer of acrylic acid ester-styrene, significantly improves the mechanical properties of the mortar, while it affects the capillarity rise of the sample to a lesser extent. Despite the above mentioned issues it can be concluded that this is the best additive, considering its effect on mechanical and physical properties of the mortars.

R e f e r e n c e s

[1] JennI A., Holzer L., ZurbrIggen R., Herwegh M., *Influence of polymers on microstructure and adhesive strength of cementitious tile adhesive mortars*, Cem Concr Res, 35, 2004, 35-50.

[2] Ohama Y., *Principlesof latex modification and some typical properties of latex modified mortars and concretes*, ACI Mater, J 1987, 511-518.

[3] Ru Wang, Pei-Ming Wang, Xin-Gui Li., *Physical and mechanical properties of styrene – butadiene rubber emulsion modified cement mortars*, Cement and Concrete Research 35, 2005, 900-906.

[4] Silva D.A., Roman H.R., Gleize P.J.P., *Evidences of chemical interaction between EVA and hydrating Portland cement*, Cement and Concrete Research 32, 2002, 1383-1390.

[5] Stanisz A., *Przystępny kurs statystyki z zastosowaniem Statistica na przykładach z medycyny*, StatSoft Polska Sp. z o.o., Kraków 2007.

[6] Fox J., *Applied Regression Analysis, Linear Models and Related Methods*, Sage Thousand Oaks, 1997.

[7] PN-EN 196-1: 2006: Methods of testing cement. Determination of strength.

WACŁAW BRACHACZEK*, WOJCIECH SIEMIŃSKI**

RESEARCH ON THE INFLUENCE OF COLLOIDAL SILICA ADDITION ON WATER VAPOUR PERMEABILITY OF PAINT COATING

BADANIE WPŁYWU DODATKU KRZEMIONKI KOLOIDALNEJ NA PRZEPUSZCZALNOŚĆ PARY WODNEJ POWŁOK MALARSKICH

Abstract

In the paper the influence of colloidal silica addition with different amounts of organic resin in facade paints formulations on the change of water vapour permeability of hardened coatings was researched. The results were obtained by means of experiments. To quantify the ability of paint to diffuse water vapour, Sdfactor, defined as equivalent to the thickness of non-rotating air layer, was used. For the quantitative determination of the relationship between water vapour permeability and the share of analyzed components in the formulation of paint a statistical model based on multiple regression was applied. Statistical analysis of the results showed that the effect of changes in the amount of colloidal silica in the formulation of paint on Sd value is small, compared to organic resin share changes.

Keywords: colloidal silica, water vapour permeability, coating

Streszczenie

Przebadano wpływ dodatku krzemionki koloidalnej przy różnych ilościach żywicy organicznej w recepturach farb fasadowych na zmianę przepuszczalności pary wodnej przez utwardzone powłoki. Wyniki badań uzyskano na drodze eksperymentalnej. Do skwantyfikowania zdolności powłok malarskich do dyfuzji pary wodnej posłużono się współczynnikiem *Sd* definiowanym jako równoważna grubość nieruchomej warstwy powietrza**.** Do ilościowego określenia związków pomiędzy przepuszczalnością pary wodnej a udziałem analizowanych składników w recepturze farby posłużono się modelem statystycznym opartym na regresji wielorakiej. Sadystyczna analiza uzyskanych wyników wykazała, że wpływ zmian ilości krzemionki koloidalnej w recepturze farby na *Sd* value jest niewielki w stosunku do zmian udziałów żywicy organicznej.

Słowa kluczowe: krzemionka koloidalna, przepuszczalność pary wodnej, powłoki malarskie

* Ph.D. Eng. Wacław Brachaczek, Faculty of Materials and Environmental Sciences, University of Bielsko-Biala.
** M.Sc. Wojciech Siemiński, Sempre Farby sp. z o.o., 43-301 Bielsko-Biała, ul. Gen. J. Kustronia 60.

Designation

C_{PR}	–	proportion by weight of aqueous solution of colloidal silica
C_{PR}	–	proportion by weight of aqueous dispersion of organic resin
S_d	–	factor, diffusion equivalent air layer thickness [m]
V	–	coefficient of diffusion of water vapour [g/(m²·d)]
$m_1 - m_2$	–	the difference in mass of the container between the two measurements [g]
$t_2 - t_1$	–	the time between two consecutive measurements expressed in [h]
A	–	the surface of the tested sample expressed in [m²]

1. Introduction

Colloidal silica is an aqueous dispersion of amorphous silicon dioxide (SiO_2) in the form of spherical, non-crosslinked particles. Surface of each such particle is fully hydroxylated, the size, as in the case of colloids, ranges from 5 to 75 nm. There are many literature references describing the possible use of colloidal silica for the manufacturing of paints for different applications. In paints containing an organic binder, the addition of colloidal silica improves the adhesion to the substrate, increases coating's hardness and resistance to weathering. Inorganic paints can be used as the main component or as the primary binder. Furthermore, the addition of colloidal silica increases the elastic modulus of the cured film, which in turn allows to reduce the amount of organic binder in paint formulations without the loss in mechanical properties of coatings. An important parameter affecting coatings' long-term functionality and enabling transport of the accumulated moisture by diffusion of water vapour is water vapour permeability. In the paper paint formulations containing various amounts of organic binder and colloidal silica in terms of water vapour permeability were tested.

2. Experimentalsection

2.1. Material

Tests were conducted on coatings made from the paint produced in laboratory scale from the formulations comprising: filler: $CaCO_3$ (in an amount of about 30% in comparison with all components of a formula), quartz powder (7%), thickening agent: Methyl Hydroxy Ethyl Cellulose MHEC (0.45%), Pigment: Titanium dioxide Rutil (17%), dispersing agent: sodium salt of poliacrylic acid (0.4%), silicone defoamers (0.2%) and water (qs to 100%). First the pigments, fillers and coating assistants were dispersed in water to give a base, which was then mixed in appropriate weight proportions with aqueous dispersion of a copolymer of n-butyl acrylate and styrene (incl. 50% solids) and an aqueous solution of colloidal silica (incl. 50% solids, particle size 12 nm, pH 7.5). Weight percentages of aqueous dispersion of organic resin for all ingredients of tested paints formulations (C_{PR} [%]) were: 13, 16, 19, 22 and 25% for each part of organic resin, weight shares of aqueous solution of colloidal silica (C_{SI} [%]) were 0, 3, 6, 9 and 12%. Coating thickness in the hardened state was 0.24 [mm].

2.2. Measurement of S_d [m] factor, diffusion equivalent air layer thickness by Wet-Cup scale method

The ability of diffusion of water vapour of the decorative and protective coating is determined by the value of diffusion-equivalent air layer thickness S_d. It means that the thickness of the stationary air layer [m], under the same measurement conditions has the same coefficient of diffusion of water vapour V [g/(m²·d)] as the tested coating. The study was conducted on a sample of paint that had a thickness of 180 μm, using a Wet-Cup method. The equipment and materials for the study were prepared in accordance with PN-EN ISO 7783-2: 2001 [8]. For this purpose glass pans were used which, after filling with a saturated solution of ammonium dihydrogen phosphate were sealed with a porous material made of porous polyethylene PE-HD, at which the tested coating was previously applied by brush. The space between the wall of the capillaries and the sintered disc was sealed. Thus prepared dish was weighed on an analytical scale and placed in a climate chamber (see Fig. 1).
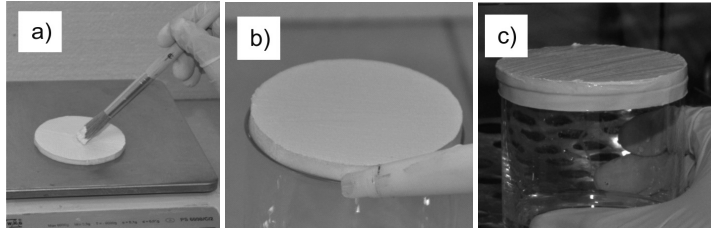
Fig 1. Preparation of the samples to determine the water vapour transmission rate

The amount of steam, which diffused through the tested coating was determined by measuring the weight. The change in mass of water, on the basis of which the S_d value was determined, was calculated as the average value of three successive measurements at subsequent intervals after equilibrium was achieved, and it was carried out on three separate coatings of the same material. For each tested sample, the values of diffusion equivalent air layer thickness Sd according to the formula (1), were determined:

$$S_d = \frac{20 \cdot A \cdot (t_1 - t_2)}{24 \cdot (m_2 - m_1)} \tag{1}$$

where:

$m_1 - m_2$ – the difference in mass of the container between the two measurements expressed in [g],

$t_2 - t_1$ – the time between two consecutive measurements expressed in [h],

A – the surface of the tested sample expressed in [m²].

The S_d value of diffusion equivalent air layer thickness of the coatingwas calculated as the difference of the substrate Sd with a coating without substrate S_d,

$$S_d(\text{coating}) = s_d(\text{substratewithcoating}) - S_d(\text{substrate}) \tag{2}$$

3. Results and discussions

The results of studies on permeability of water vapour through the coating containing various amounts of colloidal silica and organic resin were presented in graphic form in Figure 2.
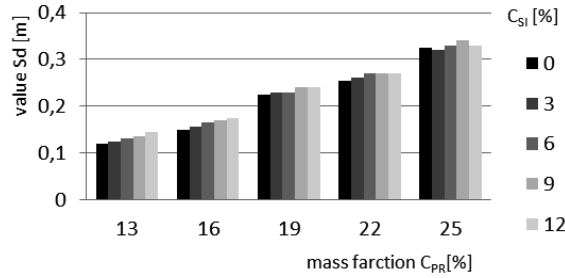
Fig. 2. Results of studies on permeability of water vapour through the coating, where: S_d – factor, diffusion equivalent air layer thickness [m], C_{PR} – proportion by weight of aqueous solution of colloidal silica, C_{PR} – proportion by weight of aqueous dispersion of organic resin

3.1. Analysis of variance according to a double classification (ANOVA)

In order to check whether simultaneous changes in the mass fraction of the analysed ingredients have a statistically important impact on the value S_d, a correlation matrix allowing for the calculation of Pearson's coefficients of correlation and assessment of their significance was developed. With this purpose in view, statistical inference with the use of ANOVA analysis of variance according to a double classification was conducted [4, 5].

Table 1 presents the results of the analysis of variance in the aspect of the assessment of impact of the change in the fraction of the analysed ingredients on the value of ds The calculated values of statistics $F(C_{PR})$ and $F(C_{SI})$ were compared with the critical values of $F(C_{PR}, \alpha)$ and $F(C_{SI}, \alpha)$ read in the Fisher-Snedecor distribution table [5].

Table 1

The results of a test based on analysis of variance according to a double classification ANOVA

Value S_d [m]						
	SS	dg. of freedom	MS	F	F_{crit}	p
free term	1.111	1	1.111	16832.06		0.000000
C_{PR} [%]	0.159	4	0.039	601.3	3.49	0.000000
C_{SI} [%]	0.004	4	0.0011	16.61	3.26	0.000015
error	0.0011	16	0.00007			

where:

F – computational value of F-Snedecor statistics,

$F_{\text{Crit.}}$ – critical value read from F-Snedecor distribution tables at the significance level $\alpha = 0.05$ and the number of the degrees of freedom $(w-1)$ and $(z-1)$,

SS – total of squares of differences in the dependent variable and its mean,

MS – mean square,

C_{PR} – mass fraction of polymer resin [%],

C_{SI} – mass fraction of colloidal silica [%].

Having analysed the results of ANOVA tests, it can be stated, that the simultaneous impact of changes in the values of C_{PR} % and C_{SI} %, ds depends on the change in the fraction of both ingredients.

3.2. Calculation of substitute characteristics, assessment of the significance of the identified regression functions

In order to quantify the relationship between simultaneous influence of the shares of the analyzed components C_{SI} [kg/t], C_{PR} [kg/t] in the formulation and S_d [m], a linear multiple regression model was established. In this case, the shares of the analyzed components were correlated with S_d by equation:

$$Y = b_0 + b_1 x_1 + b_2 x_2 + ... + b_k x_k + \varepsilon \tag{3}$$

where:

b_i – model parameters (regression coefficients) describing the impact of the i-th variable,
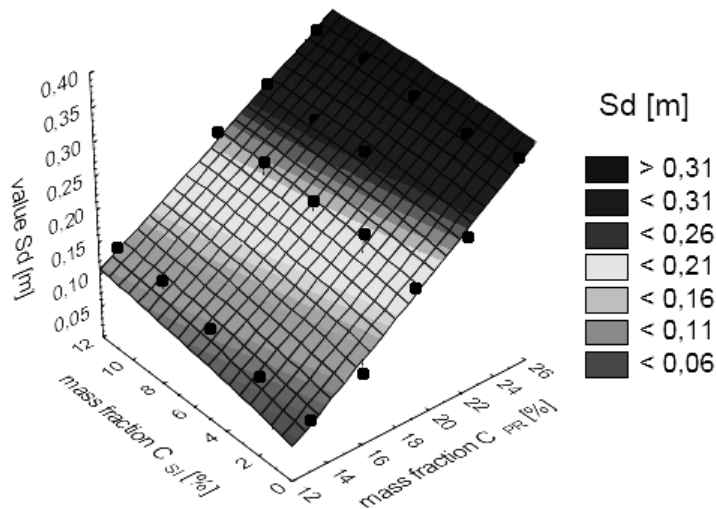
ε – error factor.

Fig. 3. Surface chart of the regression function $\hat{ds} = f(C_{SI}; C_{PR})$

Values of statistics summarising regression functions

$N = 25$	$b*$	St. Error of $b*$	b	St. Error Of b	$t(22)$	p
	Summary of dependent variable regression: ds [m] $R = 0.9834709$ $R^2 = 0.96720752$ corrected: $R2 = 0.96422639$ $F(2.22) = 324.44$ $p < 0.00000$ Standard error of estimation: 0.015					
free term			-0.15973	0,015023	-10.6325	0.000000
C_{PR} [kg/t]	0.970274	0.038608	0.018533	0.000737	25.1315	0.000000
C_{SI} [kg/t]	0.160549	0.038608	0.003067	0.000737	4.1585	0.000000

Table No. 2 shows that the model is linear with respect to the *ds* parameter. Linearity was checked by test *F*. The *p* level for this test is 0.000, the *R* correlation factor was 0.98347 which means that there is a strong linear relationship between the variables. The standard error of estimate is 0.015. This means that the predicted values of the ds variable differ from empirical values on average by 0.015 m.
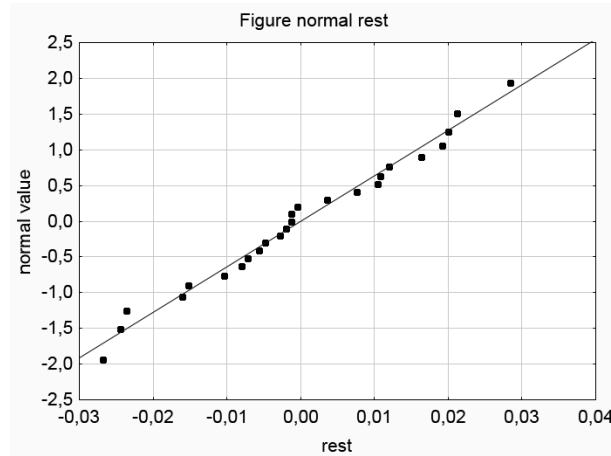
Fig. 4. Normality residues chart

In order to verify whether the residues have a normal distribution, normality residues chart was created, Fig. 4. The analysis of residuals was based on Cook's distance measurement. It was found that all the statistic values are of the same order, and there is no different case affecting the load of the regression equation. On the basis of the analysis of the residuals, the correlation factor and determination, it can be assumed that the adjustment of the model to empirical data is proper. The multiple regression equation calculated in this way is:

$$d_S = 0.018533 \cdot C_{PR} + 0.003067 \cdot C_{SI} - 0.15973 \pm 0.015 \qquad (4)$$

This means that if the C_{SI} increases by 1 kg, ds will then rise by about 0.018533 [m]. Similarly, if the amount of colloidal silica is increased by 1 kg, ds will increase by 0.003067 [m]. The relatively large error of the free term indicates that it should be used with caution when predicting random variable.

Changes in proportion by weight of organic resin and colloidal silica affect the size of Sd with varying intensity. The change of share of organic resin has greater influence on the analyzed parameter than the change in the quantity of colloidal silica. The observed dependences can be explained by a difference in binding the mineral components of the coating by organic resin and colloidal silica. The aqueous dispersion of a copolymer of n-butyl acrylate and styrene used in the paint formula, is undergoing a film-forming material pervious to coalescence by evaporation of water. Thus obtained film is flexible, durable and resistant to water, with high adhesion to mineral surfaces as well as surfaces made of plastics and non-metals. The colloidal silica that is involved in the binding process, binds the mineral components as a result of silicification reaction. The active functional groups of colloidal silica are involved in the reaction: $-Si(OH)_2$, mineral components of the coating and the substrates, mainly calcium carbonate and silica sand. Thus formed structure is an open-porous one, of high permeability with respect to water vapour. Large diffusivity in relation to water vapour was obtained for the coatings for which the weight fraction of aqueous organic resin does not exceed 13%. In that case, irrespective of the content of colloidal silica, the range of changes in S_d equivalent air layer does not exceed 0.14 [m]. Such coatings, due to the volume of water vapour permeability factor, according to DIN EN 1062-1: 2005 [7] are classified as Class I: high diffusivity of water vapour. Application of colloidal silica in the recipes will also have a positive impact on other properties of cured coatings. Chemical bonding method of colloidal silica will exert a positive impact on the stability and adhesion of coatings to mineral substrates. Together with a decrease in the share of organic resin, the coating's tendency to soiling will be reduced. When designing paint, one should consider the fact that reduction of the share of polymer resin will be connected with an increase in the surface absorption of coatings for water and it may be necessary to use hydrophobicizing agents, which may have an impact on the value of Sd factor.

The applied statistical method, that is based on multiple regression can be a useful tool to quantitatively assess the relations between the simultaneous influence of paints' ingredients and other parameters of coatings, such as surface water absorption, abrasion resistance, etc. A well designed program of studies however will reduce the number of time-consuming research, and thus the time of developing the technology of new products will be reduced, which will bring tangible economic benefits.

4. Conclusions

On the basis of experimental research it was estimated that there is a correlation between the change in the quantity of organic resin and colloidal silica in the formulation of paints and water vapour permeability quantified by relative diffusion resistance Sd of cured coatings. Based on statistical analysis it can be concluded, that this relationship is of a positive character, statistically highly linear.

The effect of changes in the amount of organic resin in a formulation is greater than the effect of changes in the amount of colloidal silica on water vapor permeability.

R e f e r e n c e s

[1] Bergnah E., *Colloid chemistry of silica* in Colloidal Silica Fundamentals and Applications, CRC Press Taylor & Francis Group, Boca Ration 2005, Vol. 131, 9.

[2] Otterstedt J.E., Greenwood P., *Some Important, Fairly New Uses of Colloidal Silica Soll* in in Colloidal Silica Fundamentals and Applications, Taylor & Francis Group, Boca Ration 2005, 737.

[3] Brachaczek W., *Masa tynkarska polikrzemianowo-silikonowa*, Patent nr 214638, 2009.

[4] Stanisz A., *Przystępny kurs statystyki z zastosowaniem Statistica na przykładach z medycyny*, StatSoft Polska Sp. z o.o., Kraków 2007.

[5] Dunn O.J., Clark V.A., 2nd Ed., Applied Statistics: Analysis of Variance and Regression, John Villey, New York 1987.

[6] Fox J., *Applied Regression Analysis, Linear Models and Related Methods*, Sage Thousand Oaks, 1997.

[7] Farby i lakiery. Wyroby lakierowe i systemy powłokowe stosowane na zewnątrz na mury i beton. Część 1: Klasyfikacja.

AGNIESZKA BUCKA*

"A SECOND CHANCE" – THE CONCEPT OF REVITALIZING THE "JAWISZOWICE" STATE COAL MINE

„DRUGA SZANSA" – KONCEPCJA REWITALIZACJI PAŃSTWOWEJ KOPALNI WĘGLA KAMIENNEGO „JAWISZOWICE"

Abstract

The paper presents the problem of degradation of the former industrial complex PKWK "Jawiszowice" in Brzeszcze with its buildings and technical infrastructure, and examines the possibility of its re-use. It emphasizes the benefits of the area revitalization in the broad sense that seems to be the most sensible decision which may be made after the termination of extraction of the raw material. The main aspect is the implementation of innovative and creative solutions which consequently enable the creation of the development not only for the city of Brzeszcze but for the entire region. This example – which is the subject of the present discussion – was also the subject of author's previous studies conducted in the framework of the masters' thesis.

Keywords: revitalization, post-industrial areas, Jawiszowice

Streszczenie

W artykule przedstawiono problem degradacji dawnego kompleksu przemysłowego PKWK[1] „Jawiszowice" w Brzeszczach wraz z jego zabudową i infrastrukturą techniczną, a także rozpatrzono możliwości ponownego ich wykorzystania. Podkreślono korzyści płynące z rozumianej *sensu largo* rewitalizacji obszaru poprzemysłowego, zdającej się być najrozsądniejszą decyzją, jaką można podjąć w związku z zakończeniem eksploatacji surowca. Główny aspekt stanowi wdrożenie innowacyjnych i kreatywnych rozwiązań, które w konsekwencji umożliwią stworzenie przestrzeni rozwoju nie tylko dla miasta Brzeszcze, ale i całego regionu. Przykład będący tematem rozważań jest również przedmiotem wcześniejszych studiów autorki prowadzonych w ramach pracy magisterskiej.

Słowa kluczowe: rewitalizacja, obszary poprzemysłowe, Jawiszowice

---

* M.Sc. of Architecture Agnieszka Bucka, Department of Civil Engineering and Building Physics, Faculty of Civil Engineering, Cracow University of Technology.

[1] For the purpose of this article I follow K. Lenartowicz terminology [2]: The State Coal Mine Jawiszowice (PKWK Jawiszowice). Originally the complex was called Jawiszowice Mine, while the current name is KWK Brzeszcze Silesia – Ruch II.

1. Introduction

1.1. Revitalization of post-industrial areas

1.1.1. Western Europe example – "Zollverein" mine in Essen

"Zollverein" mine is one of the most valuable examples of industrial construction. It is worth mentioning that at the time of its heyday, it was the largest and most modern mining facility in the world. The architecture of the complex consists of simple geometric solids, slammed into cubes of steel frame construction, filled with red brick.

In 1986, coal extraction has been suspended [4], and a broad spectrum of social and spatial activities that was later performed, opened a new chapter in the history of the mine. At the moment, the Zollverein industrial complex is a model example of revitalization of post-industrial structures, and is being mentioned alongside such projects as the revival of the steelworks in Duisburg and other industrial Ruhr area. Not without significance is the fact that on 14 December 2001, the group of Zollverein Coal Mine buildings has been inscribed into the UNESCO list of World Heritage under the name "Zollverein Coal Mine Industrial Complex" [3].
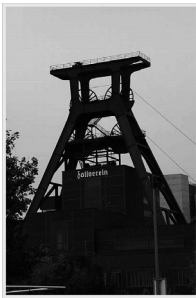
Fig. 1. Mine and coking plant Zollverein in Essen [10]

Fig. 2. Mine and coking plant Zollverein in Essen [10]

1.1.2. An example from Poland – "Julia" mine in Wałbrzych

In 2014, the revitalization of the "Julia" mine in Walbrzych is to be completed [7], remade – in accordance with the draft zoning made by the *Nizio Design International* studio – into a center of cultural and creative industries, as well as a sports and leisure complex. Designers working on the new look, intend to use large-scale multimedia technologies that have recently been gaining popularity [7].

Fig. 3. "Julia" mine in Wałbrzych – condition of buildings before renovation [9]

Fig. 4. „Julia" mine in Wałbrzych – visualization [8]

2. The Idea

2.1. PKWK „Jawiszowice" revitalization

2.1.1. History draft

The mining history of the area dates back to the eighteenth century, however, the actual date of facility construction is the beginning of the twentieth century. The establishment of the mine resulted in the rapid growth of Jawiszowice, turning it into a thriving industrial center. Exhaustion of deposits in the 70's was the reason that coal mining became unprofitable. The property was gradually withdrawn from service, and the production was totally discontinued in 1995. In the next years, some of the buildings were sold to private investors, others were demolished, and the rest gradually fell into ruin. The complex has also a rich historical past – during World War II it was a prisoners' labor camp [5]. According to the author of the article, Agnieszka Zaborska-Jagiello [6], some of the PKWK "Jawiszowice" buildings clustered around Andrew III Shaft were included in the provincial register of monuments as a modernist industry building group – but this, in practice, does not necessarily translate into adequate measures to protect the monument.

2.1.2. Main assumptions of revitalization concept

The main idea of revitalization is to transform the industrial area into an educational and cultural center, with the supplement in the form of numerous sports, recreational and entertainment, tourism and museum facilities. The project fits in with the popular in Europe – and tested in the revitalization of other mining objects – trend of so-called "creative industries", while taking into account the economic and cultural needs of the region. Naming of the buildings has been chosen to combine their old function with the new one, while maintaining the nomenclature proper for the mining industry. For many existing buildings that undergone revitalization and in different zones of the complex, new names have been adopted which evoke the coal exploitation: for example '*The Mine of Knowledge*' (a museum), '*The Theatre of Coal-Black Humor*' (a theater), '*SPA-lony Shift*'[2] (a SPA) and 'Coal Sketches' (an art gallery), '*Excavation*' (a cultural centre), '*Extraction*' (an acting school), '*KOKS*' (the Original Arthouse Cinemas Complex[3]), '*The Processing Hall*' (a school of creative photography), '*Tunnel*' (a school of interior and space design), 'Headroom' (the management office).

The article describes the general concept of development of the land surface of the mine in the western part of the establishment with its zoning: development, arts, culture, education, museum, sports, shopping, the seat of the administrative staff and complex management, and – in the eastern part – two zones combined: the outdoor and sports area (preserved in the naturalistic style, open-air stage on a hill, an amphitheater and a reservoir equipped with a port for rafts and boats). The mine buildings fit in with the planned large-scale green areas such as forests (the project includes the creation of spaces for undertakings such as a rope course, paintball, quad and cross tracks, skate park, walking paths) and reservoirs (Soła river and ponds created with mining subsidies), which are communicated with each

---

[2] This name is a wordplay: '*spalony*' in Polish means '*burnt*' (translator's note).

[3] Also a wordplay: '*koks*' means '*coke*' and is at the same time an acronym for the Polish name of the complex (translator's note).

other by means of a rollers and bicycle routes and a waterway for boats and rafts. In terms of communication the following are planned: multiple entry points for cars and conveniently located car parks surrounded by protective greenery, a connection of the establishment to the city by a railcar line using existing and unused railroad tracks.
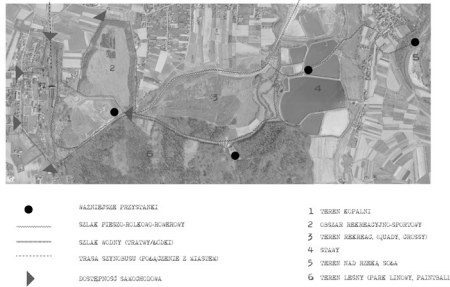

Fig. 6. The concept of urban revitalization of the PKWK "Jawiszowice" area (author's archive)

Fig. 5. The environmental analysis of the site PKWK "Jawiszowice" and its surrounding areas (author's archive)

The whole premise closes with the newly designed building of the Art Schools Centre "ARTySZYB" ("ARTySHAFT"). The school in its idea refers to the assumptions of Walter Gropius implemented at the Bauhaus. The name itself combines the former place of work of hundreds of people in the underground of the 'shafts' with the newly established buildings of art where, instead of working hard in tough conditions, people are focusing on integration, education, artistic creation and active leisure. It constitutes a denial of the past in relation to the interior form, thanks to wide walking paths, well-lit and vast interiors, the transparency of the newly designed parts of the object, and also to its character: full of vitality. The building is, at the same time, an integral part of both the premises and the greenery (in particular, through the adoption of a green roof), and it consists a contrasting element due to its modern form. It is designed to realize the change that has occurred as a result of the forbearance of its industrial use and of buildings adaptation for educational and artistic functions.
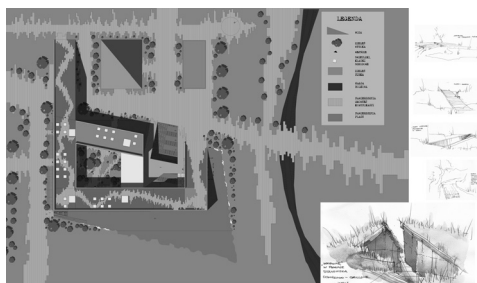

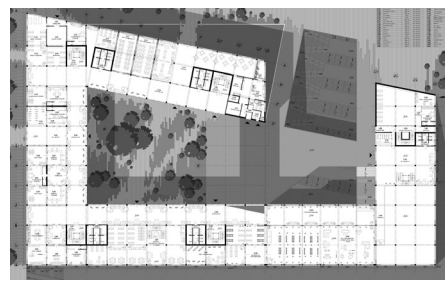Fig. 7. *Art Schools Centre "ARTySZYB"* – positioning (author's archive)

Fig. 8. Centrum Szkół Artystycznych "ARTySZYB" – a groundfloor sketch with its environment (author's archive)

Using different finishing materials, resulted in a clear difference between the structure of old red brick buildings and a contemporary interference in the form of white-plastered concrete and large glazed surfaces, generating the impression of lightness that stands in opposition to the character of the buildings built in the traditional technology. The main idea of the project is to highlight the antagonisms intensified by the wordplays in the naming and a game of illusion and allusion of two different worlds: the underground – full of gloom and narrowness, accompanying the miners – and the surface, which is reminiscent of light and space.

The entire complex has been designed in such a way as to create a wide range of options to suit the widest possible range of users. The proposed facilities are to counteract the lack of prospects, characteristic for many small towns, and the concepts of proposed functions – to give the possibility to retrain and give employment opportunities to the population that is losing their jobs due to downsizing in the mining industry. For some of the buildings, their features are flexible, giving the possibility to produce income from their usage (renting for purposes such as: events, fairs, workshops, concerts, conferences, sports activities etc.).

3. Conclusions

The presented concept meets the problems and issues described by the author (Daria Grochowska) in the article [1], which are: sustainability, accessibility, diversification, open space, compatibility, incentives, adaptability, density and identity of the place. The key role of the revitalization is to optimize the balance of development of the economic and ecological area, with the use of energy-efficient and innovative solutions and technologies that are implemented in the construction of new facilities and the renovation of the existing ones.

Using the unquestionable advantages of the location and the rich history of PKWK 'Jawiszowice', the author tried to transfer western trends to Polish reality, while respecting the cultural values of the region. It is hoped that these studies will be useful in the revitalization works of mines and other objects of this type in Poland.

References

[1] Grochowska D., *Nowe życie „miejskich przegranych:. Rewitalizacja kopalni węgla kamiennego „Mysłowice" i terenów przyległych*, czasopismo techniczne, z. 1, 1-A/2012 (rok 109), 200-203.

[2] Lenartowicz J.K., *Potencjał dziedzictwa techniki w rewitalizacji. Państwowa Kopalnia Węgla Kamiennego Jawiszowice jako ognisko Strategicznej Interwencji w gminie – prolegomena projektu rewitalizacji*, czasopismo techniczne, z. 1-A/2011 (rok 108), 49-58.

[3] Pasko K., Staszewska-Ludwiczak A., *Przystosowanie wybranych obiektów dziedzictwa poprzemysłowego na potrzeby bazy hotelarskiej i turystycznej – przykłady z Polski i Europy*, materiały pokonferencyjne z IV Konferencji Naukowo-Praktycznej pt „Dziedzictwo przemysłowe jako strategia rozwoju innowacyjnej gospodarki", Zabrze 6–7 września 2007, 100.

[4] Pluta K., *Projektowanie urbanistyczne jako narzędzie kształtowania przestrzeni publicznych w procesie rewitalizacji terenów przemysłowych i kolejowych*, czasopismo techniczne, z. 12, 3-A/2012 (rok 109), 110.

[5] Senkowska S., *Podobóz Jawischowitz*, Odgłosy Brzeszcz, Nr 9 (141), wrzesień 2003, 14-15.

[6] Zaborska-Jagiełło A., *The state coal mine Jawiszowice in Brzeszcze. The history, present state, architecture, vision of revitalisation with the partucipation of creative industries*, AGH Journal of Mining and Geoengineering, vol. 36, No. 1, 2012, 344.

[7] http://architektura.muratorplus.pl/projekty/nowa-inwestycja-w-walbrzychu-rewitalizacja-kopalni-julia_80526.html (access: 02.07.2014).

[8] http://www.nizio.com.pl/pl/rewitalizacja_dawnej_kopalni_julia_w_walbrzychu.html (access: 02.07.2014).

[9] http://www.renowacjeizabytki.pl/index.php?option=com_content&view=article&id=188:rewitalizacja-zabytkowej-kopalni-julia-w-wabrzychu&catid=9 (access: 02.07.2014).

[10] http://www.zollverein.de (access: 02.07.2014).

KORNELIA CABAŁA, SEBASTIAN ZAWORSKI, JOLANTA GINTOWT[*]

THE INFLUENCE OF FITTING OF A WINDOW ON A HEAT TRANSFER COEFFICIENT AND AN ENERGY BALANCE OF A BUILDING

WPŁYW MONTAŻU OKIEN NA STRUMIEŃ CIEPŁA I BILANS ENERGETYCZNY BUDYNKU

A b s t r a c t

The project concerns windows and their properties. Four windows were considered to provide computations. Two of them were common windows and the other two – passive windows. The analysis focuses on a role of a fitting in heat losses, explains important aspects of choosing a window and shows main types of methods of mounting a window. The paper proves how big the influence of fitting a window is on a heat transfer coefficient value and shows what the losses steming from inproper fitting are. The project submits that fitting factor should be considered while calculating the heat transfer coefficient value and that windows ought to be mounted in an insulation to minimize heat losses.

Keywords: heat transfer, passive building, thermal bridges, montage, heat balance, window

S t r e s z c z e n i e

Analiza dotyczy montażu okien. Obliczenia przeprowadzono dla czterech typów okien: dwóch powszechnie stosowanych i dwóch pasywnych. Projekt koncentruje się na roli montażu w stratach ciepła, wyjaśnia, co jest ważne przy wyborze okna i określa, jakie są główne konsekwencje. Analiza podnosi że zagadnienie montażu okna powinno być brane pod uwagę na etapie obliczeń współczynnika przenikania ciepła okna, a nie dopiero przy obliczaniu wartości współczynnika przenoszenia ciepła.

Słowa kluczowe: przepływ ciepła, budynek pasywny, mostek termiczny, montaż, bilans energetyczny, okno

[*] Kornelia Cabała, Sebastian Zaworski, M.Sc. Eng. Jolanta Gintowt, Institute of Materials and Building Structures, Faculty of Civil Engineering, Cracow University of Technology.

Designations

A_g – surface glazing [m²]
A_f – surface frame [m²]
U – the heat transfer coefficient [W/m²K]
U_f – the heat transfer coefficient for a frame [W/m²K]
A_f – *the* area of a frame [m²]
Ψ_g – the linear heat transfer coefficient (frame bonding) [W/mK]
S_g – the length of linear heat transfer coefficient (frame bonding) [m],
S_f – the length of a thermal bridge along window frame – wall bonding [m]
Y_f – the linear heat transfer coefficient of a thermal (wall bonding) [W/m K]
l_f – the length of linear heat transfer coefficient (wall bonding) [m]
g – coefficient of a solar radiation permeability (here: $g = 1$)
z – shading coefficient (here: $z = 1$)
ΔT – the temperature difference between inside and outside the building (here: $\Delta T = 35$ K)
t – number of hours in a month (here: $t = 720$ h)

1. Introduction

1.1. Topic of the project

The topic of the project is the influence of fitting a window on a heat transfer coefficient and an energy balance of a building. It is essential for each house to choose the best type of a window and to fit it in a proper way. It is not enough to choose windows with high insulation properties and great energy balance – but the surrounding of a window and its fitting are also important. They should be mounted in such a way that eliminates thermal bridges [1, 12, 13] and that makes fitting connections impermeable [1–6].

Criteria of assessing the window: impermeability, fitting, heat transfer coefficient U [W/m²K], coefficient of a solar radiation permeability g, shading coefficient z, heat loss Q [kWh]. The analysis is connected with two factors mentioned above: fitting and heat loss.

1.2. Means of mounting a window:

Although the first one is causing the greatest heat losses, it is the most popular way of mounting in Poland [7–9, 11, 12]. It is called "traditional fitting", where a window is located on internal edge of the wall. It is shown in Fig. 1a. The amount of heat loss through thermal bridges will be smaller in case of "flush fitting", where the window is located along the isolation, which is not covering the frame of the window as it is shown in Fig. 1b. Windows should be situated on the outside edge of the wall to stay in the insulating layer, which is additionally covering the frame of the window. This solution is recommended in passive buildings [1, 10, 12]. In this case windows should not be open able, as the suitable amount of air is provided by a special circulating system. Making the windows openable would also cause a problem of stability. That is why the solution comes with anchors which help the window stay in the insulation as shown in Fig. 1c.
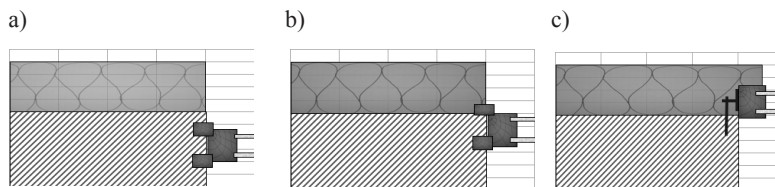
Fig. 1a) Traditional fitting, b) Flush fitting, c) Fitting in an insulation

2. Purpose of the project

The purpose of the project is to show the influence of fitting of a window on the value of heat transfer coefficient and to prove that a formula for calculating the heat transfer coefficient of the window which exists in Poland should include fitting and take into account consistent with [10] a method for determining the outside temperature.

3. Theses of the project

An inappropriate fitting of a window causes large amounts of heat losses and at the same time increases the cost of heating. Balancing gains and losses through windows for passive houses, nearly to zero-energy buildings, should be calculated according to the formula PHI [10].

4. Subject matter

The subject matter are four windows: two common windows (Aluplast IDEAL® 4000 [14] and Aluplast ENERGETO® 4000 [15]) and two passive windows (Internorm HF® 200 [16] and Oknoplast WINERGETIC PLUS® [17]).

5. Methods of analyses

The heat transfer coefficient calculations were done basing on the following formulas:

$$U_W = \frac{\sum A_g U_g + \sum A_f U_f + \sum l_g \Psi_g}{\sum A_g + \sum A_f} \tag{1}$$

In agreement with [12]

$$U = \frac{U_g \cdot A_g + U_f \cdot A_f + \psi_g \cdot s_g + \psi_f \cdot s_f}{A_g + A_f} \tag{2}$$

In agreement with [10]

Both formulas consider glazing, frame and bonding glazing – frame of a window. They differ from each other in a way that one of them does not consider the influence of fitting.

The formula for a heat loss calculation:

$$Q = \left[\left(U_w \cdot A_w \cdot g \cdot z \right) + \left(s_f \cdot \psi_f \right) \right] \cdot \Delta T \cdot t \cdot 10^{-3} \qquad (3)$$

According to [12]

$$Q = U_W \cdot A_W \cdot g \cdot z \cdot \Delta T \cdot t \cdot 10^{-3} \qquad (4)$$

According to [10]

The calculations of a heat loss for common windows were done basing on the first of the formulas. That is because in Poland fitting is considered in calculations only at this stage. In computation for passive windows the second formula was used. Additionally, to show significant influence of fitting on a heat loss it was assumed that common windows are mounted in a wall, as it is generally done in Poland. On the other hand it was assumed for passive windows that they are mounted in an insulation, according to rules for passive buildings.

For the purposes of comparison, the difference in calculation of a heat balance resulting from the different outside temperatures has been omitted (computational temperature is selected from: the coldest and warmest sunny/cloudy day) in [12] and [10].

6. Results

6.1. The value of a heat transfer coefficient

The chart below shows a value of a heat transfer coefficient of a window. It is divided according to a window model (first two of them are common windows and the other two are passive windows) and also according to a form of a calculation formula. The white color represents the formula which is in line with the Polish norm, which does not consider fitting. Light and dark blue colors represent the formula according to PHPP. "Proper fitting" should be understood as fitting which fulfills requirements of passive buildings. In turn an "improper fitting"is fitting failing to meet those requirements of passive buildings. In turn a bad montage is a montage which do not satisfy that demands.

Analyzing the chart, one should notice that an improperly-mounted passive window (Oknoplast Winergetic Plus®) has comparable value of a heat transfer coefficient as a well-mounted common window (Aluplast Energeto® 4000). One A big difference between a well- and badly-mounted window is also clear. In this case it equals 0.432 [W/m²·K] (Internorm® HF 200). Both factors mentioned above show the significance of influence of fitting on a heat transfer coefficient of a window.
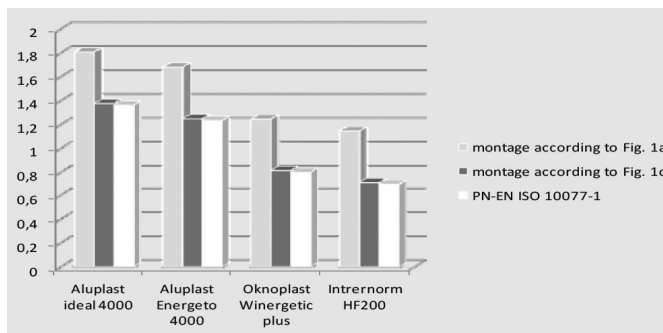
Fig. 2. Heat transfer coefficient U [w/m²K]

Window – *U* coefficient

Window	PN-EN ISO 10077-1	According to Fig. 1c	According to Fig 1a
Aluplast IDEAL® 4000	1.360	1.375	1.807
Aluplast ENERGETO® 4000	1.234	1.249	1.680
Oknoplast WINERGETIC PLUS®	0.800	0.815	1.246
Internorm HF® 200	0.699	0.714	1.146

6.2. Comparative analysis of the heat loss through windows

The chart shows a heat loss through an analyzed window in a period of one month. Time interval adopted for the purposes of this analysis seems to be sufficient. One should notice that the difference between a passive window mounted in insulation and a common window mounted in a wall is almost tripled and equals 91.11 [kWh]. It shows how great the losses created by a bad fitting are. It is shown in Fig. 3a. The difference resulting from the use of [10] and [12] for the calculation of the heat demand is approximately 25%. (An only loss associated with heat transfer through windows). This is a value that should not be ignored. This is shown in Fig. 3b.
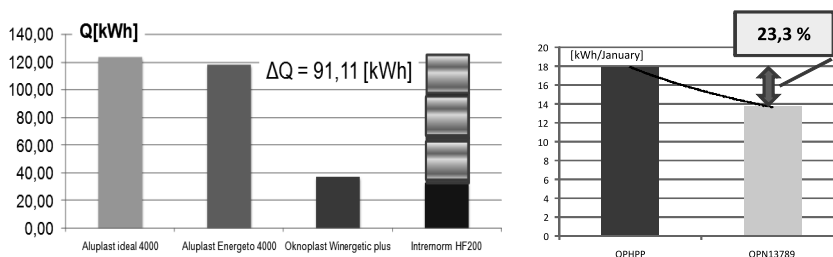

Fig. 3a) The heat demand for heating-window [kWh], b) PHPP and PN 13789 methods

7. Conclusions

To minimize heat losses and to eliminate thermal bridges windows should be mounted in an insulation. The fitting should be considered in a formula for a heat transfer coefficient because fitting considerably influences its value. It seems that the use of a formula for calculating the heat demand for passive houses, nearly-zero buildings, plus building, proposed by the Passive House Institute in Darmstadt, and entered in the PHPP, is justified.

References

[1] Feist W., Schlagowski G., *Podstawy budownictwa pasywnego*, Pol. Inst. Budownictwa Pasywnego, Gdańsk 2006.

[2] Chwieduk D., *Recommendation for energy concept of building*, Technical Transaction, Civil Engineering, 2-B/2012, Wyd. Politechnika Krakowska, ISSUE 3, YEAR 109.

[3] Chwieduk D., *Pozyskiwanie oraz konwersja termicznej energii słonecznej w budynku*, IPPT PAN, Warszawa 2006.

[4] Jędrzejuk H., Marks W., *Evolutional optimization of energy-saving buildings*, ARCHIVES OF CIVIL ENGINEERING, LI, 3, 2005, 395-413.

[5] Kisilewicz T., *Window sizing procedure for energy efficient buildings*, Czasopismo Techniczne. Budownictwo, Politechnika Krakowska, Kraków 2006.

[6] Gintowt J., *Ecological aspects of passive house as an example of completion of an investment,* Wyd. Politechnika Krakowska, Czasopismo Techniczne 2011.

[7] Dz.U. 2013 poz. 45, Rozporządzenie Ministra Transportu, Budownictwa i Gospodarki Morskiej z dnia 3 stycznia 2013 r. zmieniające rozporządzenie w sprawie metodologii obliczania charakterystyki energetycznej budynku i lokalu mieszkalnego lub części budynku stanowiącej samodzielną całość techniczno-użytkową oraz sposobu sporządzania i wzorów świadectw ich charakterystyki energetycznej.

[8] Rozporządzenie Ministra Infrastruktury w sprawie warunków technicznych, jakim powinny odpowiadać budynki i ich usytuowanie z dnia 12 kwietnia 2002.

[9] PN-EN ISO 10077-1, 2007.

[10] Program: PHPP (Passive House Design Package).

[11] PN-EN ISO 14683 of 2008.

[12] PN EN ISO 13789, Właściwości cieplne budynków, Współczynnik start ciepła przez przenikanie. Metoda obliczania.

[13] PN EN ISO 14683, Mostki cieplne w budynkach. Liniowy współczynnik przenikania ciepła. Metody uproszczone i wartości orientacyjne.

[14] http://www.aluplast.net/eng-int/produkte/kunststofffenster-systeme/ideal-4000.php

[15] http://aluplast.com.pl/index.php?module=katalog&kategoria

[16] http://www.internorm-krakow.pl/hp-okna-da-hf200.php

[17] http://oknaidrzwib2b.pl/produkty/k/108-okna

IRENEUSZ CHRABĄSZCZ, MAREK DUDZIK, JANUSZ PRUSAK[*],
WALDEMAR STEC[**]

INITIAL ANALYSIS OF THE POSSIBILITY TO SUBSTITUTE A GIVEN TRAM SUBSTATION WITH SEVERAL ONES SMALLER IN SIZE

WSTĘPNA ANALIZA MOŻLIWOŚCI ZASTĄPIENIA OBIEKTU WYBRANEJ PODSTACJI TRAMWAJOWEJ KILKOMA O MNIEJSZYCH GABARYTACH

Abstract

The article addresses – based on an existing section of a tram line – the evaluation of the capability to substitute an existing train substation (as a civil structure) with several smaller ones. Taking into consideration the real estate prices and the shortage of available plots in the centers of larger cities, the localization of a substation building poses a significant location and budget challenge, when it comes to new tram lines. Additionally, such objects (substations) often spark concern and protests among the tenants of the nearby houses, as they are considered to be the source of a dangerous electromagnetic radiation and, sometimes, noise. The possibility to significantly reduce the size of those objects would mitigate the aforementioned challenges – both environmental and budget-related.

Keywords: tramway system substations, rectifier sets

Streszczenie

W artykule dokonano, na przykładzie rzeczywistego odcinka linii tramwajowej, oceny możliwości zastąpienia istniejącej podstacji trakcyjnej (jako obiektu budowlanego) kilkoma mniejszymi podstacjami. Biorąc pod uwagę ceny gruntów i brak wolnych działek w centrach dużych miast, umiejscowienie budynku podstacji stanowi istotną trudność lokalizacyjną i kosztową w przypadku nowych linii tramwajowych. Dodatkowo obiekty te (podstacje) często budzą niepokój i protesty wśród mieszkańców okolicznych kamienic, gdyż traktowane są jako źródło niebezpiecznego promieniowania elektromagnetycznego, a niekiedy hałasu. Możliwość znacznego zmniejszenia tych obiektów ograniczyłaby wspomniane wyżej trudności zarówno kosztowe, jak i środowiskowe.

Słowa kluczowe: tramwajowe podstacje trakcyjne, zespoły prostownikowe

[*] Ph.D. Ireneusz Chrabąszcz, Eng. Ph.D. Eng. Janusz Prusak, M.Sc. Eng. Marek Dudzik, Institute of Industrial Electrical Engineering and Technical Information Technologies, Faculty of Electrical and Computer Engineering, Cracow University of Technology.

[**] MA, Eng. Waldemar Stec, a graduate of Faculty of Electrical and Computer Engineering, Cracow University of Technology, specializing in Electrical Engineering in Transport.

1. Introduction

Electric rail transportation (trams), for over a century, has been an efficient mean of passenger transport in both bigger and smaller metropolitan areas in Poland. Currently Poland [1] has 14 tram networks that are being used by 16 entrepreneurs (in Łódź there are three providers present), trams operate in 11 voivodeships. On the streets of Kraków, electric trams appeared on March 16th 1901.

From a technical point of view, the main advantage of trams [2] is their low demand for energy, as compared to other mechanical means of transport (especially passenger motor cars). Ecological factors present themselves in an especially favorable light. Trams in their place of operation do not pollute the atmosphere with any exhaust fumes (e.g. CO_2). Additionally, which isn't without significance, this mean of transport utilizes national energy resources (the operation of power plants is based on lignite and bituminous coal) and for that reason the operational costs are less susceptible to the fluctuations of oil prices on global markets. What's specific about this mean of transport is that trams (as well as other vehicles of electric traction) require a constant supply of energy provided from a specialized power system. This is caused by the fact, that they are non-autonomous as vehicles, as they don't posses their own energy source.

2. Power supply of electric railway transportation

Traction substations constitute the most basic element of the tramway system power supply. These are road structures equipped with conversion devices, which adapt the voltage parameters of the national power system to the requirements of the railway rolling stock.

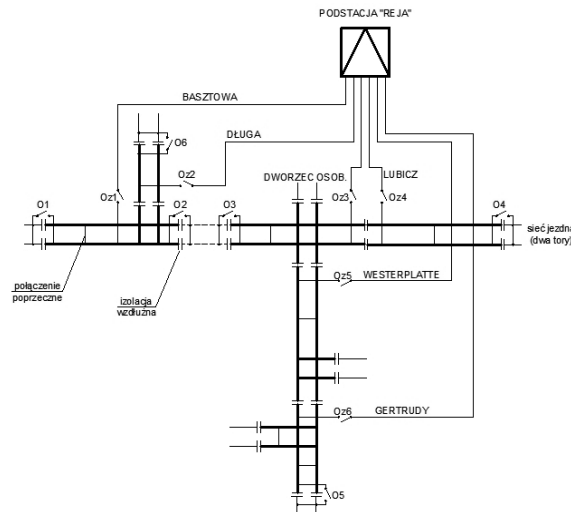

Fig. 1. Schematics of connection between tramway system substations direct current system and the traction network based on an existing „Reja" substation (Oz1, …, Oz6 – isolating switches for power supply, O1, …, O6 – section isolating switches)

Traction substations are powered from a power system, through overhead and cable transmission lines of voltages ranging from 6 to 110 kV. Tramway system substations are most commonly powered by cables of a voltage between 6 and 15 kV [5]

In tramway systems a one-directional power supply system is most commonly used [3–5]. This means that the substation power supply is divided into a sequence of sections, where each one is powered by a separate cable (power supply) from the traction substation.

Figure 1 presents an existing area of power supply of a tramway system „Reja” substation in the center of Kraków [6].

The dimensions of a traction substation building depend, among others, on the power of conversion devices installed in them. For a presented „Reja” substation, it is the power of over 3 MW. The decrease of the installed power should translate into the decrease of the substation size.

Figure 2 presents the proposed way of providing power to the traction network from substations, that are substantially lower in capacity. It is assumed that every power supply (power supply cable) will be connected with a separate mini-substation.
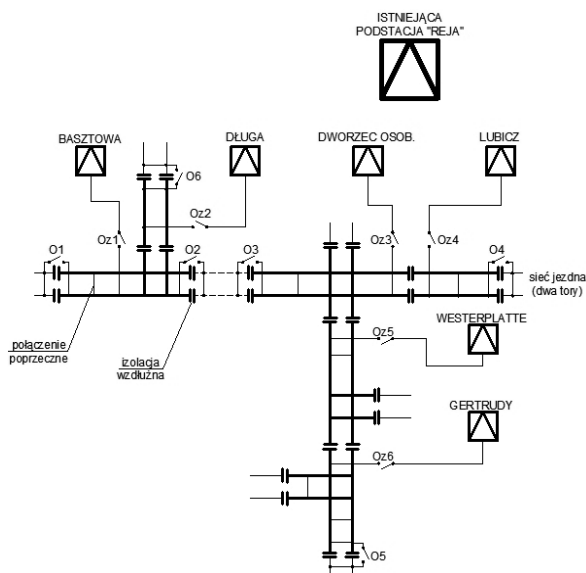
Fig. 2. Connection schematics of a hypothetical tramway system direct current mini-substations with the traction network based on an example of the existing „Reja” substation's power supply area (Oz1, …, Oz6 – isolating switches for power supply, O1, …, O6 – section isolating switches)

3. Results of Calculations

The selection of rectifier sets for mini substations was based on traction electricity runs in the power supply cables (power supplies), that were obtained through simulation, using a method of so-called theoretical passage [7].

Figure 3 presents the current of power supply load – Basztowa, and Fig. 4 the current of power supply load – Długa.

Fig. 3. Basztowa power supply: current of load

Fig. 4. Długa power supply: current of load

In the above figures (Figs. 3 and 4), significant differences between the loads of presented power supplies are conspicuous. This remark pertains to remaining power supplies within reasonable supply area. This variation is a result of a frequency of tram communication, their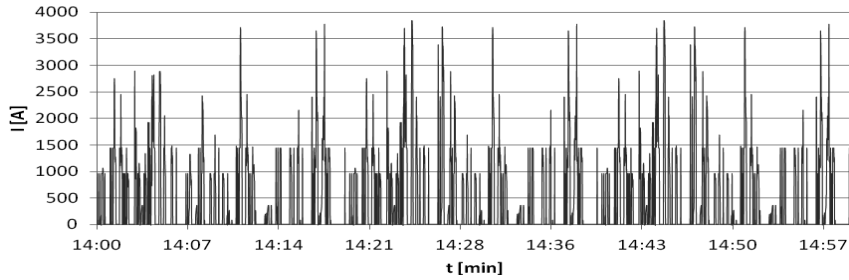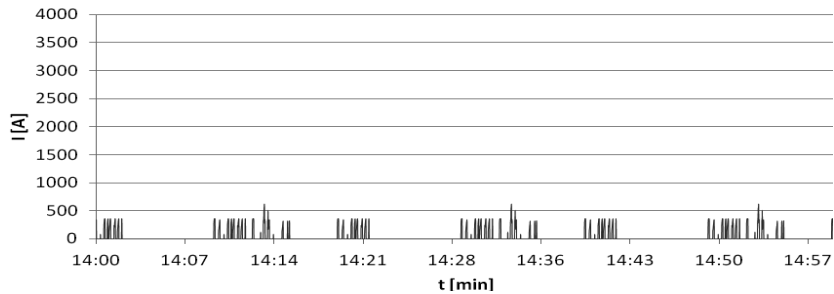 traction characteristics, line profiles and distances between stops. On hypothetical mini substations rectifier sets (explanation: „transformer with diode rectifiers) in the fifth class of overload capacity could be used. Such groups are used at modernized tram substations. Rated current of such group on the side of direct current – 660 V equals 1200 A with the V class of overload capacity [8, 9]. The amounts of overload in this class equal:

100% – permanent load (1200 A),

150% – 2-hour load (1800 A),

200% – 1-minute load (2400 A).

The selection of the amount of rectifier sets is based on the comparison of their permanent current-carrying capacity, with the permanent load of the substation and the temporary current-carrying capacity, that stems from the class of the rectifier sets with the maximum instantaneous current of the substation [5]. From the calculated amounts of rectifier sets (under different loads), the highest is picked and rounded up to an integer. The result is the amount of necessary rectifier sets – required by a given mini substation.

Table 1 presents the results of calculations of rectifier sets amount on hypothetical, reduced in size tram substations [7].

Determining the amount of rectifier sets on hypothetical substations [5]

Substation	I_{max} [A]	$I_{1m\text{-prost}}$ [A]	$I_{c\text{-podst}}$ [A]	$I_{c\text{-prost}}$ [A]	n
Lubicz	1922	2400	107	1200	1
Basztowa	3840	2400	353	1200	2
Dworzec Osob.	2880	2400	261	1200	2
Westerplatte	2880	2400	252	1200	2
Gertrudy	1825	2400	132	1200	1
Długa	617	2400	27	1200	1

Where:

$I_{c\text{-podst}}$ — average substation constant current,
$I_{c\text{-prost}}$ — rectifier set constant current,
I_{max} — maximum substation instantaneous current,
$I_{1m\text{-prost}}$ — 1-minute overload current of rectifier set.

4. Closing Remarks

As it can be seen (Table 1), for the traffic situation being analyzed, when supplying power from the hypothetical mini substations, a total of nine rectifier sets should be used in all those substations, which means over twice as many as they are currently used in a real substation (4 units).

Providing power from mini substations to an area of such load diversity as the "Reja" substation is currently not viable using devices available on the market. Because of the capacity, which should be installed, the degree of size reduction of the substation objects will be inadequate to the expectations.

Reducing the (building) size of tramway system substations is a necessity, due to environmental and economic factors (lack of space and real estate prices in cities). Thanks to that, as building structures, they will be less conspicuous and will not spark concern among the nearby tenants, as it is currently the case.

In order to achieve that, the analysis for loads of tramway system power supplies should be carried out and conclusions regarding changes in project methodology should be drawn on the basis of their results. Additionally, substations of the new type will require new technical and design solutions.

R e f e r e n c e s

[1] Wojcieszak J., *Komunikacja tramwajowa w Polsce*, TTS Technika Transportu Szynowego, nr 9/2003, 31-50.

[2] Verkehr auf Schienen: *Herausforgerungen an die Elektrotechnik*, Siemens – Aktiengesellschaft–Berlin, Muenchen 1979.

[3] Mierzejewski L., Szeląg A., Gałuszewsk M., *System zasilania trakcji elektrycznej prądu stałego*, Wydawnictwa Politechniki Warszawskiej, Warszawa 1989.

[4] Chrabąszcz I., Prusak J., Drapik S., *Trakcja elektryczna prądu stałego. Układy zasilania*, podręcznik INPE dla elektryków, zeszyt nr 27, Bełchatów 2009.

[5] Kałuża E., Bartodziej G., Ginalski Z., *Układy zasilania i podstacje trakcyjne*, Politechnika Śląska, Skrypty uczelniane nr 1220, Gliwice 1985.

[6] *Dokumentacja obszaru zasilania prostownikowej podstacji trakcyjnej, „Reja"*, ZIKiT, Kraków 2007.

[7] Stec W., *Ocena wartości prądów obciążenia kabli zasilaczy i kabli powrotnych tramwajowych podstacji trakcyjnych w aspekcie miniaturyzacji tych podstacji*, praca magisterska, Politechnika Krakowska, 2011.

[8] Rysunek ofertowy prostownika PD-12/08k firmy Woltan.

[9] Zespół prostownikowy 12-pulsowy. Prospekt firmy Enika.

MAGDALENA CHUDY*

THE INFLUENCE OF ARCHITECTURE ON ENVIRONMENT – REGENERATIVE DESIGN

WPŁYW ARCHITEKTURY NA ŚRODOWISKO – PROJEKTOWANIE REGENERACYJNE

Abstract

Facing the climate change and scarcity of natural resources, it is essential to treat architecture and the whole urbanized environment as a part of one complex system creating nature. A building takes construction materials from nature and has an influence on water and soil conditions, biodiversity, air pollution, microclimate. Consequently, an existing building becomes a part of ecosystem having both beneficial and/or negative impact on nature. In order to construct an architectural object in compliance with current requirements, it is necessary to demonstrate a holistic knowledge of environmental conditions and foresee how they will be affected by a performing building.

Keywords: regenerative design, ecosystems, urban planning, architecture

Streszczenie

W obliczu zmian klimatycznych oraz kurczenia się zasobów surowców naturalnych konieczne jest pojmowanie architektury i całego środowiska zurbanizowanego jako części jednego złożonego systemu tworzącego środowisko przyrodnicze. Budynek czerpie ze środowiska naturalnego surowce potrzebne do konstrukcji oraz wpływa na warunki wodne, glebowe, bioróżnorodność, zanieczyszczenie powietrza, mikroklimat. W konsekwencji powstały budynek staje się elementem ekosystemu, który może działać na jego korzyść lub niekorzyść. Aby obiekt architektoniczny odpowiadał wymaganiom obecnie stawianym, należy posiąść holistyczną wiedzę na temat uwarunkowań przyrodniczych oraz przewidzieć, jak wpłynie na nie działający budynek.

Słowa kluczowe: projektowanie regeneracyjne, ekosystemy, urbanistyka, architektura

* M.Sc. Arch. Magdalena Chudy (Ph.D. Student), Faculty of Architecture, Cracow University of Technology.

1. Introduction

In the 1980s, in the face of climate change and the shrinkage of non-renewable natural resources, the idea of sustainable development emerged. According to this theory, natural resources should be used in such a way as to enable the existence and development of future generations. Within sustainable development, there are two approaches: technological and biological. The technological approach became a ground for the development of "Green buildings" and so-called eco-efficient design which are mainly based on the development of technology and engineering. The concept of *regenerative design*, meanwhile, is derived from the biological approach. Regenerative design is based on ecology and it uses in its theory the rules governing living systems.[1] The principles of sustainable design are now focusing on causing the "lesser harm"; that is reducing the usage of natural resources, energy consumption and, as a consequence, CO_2 emissions, whereas regenerative design goes a step further and concentrates on creating, combining and improving natural and artificial systems [2].

2. Case studies

2.1. Designer: Terrapin Bright Green, LLC. Project: 111 Eight Avenue, NY, USA

Eight Avenue is the best known project of Terrapin Bright Green, LLC using *Deep Ecological History.* The name of the project is the address of 87 year old estate situated in the western part of Manhattan, which was subjected to a regeneration. The problem of the building was an excess water usage in comparison to other buildings of the same size. In addition, in a building's basement sump pumps constantly pumped clear cool water. To find a solution to this problem, the designers used a map elaborated by Mannahatta Project. The map depicts the reconstruction of Manhattan's ecosystems just before the first contact with Europeans (1609). The historic map was created on the basis of old maps, soil and geology information to reflect the ecosystems in Manhattan during Native American domination. The map's analysis let the designers to estimate solar energy, water, coal resources and biodiversity on the plot of 111 Eight Avenue around year 1609. The historical data became guidelines for the regeneration project. Proposed solutions assumed a usage of storm water and the water pumped from the basement for the cooling tower. In consequence, the potable water and energy consumption should decrease radically. Deep Ecological History was used to investigate relations between natural ecosystems and the building, in order to improve quality of environment, architecture and economy [3].

2.2. Designer: Perkins+Will Canada. Project: Livind with Lakes Centre, Uniwersytet Laurentian, Sadbury, Ontario, Canada.

Canadian architectural office Perkins+Will develops its own regenerative design research program. The Living with the Lakes Centre project located in the surrounding of Lake Ramsey: the drinking water reservoir, and next to an industrial area which is responsible for air contamination; was designed in collaboration with the university's researchers and scientists. Thanks to the materials used, the building came into interaction with the surrounding and affected it in a positive way. Limestone, which is the main material on the façade and in the landscape neutralizes the acids contained in storm water [4].

2.3. Designer: Perkins+Will Canada. Project: Van Dussen Botanical Garden Centre, Vancouver, Canada

The project used the knowledge of the influence of building materials on human health and the environment. The list of dangerous substances called 'Precautionary List' was first created by Perkins+Will researchers and then developed by scientists at the Yale University. Precautionary was the main strategy of the project. Materials used to construct the building were as little processed as possible, to be sure that they didn't contain any dangerous substances and to enable its recycling [4].

2.4. Consultants: Regenesis Group. Project: Loreto Bay Villages, Agua Viva, Mexico

The aim of the project was to regenerate former estuary which degenerated into dry lands over the last 300 years. The project involved the private investors, the government of Mexico, designers, local inhabitants and Regenesis Group as the regenerative solutions suppliers. The plan of land development consisted of several phases. The task for the Regenesis Group was to help the designers understand 'genius loci' and the *Story of the Place* which meant to be regenerated. Restored mangrove, oceanic and river ecosystems should coexist and exchange the energy. Designed river channels should top up the web of public spaces and create friendly and healthy environment for people [5].

2.5. Designer: 606 studio. Project: Regeneration of the south – east part of Los Angeles, California, USA

The designer's proposal for the south-east part of the city, which is struggling with social issues such as unemployment, limited access to public services and transportation, as well as, ecological problems (alarming air contamination and heat island caused by excess usage of cars) was to start processes aiming at the regeneration of the neighborhood. The most important actions included using empty sites for mini-parks, recreation spaces for local community and mixed-use zones (including such functions as: commercial, office, public services, industrial and residential). Part of environmental issues were addressed along with transportation difficulties. Stops of the newly-designed cable railway were placed at the strategic city spots. At the same time, pedestrian and bicycle paths were created to minimize air contamination. Additionally, an urban forestry program was started (it is volunteer-based planting of trees along main roads).The problem of the heat island was solved by introducing refinery and using filtered water for watering new vegetation and supplying ponds in parks. Greenery and water in public spaces are supposed to improve microclimate through increased humidity and reduced temperature [6].

3. Conclusions

The concept of regenerative design, which goes beyond the scope of sustainable design, seems to be a bold and reasonable alternative to the mindless urban development. Its basis – the idea of harmoniously combining not only the landscape, but also the environmental aspects of the site, with the tasks faced by an architect or a planner, can be a remedy for the expansion of cities onto new still undeveloped areas. The question arises whether a person

is actually able to create a system fully replacing the natural processes. Perhaps regenerative design best meets its role in repairing degenerated, already urbanized areas, as was the case with the previously discussed projects: 111 Eight Avenue and regeneration of the south-east part of Los Angeles. In both projects, the authors focused on initiating recovery processes of degraded buildings or areas, in order to gain the objects for the benefit of the environment. The proof of the fact that, in certain cases, the introduction of people together with buildings to the degenerated areas can also be beneficial for the environment is a settlement Loreto Bay Villages, Mexico. Reintroduction of plants, animals and people to the dry basin shows that regenerative design, which is intended to protect ecosystems, also refers to humans as a part of the natural system. Health and human living conditions are prioritized, along with other living organisms.

Paradoxically, it can be stated that the challenge for regenerative design is to look beyond the ecology and functioning of ecosystems, as once dared to look beyond the land where the building is designed. Consideration of all infrastructure networks (research centers, factories, vehicles and all of the positive and negative impacts related with their functioning), that allow for the creation of buildings, and attempt to balance them could complete the concept of regenerative design.

R e f e r e n c e s

[1] Mang P., Reed W., *Designing from Place: Applying the Ecological Worldview and Regenerative Paradigm*, BRI Draft, 2011, 2, http://www.yestermorrow.org/assets/ Uploads/PDFs/Designing-from-Place-Applying-the-Regenerative Paradigm.pdf, access: 08.09.2013.
[2] Lake David, cyt. za Nicolette M., *Beyond LEED: Regenerative Design*, In Landscape Journal nr 31:1-2, University of Wisconsin Press, 229, http://www.biblos.pk.edu.pl/, access: 01.07.2013.
[3] Browning B., Terrapin Bright Green, LLC, *Letting Deep Ecological History Determine Building Performance Metrics*, Beyond LEED Regenerative Design Symposium, UTSOA, 2012, http://soa.utexas.edu/beyondleed/index.html, access: 15.07.2013.
[4] Busby P., Richter M., Driedger M., *Towards a new relationship with nature. Research and regenerative design in architecture*, [In] AD, John Wiley & Sons Ltd., 2012, 95-96, http://www.biblos.pk.edu.pl, access: 05.07.2013.
[5] http://www.regenesisgroup.com, access: 25.08.2013
[6] Lyle J.T., *Regenerative Design for Sustainable Development*, John Wiley & Sons Inc., New York 1994, 127-129.

RAFAŁ DĄBROWA, KAZIMIERZ WOJTAS*

CONTROLLABILITY OF INDOOR AIR QUALITY PARAMETERS IN A TEST CHAMBER OF ZOOLOGICAL INSTITUTE

OCENA MOŻLIWOŚCI REGULACJI PARAMETRÓW KLIMATU WEWNĘTRZNEGO W KOMORZE BADAWCZEJ INSTYTUTU ZOOLOGII

Abstract

Breeding laboratory chambers require a wide range of indoor air parameters, which implies the need to use special equipment for air treatment and very accurate and fast automatic adjustment. The article presents the results of an experimental study conducted in the existing breeding chamber. The work is based on numerous observations as well as on-site measurement series of indoor climate parameters. The conclusions seem to be important for future design projects.

Keywords: indoor air quality, climatic chamber, close control air conditioning, laminar air flow, comfort

Streszczenie

Komory hodowlane są przykładem pomieszczeń o bardzo wysokich wymaganiach w zakresie parametrów powietrza wewnętrznego, co z kolei implikuje konieczność zastosowania specjalnych urządzeń w wykonaniu higienicznym oraz bardzo dokładnej i szybkiej regulacji parametrów. W artykule przedstawiono wyniki badań parametrów powietrza w ujęciu dynamicznym w istniejącym obiekcie Instytutu Zoologii UJ. Wnioski z przeprowadzonych analiz mają duże znaczenie dla projektowania systemów klimatyzacji tego typu obiektów.

Słowa kluczowe: jakość powietrza wewnętrznego, komfort wewnętrzny, precyzyjna regulacja parametrów powietrza, laminarny przepływ powietrza

* M.Sc. Eng. Rafał Dąbrowa, Ph.D. Eng. Kazimierz Wojtas, Institute of Thermal Engineering and Air Protection, Faculty of Environmental of Engineering, Cracow University of Technology.

Designations

Φ_N –   heat exchanger nominal capacity [kW]
Φ –   transient heating capacity of the air heater [kW]
V_a –   air flow rate [m³/h]
t_{out} –   air temperature at the outlet of the heat exchanger, [°C]
t_{in} –   air temperature at the inlet to the heat exchanger [°C]
t_{sN} –   supply water temperature in nominal parameters [°C]
t_s –   water temperature at the inlet of air heater [°C]
t_r –   water temperature at the outlet of air heater [°C]
m_{wN} –   nominal water mass flow rate [kg/s]
$c_{p,a}$ –   specific heat of air at constant pressure [kJ/(kg*K)]
M –   mixing ratio of the water in a 3-way mixing valve [–]
a –   exponential parameter of the heat exchanger [–]
LPHW   –   Low Pressure Hot Water Heater coil

1. Introduction

Laboratory breeding chambers are the examples of rooms, where very high requirements of the internal climate quality at a wide range of air parameters, go hand-in-hand with the need for accurate and fast automatic adjustment of the indoor comfort level parameters. Unfortunately, due to some unfavorable characteristics of certain air treatment and control system components, achieving these two objectives simultaneously is very difficult. The article contains an analysis of thermodynamic and technical impact of various characteristics of the selected items of the existing air conditioning installation at the breeding chamber laboratory of the Institute of Zoology of Jagiellonian University in Kraków.

2. Analysis of the indoor air parameters required for breeding chambers

Breeding chamber tested for the research is a tight, hermetic room (without windows), equipped with the necessary technology to carry out the experiments, which in this case involve breeding of rats. The following table lists the basic requirements concerning the indoor climate, set out in the regulation of the Minister of Agriculture [3], as well as in the analyzed literature [5]. Those two were compared with the requirements laid down by the Institute of Zoology, on which base the project was realized. Several important pieces of information come out from the table below. The first one is the high ventilation air exchange rates, which are obligatory due to the secretion of breeding animals and unpleasant smell of rats. The second one is that, in the documents [3, 5] there is no data on either accuracy of temperature control, or air velocities in the breeding area of the room. As it can be seen in the table 1, the Institute has set the highest and widest requirements of those three, which – in the existing conditions – became very difficult to acquire by the A/C system installed and finally made the reason for the job reported.

The requirements of the internal climate parameters for breeding chambers

Parameter	Unit	Regulation [3]	Article [5]	The requirements of the Institute of Zoology
Temperature	[°C]	20–24	20–22	10–37 (±1 K)
Relative humidity	[%]	55 (±10)	55 (±5)	50–80% (±5%)
The minimum room exchange rates	[1/h]	15–20	10–20	15
Acoustic pressure level	[dB]	35	–	–
Air velocity	[m/s]	–	–	–

3. Dimensioning of air conditioning equipment for the breeding chamber

General characteristics of the test chamber are: partitions made of stainless steel, properly insulated brick exterior wall, hermetic, airtight, non-absorbable walls and surfaces, lack of windows (see Fig. 1).
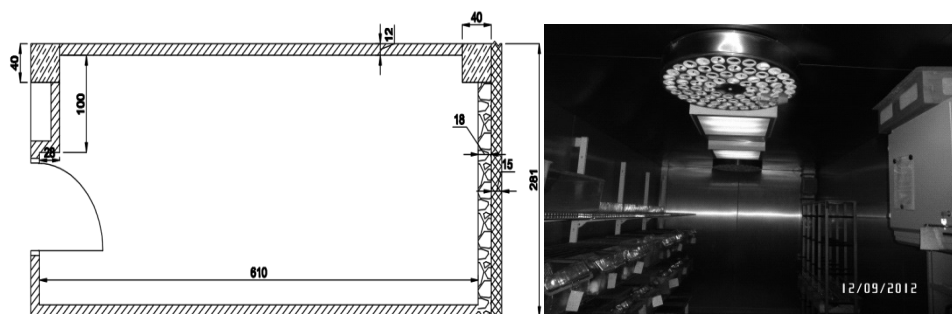

Fig. 1. Projection of the test chamber. On the right – photo of its interior

During the first step of the work reported, detailed thermal calculations of air treatment processes were provided, in order to make an assessment of existing A/C system components sizes and characteristics. As the result of those, the final scheme of the installation was set, like the one shown in the Fig. 2.

When sizing the components of Air Handling Unit (AHU), it was crucial to remember, that the indoor air parameters have to be adjusted and stabilized precisely and continuously, all year around – 8760 hours in a year – regardless the random changes of the external air parameters, as well as the impacts of the safety control devices and procedures installed for the AHU's equipment protection (i.e. protection of cross flow recuperator and LPHW coil

against freezing, startup of each of the heat exchangers, set point change, abrupt change in air flow, etc.) Due to the multitude of problems, which disrupt the regulation process, this paper is limited to the analysis of the impact of two issues, which – according to the authors – have a dominant influence on the quality of indoor comfort in the chamber, ie:

a) distribution of the conditioned air in the room's space,

b) impact of control valve's actuator and LPHW heat exchanger's operating characteristics.
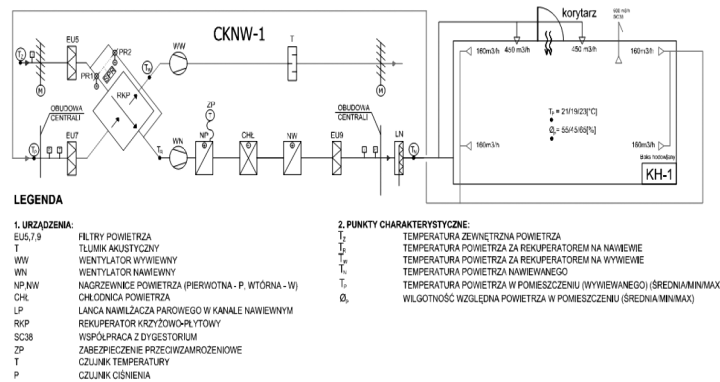

Fig. 2. Technological scheme of the AC system operating in the tested breeding chamber

4. Comparison of the room's air distribution systems

To achieve the most convenient distribution of air parameters in the tested room, two basic air discharge solutions were compared: mixing (induction) of air discharge devices and ceiling laminar displacement air flow. Laminar air discharge devices require a large area of ceiling to minimize the air discharge velocity. One of system's characteristic features is a homogeneous unidirectional airflow, achieved at low air speed. It offers very high ventilation efficiency and a very high level of thermal comfort (i.e. low value of the Draft Ratio – DR). Using the advantages of the laminar discharge and aiming for high comfort level of the controlled space in the test chamber, we were provided with detailed calculations for sizing the installation, when applying this kind of distribution system. As the result, two laminar diffusers were selected, for which the air velocity along the height of the room was determined. Subsequently, the designed installation framework was characterized by the airflow supply, V_N = 2700 m³/h and air flow exhaust, V_W = 2830 m³/h. This system was finally chosen for comparison with the existing mixing (induction) air supply system (see Fig. 1), consisting of 2 spin slot diffusers with a capacity 305 m³/h each and 4 exhaust grilles with a capacity 160 m³/h each. For the proposed laminar air flow system, based on the characteristics of software selected by the manufacturer, the values of air velocity in the test zone of the chamber (height between: 0.5 and 2.0 m) were determined (between 0.10 to 0.15 m/s). Assuming, that the Turbulence Factor (Tu) for laminar airflow is not grater then 5%, DR comfort index values were calculated for sample air temperature (t_a = 20°C). The final result

of these calculations proved, that the DR index value in such case is between 5.0% and 10.0% PD (Percentage of Dissatisfied) and since that, the controlled space of the chamber performs at the highest comfort level (class I according to [5]). On the other hand, the existing air supply system is characterized by high values of the turbulence factor (Tu up to 40%) and uneven airflow speed, which decreases, as the air is moving away from the diffuser. Using manufacturer's simulation program [7] it was determined that the air velocity in the room's space can vary from 0.32 m/s ($h = 2.0$ m) and 0.18 m/s ($h = 0.5$ m). For these air velocity values and the air temperature applied ($t_a = 20°C$), the range of DR index is respectively between the values: 50% and 23.0% PD. As it could be forecasted, these values are much higher than those for laminar discharge system and they are outside of the IIIrd category of comfort (in accordance with [5]).

4.1. *On-site* tests for indoor comfort parameters in the breeding chamber validation

T a b l e 2

Summary of the measurement points

Mesurement point	Air temperature	Air velocity	Draft factor
	t_a	w_a	*DR*
[–]	[°C]	[m/s]	[% PD]
1	20	1,5	446,7
2	20	0,11	11,7
3	20	1,23	331,1
4	20	0,3	44,9
5	20	0,2	26,3
6	20	0,32	49,0

Since the comfort index values for the applied distribution system are on the edge of "satisfaction range of the end-user", it was compulsory to validate the air velocity in particular points of the chamber space. During the experiments, the air velocity – as well as the air temperature – were measured (with laboratory anemometer and Cu-Const thermocouples). The values were averaged for an over 1-hour period of time and recorded simultaneously at 6 individual test points. Table 2 shows the example of air velocity measurement, which proved that the "a priori" calculations made with the software were valid (besides points 1 and 3 which are situated outside the test zone of the chamber – close to the air diffuser and the wall). As the result, it can be finally stated, that the air distribution system chosen for the analysed project is not the main cause of problems with indoor climate parameters control.

5. Control loop characteristics of the LPHW coil

The main problem that occurs in the close control air conditioning systems, is maintaining the comfort parameters of indoor air in a specific, narrow range of deviation from the set point, as well as the high stability of the signal waveform in real time, regardless of the interferences caused by: user (exploitation and operating procedure), dynamic changes of the outside air parameters, as well as the technical and operational characteristics of the individual items involved within the temperature control loop (as shown in the Fig 3). After the preliminary examinations, it was concluded, that the air temperature control instability was primarily caused by the properties of the technical equipment involved in the control process of LPHW coil – especially valves and actuators.
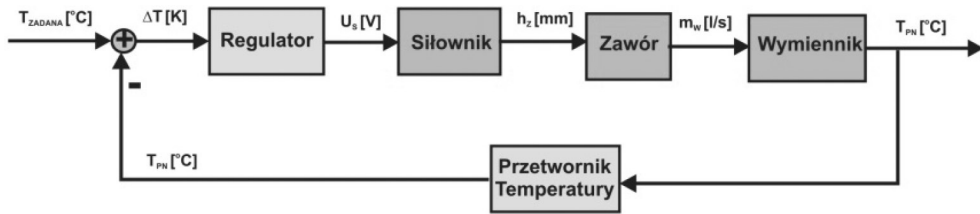

Fig. 3. Block diagram of the heater's temperature control loop

5.1. Valve and actuator operating characteristics

The control loop of the LPHW heater operating in the experimental installation consisted of a 3-way mixing control valve, featuring: equal percentage characteristic (Fig. 4), the flow rate factor $k_{vs} = 1.60$ m³/h and the minimum flow rate factor $k_{vr} = 0.032$ m³/h. The latter factor is also referred to as a "range of controllability" of the valve, as it gives out the minimum value of water flow, upon which the valve maintains the flow control characteristic declared by the manufacturer (below this value it is "unknown zone of control"). Based on those two, the valve's range is defined by the ratio $R = k_{vs}/k_{vr}$. The tested valve was characterized by the value of $R = 50$. The control characteristic of the applied actuator is of a step-wise type (Fig. 5).
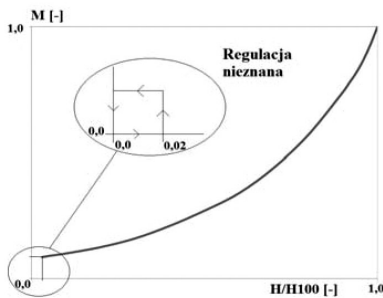

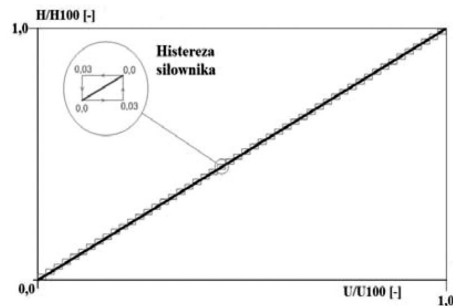Fig. 4. Equal percentage valve characteristic

Fig. 5. Control characteristics of a step-wise actuator

5.2. Low Pressure Hot Water coil characteristic

The goal of mathematical modeling of the analyzed heat exchanger was to acquire a capacity control characteristic, describing the change of the air temperature, as a function of mixing degree of 3-way valve placed at the inlet of the heat exchanger (see the model in the Fig. 6). Assuming that the mass flow rate of the water flowing through the LPHW coil is constant, the mixing ratio M of the control valve is the key factor, the water inlet temperature depends on. The M coefficient is defined as the ratio of the water mass flow rate, flowing through the valve from the heat generation system (m_w with t_{sN} temperature), to the nominal heat exchanger water flow (m_{wN} = idem). Scheme of the hydraulic system model is shown in Fig. 6. The final control curve characteristic was determined by applying the Trefny's model [1].

Fig. 6. Model of the tested heat exchanger
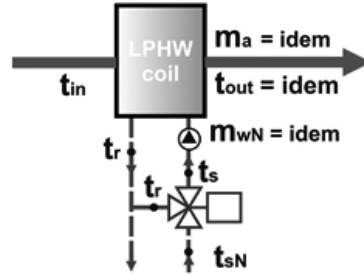
The main assumptions used in the calculations:
- V_a = 610 m³/h (idem),
- t_{out} = 37°C (idem),
- t_{in} = var $\in$ <–20÷37°C>,
- t_{sN} = 70°C (idem),
- Φ_N = 11.59 kW,
- m_{wN} = 760 kg/h = 0.21 kg/s (idem),
- $c_{p,a}$ = 1.005 kJ/kgK.

Control characteristic of the heater was determined by the following formulas:

$$\Delta t_a = t_{out} - t_{in} = \frac{\Phi(M)}{m_a \cdot c_{p,a}} \tag{1}$$

$$\Phi(M) = \Phi_N \cdot \frac{1}{1 + a \cdot \left(\dfrac{1-M}{M}\right)} \tag{2}$$

where:

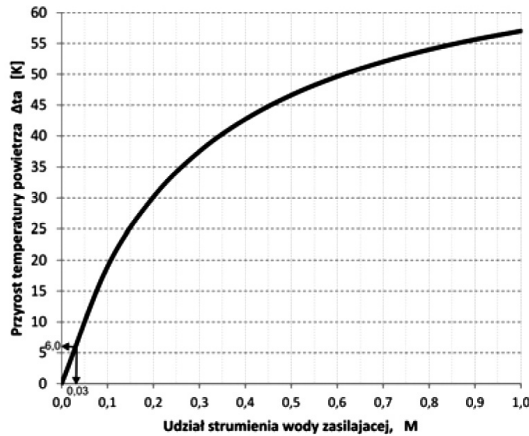$$a = \frac{t_{sN} - t_{rN}}{t_{sN} - t_{inN}} \tag{3}$$

Fig. 7. Control characteristic of the tested LPHW coil

The simulations were performed for a variable temperature of the heater's air inlet. The air temperature rise in the heater is presented as a function of relative water flow (M) supplied through the control valve (see Fig. 7).

5.3. The maximum error of air temperature control loop

When analysing the temperature control loop (Fig. 3), it can be concluded, that – as the result of maximum "dead zone" value of water flow performed at the inlet of the heat exchanger – the maximum air temperature deviation at the outlet of the heater can be finally derived from the control characteristics of the heat exchanger (Fig. 7). Because the control signal flowing through both devices of the temperature control loop is in a serial connection manner (Fig. 3), the maximum value of the output signal's "dead zone" is the result of the maximum "errors" of both devices – the valve and the actuator. As the tested valve hysteresis was equal $\Delta M = 2\%$ (at the starting point, as a result of the range $R = 50$ – see Fig. 4), while the hysteresis of the actuator declared by the manufacturer's technical information equals $\Delta U = 3\%$ (see Fig. 5). This means, that the maximum possible deviation ("static displacement") of the output signal of the complex object, made of actuator and control valve (which is also an input signal to the heat exchanger) may reach, in the worst case, the value of 3%. Consequently – based on the determined heat exchanger characteristic – the maximum outlet air temperature deviations can reach 6.0 K (Fig. 7).

6. Conclusions

Based on the analyses and on-site experiments conducted in a real, operational breeding chamber, it can be concluded, that obtaining high comfort indexes in such "unusual space", can be acquired by maintaining accuracy and stability of the air parameters supplied by the Air Handling Unit. High quality control devices, such as a valve or an actuator, can help achieving this goal. Similar value of importance should be also paid to other issues, such as:

- indoor air distribution structure and components applied,
- range of indoor parameters required (should be as narrow as possible),
- stability of flow control in the hydraulic systems supplying the heat exchangers,
- finally, the most attention should be paid to the control structure and strategy at the initial range of capacity of each heat exchanger applied.

R e f e r e n c e s

[1] Junkers B., *Regulacja urządzeń wentylacyjnych i klimatyzacyjnych*, Arkady, Warszawa 1980.
[2] Zawada B., *Układy sterowania w systemach wentylacji i klimatyzacji*, Oficyna PW, Warszawa 2006.
[3] Rozporządzenie Ministra Rolnictwa i Rozwoju Wsi z dnia 10 marca 2006 r. w sprawie szczegółowych warunków utrzymywania zwierząt laboratoryjnych w jednostkach doświadczalnych, jednostkach hodowlanych i u dostawców.
[4] PN EN ISO 7730: 2006 – Ergonomia Środowiska wewnętrznego. Analityczne wyznaczanie i interpretacja komfortu termicznego z wyznaczaniem wskaźników PMV i PPD oraz kryteriów lokalnego komfortu termicznego.
[5] PN-EN 15251: 2007 – Indoor environmental input parameters for design and assessment of energy performance of buildings addressing indoor air quality, thermal environment, lighting and acoustics.
[6] Dąbrowa R., *Weryfikacja projektu systemu klimatyzacji komory hodowlanej w aspekcie parametrów klimatu wewnętrznego na wybranym przykładzie laboratorium Instytutu Zoologii UJ*, praca dyplomowa magisterska, Politechnika Krakowska, Kraków 2013.
[7] Stifab Farex, ProAir 1.2.8, Selection software of the air distribution systems.

MAREK DUDZIK*, DAWID ŁĄTKA, MICHAŁ REPELEWICZ**,
EDWARD STEWARSKI***, ANNA M. STRĘK****

A PRELIMINARY FEASIBILITY STUDY OF A SHORT-TERM PROGNOSIS OF MINING TOWERS TOPS' DISPLACEMENTS WITH THE USE OF ARTIFICIAL NEURAL NETWORKS

WSTĘPNE STUDIUM WYKONALNOŚCI KRÓTKOTERMINOWEJ PROGNOZY PRZEMIESZCZEŃ SZCZYTÓW WIEŻ GÓRNICZYCH Z WYKORZYSTANIEM SZTUCZNYCH SIECI NEURONOWYCH

Abstract

Mining industry is a key sector of many national economies, thus even a small crack in a mining site echoes nationwide. This strategic sector is subjected to special safety care in every aspect, including operational safety of engineering structures. The newest technologies are employed to diagnose and monitor the working structures and buildings. In this article we propose an innovative idea of combining GPS monitoring system with artificial neural network prognosing to build a prediction tool for displacement of mining shafts in operational conditions. The paper describes a training of a neural network system whose task is to prognose the displacements of the top of a mine shaft tower in direction in a selected period of time. The data used for the training come from the GPS monitoring of displacements of the top of the S 1.2 mining shaft tower. The tower is located in the mining works LW "Bogdanka".

Keywords: artificial neural network, artificial neural network training, displacement of the top of mining shaft tower, GPS monitoring

Streszczenie

Przemysł wydobywczy jest kluczowym sektorem wielu gospodarek narodowych, w związku z tym nawet najmniejsza usterka w obrębie kopalni zawsze odbija się echem w całym kraju. Ten strategiczny sektor jest więc poddany szczególnej trosce o bezpieczeństwo, w każdym aspekcie, włączając bezpieczeństwo eksploatacji konstrukcji inżynierskich. Najnowsze technologie są używane do badania i monitorowania pracujących obiektów i budowli. W tym artykule proponujemy nowatorski pomysł połączenia monitoringu GPS z prognozowaniem za pomocą sztucznych sieci neuronowych w celu zbudowania narzędzia prognozowania przemieszczenia szybów kopalni w warunkach eksploatacyjnych. Artykuł prezentuje trening sztucznej sieci neuronowej, której zadaniem jest prognozowanie przemieszczenia szczytu wieży szybu kopalnianego dla jednego kierunku w wybranym okresie czasu. Analizowane w artykule wyniki pomiarów pochodzą z monitoringu przemieszczeniowego szczytu wieży szybu S 1.2 w kopalni LW „Bogdanka". Uzyskane wyniki obliczeń dla wybranego fragmentu okresu letniego prezentują się obiecująco.

Słowa kluczowe: sztuczna sieć neuronowa, trening sztucznej sieci neuronowej, przemieszczenia szczytu wieży szybu kopalnianego, monitoring GPS

* M.Sc. Eng. Marek Dudzik, Institute of Industrial Electrical Engineering and Computer Technology, Faculty of Electrical and Computer Engineering, Cracow University of Technology.
** M.Sc. Eng. Dawid Łątka, M.Sc. Eng. Michał Repelewicz, Institute of Building Materials and Structures, Faculty of Civil Engineering, Cracow University of Technology.
*** Ph.D. Eng. Edward Stewarski, AGH University of Science and Technology, Faculty of Mining and Geoengineering, Department of Geomechanics, Civil Engineering and Geotechnics.
**** M.Sc. Eng. Anna Stręk, AGH University of Science and Technology, Faculty of Mechanical Engineering and Robotics, Department of Strength and Fatigue of Materials and Structures.

1. Introduction

GPS measurements – a modern satellite technology – became increasingly popular in various applications. They may be used, for example, for monitoring [1], displacements analyses and displacements prognoses of mine shafts towers. Such prognoses might prove to be important in safety systems, thanks to the possibility to inform the miners working underground about a potentially hazardous state. One of the tools used for displacement prognoses might be a novel idea of the said GPS measurements combined with neural networks. We present the concept in this article.

The paper shows a training of a neural network system which was designed to prognose the displacements of the tower top of a mining shaft. The aim of this preliminary training study was to verify whether the designed neural network could be trained based on the GPS measurement data (feasibility study). The used data came from the GPS monitoring in the mining works LW "Bogdanka" [1] and comprised measurements of the displacements of the S 1.2 mining shaft tower top. The presented results refer to the displacements in one direction in a selected period of the summer season: from 31st July 2013 03:01:00 AM to 3rd August 2013 08:00:00 AM.

However, the condition that neural displacement prognoses in the mining industry lead to safety betterment is that they have to be feasible and accurate. Implementation of algorithms which fulfill these two requirements might, apart from the improvement of life protection, also result in lowering potential costs, which could arise due to stability loss of the monitored structures.

2. Artificial neural network

The artificial neural network that was designed for the analysis and prediction of the displacements of the S 1.2 tower top is shown in Figure 1.
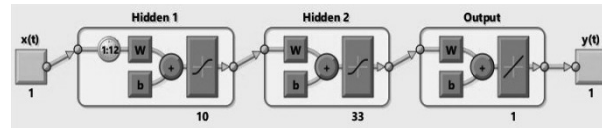

Fig. 1. The assumed artificial neural network structure

The chosen structure was a focused time-delay neural network structure with two hidden layers (Hidden 1, Hidden 2). On the other hand, it is worth noticing, that the chosen structure also corresponded to a feedforward neural network type, but for the tapped delay data line vector implemented before the input port of the first hidden layer. This vector was the basis of the input data for the neural network training. On the basis of these vector data the neural network prognosis $y(t)$ was calculated (Fig. 1).

The first hidden layer consisted of 10 neurons. At the input of this layer one input signal was assigned. At the output – 10 output ports were assigned. Before this first hidden layer a vector of 12 delays was implemented. This means that input signal in the first hidden layer was a vector data consisting of 12 elements. The elements were considered displacement delayed from 1 to 12 minute. The activation function in the hidden layer was a hyperbolic tangent sigmoid transfer function (tansig).

The second neural network hidden layer consisted of 33 neurons. This layer had 10 input ports and 33 output ports. There were no delays implemented for the second hidden layer. The activation function in the second hidden layer was a hyperbolic tangent sigmoid transfer function (tansig).

The output layer (Output) used a linear activation function. At the entrance of the output layer there were 33 input ports. At the output of this layer there was one output port implemented. The signal that was produced at this last port was the desired prognosis. There were no delays implemented for the output layer.

The presented network was constructed arbitrarily. The architecture of the chosen ANN may be studied in other variants, for example networks with another number of neurons and layers may be built and compared to the one presented here. This might be a further project development stage.

3. Input data

The recorded displacement data were imported from the GPS using the Trimble program. The data were imported in three directions (X, Y, Z). Basing on a referent comparative data sheet provided with the input data, the direction X was identified as the northing position, the direction Y as the easting position and the direction Z as the height position. The paper presents the analysis for the training in one chosen direction – the X direction, that is the northing.

In order to transform the tower top's position values to the most convenient form for calculations, those values were processed in the following way. A reference point was chosen as a mean value of all analysed data. Next, the value of the reference point coordinate was simply subtracted from the analysed coordinates X, in order to shift vectors in the direction X.

Calculations were performed using Excel and Matlab Simulink programs. The assumed sampling time was 1 minute, because the prognosis was a short-term prognosis and was supposed to foresee an instantaneous value of the displacement in the chosen X direction to be read by the GPS device one minute later.

The data chosen for the artificial neural network training comprised the instantaneous values of the displacements of the S 1.2 tower top. The displacements in the X direction (relative to the reference position) ranged from –0.0358 to 0.0392 m. Such a small order of magnitude of the data values and their changes might have reduced the efficiency possibility of the neural network training; therefore, the values were multiplied by 10^4.

4. Neural network efficiency results

Results presented in the paper were obtained for the following neural network training settings:

- sample time = 60 sec;
- performance goal = 0;
- learning rate = 0.01;
- momentum = 0.9;

- maximum validation failures = 12;
- maximum number of epochs to train = 33333;
- minimum performance gradient = 1e-10;
- epochs between displays (NaN for no displays) = 25;
- maximum time to train in seconds = infinite.

In order to train the designed artificial neural network, the one-way network (up to 3 layers) training was used according to the Leveneberg-Marquardt algorithm.

Figure 2 shows the error histogram obtained from the artificial neural network training with a teacher. On the abscissa axis there are marked absolute error values calculated as the difference between the actual value measured by the GPS device (target) and the response of the neural network $y(t)$ (output). On the ordinate axis there are marked instances. The absolute value of the maximum absolute error obtained from neural network training was $101.3 \cdot 10^{-4}$ m ≈ 0.0101 m, which means that the value was about 10 mm.
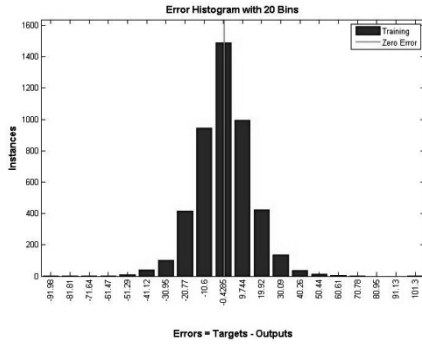

Fig. 2. The neural network training with teacher error histogram
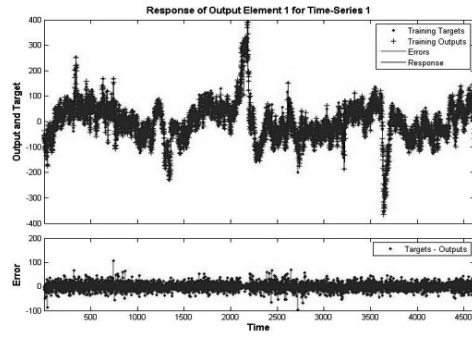

Fig. 3. The comparison of the prognosed displacement with the actual measured data

The comparison of the displacement values in the X direction prognosed by the neural network with the actual measured and recorded displacement values for the considered period is shown in Figure 3. Dot markings in Figure 4 correspond to actual measured values of the displacement. Cross markings refer to the neural network displacement prognosis values. Orange lines represent the instantaneous values of absolute errors (target minus the neural network output $y(t)$). These values are plotted for neural network input signal after changing the order of magnitude by the factor of 10^4.

Figure 4 presents the artificial neural network training performance graph. The ordinate axis corresponds to the neural network training performance function values. The mean square error (mse) was chosen as the neural network training performance function. On the abscissa axis there are neural networks training epochs marked. The best neural network training with a teacher performance was reached for the epoch 33333 and it was equal to 215.7194 of the mean square error value. This value was achieved for neural network input signal values after changing their order of magnitude by 10^4. From the epoch 1 to 33333 one can observe a downward trend. This means that the ANN for each new training epoch achieved a better performance training value. There was no such situation while training for which validation failure occurred one after another for 12 times. Therefore, in accordance to neural network training settings, the epoch 33333 was recognized as the global minimum for the training aim for the set neural network structure (Fig. 1). The mentioned epoch number was set as the maximum number of epochs to train; hence, the training process was completed for this epoch.

Figure 5 presents the regression results for the training for all data assigned to the ANN training with a teacher. Here the ordinate axis represents the neural network output $y(t)$ after

their multiplication by 10^4. On the abscissa axis there are shown values measured by the GPS device (targets) after their multiplication by 10^4. Values returned by the ANN $y(t)$ should be convergent to the abscissa axis values (values measured by the GPS). The $R = 1$ regression result means that there exists an unequivocal relation between the actual value (target; from measurement or simulation) and the neural network output value [2]. The regression for the data assigned to the training reached $R = 0.98052$. The total number of data samples assigned to the network training was 4625.
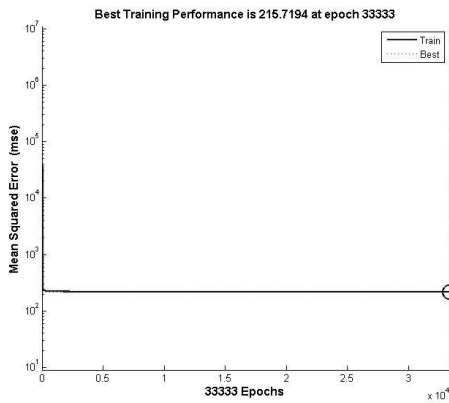

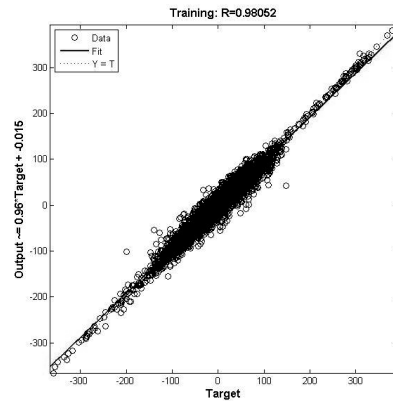Fig. 4. Artificial neural network training
performance graph

Fig. 5. The regression results for data assigned
to the ANN training with a teacher

4. Conclusions and future development of the proposed GPS+ANN method

The neural network training results obtained for the summer period are promising. However, due to different environmental conditions in each season of the year, the applicability of the described neural network system should be assessed for each season separately, as well as for transitional periods between them.

The authors used a focused time-delay neural network (FTDNN) structure type. Nevertheless, they do not preclude the use of a distributed time-delay neural network (DTDNN) structure type.

The subsequent studies of the issue may attempt to reduce the mentioned training error by increasing the maximum number of epochs to train in the artificial neural network training process. Artificial neural networks with one and two hidden layers might also be analyzed, as well as other neural sub-architectures. The research may be performed also for the values imported from the GPS device in other directions (north, east, vertical). Another path of development is to extend the neural network prognosing possibilities by adding the ability to prognose not only regular operating conditions but also catastrophe and failure states. Also, indirect variables, such as the radii vectors, which can be calculated from the imported data, might be studied. The shown prognosis is a short-term one. Naturally, there rises the problem of lengthening the prediction period to a time sufficient (for example) for workers' evacuation; this may be achieved by developing the studied ANN or alternatively proposing a different one to compare them.

Last but not least, the aim of the feasibility study was just to preliminarily state whether it is possible at all to build a network relevant for such mining shaft displacement predictions. Now, having the training phase behind, another data set should be used as material for testing, while only such a procedure can actually give more precise information as to how to develop the studied ANN to the target safety GPS+ANN system that could find actual application.

References

[1] Tajduś A., Stewarski E., *Monitoring satelitarny GPS mikroprzemieszczeń szczytów wież szybowych w kopalni LWBogdanka (Komunikat)*, Bezpieczeństwo Pracy i Ochrona Środowiska w Górnictwie, vol. 1, 2013, 26-30.

[2] Kobielski A., Drapik S., Dudzik M., Prusak J., *Wstępne studium efektywności zastosowania sieci neuronowych w badaniach obciążeń kolejowych podstacji trakcyjnych*, XIV Konferencja naukowa Jakość, Bezpieczeństwo, Ekologia w Transporcie QSET 2013, 05–07 czerwca 2013 Niepołomice, Politechnika Krakowska Wydział Mechaniczny, Instytut Pojazdów Szynowych.

[3] Mathworks: http://www.mathworks.com/help/nnet/gs/time-series-prediction.html.

[4] Kosek W., *Metody Analiz Widmowych, Filtracji i Prognozowania*, Centrum Badań Kosmicznych PAN, Bartycka 18A, 00-716 Warszawa, http://www.cbk.waw.pl/~kosek/tsa/wyklad3.html.

ANNA DUDZIŃSKA[*]

THE ATTEMPT OF EVALUATION OF THERMAL COMFORT CLASS IN A PASSIVE SCHOOL BUILDING ON THE BASIS OF SHORT-TERM IN SITU RESEARCH IN CONTEXT OF PN-EN 15251 STANDARD

PRÓBA WYZNACZENIA KLASY KOMFORTU CIEPLNEGO W PASYWNEJ SZKOLE NA PODSTAWIE KRÓTKOTERMINOWYCH BADAŃ IN SITU W ODNIESIENIU DO STANDARDÓW NORMY PN-EN 15251

A b s t r a c t

In this paper, the classification of thermal conditions within a passive school building in Budzów in a narrow time spectrum, in accordance with PN- EN 15251 standard requirements is presented. Results of the short-term initial measurements made within the school building are shown. On their basis, a preliminary evaluation of the environment category was performed.

Keywords: thermal comfort class, PMV, PPD, DR, PD

S t r e s z c z e n i e

W artykule zamieszczono informacje na temat warunków termicznych w wąskim przedziale czasowym wewnątrz pasywnej szkoły w Budzowie w odniesieniu do wymagań normy PN--EN 15251. Przedstawiono wyniki krótkotrwałych, próbnych pomiarów prowadzonych w tym obiekcie i na tej podstawie dokonano wstępnej oceny katergorii środowiska.

Słowa kluczowe: klasa komforut cieplnego, PMV, PPD, DR, PD

[*] M.Sc. Eng. Anna Dudzińska, Institute of Materials and Building Structures, Faculty of Civil Engineering, Cracow University of Technology.

1. Introduction

After Polish accession to the European Union, it was necessary to implement the 2002/91/ EC Directive of the European Parliament and the European Council dated 16th December 2002. Concerning the energetic effectiveness of buildings. Its main goal is to stimulate the economy in EU member countries to create buildings characterized with the lowest possible energy demands, as well as, respective indoor microclimate and profitability of the investment. According to the Directive's requirements, all newly erected or rented buildings are to be certified. Energetic quality certificates need to account for the heat capacity, cooling system and passive heating, thermal bridges, anti-solar protection, heating systems and electricity systems powered by renewable energy sources, as well as, indoor climate conditions.

Classification of the building in context of the thermal comfort is performed in accordance with the PN-EN 15251 standard [1]. Analysis should be carried out exclusively for closed environments in the period of their highest thermal effort. It is suggested that the measurement period was several days long. However, for the preliminary analysis of the indoor conditons purposes, a several hours long period with high outdoor air temperatures was selected. Preliminary in situ tests of such type enable us to evaluate the indoor environment. In case of disadvantageous results (bad indoor conditons), these tests will be the basis for the further thorough thermal analysis for longer time periods.

2. Assumptions of PN-EN 15251

PN-EN 15251 [1] classifies objects into the respective thermal comfort classes on the basis of assumed requirement level. In this document, three environment categories are distinguished:

- Category A – rooms fulfilling high requirements. It is recommended for rooms in which sensitive and weak people live. E. g. small children, disabled or ill people.
- Category B – rooms fulfilling medium requirements (normal requirements). This category is designed for new and modernized buildings.
- Category C – rooms fulfilling moderate requirements. It is designed for building used at the acceptable level [2].

The above classes allow to decide, into which group the existing or planned building should be classified. They determine criteria for their respective level. Several factors affect the thermal comfort evaluation:

- Air temperture and spatial distribution of temperature within the room,
- Temperature of the surrounding space,
- Air moisture,
- Air velocity.

The analysis of the above parameters in each room decides on the whole building's thermal comfort class.

Coefficients PMV, PPD, DR and PD (computed in accordance with PN-EN ISO 7730:2006 [3]) are used in the evaluation of the thermal environment conditions. PMV coefficient (Predictive Mean Vote) determines the predicted mean vote according to the 7-grade psychophysical scale of thermal feeling – from +3 (hot) to –3 (cold). PPD coefficient (Predicted Percentage of Dissatisfied) determines the predicted percentage of people,

who would be dissatisfied with the thermal comfort within the room. The aforementioned coefficients determine the thermal comfort with reference to the whole body. Human can feel the so-called "local discomfort", which is related to different factors. Percentage of people dissatisfied with the air velocity within the room (draught) is specified into DR (Draught Rating) coefficient. Local thermal feeling related to either too cold or too hot floor due to the height and the asymmetry of the heat radiation is accounted for in PD coefficient.

T a b l e 1

Recommended values of the thermal comfort coefficients for respective room classes [1]

Room category	Thermal feeling of the whole body		Local discomfort			
			PD [%]			
	PMV	PPD [%]	DR [%]	Vertical air temperature difference [%]	Hotter or colder floor [%]	Asymmetry of the heat radiation [%]
A	−0.2 < PMV < +0.2	< 6	< 15	< 3	< 10	< 5
B	−0.5 < PMV < +0.5	< 10	< 20	< 5	< 10	< 5
C	−0.7 < PMV < +0.7	< 15	< 25	< 10	< 15	< 10

The classification is performed on the basis of design data, measurements and numerical simulations. Representative rooms in a building are analysed.

3. The first passive school building in Poland

The first passive school building was erected in Bremen-Sebaldsbruck (Germany) in 2001. Eleven years later, a similar structure – characterized by great energy savings – was built in Poland. This school, located in Budzów (Lower Silesia), is heated with the special devices using the energy produced by students as well.

Fig. 1. The passive school building in Budzow

The school building is characterized by great tightness. Thus, the energy recovery ventilation is used to recover the generated heat. Thermal transmittance coefficients for walls are equal to about 0.1 W/m²K, whereas they are equal to 0.8 W/m²K for windows, and the energy demand for heating purposes equals to about 15 kWh/m²year [4].

Measurements were made on the 17th of June at about midday (from 10 a.m. to 1 p.m.). In a representative classroom (located at the east side of the building), there were 30 students and a teacher.

The calibration of activity, metabolism and cloth coefficients was made. Students' activity in a siting position is rather small. Thus, the value of the generated energy was assumed as 1.591 met. Clo value for the light clothes was set as 0.5 accounting for the thermal resistance coefficients.

4. Results

The values of PMV and PPD for the analysed school classroom are presnted in Fig. 2. Predicted Percentage of Dissatisfied equals about 17%.
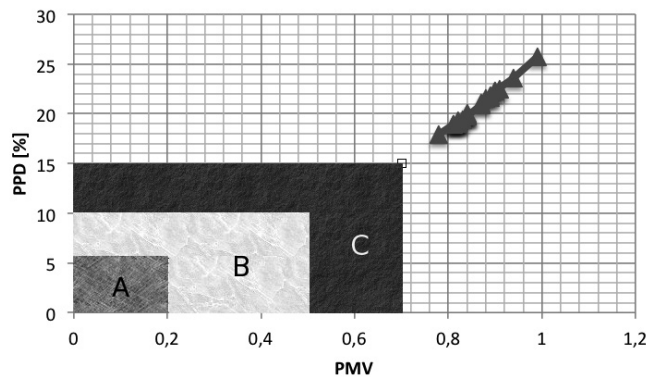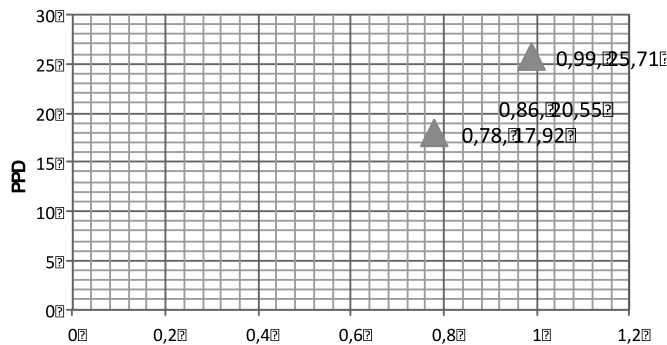

Fig. 2. Values of PMV and PPD coefficients

Fig. 3. Minimum,medium and maximum values of PMV and PPD coefficients

The value of DR coefficient for the whole measurement period is equal to 0. It was evaluated according to the following formula:

$$DR = (34 - t_{a,1}) \cdot (v_{a,1} - 0.05)^{0.62} \cdot (0.37 \cdot v_{a,1} \cdot T_u + 3.14),$$

where:

$t_{a,1}$ – air temperature at the point [°C];
$v_{a,1}$ – mean air velocity at the point [m/s], $v_{a,1} < 0.5$ – we assume that $v_{a,1} = 0.5$;
T_u – turbulence intensivity at the point ranging from 10% to 60% (value of 40% was assumed) [3].

PD coefficient, the indicator of the local discomfort due to the differences in vertical temperature distribution, too cold or too hot floor and the asymmetry of heat radiation, was not measured beacause of the gauge limitations.

T a b l e   2

Values of the evaluated thermal comfort coefficients

Thermal feeling of the whole body		Local discomfort			
		PD [%]			
PMV (medium)	PPD (medium) [%]	DR [%]	Vertical air temperature difference [%]	Hotter or colder floor [%]	Asymmetry of the heat radiation [%]
0.86	20.55	0	No data	No data	No data

5. Conclusions

On the basis of results of measurements one can conclude that:
- Mean value of PMV coefficient is equal to 0,86. It means that, according to PN-EN 15251 [1], it does not match for any of the presented environment categories.
- The evaluated values of the predicted mean vote denote a "hot" microclimate within the school classroom, according to Fanger criterion [5]. It should be noticed that the masurements were not made in the period of maximum outdoor temperature. It can be predicted that temperature increase would result into further deterioration of thermal comfort within the classroom.
- Over 20% students having classes in the analysed school classrom are not satisfied with its thermal conditions. It is reflected by the mean value of PPD coefficients (20.55).
- Local discomfort coefficient (DR), determinig the percentage of users sensitive to the air motion of high velocity, equals 0 for the whole analysis period. It comes from the low air velocities ($v_a < 0.05$) ranging from 0.00 to 0.03 m/s.
- The percentage of users dissatisfied with the differences in vertical temperature distribution, too hot/cold floor or the asymmetry of heat radiation was not evaluated. It was due to the gauge limitations, which are able to measure the temperature at only one height.
The preliminary analysis of the environment category within the school does not allow us to classify the object into any of the thermal comfort classes specified in PN-EN 15-251. Due

to the incomplete measurements set, limited range and time period of the analysis, the full description of the thermal conditions is not provided. Future research effort is to analyse the microclimate in a period of low outdoor temperatures using a gauge equipped with three probes located at different elevations. It will provide a reliable building evaluation.

Due to the incomplete set of results (limited range and measurement period), one obtains only the temporary overview of environment conditions. However, the possibility of uncomfortable thermal situation can be observed, which may affect the performance of the human body. It should be verified if the functioning of the object beside the thermal comfort range exceeds 10% of the whole year, which is the obligatory limitation. Thus, futher microclimate measurements are planned for several days periods with the maximum outdoor air temperatures, as well as, the statistical analysis. They will enable more reliable building evaluation, including its categorization.

References

[1] EN 15251:2007, Indoor environmental input parameters for design and assessment of energy performance of buildings addressing indoor air quality, thermal environment, lighting and acoustics, (PN-EN 15251:2007, Kryteria środowiska wewnętrznego, obejmujące warunki cieplne, jakość powietrza wewnętrznego, oświetlenie i hałas (oryg.).

[2] Sudoł-Szopińska I., Chojnacka A., *Thermal comfort within office rooms in accordance with norms*, Central Institute for Labour Protection – National Research Institute, Labour Protection 6/2007.

[3] EN ISO 7730:2005 Ergonomics of the thermal environment – Analytical determination and interpretation of thermal comfort using calculation of PMV and PPD indices and local thermal comfort criteria.

[4] Executive project by architect Bożena Bończa-Tomaszewska, Bończa-Studio (in Polish).

[5] Fanger P.O., *Thermal comfort*, Arkady Publishing House, Warsaw 1974.

MAŁGORZATA FEDORCZAK-CISAK*, JADWIGA STOCHEL-CYUNEL**

ACTIVE AND PASSIVE BUILDINGS IN THE CONTEXT OF USAGE PARAMETERS (INDOOR CLIMATE)

BUDYNKI AKTYWNE I PASYWNE W KONTEKŚCIE PARAMETRÓW UŻYTKOWANIA (KLIMATU WEWNĘTRZNEGO)

Abstract

In the last three decades, the issues of energy use and consumption have become one of the most important problems of the European market of real-estate development. The UE regulates it through legislation, standards and guidelines for both design and use of buildings. This paper lists the types of low-energy buildings, in the context of the requirements necessary for their design and construction. It also describes the initial experience with the use of these objects in terms of their advantages and disadvantages. Particular effort was made to compare the obtained parameters and comfort in active and passive objects. This paper provides an overview of low energy buildings, in order to introduce a series of articles presenting researches of individual authors.

Keywords: sustainable building, low-energy buildings, passive buildings, active buildings

Streszczenie

W ciągu ostatnich trzech dekad zagadnienia użycia energii i jej konsumpcji stały się jednym z najważniejszych problemów budownictwa europejskiego. W UE uregulowano je przez akty prawne, normy i wytyczne do projektowania i użytkowania obiektów budowlanych. Artykuł zestawia typy budynków niskoenergetycznych w kontekście wymagań niezbędnych przy ich projektowaniu i budowie oraz opisuje pierwsze doświadczenia z użytkowania tych obiektów z uwzględnieniem ich wad i zalet. Szczególną uwagę autorzy zwrócili na porównanie uzyskanych parametrów końcowych oraz komfortu użytkowania w obiektach pasywnych i aktywnych. Praca ta, przedstawiająca przegląd budynków niskoenergetycznych, jest wstępem do całego cyklu artykułów, w którym autorzy zaprezentują własne badania i analizy.

Słowa kluczowe: budownictwo zrównoważone, budynki niskoenergetyczne, budynki pasywne, budynki aktywne

* Ph.D. Eng. Małgorzata Fedorczak-Cisak, Institute of Building Materials and Structures, Faculty of Civil Engineering, Cracow University of Technology.
** M.Sc. Eng. arch. Jadwiga Stochel-Cyunel, JSCDESIGN, Polska.

1. Legal regulations

The strategy of Poland's development is coherent with the European strategies, including those referring to low-energy building. In the field of properties development, the requirements and decisions of the European Commission (the Union Directives, Access Treaty, the Kyoto Protocol) are of special importance for Poland, as the attempts to implement them can be noticed. It is especially important to meet the deadline determined in the Directive 31/2010 EPBD RECAST, in which the date of introducing the standard of "Net zero energy building" is settled.

A building of net zero energy demand – according to a definition given in the Directive 31/2010 EPBD RECAST – is a building of a very high energy characteristic. Net zero or a very small amount of demanded energy should come, to a very high degree, from renewable energy sources, produced on the spot or nearby.

In the light of such demands, building in Poland and other European Union countries faces a thorough change from traditional building, to that of very much lowered energy demand. This is connected with operations in many fields, as well as the necessity to meet the new challenges.

The European Union expects its Member Countries to define the "buildings of net zero energy demand", adjusted to the regional conditions. National definitions of a "net zero energy building" are being shaped now, while the buildings with lowered energy demand are built in the European countries, according to different standards and experiences. In Europe, the idea of passive buildings is the most developed one – especially in Germany, Austria and Scandinavia (more than 15000 of the buildings meeting the Passive House standards). Recently, the idea of designing active buildings has appeared.

2. Passive Buildings. Designing guidelines. Examples of realisation

The idea of passive buildings originated in Germany, in the Institute of Passive Buildings. In this Institute, the parameters of such objects were determined. According to the definition, a Passive House is a building, which meets proper standards of energy-saving, provides comfort of usage and has low exploitation costs. The type of building promoted by the Institute in Darmstadt allows saving up to 90% of the energy, in comparison to the average energy consumption in the existing buildings in the central Europe and over 75% in comparison to the average for newly erected buildings. Energy saving concerns not only moderate climate zones. The passive objects localized in warm climate zones–where cooling is demanded – show much smaller energy usage than standard buildings. Passive houses use less than 1.5 l of oil or 1.5 m^3 of gas to heat one square meter of living area a year–considerably less than in typical "low-energy" buildings. The criteria for Passive Buildings – in comparison to the Polish standards – are very difficult to meet. According to the directives of the Institute in Darmstadt.
1. The annual heating demand may not exceed 15 kWh/(m²a).
2. *U*-values of opaque exterior components must be less than 0.15 W/(m²K).
3. *U*-values of windows must be less than 0.8 W/(m²K).
4. *G*-values must be around 50% (total solar transmittance).

5. Translucent areas oriented towards the west or east (±50°), translucent areas inclined at an angle of 75° to the horizontal may not exceed 15% of the useful areas, or they must be equipped with temporary solar protection with a reduction factor of at least 75%.
6. Maximize passive solar gain.
7. The use of specific primary energy for all domestic applications (heating, hot water and domestic electricity) must not exceed 120 kWh/(m²a) in total.
8. Ventilation with highly efficient heat recovery – 75% of the heat from the exhaust air is transferred to the fresh air again by means of a heat exchanger.
9. Uncontrolled leakage through gaps must be smaller than 0.6 of the total house volume per hour during a pressure test at 50 Pascal (both pressurised and depressurised).
10. Thermal bridges, which cannot be avoided, must be minimised as far as possible.

Passive buildings use mainly solar energy, gained through glazing areas facing south and stored in massive walls of high thermal capacity. Thanks to high tightness and good thermal insulation of the external walls, as well as effective systems of mechanical ventilation with heat recovery, the passive houses minimize heat losses. The location of the building is of significant importance, as well as the shape of the exterior shell – relative to the geographical direction.

The first passive building in Poland – certified by the Institute of Passive Houses in Darmstadt – was built in 2006 in Solec, near Wrocław.

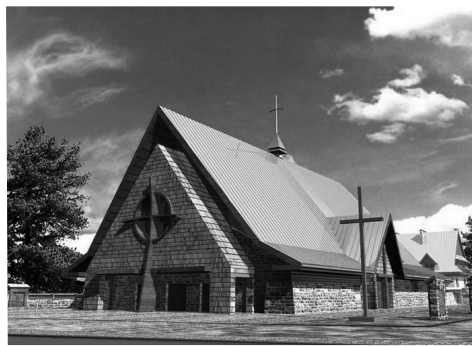Fig. 1. Passive house in Solec near Wrocław

Fig. 2. Passive church in Nowy Targ, Równia Szaflarska

The first "passive" church was opened in Nowy Targ, Równia Szaflarska. It was erected according to the project of architects Tomasz Pyszczek and Marcin Stelmach.

The object of 1740 m² was designed for a congregation of 500. The structure incorporated solutions typical for passive buildings, such as: compact building structure, high thermal insulation of the all building components of the exterior shell of the house (walls $U = 0.1$ W/m²K, windows $U = 0.8$ W/m²K), low-temperature underfloor heating with heat pump powered by a drilled well, as well as mechanical ventilation with a very efficient heat recovery.

Recently, a pressure test has been carried out in the church – the result of 0.59 l/h proved sufficient tightness of the casing on the passive object level.

3. Active Buildings. Designing guidelines. Examples of realisation

The idea of an active house originated as an alternative for energy efficient passive building, in a rigorous way forcing new directions for glazing and mechanical ventilation in the objects. It is based on similar architectural and building concepts, referring to material solutions, the object airtightness, shape of the building envelope and its optimal position, regarding the siting relative to the geographical direction – yet at the same time favoring natural light, natural ventilation and by using windows with automatically controlled opening system. At the increased glazing areas, active buildings are protected against overmuch heat gains through a system of automatically steered external roller-blinds and solar shading. The basic assumption in such types of buildings is to make use of solar energy, geothermal energy or wind energy in a most effective way, while remaining comfortable for the user.

In the designing process of an active building, it is important to analyse the possibility of limiting the negative influence of the object on the environment, starting from the phase of entering the building site, through the building process, up till the final usage of the object. Energy efficiency and saving water, the care about the quality of air, the rational choice of the building materials, technical service of the appliances – all these are priorities to be taken into account, when designing and constructing active buildings.
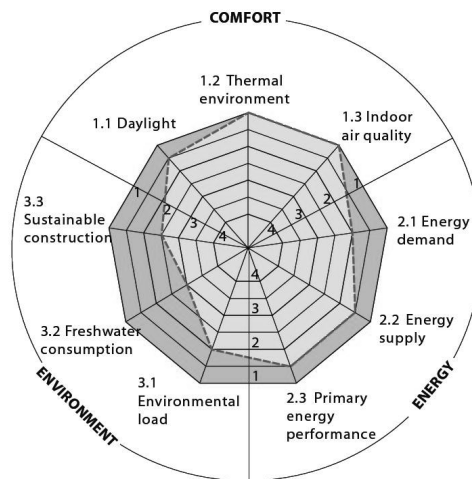

Fig. 3. Active house radar

Similarly to the passive houses, the annual energy demand of the active ones is minimized and heat transfer losses from exterior envelope of the building are limited to a minimum. Active buildings are able to "produce" electric energy or any other energy from the renewable sources, which should compensate the so-called climate payback, taken out by the house building – relative to the environment and society.

In the years 2009–2011, within the Model 2020 research project, six houses were erected in Europe, which met the criteria of active buildings. The houses were inhabited by families, which took part in the tests on users' comfort in the objects.

Fig. 4. Solar-Activhouse, Kraig, Austria

Fig. 5. Home for Life, Lystrup, Denmark

In those buildings, a hybrid ventilation was used, which means natural ventilation in summertime and mechanical ventilation (with heat recovery) during wintertime. In the transition seasons of spring and fall, the hybrid ventilation is switched on and off under the influence of outdoor temperature changes.

4. Experience gained from active and passive buildings usage

In the active Home for Life, tests were carried on the user's comfort, during the two years of usage. The results were published in REHVA – Federation of European Heating, Ventilation and Air-conditioning Associations in the article: *Using cooling ventilation system and solar shading to achieve good thermal environment in a Danish Active House*. The conclusions presented by the authors:

1. The building reaches good heat efficiency, which should be seen in connection to the high level of natural daylight.
2. Automatic control of the window openings and the solar shading elements positively influences indoor climatic conditions.
3. Cooling through window openings plays especially important role in maintaining heat comfort within the building – no significant overheating of the building was noticed in the summertime.
4. Small episodes of overcooling were observed during wintertime, keeping a favourable balance between the optimal interior temperature and usage of energy.

In Poland, the analysis was carried out on the microclimate in the passive sports hall in Słomniki. When taking measurements during high external temperatures, it was noted that:

1. In the case of a small physical activeness, the user will experience ideal conditions for his organism.
2. In the case of high physical activeness and with a bigger number of users, the increase of temperature and humidity will endanger the thermo-regulation processes of a competitor.
3. Blocking out roller blinds appeared to be necessary – in the afternoon hours, the outdoor light breakers were not able to reduce heat gains.

5. Conclusions

The results of both measurements are difficult to compare due to the difference in time of the carried out tests. The active house underwent measurements during a two years period, while the hall testing was carried out during just a few days of very high outdoor temperatures.

While in the passive houses an excessive heat recovery in the summertime appears to be a problem, in the active houses overcooling was noted in winter months.

Moreover, in the sports hall – at the same values of indoor climatic conditions – the competitors felt discomfort, while the audience enjoyed proper comfort.

This suggests the necessity of creating a space separation system, according to the physical activeness of the users.

Low-energy buildings demand a different way of designing than traditional buildings. The zero energy buildings create more technological problems, rather than architectural ones.

Meeting the requirements when designing the energy efficient buildings (PHPP, Active Houses Qualitative Parameters, etc.) is a necessary, yet it is not sufficient for effective functioning of the object, as a space of optimal indoor comfort.

It would be justified to introduce the necessity to carry out model analysis, as well as computer simulations at the designing stage.

Cooperation between architects, technologists, building physicists, constructors and contractors – from the very first stages of the project – is an indispensable condition when creating buildings, which would function effectively.

The authors are in the course of research on low-energy buildings, with the comfort and quality of the internal environment, which also affects comfort, acoustics, vibration, amount of daylight and air pollution. The following publications will presented the results of this work, along with suggested steps for optimizing the design of low energy buildings. The selection of materials, installations or building integration (BMS) are the target and the main concern of this research.

R e f e r e n c e s

[1] Dyrektywa 31/2010 EPBD RECAST, http://www.zb.itb.pl/files/zb/epbd_recast.pdf.

[2] Feist W., Schlagowski G., Kołakowska R., *Podstawy budownictwa pasywnego*, Polski Instytut Budownictwa Pasywnego, Gdańsk 2006.

[3] The Federation of Swiss Architects (Bund schweizer Architekten), Werk, Bauen + Wohnen, Vol. 81, Verlegergemeinschaft Werk, Bauen + Wohnen, 1994, 78.

[4] *Pasywna świątynia na Podhalu*, Izba Architektów Rzeczypospolitej Polskiej, zawód: ARCHITEKT, nr 2/2009, 30.

[5] Eriksen K.E., Rode C., Gillet P.-A., *Active House Specification – evaluation of comfort, energy and environment in buildings*, The REHVA European HVAC Journal, Vol. 50, May 2013, 10.

[6] Sartori I., Napolitano A., Voss K., *Net zero energy buildings: A consistent definition framework*, http://pubs.iea-shc.org/publications/downloads/DA-TP6-Sartori-2012-02.pdf.

[7] Foldbjerg P., Asmussen T., *Using ventilative cooling and solar shading to achieve good thermal environment in a Danish Active House*, The REHVA European HVAC Journal, Vol. 50, May 2013, 36.

[8] Dudzińska A., *Analiza obciążenia termicznego w pasywnej hali sportowej w czasie występowania wysokich temperatur zewnętrznych*, IZOLACJE, Vol. 179, wrzesień 2013, 26.

PIOTR FIELEK, ALICJA KOWALSKA-KOCZWARA[*]

ANALYSIS OF SUBSOIL MODELING INFLUENCE ON DYNAMIC CHARACTERISTICS OF REINFORCED CONCRETE BUILDING

ANALIZA WPŁYWU MODELOWANIA PODŁOŻA GRUNTOWEGO NA CHARAKTERYSTYKI DYNAMICZNE BUDYNKU ŻELBETOWEGO

Abstract

The paper is devoted to issues related to creation of subsoil models. At the beginning of the paper, the model of the building chosen for the analysis was described. The procedures for calculation of different models of the subsoil were also described. The final part of this paper presents results of the analysis of natural frequencies of reinforced concrete building with regard to the different models of the interaction between subsoil and the structure, and the conclusions drawn from this analysis are also presented.

Keywords: model of the subsoil, dynamic characteristics, the dynamics of buildings, coefficient of elasticity, modal analysis

Streszczenie

Artykuł jest poświęcona zagadnieniom związanym z kształtowaniem modeli podłoża gruntowego. Na początku opisano model budynku wybranego do analizy. Opisane zostały również procedury obliczeniowe różnych modeli podłoża gruntowego. Końcowa część prezentowanej pracy zawiera wyniki analizy drgań własnych budynku żelbetowego z uwzględnieniem różnych modeli współpracy podłoża gruntowego z konstrukcją oraz wnioski, które z tej analizy wyciągnięto.

Słowa kluczowe: model podłoża gruntowego, charakterystyki dynamiczne, dynamika budowli, zastępczy współczynnik sprężystości K_{Z}, analiza modalna

[*] Eng. Piotr Fielek, Ph. D. Eng. Alicja Kowalska-Koczwara, Institute of Structural Mechanics, Faculty of Civil Engineering, Cracow University of Technology.

1. Denotations

K – substitute modulus of elasticity of soil [kN/m]

K_x, K_y, K_z – substitute modulus of elasticity of soil in x, y and z direction respectively [kN/m]

$C_x C_y C_z$ – uniform deflection factor in x, y and z direction respectively [MN/m³]

F – foundation area [m²]

C_0 – dynamic coefficient of the subsoil [MPa/m]

a, b – foundation dimensions [m]

Δ – correction factor [m⁻¹]

p – static foundation pressure on the soil from characteristic loads [MPa]

Δu – total settlement [m]

1. Introduction

Computational methods are now a widely used tool in the building design. Interaction between subsoil and the structure is frequently omitted and replaced by rigid supports. Numerical results (predicted displacements or deformations) derived from the model of the rigid connection between subsoil and the structure are different from those obtained as a result of in-situ measurements. Different models of the subsoil, which were created over the past years (ex. [1–5]), are helpful in this subject.

The subsoil parameters which could be delivered from [6] are used for modeling subsoil in commercial engineering programs. Engineer should be careful when they consider dynamic loads. The parameters of the subsoil used for dynamic modeling should be received from dynamic measurements (according to [7]) or from experience and knowledge of the investigator. In Poland for example this problem could be solved by using procedures included in [8].

In order to illustrate the problem of selection of a subsoil model, an example of reinforced concrete building was made, taking into account its cooperation with the substrate through the use of substitute soil elasticity modulus. Substitute modulus of elasticity of soil K was calculated in two ways: counting "by hand" in accordance with the recommendations contained in [8] and using the subsoil calculator contained in one of the commercial engineering programs. Then, modulus K calculated in this way was used for modal analysis of the building to determine the effect of K on the characteristics of the natural vibration, and in particular on the natural frequency of the structure.

2. The model of the chosen building

The four-storey framed, reinforced concrete building was chosen for analysis. Building dimensions in plan are 20.80×18.00 m and the height is equal to 19.70 m. The bearing structure are columns with dimensions of 35×45 cm (external columns) and 35×35 cm (internal), substrings 35×60 cm, ribs 25×40 cm, slab with a thickness of 10 cm, and spread footings with dimensions in plan 2.5×2.5 m and a height of 80 cm. A stock character of the

building was assumed, that is why the estimated load of individual footings are as follows: 3000 kN for the internal feet, 1500 kN for the external feet, and 750 kN for the corner feet.

Three models of the ground were adopted to compare the effect of the method of subsoil modelling on the dynamic characteristics of the building. In the first model, the building is rigidly supported; in the second model, the building is founded on loamy sand (IL = 0.1), whereas in the third model: on gravel-clay (IL = 0.2). For the last two models, the coefficient K was calculated using the recommendations contained in [8] and using the subsoil calculator contained in Robot Structural Analysis. Then, a thus obtained coefficient K was used in FEM models of the building and calculations of natural frequency of the building were being made. This has led to five variants of computational model that has been compared to each other. Building model constructed in Robot Structural Analysis is shown in Fig. 1.
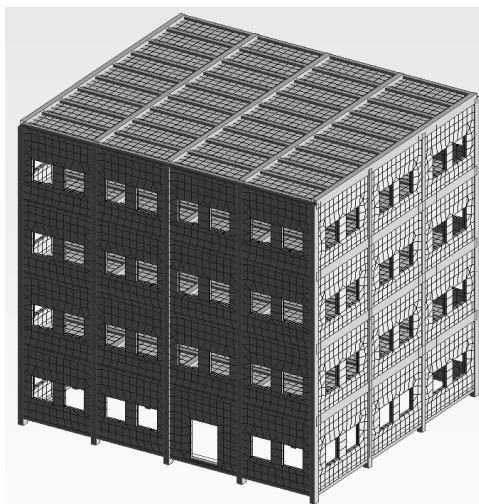

Fig. 1. FEM model of chosen building

3. The calculation of coefficient K in accordance with [8]

The procedure of calculation of the dynamic stiffness of the subsoil according to [8] is shown below. This procedure shows detailed calculations made for loamy sand but the algorithm is identical to the second soil.

Loamy sand (IL = 0.1) corresponds to III category of soil (soil medium stiffness: loamy sands, dusts, clay and loam hard plastic, IL = 0–0.25). The value of the dynamic coefficient of the substrate C_0 for this type of soil is 16 to 20 MPa/m. For the calculations a value of 16 MPa/m was chosen. The coefficient K_z (substitute modulus of elasticity of soil K in z direction) in accordance with [8] is calculated from the following formula:

$$K_z = C_z \cdot F. \tag{1}$$

Coefficient C_z contained in the formula (1) is determined using the relationship:

$$C_z = C_0 \left[1 + \frac{2(a+b)}{\Delta \cdot F} \right] \sqrt{\frac{p}{0.02}} \qquad (2)$$

where:

C_0 – was adopted 16 [MPa/m],

$\Delta = 1$ [m^{-1}].

Obtained from the above formulas values of coefficient K_z are listed in table 1.

Ta b l e 1

The values of Kz obtained in accordance with [8]

Soil Foundation type	Loamy sands	Gravel-clay
	K_z [kN/m]	
Internal footing	1274000	2069818
External footing	900700	1463582
Corner footing	636900	1034909

It was also necessary to adopt values of the coefficients K_x and K_y, because the elastic foundation in the model takes into account not only the vertical elasticity, but also horizontal elasticity. The coefficients K_x and K_y were determined using the simple relationship:

$$K_x = K_y = 0.7 K_z \qquad (3)$$

resulting directly from equation (4):

$$C_x = C_y = 0.7 C_z \qquad (4)$$

4. The calculation of coefficient K using subsoil calculator

Using available computer programs is the easiest way to take into account the interaction between soil and the building. The Robot Structural Analysis Professional holds a subsoil calculator, so the building designer can easily determine the modulus of elasticity of the subsoil K_z. The type of foundation (slab, continuous footing, footing), the dimensions of the foundation, and the estimated load must be defined to obtain the coefficient K_z from this calculator. A detailed procedure for calculating the coefficient K is contained in [9]. Soil under the foundation is split into bands with a thickness of 0.2 m. The average tension delivered from the formula Boussnesqu'a is determined in the middle of each band. Then, the average subsoil settlement in each band is determined from the relationship between tension and compression modulus. Total settlement is the sum of settlements in successive bands. Total settlement is associated with coefficient K by the formula:

$$K_z = \frac{1}{\Delta u} \qquad (5)$$

In Table 2 the values of coefficient K_z obtained from subsoil calculator are summarised.

The values of Kz obtained from subsoil calculator of Robot program

Soil Foundation type	Loamy sands	Gravel-clay
	K_z [kN/m]	
Internal footing	202896	163420
External footing	216503	173087
Corner footing	237853	190156

When comparing Table 1 and 2, huge differences can be observed between the values of the coefficient K_z obtained according to standard [8] and values of the coefficient obtained using subsoil calculator. Subsoil Calculator is based on the standard [6], which is used to determine the so-called static modulus of soil elasticity, while the procedure included in [8] is used to determine the dynamic modulus of soil elasticity. Static coefficient K_z is not suitable for dynamic calculations. For this type of calculations, it is necessary to use the dynamic coefficient K_z calculated according to [8].

5. Modal analysis taking into account the different models of interaction between soil and the structure

Differences in the coefficient K_z, although very large, may not lead to significant differences in the dynamic calculations. In order to analyse the influence of the coefficient K_z on quality of analysis, calculations of natural frequency of the building were performed. The three variants of the model were considered: rigid supports and the elastic foundation with to two types of soil using the static and dynamic K_z coefficient. The following table shows the results (first 10 natural frequencies) for all model variants.

The values of the natural frequency for all variants of the model

No.	Rigid support Frequency f [Hz]	Loamy sand Frequency f [Hz]		Clay-gravel Frequency f [Hz]	
		K_z stat.	K_z dyn.	K_z stat.	K_z dyn.
1	3.16	**2.36**	2.73	2.28	2.83
2	4.07	2.41	2.91	2.32	3.09
3	6.29	4.01	4.72	3.90	4.97

4	9.15	7.40	8.62	6.98	8.77
5	10.93	7.69	10.00	7.40	10.35
6	11.76	8.55	10.59	8.18	10.96
7	12.20	8.96	10.95	8.63	11.25
8	12.31	9.22	11.33	8.83	11.70
9	12.44	9.33	11.82	9.07	12.19
10	12.87	10.73	12.52	10.32	12.60

The calculation results obtained from the model of the subsoil with the use of dynamic coefficient K_z mostly correspond to real behaviour of the structure (ex. [10]). The results from a rigid support overstates the value of the natural frequency, which can lead to an incorrect assessment of the stiffness of the structure (the higher the frequency, the greater its rigidity). The results obtained from the use of static coefficient K_z underestimate the value of the natural frequency, which are on the safe side.

6. Conclusions

The main purpose of this article is to sensitize designers who use modern FEM programs on calculation results which they obtain. First of all, it is important to verify the algorithm, which is used by the program in the calculations and check if the chosen algorithm is suitable for calculations that we should do. Errors in numerical calculations are not the fault of the program, but the user who did not check their contents.

It is shown in only one aspect of coefficient K_z that, in the case of non-standardcalculations (e.g. such as in this case – the dynamic calculation), the designer should pay particular attention to the quality of the numerical results. In such cases it is always worth to perform even a simple manual check of the results using the recommendations specified by the standards.

References

[1] Gwóźdź-Lasoń M., *Computational models of the subsoil in terms of the various methods and technologies of strengthening.* Doctoral dissertation, Cracow University of Technology, Kraków 2007.
[2] Fedorowicz L., Kadela M., *Model calibration of line construction–subsoil assisted by experimental research*, AGH Journal of Mining and Geoengineering, Vol. 36, No. 1, Kraków 2012.
[3] Makovička D., Makovička D. Jr., *Seismic Response of a Structure under Various Subsoil Models,* Journal of Mechanics Engineering and Automation, Vol. 4, 2014, 78-84.

[4] Ulitsky V.M., Shashkin A.G., Shashkin K.G., Vasenin V.A., Lisyuk M.B., Dashko R.E., *Interaction between structures and compressible subsoils considered in light of soil mechanics and structural mechanics*, Proceedings of the 18th International Conference on Soil Mechanics and Geotechnical Engineering, Paris 2013, 825-828.

[5] Edgers L., Sanayei M., Alonge J.L., *Modeling the effects of soil-structure interaction on a tall building bearing on a mat foundation*, Civil Engineering Practice Fall/Winter 2005, 51-68.

[6] EN 1997-2 (2007) (English): Eurocode 7: Geotechnical design- Part 2: Ground investigation and testing [Authority: The European Union Per Regulation 305/2011, Directive 98/34/EC, Directive 2004/18/EC].

[7] EN 1998-1 Eurocode 8, Design of structures for earthquake resistance. Part 1: General rules, seismic actions and rules for building, 2005.

[8] Lipiński J., *Fundamenty pod maszyny*, Arkady, Warszawa 1985.

[9] Robot – manual. 2009 Autodesk Inc.

[10] Kowalska A., *Analysis of the influence of non-structural elements on dynamic characteristics of the building*, Doctoral dissertation, Cracow University of Technology, Kraków 2007.

KATARZYNA FILA, MAGDALENA FURMAN, JOLANTA GINTOWT[*]

ILUMINATION OF ARCHITECTURE. THE PROBLEM OF LIGHT POLLUTION

ILUMINACJA ZABYTKÓW. PROBLEM ZANIECZYSZCZENIA ŚWIATŁEM

Abstract

This paper is an attempt to briefly present the problem of light pollution, concerning the illumination of both historical and architectural objects and its influence on environment. According to the measurements conducted in Kraków and Frankfurt am Main, the comparison and the analysis of the problem will be provided.

Keywords: light pollution, illumination of architecture, Unified Glare Rating

Streszczenie

Niniejsza praca jest szkicową próbą przedstawienia problemu zanieczyszczenia światłem związanym z iluminacją obiektów zabytkowych na przykładzie analizy porównawczej natężenia światła na rynku głównym we Frankfurcie nad Menem oraz w Krakowie.

Słowa kluczowe: zanieczyszczenie światłem, iluminacja zabytków, wskaźnik UGR

[*] Katarzyna Fila, Magdalena Furman, M.Sc. Eng. Jolanta Gintowt, Institute of Building Materials and Structures, Faculty of Civil Engineering, Cracow University of Technology.

1. Introduction

Light in its form is a flexible and simple to manipulate matter, that allows achieving the desired goals easily. These days – thanks to the technical development – people are able to operate with light's intensity, color, or play with the ways of its propagation. The field, which involves light waves is called illumination and is defined as "applying light, in order to show objects and their surroundings".

Designing illumination requires insightful analysis of its influence on perception and artistic values (Fig. 1). Subjects of illumination may differ – they may include buildings, details of the building, streets, signs, monuments, as well as any structure and video mapping subject. Main purpose of illumination is to improve security of an object, or its attractiveness, understood as distinction from its surroundings.

Fig. 1. Light illumination of the historic objects in Kraków and Frankfurt

Excessive light has negative health effects on human body. Mainly, it can cause an effect called "glare", which results in a feeling of discomfort, reduced ability to recognize objects or simply problems with sleep. Lights also confuse animals, especially birds, which can be light-blinded and hit the walls of the buildings. While light remains an essential part of historical spots of old towns, we have to bear in mind, that proper design and application is required in every stage of illumination, in order to avoid the negative outcomes of what we call the "light pollution". In the paper [11] – are presented examined the effect of night shift work on breast cancer. In the paper [1] – are presented problems with astronomical survey of the sky.

2. The problem of light pollution

Putting esthetic values aside, it is worth to notice a problem of high emission of artificial light. "Light pollution" is defined as an excessive presence of artificial light in comparison to the natural luminosity of the night. Light scattered in atmosphere is perceived as "sky glow" – or so called "light fog". This fog is related to the overall air pollution. Air pollution enhances light pollution trough increasing the amount of scattered light. It is easy to notice that nowadays the problem of photo-pollution increases – even if it is not as well known as air pollution and not such easily detectable. Light pollution can be determined as emission

of disturbing light. Disturbing light is an undesired light, that can cause irritation, interrupted vision, distraction or reduction of vision. The light pollution causes unnecessary escape of light to the areas, which are not supposed to be illuminated or are not the subject of the given illumination (ex. street lamps on the side of the buildings). Another side effect results in excessive light – the presence of lights, which are actually not needed; too bright, too numerous and without any particular purpose. The third side effect is the so-called light chaos, caused by a badly designed illumination, consisting of lights, which are poorly shielded or not shielded at all, badly installed, poorly directed or situated. Finally, the urban glow, often caused by street lighting and commercial premises lighting, which is usually pointed upwards and thus contributes to the phenomenon called "light fog" [2–10].

In our paper we would like to prove, that what looks pretty is not necessary good. As far as sound goes, people are aware of the term "noise pollution" but they are not aware of light pollution.

3. Method of measurements

The analysis features the illumination of historic urban areas; two European markets, which differ in surface and surroundings (Fig. 2).

The measurements were conducted during summer (no snow) on the main squares of Frankfurt am Main and Cracow. The sky was clean and relatively dark. The following results were obtained, according to the eyesight level values. All measurements were taken with use of photometer (Mastech MS6612 37450 – 0). The difference in the number of analysis points (positions at which the measurement was held) is caused by the difference of the area's surface – Cracow's area (0.03 km²) is about 3 times bigger than Frankfurt am Main (0.01 km²).
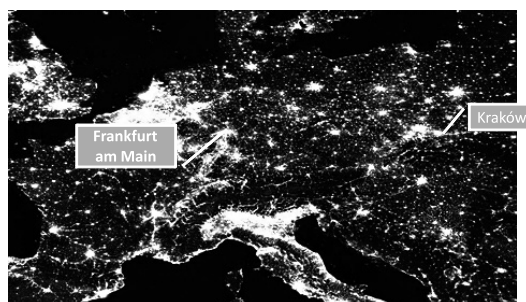

Fig. 2. Location of the examined objects on the light pollution map

4. Results

Firstly, it is very important to remember, that not only the areas vary, but so does the significance of those two places. The main square in Kraków is the city center, not only full of restaurants, but also of significant, internationally known monuments. In comparison, the main square in Frankfurt am Main is of lesser importance. This difference is easy to notice

during analyzing the diagrams above. In case of Kraków, the biggest amplitude is observed near the lanterns, the main sources of light needed in order to illuminate the monuments (e.g. Saint Mary's Basilica), as well as the openings of the main streets (Szewska, Floriańska). According to the results from Frankfurt am Main, the highest values were obtained in front of two spotlights illuminating the Church of Saint Nicolaus.
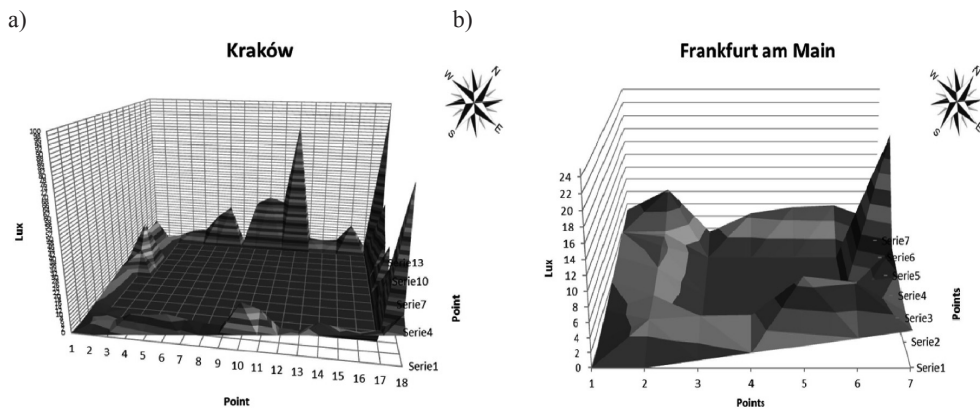
Diagrams no 3 and no 4 reveal the difference of luminous flux on the walls of squares.

Fig. 3. Distribution of luminous flux on the Main Square, measured on the eyesight level:
a) in Kraków, b) in Frankfurt am Main

Fig. 4. Glare effect on the Main Square in Frankfurt am Main (left side) (author: B. Rudnik)

In order to better understand the problem, we were also measuring the luminous flux on one side of the Main Square in Kraków – the NE wall. Moreover, the research was carried out in six different positions – from the base to the eyesight level, as shown on the Fig. 4. The highest amplitude – as mentioned above – is observed near lanterns located at the openings of the streets. What was noticed during the measurements is that the value of the luminous flux decreased as the street movement increased. Additionally, on the main market square in Frankfurt am Main, the glare effect was observed, which dimmed the surrounding area. This

effect was caused by a point light located in the southern part of the market. In Cracow, the main market sqare lighting is evenly distributed (Fig. 5 and 6).

Luminaries: the market in Frankfurt am Main and Cracow luminaries does not cause light scattering upwards. The shape of luminaries affects the scattering of light on the sides (Frankfurt) or concentrates the light downwards without scattering it sideways Cracow (Fig. 6).
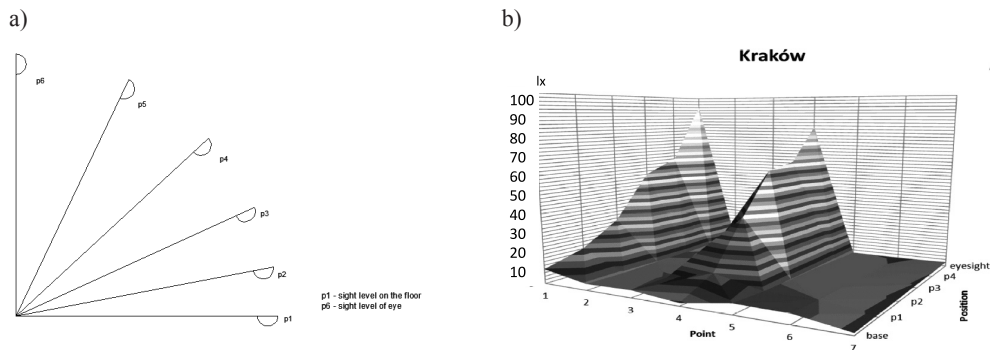
a)

b)

Fig. 5a) The position of photometer, b) The distribution of the luminous flux on the Main Square in Kraków at six different positions of the photometer for NE wall

a)

b)
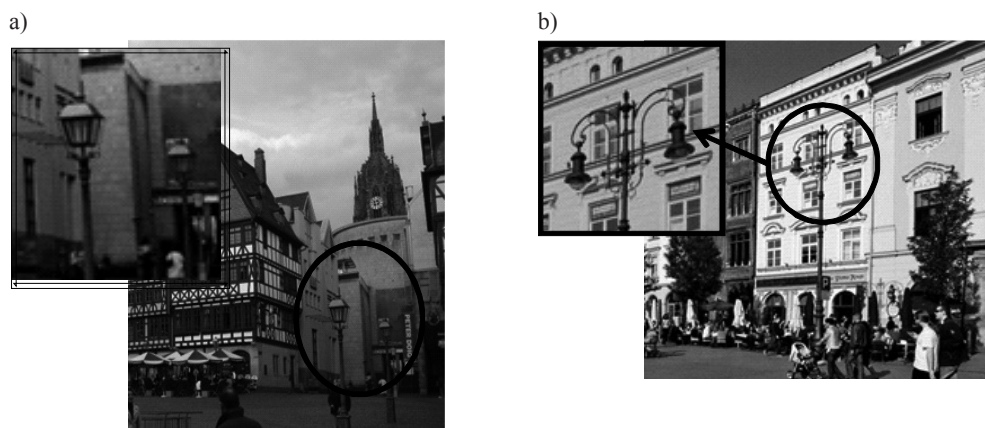
Fig. 6. Luminaries: a) in Frankfurt am Main, b) in Cracow

5. Conclusions

In this paper we demonstrated, that the choice of the shape of the light fittings for the historic sites can not be accidental, and even small differences in their shape are affecting the environment significantly. However, the lighting of historic areas is important for aesthetic

perception of the historic monuments. Selection of lighting fixtures because of their shape referring to the historical location, is not a sufficient criterion, as there may still cause various disturbing effects, such as glare. In order to properly evaluate the lighting in public open spaces, a Unified Glare Rating – simmilar to the one used in evaluation of the closed spaces – should be used as the basic parameter. Further direction of research should address the impact of night lighting on the health of both residents and nocturnal animals, as well as astronomical observations carried out in the historical areas.

References

[1] Smith M.G., *Protection of existing and potential observatory sites*, Proceedings of the International Astronomical Union, Woodruff T. Sullivan Arts and Sciences, Astronomy, 1 (T26A), 2005, 381-382.

[2] Ratajczak J., *Oświetlenie iluminacyjne obiektów architektonicznych*, Politechnika Poznańska, Poznań 2009.

[3] Śpik A., *Iluminacja obiektów zabytkowych architektury*, Warszawa 1976.

[4] Żagan W., *Iluminacja obiektów*, Oficyna Wydawnicza Politechniki Warszawskiej, Warszawa 2003.

[5] Rzepiński R., *Dekorowanie światłem – technika iluminacji*, Konferencja „Światło w architekturze – kształtowanie przestrzeni miejskiej (projektowanie, technika, finansowanie)", Warszawa, 5–6 października 2000.

[6] Hryszkiewicz D., *Iluminacje obiektów zabytkowych w Gdańsku, Malborku i Gniewie. Między koncepcją a realizacją*, Sympozjum „Iluminacja zabytków", Warszawa, 6–7 kwietnia 2006.

[7] Brzozowski S., *Oświetlenie elewacji budynków*, „Technika Świetlna '96. Poradnik – Informator", Warszawa 1996.

[8] Bąk J., Pabjańczyk W., *Podstawy techniki świetlnej*, Wydawnictwo Politechniki Łódzkiej, Łódź 1994.

[9] Leniarski L., *Oświetlenie obiektów sakralnych*, „Technika Świetlna '96. Poradnik – Informator", Warszawa 1996.

[10] *Guidance Notes for the Reduction of Obstructive Light*, ILE, 2005.

[11] Stevens R.G., BraInard G.C., Blask D.E., Lockley S.W., Motta M.E., *Adverse health effects of nighttime lighting*: *comments on american medical association policy statement*, Am J Prev Med. 2013 Sep, 45 (3), 343-346.

[12] PN 84/E-02033: *Oświetlenie wnętrz światłem elektrycznym*.

[13] ISO 8995: 1989. Principles of visualergonomics. The lighting of indoor work systems.

[14] Rea M., *Vision and perception w Lightin Handbook, Rreference &Application*, IES of North America, IESSNA, New York 1993.

EWELINA GAWELL, ANNA NOWAK, JOANNA PIETRZAK[*]

MODELING OF BIOCLIMATIC SKYSCRAPERS' FACADES WITH GENERATIVE DESIGN METHODS

KSZTAŁTOWANIE ELEWACJI WIEŻOWCÓW BIOKLIMATYCZNYCH METODAMI GENERATYWNYMI

Abstract

Today, the architectural design process is based on developing digital technologies, and the interest in „fitting" buildings into a local microclimate is increasing. The article brings up the subject of modeling skyscrapers' facades to present the tendency of the generative design methods in the design process of bioclimatic building. As a result, each individual element is adapted to the local microclimate. The results of the design integrated with modeling based on generative methods are mostly unconventional shaped structural forms.

Keywords: bioclimatic skyscraper, facade modeling, generative design methods

Streszczenie

Obecnie proces projektowania opiera się o coraz lepsze wykorzystanie technologii cyfrowych, a zainteresowanie poszukiwaniem budynków „wpisujących się" w lokalny mikroklimat wzrasta. Podjęta tematyka kształtowania elewacji wieżowców ma na celu przedstawienie tendencji do wykorzystywania generatywnych metod w projektowaniu obiektów bioklimatycznych. W ich rezultacie każdy element budynku może być dostosowywany do warunków istniejących w miejscu jego wbudowania. Wynikiem wprowadzenia generatywnego modelowania są często formy strukturalne o niekonwencjonalnych kształtach.

Słowa kluczowe: bioklimatyczny wieżowiec, kształtowanie fasady, generatywne modelowanie

[*] M.Sc. Eng. Ewelina Gawell, M.Sc. Eng Anna Nowak, M.Sc. Eng. Joanna Pietrzak, Department of Structural Design, Construction and Technical Infrastructure, Faculty of Architecture, Warsaw University of Technology.

1. Introduction

Recently, there has been a growing interest in *bioclimatic design,* which is *"*the passive, low-energy design approach that makes use of the ambient energies of the climate of the locality to create conditions of comfort for the users of the building" [1]. The implication of digital tools facilitates greatly the design of bioclimatic skyscrapers.

The methods of designing the bioclimatic structures are also used in European high-rise buildings. The skyscrapers erected in Europe do not compete with global implementations in the unfolding race of height and their prestige is decided by, among other things, bioclimatic solutions. One of the key issues in the design of a tall, bioclimatic building, is the proper structuring, as well as the technical and technological solution of the elevation. The desired goals are: to maximize access to daylight and use of natural ventilation [2], heating and cooling, to minimize heat gain or loss and to prevent a glare.

The development of digital technologies contributed to the increase of research on the enclosure, defined in the architecture as the boundary between the interior and the exterior of the building. For many historic structures, the cladding of the enclosure defined the finishing layer, covering the actual internal structure of the building. Breaking with the treatment of the elevation as a top layer ("the costume"), determines the technological possibilities and the development in the era of optimization [3]. The enclosure is an integral part of building's structure, constituting the continuation and completion of systems in the building. In many contemporary implementations, the enclosure is an element adapting the building to the changing climate conditions, compared to a *skin*. The multitude of factors affecting the exterior and the functionality of the enclosure, as well as the development of the newest technologies and digital tools, currently make interdisciplinary design one of most interesting trends in shaping bioclimatic elevations.

The implementation of innovative technical surface treatment of elevation structures as an *architectural skin*, is made possible by generative tools of an architect, in which the algorithms play a key role. Thanks to the characteristic iterative structure, enabling to generate multi-option solutions, based on initial data [4], the algorithms are widely used in modeling bioclimatic facades of high-rise buildings, where the relation between climate variables is particularly important. The generative design methods allow to control and interfere with the form, generated by the program. Due to the complexity of the architectural design, architects are now closer to the digital tools, that are based on a program (e.g. for manual modeling) and include features embedded in the application. The application of the generative modeling tools allows for the search and analysis of optimal solutions, regardless of their geometrical complexity. The world's most renowned design studios create their own optimization programs, enabling the creation and implementation of a rational and often unusual engineering solutions.

2. The analysis of architectural examples

The use of generative tools in the process of architectural design, allows connecting many disciplines and issues with a single algorithm. In the complex process of generating a form, more often all possible parameters that affect the final form of the object are taken into account. As a result, the modeled form constitutes a coherent spatial arrangement, the surface

of which, separates the interior from the exterior, comprises an active layer, through which the processes, necessary to maintain the comfort of the object occupants, take place.

One of the more interesting examples of generative tools application, in the development process of bioclimatic facades of high-rise buildings, is the *Education Executive Agency and Tax Offices* in Groningen. The building, designed by UN Studio in collaboration with the DUO² consortium and implemented in the years 2006–2011, is the new headquarters for two government offices. The complex includes an office building with a parking lot, a commercial pavilion and a public park [5].
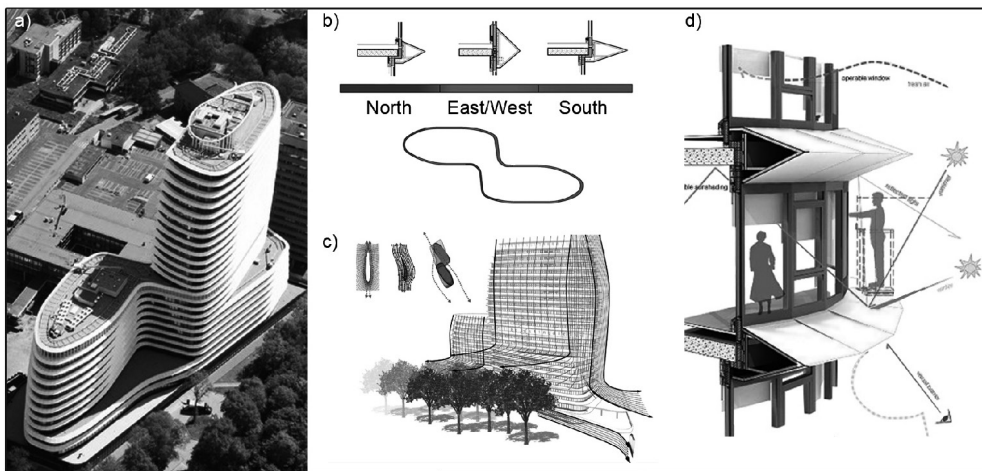
Fig. 1. Education Executive Agency and Tax Offices: a) a bird's eye view; b) shaping of elevation's elements; c) an aerodynamic shaping of building's form; d) a diagram of elevation functions

The object was formed with the use of a parametric methods in a way to obtain optimal exposure to sun rays of the interiors, as well as to enable natural ventilation through windows. A smooth, bionic form was shaped as a result of the aerodynamic analysis, the aim of which was to minimize turbulence around the building. The facade which combines all the necessary features of a bioclimatic "skin" using a relatively simple technology, thanks to the use of generative tools, played a special role in the project. The characteristic elements of the elevation are horizontal ribs, surrounding the building at the ceiling level, the profile of which varies smoothly, depending on the orientation of the corners of the world [6]. These bands are used as elements controlling the gusts of wind, a visual barrier and, depending on the season, reflecting the sunlight outside the building or to its interior. Furthermore, the shaping of the facade prevents the building's overheating process and the specially designed building projection and horizontal bands of windows, allow visual contact with the environment, as well as better lighting of the interior with natural light.

An interesting example of the use of generative design methods is also the building *Tour Phare*, located in the Parisian office district La Défense. The completion of the 300-meter high skyscraper designed by Morphosis is planned for 2017. The building is expected to include a public space on the ground floor, office space and restaurants.

The main objectives of the project were: to maximize the use of daylight, wind energy and to minimize the effect of overheating of the building. As a result, the orientation and the form of the skyscraper have been designed in accordance with the position of the sun. The flat northern facade will be fully glazed and the "waving" east-south-west elevation will be additionally covered with a set of diagonally placed perforated stainless steel panels. The multi-layer skin, thanks to its curvature and construction, will improve the energy efficiency and working conditions [7].
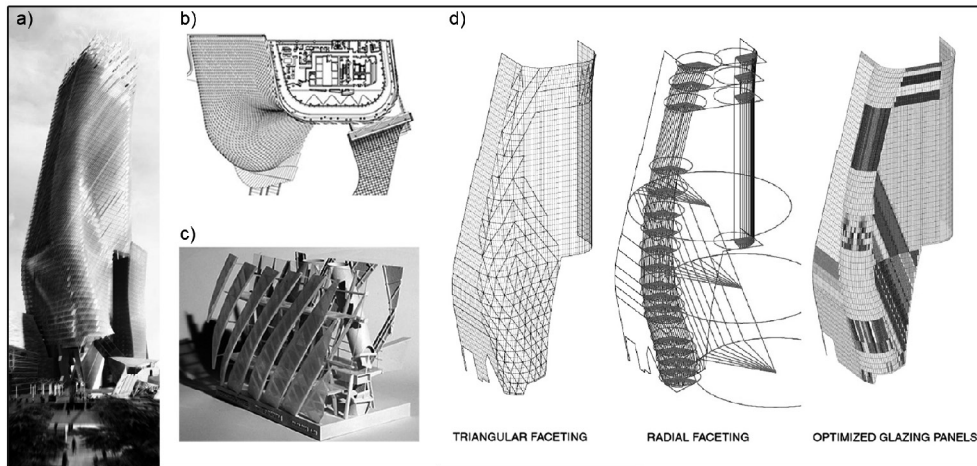
Fig. 2. Tour Phare: a) a visualization; b) the plan of the 65th floor; c) a model showing construction of the waving enclosure; d) diagrams showing the evolution of the waving façade's glazing

Project was begun on Bentley software form Microstation and a programmer was hired to write scripts for a customized parametric model. Later on, architects finished the project using Digital Projects [7]. The complexity of the waving facade required drawing up of a detailed design regarding, inter alia, the panelization i.e. the division of the facade and the support structure into production elements. Optimizing the form of the panels was made possible by the use of appropriate algorithms for generating divisions, which meet the functional, visual, material and economic requirements. In the pursuit to maximize the amount of repeatable elevation elements, the optimization of both the geometry of the panels and their supporting structure, as well as the method of combining individual elements, was obtained. However, to achieve the greatest possible efficiency, each of the 5000 panels has a different angle alignment. Moreover, the maximum length of steel panels was determined due to a different wind load of the different parts of the building [7].

The generative design methods are a very effective tool for presenting a loose complex architectural form, through the use of an easy to describe geometry and translating it into building elements. An example would be the project of the office building *Bishopsgate Tower* in London, designed by Kohn Pedersen Fox Associates. This skyscraper was designed with the facilities provided by parametric modeling software, namely Bentley's Generative Components [8]. The geometry of the object was chosen as a result of the generative modeling

and it is based on algorithms used to adapt the project to a few simple design restrictions, inter alia, the model of the building was built entirely from lines and tangent arcs.

One of the key issues in design was the solution to the elevation of the building. The object was to be entirely glazed and the double elevation was formed by repeatable rectangular modules. The inner layer of the elevation is a continuous housing, equipped with operable windows, while the outer one is comprised of separated, slightly overlapping panels. In the basement, a curvilinear glass facade creates a canopy over the pavement, which improves the wind conditions at the surrounding ground level.
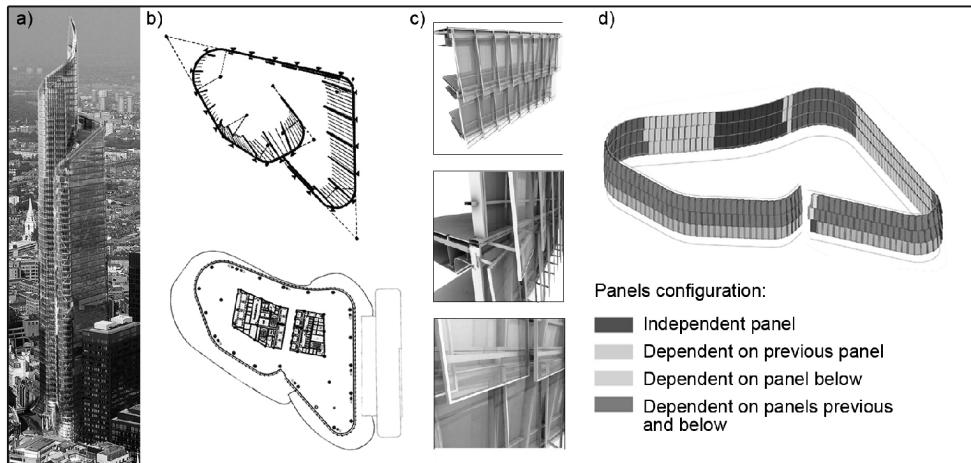
Fig. 3. Bishopsgate Tower: a) a visualization; b) a diagram of the building geometry and a typical floor plan; c) a model of elevation – visualizations; d) a diagram of the elevation panels configuration

The shaping of the facade and the setting of its elements, were generated by a properly "specialized" optimization algorithm. In particular, an iterative process for the purpose of minimizing the voids in the double facade was carried out, which maximized usable space. Furthermore, an important goal was to define such a configuration of panels, which would prevent their collision, in close adjacency and visual continuity, while maintaining the required appropriate vents between overlapping outer panels [8].

3. Conclusions

The European projects, presented in this article, are examples of new generation bioclimatic skyscrapers. Their creation was contingent upon the introduction to the design process of multi-criteria optimization, as a result of which, each element of the building may be adapted to the conditions in the place of its erection. The presented trends in architectural design, involve the use of generative design methods.

Shaping of the "bioclimatic" elevations is an important factor in increasing comfort of tall buildings. Treating the outer divider as an *architectural skin* is a difficult task in finding

more effective tectonic and functional solutions, the essence of which results from the microclimatic conditions and the adaptation of the object in given environment. The use of algorithms in the complex process of modeling the form of an object, along with the system of connections and relations, enables to generate heterogeneous structures, which constitute a synergistic solution in an interaction of many disciplines. The use of the generative methods in the design of bioclimatic elevations, pertains not only to the shaping the surface, but also to the systems that are responsible for the processes, taking place between the building and its surroundings.

The search for optimal engineering solutions is becoming an important factor in determining the value of modern architecture. One of the indicators of this trend is the use of generative methods in the design of bioclimatic elevations of tall buildings, which results in interesting and original structural forms, with a considerable degree of complexity that goes beyond the traditional design.

References

[1] Yeang K., *The green skyscraper: the basis for designing sustainable intensive buildings*, Prestel, Munich, London, New York 1999.

[2] Wood A., Salib R., *Natural Ventilation in High-Rise Office Buildings: An output of the CTBUH Sustainability Working Group*, Council on Tall Buildings and Urban Habitat, Chicago 2013.

[3] Januszkiewicz K., *O projektowaniu Architektury w dobie narzędzi cyfrowych. Stan aktualny i perspektywy rozwoju*, Oficyna Wydawnicza Politechniki Wrocławskiej, Wrocław 2010.

[4] Rokicki W., Wysokińska E., *Algorytmy w kształtowaniu form strukturalnych*, Materials from Academic and Technical Conference ARCHBUD 2012 "Problems of Modern Architecture and Construction", Oficyna Wydawnicza Wyższej Szkoły Ekologii i Zarządzania, Warszawa 2012, 243-252.

[5] Cilento K. (26.04.2011) EEA + Tax Office/UNStudio, http://www.archdaily.com/130671, access: 30.09.2013).

[6] Zielonko-Jung K., *Kształtowanie przestrzenne architektury ekologicznej w strukturze miasta*, Oficyna Wydawnicza Politechniki Warszawskiej, Warszawa 2013.

[7] Johnson S., *Performative Skyscraper: Tall Building Design Now*, Balcony Press, Los Angeles 2014.

[8] Hesselgren L., Charitou R., Dritsas S., *The Bishopsgate Tower Case Study*, International journal of architectural computing, issue 01, vol. 05, 61-81, http://www.formpig.com/pdf/formpig_bishopsgate%20 tower%20study_kpf%20dritsas%20hesselgren%20charitou.pdf, access: 1.09.2014

JOLANTA GINTOWT, PAULINA ŁYSIK*

COMPARATIVE ANALYSIS OF THE CRITERIA USED TO SELECT THE OPTIMAL ENERGY SAVING VARIANTS IN BUILDINGS. SELECTED ISSUES

ANALIZA PORÓWNAWCZA KRYTERIÓW STOSOWANYCH DO WYBORU OPTYMALNYCH WARIANTÓW ENERGOOSZCZĘDNYCH W BUDOWNICTWIE. WYBRANE ZAGADNIENIA

Abstract

Comparative analysis of multi-criteria Pareto and SPBT optimization, for a single-family, detached residential building used as an example. Main elements of interest include minimum power and minimum cost of investment.

Keywords: multi-criteria optimization, Pareto, Kuhn-Tucker, SPBT

Streszczenie

Analiza porównawcza dla kryterium optymalizacji wielokryterialnej w sensie Pareto i SPBT na przykładzie budynku mieszkalnego jednorodzinnego, wolnostojącego. Funkcjami kryterialnymi są minimum energii i minimum kosztów inwestycyjnych, zmiennymi decyzyjnymi – izolacyjność termiczna przegród zewnętrznych, wielkość przeszklenia, orientacja budynku względem stron świata.

Słowa kluczowe: optymalizacja wielokryterialna, Pareto, Kuhn-Tucker, SPBT

---

* M.Sc. Eng. Jolanta Gintowt, Institute of Building Materials and Structures, Faculty of Civil Engineering, Cracow University of Technology.

** Paulina Łysik, student, Cracow University of Technology.

Designations

$f(x)$ –   vector of objective function
x –   vector of decision variables
r –   positive multiplier, controls the magnitude of the penalty terms
$h(x)$ –   vector of equality constraints
Gj –   Heaviside operator
$g_j(x)$ –   vector of inequality constraints,
ρ_i –   random number <0;1>
$P[f(x)]$ –   preference function (substitute function)
F_1 –   criterion function, energy [kWh]
$F2$ –   criterion function, investment cost [zł]
$g(i)$ –   boundary conditions
$x(5)$ –   thermal resistance [m^2K/W]
$x(6)$ –   simplex sides of the base of the building

1. Optimization method to determine reasonably low energy consumption

1.1. Unconstrained Minimization

One of the most developed groups of numerical optimization methods is the iterative type [1]. For this method, a point is established on the basis of the previously obtained results, which indicates where the minimum is likely to be, or the general direction in which it is likely to lie. This approach includes, without limitation, the following methods: Direct Search Method of Hooker and Jeeves, Simplex Method of Nelder and Mead, Variable Metric Method of Davidon-Fletcher-Powell. These methods however, should not be used to evaluate energy-efficient buildings, as they primarily determine the technical requirements, such as maximum heat transfer coefficient. In this case it is possible finding a local optima.

1.2. Constrained Minimization

The most common approach to solving constrained minimization problems involves the use of penalty functions to convert these problems into unconstrained problems. The most popular penalty function is the one, which associates a penalty – which is proportional to the square of a violation – as in the following formula (1).

$$\min_{x \in R^n} \phi(x,r) = f(x) + r\sum_{j=1}^{p}[h_j(x)]^2 + r\sum_{j=1}^{m} Gj[g_j(x)]^2 \tag{1}$$

where:
     Gj –   Heaviside operator such that $Gj = 0$ for $g_j(x) \geq 0$ and $Gj = 1$ for $g_j(x) < 0$.

One of the widely used formulations of the transformed interior function is the one shown in formula (2):

$$\phi(x,r) = f(x) + r\sum_{j=1}^{n}\frac{1}{g_j(x)} \tag{2}$$

If any of constraint functions $g_j(x)$ approaches 0, the penalty term increases very rapidly. In this method, it is necessary to start the search from an interior, feasible starting point.

Flexible Tolerance Method. The flexible tolerance method was developed by Himmelblau. In this method, $T(x)$ is defined as a positive square root of the sum of squared values of all violated inequalities or/and equality constraints. Formula (3) describes the dependency.

$$T(x) = \left\{\sum_{j=1}^{p}[hj(x)]^2 + \sum_{j=1}^{n}Gj[g_j(x)]^2\right\}^{\frac{1}{2}} \tag{3}$$

A small value of the $T(x^t)$ implies that x^t is relatively far from the feasible region.

Exploratory Methods. The accuracy of this method depends on he density of the grid, that is why we set up the grid with points spaced together close enough to define a minimum, as determined by the inspection of each point (Combinational Method).

Random Search Method (Monte Carlo Method, Modal Method). The value of objective function is evaluated for each point and the best result is taken as the minimum. This method offers two approaches for dealing with constraints. First method: a penalty is used for violating the solution outside the feasible region. In this case, the objective function is evaluated for all generated points. Second method: each generated point is tested for violation and discarded, if it is not a feasible solution. In this case, the objective function is evaluated only for a feasible solution. We select values of x_i – vector of decision variables. Used formula (4):

$$x_i = x_i^k + \rho_i(x_i^u - x_i^k) \tag{4}$$

Usually, this method will locate the solution in the neighborhood of the global minimum.

Method for Discrete and Integer Variables. Solving optimization problems with discrete variables directly is much more difficult than solving similar problems with continuous variables.

1.3. Multi-criterion Optimization Methods

In order to solve the problem, we used the Preference Function Method, described by the formula (5):

$$P[f(x^*)] = \min_{x \in X} P[f(x)] \tag{5}$$

as a Weighting Objective Method, Normed Weighting Objective Method, Global criterion Method, Min-Max Method, Weighting Min-Max Method, Method of Ideal Vector Displacement or Constraint Transformation Method.

1.4. Method of Selecting a Set of Pareto Optimal Solution, Kuhn-Tucker method

The Pareto Optimal Solution based on a random search method.
For Kuhna-Tuckera method we formulate the Lagrange function as a

$$L(x, l) = f(x) - \Sigma \, li \, gi \, (x) \tag{6}$$

The necessary conditions for saddle point of the Lagrange function $L(x, l)$, which have to be fulfilled simultaneously, are as follows:

$$\frac{\partial L}{\partial l_i}\{\geq 0 \qquad 0 < i \leq u\} \qquad \frac{\partial L}{\partial x_j}\{\leq 0 \qquad 0 < j \leq s\}$$

$$\leq 0 \qquad u < i \leq v \qquad \qquad \geq 0 \qquad s < j \leq t$$

$$= 0 \qquad v < i \leq m \qquad \qquad = 0 \qquad t < j \leq n$$

$$l_i \frac{\partial L}{\partial l_i} = 0 \qquad x_j \frac{\partial L}{\partial x_j} = 0 \text{ and for all } i, j \tag{7}$$

1.5. Task description

Criterion functions were: minimum energy consumption for heating F_1, minimum investment costs F_2. Cooling was not analyzed. Such analysis takes several hours [11]. The optimization's decisive variables were: the thickness of wall insulation (thermal resistance of the layer), the size of the glazing on all elevations, the ratio of the sides of the base. Fixed parameters were: thermal resistance on the ground floor, flat roof, building area and ventilation air stream. The analysis' subject was a single-family building; in particular, the ground floor – fixed floor area of 120 m². The boundary conditions limiting the insulation were equal to about 10 [m² K/W] < R < 3.33 [m² K/W].

1.6. Results

Table 1 describes the results of the SPBT [years] and table 2 describes the results from Kuhn-Tucker. Due to the low thickness of the insulation, the SPBT value lies between 15 and 20 cm. This is illustrated by Fig. 1a. The solution method of multi-criteria thickness of the insulation is approx. 36 cm. This is depicted in Fig. 1 b. The difference between the results of both methods is almost 20 cm (one method recommends insulaion twice as thick as the other).

Table 1

SPBT dependence on the type of energy carrier and thickness of insulation

Thickness of insulation [cm]	SPBT [year]		
	coal	gas	electricity
10	122	69	26
20	119	67	25
30	132	74	28

Dependence of thickness x (5) and F1 and F2 (method Kuhn–Tucker)

	F1	314244	314634.6	315174.8	314950.6	314135.6
	F2	5754.035	5739.386	5721.686	5728.87	5724.476
$x(5)$	10–3.33	max	max	max	max	max
$x(6)$	2.5–1	1.119	1.2457	1.23	1.25	1.3069

a)   b)
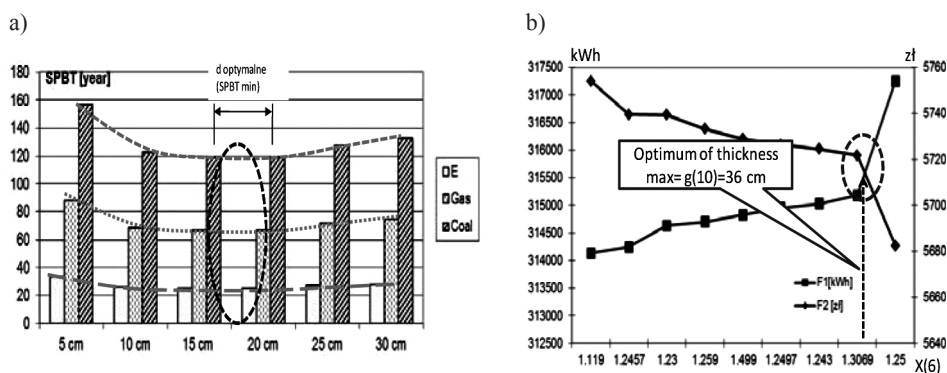
Fig. 1a) The optimal thickness of insulation, SPBT, b) the results of Kuhn–Tucker method

2. Conclusions

1. The SPBT method of choosing the optimum thickness of insulation seems to be only an estimate.
2. The difference in results between the SPBT and multi-criteria optimization methodes is not without significance.
3. It seems that one should apply advanced methods to evaluate the insulation efficiency (as opposed to the simple method which SPBT undoubtedly is).
4. The use of simple and easy ways is not a good choice among the available computational tools.

R e f e r e n c e s

[1] Osyczka A., *Computer aided mulicriterion optimization system (CAMOS)*, *Software Package in Fortran*, International Software Publisher, 1992, 56-58.
[2] Hobler T., *Ruch ciepła i wymienniki*, wyd. 3, WNT, Warszawa 1968.
[3] Bogosłowski W.N., *Procesy cieplne i wilgotnościowe w budynkach*, Arkady, 1985, 63-68.

[4] Recknagel, Springer, Hofmann, Schramek, *Poradnik. Ogrzewanie i klimatyzacja*, wyd. 1, EWFE, Gdańsk 1994, 986-989.

[5] Gordon B. Davis, Thomas r. Hoffmann, *Fortran a structured, disciplined style*, University of Minnesota, McGraw-Hill Book Company, 1970, ISBN 0-07-015901-7, 1978.

[6] Morris H. de Groot, *Optima statistical decisions*, McGraw-Hill, Inc., 122-133, 1981.

[7] Mirkowska G., *Elementy matematyki dyskretnej*, Wyd. PJWSTK, Warszawa 2003.

[8] Findensein W., Szymanowski J., Wierzbicki A., *Metody obliczeniowe optymalizacji*, Wyd. Politechniki Warszawskiej, Warszawa 1974, 158-194.

[9] Kittler R., Mikler J., *Zaklady využivania slnećneho žiarenia*, VEDA, 1986, 32-58.

[10] Kossecka E., Bzowska D., *Obliczanie dobowych sum promieniowania słonecznego na płaszczyzny nachylone przy wykorzystaniu zależności dla współczynników przezroczystości atmosfery*, Materiały konferencyjne KNT Łódź `93, Fizyka budowli w teorii i praktyce, na prawach rękopisu, 45-52.

[11] Dz. U. 2013 poz. 45, Rozporządzenie Ministra Transportu, Budownictwa i Gospodarki Morskiej z dnia 3 stycznia 2013 r. zmieniające rozporządzenie w sprawie metodologii obliczania charakterystyki energetycznej budynku i lokalu mieszkalnego lub części budynku stanowiącej samodzielną całość techniczno-użytkową oraz sposobu sporządzania i wzorów świadectw ich charakterystyki energetycznej.

[12] Jędrzejuk H., Marks W., *O korzyściach z optymalizacji budynków mieszkalnych*, Fizyka budowli w teorii i praktyce, Tom II, 2007, 109-112.

[13] Jędrzejuk H., Marks W., *Evolutional optimization of energy-saving buildings*, Archives of Civil Engineering, LI, 3, 2005, 395-413.

[14] Mikulski L., *Teoria sterowania w problemach optymalizacji konstrukcji i systemów*, Wyd. Politechniki Krakowskiej, Kraków 2007, ISBN: 978-83-7242-440-2.

[15] Jędrzejuk H., Klemm K., Marks W., *Multicriteria optimization of buildings arrangement based on wind criteria*, Archives of Civil Engineering, LIV, 4, 2008, 751-767.

PAWEŁ GUZDEK, PIOTR PETRYK[*]

WATER AND SEWAGE MANAGEMENT IN THE PAPER INDUSTRY

GOSPODARKA WODNO-ŚCIEKOWA W PRZEMYŚLE PAPIERNICZYM

Abstract

The paper industry products are materials formed as a result of a complex series of consecutive processes, which makes this industry branch a very specific and professional. In order to reduce the consumption of excessive amounts of water in papermaking processes, closed circuit water systems are used. An example of a vibrant paper mill is a Paper and Cardboard Factory BESKIDY. The paper factory is supplied with tap and well water, which covers the largest part of water demand. Excess water called as post-production circulation water, is directed to the Factory Sewage Treatment Plant. The process of purification of industrial sewage in Factory of Paper and Cardboard BESKIDY meets the requirements of the Polish Regulation of the Minister of Construction (Journal of Laws of the Republic of Poland of 2006 No.136 item 964), which means waste water – sewage management is properly carried out.

Keywords: pulp and paper industry, Sewage Treatment Plant, hydropulper device

Streszczenie

Produkty przemysłu papierniczego są uzyskiwane jako rezultat kompleksowej serii następują-cych po sobie kolejno procesów, co czyni z tej gałęzi przemysłu bardzo wąską i specyficzną branżę. W odpowiedzi na potrzebę zmniejszenia zapotrzebowania na wodę w procesie produkcji papieru, wykorzystuje się zamknięty obieg wody. Przykładem zakładu papierniczego jest Fabryka Papieru i Tektury BESKIDY. Obiekt jest zasilany wodą wodociągową oraz wodą studzienną, które po-krywają największą część zapotrzebowania na wodę. Nadwyżka poprodukcyjna wody obie-gowej jest przekierowywana do zakładowej oczyszczalni ścieków. Proces oczyszczania wody spełnia wymagania Rozporządzenia Ministra Budownictwa (Dz. U. 2006.Nr 136, poz. 964), co wskazuje na poprawnie przeprowadzony proces oczyszczania ścieków.

Słowa kluczowe: papier i przemysł papierniczy, oczyszczalnia ścieków, hydropulper

[*] M.Sc. Eng. Paweł Guzdek, Ph.D. student, M.Sc. Eng. Piotr Petryk, Ph.D. student, Institute of Water Supply and Environmental Protection, Faculty of Environmental Engineering, Cracow University of Technology.

1. The technological process of paper production

The paper products are materials used every day. Hardly anyone thinks about how great their amounts are consumed in the world, or even in Poland. Those products arise as a result of a complex series of consecutive processes, which makes the industry very specific and professional.

The basic technological processes used in the manufacture of paper products are as follows [1]:
– preparation and grinding of fiber mass,
– preparation of paper pulp,
– forming a paper web,
– compression of paper web,
– drying the paper web,
– finish paper web.

The *processes of preparation and grinding* of the pulp have to process the fiber into a water formed of predetermined concentration. Grinding serves to confer a suitable length and fiber flexibility.

Paper pulp preparation procedure provides for an adequate fiber mass in conjunction with chemicals that after the "mixing, dilution, sorting, cleaning and venting" [1] is directed to the paper making machine.

Forming a paper web of the pulp processing is assumed to form a paper web having certain structural characteristics and dryness.

Compression of paper web leads to partial drying of the paper web and obtaining its smoothness.

Drying the paper web is the post-drying elimination of the aqueous residue from earlier process, and hardening the paper.

The last process, which provides to finish the paper web production includes cooling, optimum moisture, smoothing, followed by winding the paper on a drum, and in a later stage cutting the paper web into the appropriate sizes and packing.

A very important "raw material" in the paper industry is water. It acts as both a basic component of the pulp and is used in technological and operational processes on a paper machine. The problem of water consumption in paper making processes has become an important aspect both environmentally and financial. In order to reduce the consumption of excessive amounts of water, it is used in closed circuit systems. According to Stępień [2], it allows to save up to 80% of the raw water. However, this requires pretreatment of the water in the system. The aim is to recover the raw material supplied in the form of fibers and water for reuse. The most commonly used device that the purification process is carried out within a short time is: flotation, pressure filters, centrifuges and clarifiers.

Similar solutions are offered by K. Imhoff and K.R. Imhoff [3], closing the process of water cycle in paper production system, which limited the consumption of fresh water. Imhoff [3], closing the process water system, limited the consumption of fresh water. Closed circuit also helps in the recovery of cellulose fibers, which can be reused for the production of paper products. K. Imhoff and K.R. Imhoff also propose to neutralize the colloidal suspension by adding e.g. ferrous sulfate.

Closed circuit may also affect the production cycle negatively. As noted by K. Olejnik and K. Kosińska [6] in the initial stage negative effects of the use of the same water again are

not observed. Only after reaching the limit of water consumption per unit of production in the long term, it may result as impaired recycling production processes.

We must remember that outside the water within the circulation as well as water discharges to the sewage treatment plant, technological circuits provide the loss of large amounts of water to evaporation. Despite the developed techniques, the recovery at the present time is not viable [8].

2. Water circulation in the Factory of Paper and Paperboard BESKIDY

An example of an industrial plant specializing in the production of paper products is Factory of Paper and Cardboard BESKIDY. It is the leading European manufacturer of recycled paper towel, ZZ type towel, cardboard fiber textile and cardboard protection floor. Due to the range of offered products, as well as various requirements of process water, the water system in the Factory BESKIDY is supplied in two ways. The basic unit of water supply are water wells.

In addition, in the event of loss of well capacity the water demand is covered with municipal water. Most of the water is recovered, in a closed circuit system technology.

Closed circuit is very beneficial for economic and environmental reasons. The plant significantly reduces water consumption. About 75% of post technological water is recycled, while the remaining 25% of the demand is supplied from external sources.
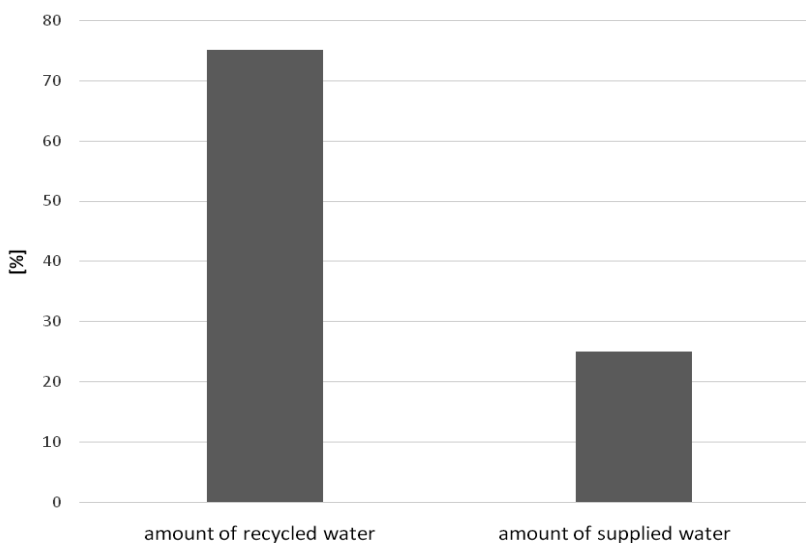
Fig. 1. Scheme amount of water used in the manufacture of paper towel

The technological process of Factory BESKIDY can be divided into two smaller ones. One is responsible for the series production of tissue paper (Fig. 1), while the second is a series of cardboard (Fig. 2).

```
┌─────────────────────┐        ┌─────────────────────┐
│     WELL WATER      │        │      TAP WATER      │
└─────────────────────┘        └─────────────────────┘
           │                              │
           ▼                              ▼
┌──────────────────────────────────────────────────────┐◄───┐
│         HYGIENIC PAPER PRODUCTION CYCLE               │    │
└──────────────────────────────────────────────────────┘    │
                      │                                      │
                      ▼                                      │
        ┌──────────────────────────────────┐                │
        │       ROTARY  WATER TANK          │                │
        └──────────────────────────────────┘                │
    ┌───────────────────│──────────────────────────────────┘
    │          ┌────────▼─────────────────────────┐
    │          │  CONTROL SYSTEM OF RECYCLED WATER │
    │          │            QUALITY               │
    │          └──────────────────────────────────┘
    └──────►┌──────────────────────────────────────┐
            │  SEWAGE TREATMENT PLANT "BESKIDY"     │
            └──────────────────────────────────────┘
```
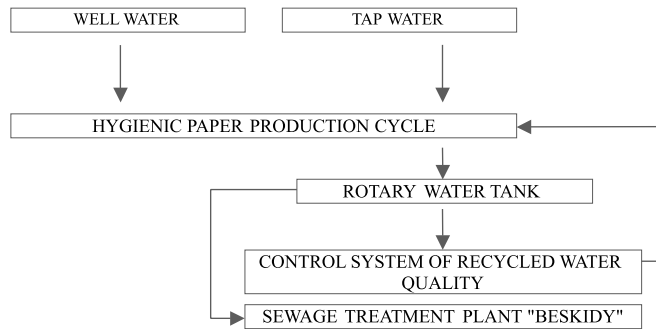
Fig. 2. Technological scheme of the water used in the manufacture
of paper towel

Process water used in the production of paper towel is derived from two sources. The first one is Wadowice Water Supply System, while the second is a factory's deep well. Tap water is used rarely, usually during maintenance and pump failure in a deep well. Well water is added to the paper, which after passing through the device that separates impurities (e.g. sand traps, sorters pressure), directs to the infusion of the paper machine, where the pulp is separated from water using a sieve. This is the first water circuit, in which, after a cleaning cycle in a battery of hydrocyclones and flotation units, water goes back to the production cycle. Well water is also used for maintenance process of a machine (rinsing screen, needle nozzle and fan). Excess water is discharged to Sewage Treatment Plant of BESKIDY Factory.

```
┌─────────────────────┐        ┌─────────────────────────────┐
│     DEEP WATER      │        │ WATER  TREATMENT PLANT "BESKIDY"│
└─────────────────────┘        │           FACTORY           │──┐
           │                   └─────────────────────────────┘  │
           ▼                              │                      │
┌────────────────────────────────────────▼──────────────────┐  │
│ CARDBOARD PRODUCTION CYCLE OF WATER  TREATMENT "BESKIDY"   │  │
│ FACTORY                                                    │  │
└────────────────────────────────────────────────────────────┘  │
      ▲                                   │                      │
      │                                   ▼                      │
┌───────────────────┐        ┌─────────────────────────────┐    │
│     TAP WATER     │───────►│     ROTARY  WATER TANK      │────┘
└───────────────────┘        └─────────────────────────────┘
```
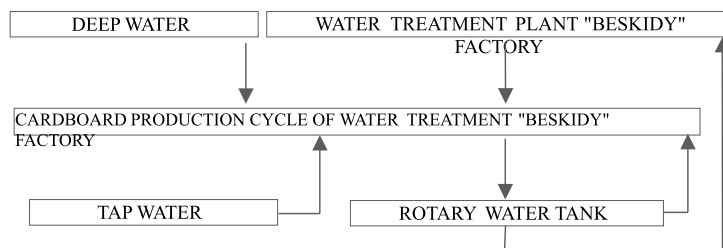
Fig. 3. Technological scheme of water used to produce cardboard

Process water used for the manufacture of cardboard (Fig. 2) is the water coming from the well as along with water pretreated in the Sewage Treatment Plant belonging to the factory.

In the little part of the process, water is used from the Water Supply System. The dominant part of the water used in the production of cardboard comes from industrial wastewater. It is directed to the hydropulper where the raw material is mixed to form a homogeneous steady mass. It is purified on the Rawk's then goes to a screen, where water is separated from the mass. Water drained in a screen is transported to the water tank rotator, where is directed to the hydropulper, and the surplus to the treatment of the factory.

3. Quality of recycled water from pretreated wastewater

"Waste product" is an excess of water from manufacturing processes in paper industry. Its various characteristics require a suitable cleaning process. The results of analysis are presented in Table 1.

Table 1

Qualitative characteristics of the effluents in the Paper and Cardbard Factory BESKIDY with values of Polish Regulation of the Minister of Construction (Journal of Laws of the Republic of Poland of 2006 No. 136 item 964), Source: Paper and Cardboard Factory BESKIDY

Factor	Unit	The value of the factor PCF BESKIDY	J.L. 2006, No. 136, it. 964
pH	[–]	7.3	6.5–9.5
BOT5	[mg $O_2 \cdot dm^{-3}$]	180	700
COD (Cr)	[mg$\cdot dm^{-3}$ O_2]	772	1000
ammonium	[mg$\cdot dm^{-3}$ N]	0.093	200
nitrite nitrogen	[mg N$\cdot dm^{-3}$]	<0.006	10
suspended o.	[mg$\cdot dm^{-3}$]	260	500
volatile phenols	[mg$\cdot dm^{-3}$]	0.012	15
chrome	[mg$\cdot dm^{-3}$]	0.037	1
chrome (VI)	[mg$\cdot dm^{-3}$]	0.03	0.2
zinc	[mg$\cdot dm^{-3}$]	0.14	5
cobalt	[mg$\cdot dm^{-3}$]	0.0076	1
copper	[mg$\cdot dm^{-3}$]	0.013	1
lead	[mg$\cdot dm^{-3}$]	0.0097	1
trichloromethane	[µg$\cdot dm^{-3}$]	<0.4	1
tetrachloromethane	[µg$\cdot dm^{-3}$]	<0.4	1.5
index of mineral oil	[µg$\cdot dm^{-3}$]	0.4	15

The values of qualitative characteristics of waste water obtained from analysis were compared with the guidance of the Polish Regulation of the Minister of Construction (Journal of Laws of the Republic of Poland of 2006 No.136, item 964). The results comply requirements of law regulation therefore were considered as correct.

4. Wastewater treatment plant in Paper and Cardboard Factory BESKIDY

Excess post-technological water of the production of paper and cardboard is directed to internal Wastewater Treatment Plant. At first the industrial "waste water" goes to the lattice. Continuing with the pump P1 it passes through the screen arc, and then is directed to the trap. It is discharged into the reservoir by P2 pumping station and then to the bioreactors. Waste water pretreated in bioreactors is stored in a buffer tank. Next, wastewater is supported by a series of technological processes. At the end of waste water treatment process, excess of post technological water is discharged to the municipal treatment plant.

5. Water consumption in the Factory of Paper and Paperboard BESKIDY

Table 2

Water demand in the Paper and Paperboard Factory BESKIDY Source: PCF BESKIDY

Month	WATER DEMAND FOR THE PRODUCTION in the year 2012			
	Well water		Municipal water	
	m^3			
	cardboard	toilet paper	cardboard	toilet paper
I	5357	6264	122	1786
II	2692	9843	53	645
III	7794	5423	239	732
IV	9175	8505	146	2
V	10975	7282	58	117
VI	22	7770	31	136
VII	4748	6813	53	176
VIII	5926	7872	75	108
IX	8424	6800	42	50
X	150	8251	38	315
XI	7257	6826	50	276
XII	3673	8505	47	25
Total	66193	90154	954	4368

From the data presented in Table 2 it is clear that higher water demand in annual summary is a characteristics of a technological cycle for paper towel. Production of cardboard: in

most cases the annual total has a lower consumption, both for well water and water from the municipal system. Apparent is the dominance of well water in the water management of factory.

6. Conclusions

Sewage water mills management require recirculation of water. Closed circuit and the repeated use of the same volume of water, significantly affect the ecological aspect of water treatment process. Well water sources militate in favor of economic considerations that provides strategic solutions for the production cycle of Paper and Cardboard Factory BESKIDY. The process of purification of industrial sewage in CPF BESKIDY conform the needs of Polish Regulation of the Minister of Construction (Journal of Laws of the Republic of Poland of 2006 No.136, item 964), which indicates a properly conducted waste water – sewage management.

R e f e r e n c e

[1] Przybysz P., *Outline of the paper-making process*, Publisher Progress, Łódź 2011.

[2] Stępień J. (ed.), *The chemical industry*, [in:] *Water and wastewater management in industrial plants*, Arkady Publishing, Warsaw 1973.

[3] Imhoff K.&K.R., *Kanalizacja i oczyszczanie ścieków*, Wydawnictwo Arkady, Warszawa 1982 (City sewer and wastewater treatment, Arkady Publishing, Warsaw 1982).

[4] Regulation of the Minister of Construction 14 July 2006 the obligations of industrial waste and the conditions for discharging wastewater into the sewage system Dz. U. 2006 No. 136, item 964.

[5] http://beskidy-wadowice.pl/

[6] Olejnik K., Kosińska K., *Wpływ jednostkowego zużycia wody świeżej w procesie roz-włókniania i mielenia na ilość substancji stałych i rozpuszczonych w wodzie technolo-gicznej*, Wydawnictwo SIGMA-NOT Sp. z o.o., Przegląd Papierniczy 67, Warszawa, lipiec 2011.

[7] Effect of the specific consumption of fresh water in the reffining and grinding processes on amount of soil and dissolved substances in process water, SIGMA-NOT Publishing, Warsaw 2011, Paper Review No. 67, July 2011.

[8] Michniewicz M., *Najlepsze dostępne techniki (BAT). Wytyczne dla branży celulozowo--papierniczej*, Ministerstwo Środowiska, Warszawa, sierpień 2005.

[9] Best Avaliable Techniques (BAT) – Guadiance for Paper Industry, Ministry of Environment, Warsaw, August 2005.

DOMINIKA KNERA, DARIUSZ HEIM*

TWO METHODS FOR MODELLING OF PHOTOELECTRIC CONVERSION IN ENERGY ANALYSIS OF BUILDINGS

DWIE METODY MODELOWANIA KONWERSJI FOTOELEKTRYCZNEJ W ANALIZIE ENERGETYCZNEJ BUDYNKÓW

Abstract

Nowadays, there is a growing interest in using of renewable energy sources, especially solar energy which can be converted into electricity by photovoltaic panels. In addition to traditional stand-alone photovoltaic systems, more and more new or modernized buildings are equipped with integrated photovoltaic systems (BIPV). The main aim of this paper is to compare two models used to calculate amount of electric power generated by photovoltaic panel. Analysed models were implemented into well-known simulation programs, ESP-r and TRNSYS.

Keywords: photoelectric conversion, mathematical models, simulation

Streszczenie

W dzisiejszych czasach można zaobserwować rosnące zainteresowanie wykorzystaniem źródeł energii odnawialnej, zwłaszcza energii promieniowania słonecznego, która m.in. za pomocą systemu fotowoltaicznego może być przekształcona na energię elektryczną. Poza tradycyjnymi wolnostojącymi panelami fotowoltaicznymi w nowych i modernizowanych budynkach, coraz częściej stosowane są systemy PV zintegrowane z budynkiem. Głównym celem tego artykułu jest porównanie dwóch modeli stosowanych do obliczania ilości energii elektrycznej wytworzonej przez fotowoltaiczny panel. Analizowane modele zostały wdrożone do znanych programów symulacyjnych, ESP-r i TRNSYS.

Sowa kluczowe: konwersja fotoelektryczna, modele matematyczne, symulacja

* M.Sc. Eng. Dominika Knera, Ph.D. Eng. Dariusz Heim, Department of Environmental Engineering, Faculty of Process and Environmental Engineering, Lodz University of Technology.

Nomenclature

λ – ideality factor parameter which define losses caused by imperfections in PV material

a – ratio of solar radiation absorbed in PV material at test conditions

a_T – modified ideality factor

e – charge on an electron, $e = 1.6 \times 10^{-19}$ [C]

q_{sw} – solar radiation absorbed in solar cell [W]

I – current flowing from solar cell [A]

I_D – diode current [A]

I_g – current which flows in solar cell when no light is present [A]

I_L – light current [A]

I_o – diode reverse saturation current [A]

I_{sh} – current through shunt resistance [A]

I_{sc} – short circuit current [A]

k – Boltzmann constant $k = 1.38 \times 10^{-23}$

P – predicted power [W]

P_{max} – maximum power point [W]

R_s – series resistance

R_{sh} – shunt resistance

T – absolute temperature of solar cell [K]

V – voltage of solar cell [V]

V_{oc} – open circuit voltage [V]

1. Introduction

1.1. Modelling the BIPV

Appropriate modelling of a BIPV system in energy simulation software is very complex and difficult. Photovoltaic systems are susceptible to the influence of many environmental factors, such as solar radiation, temperature, angle of incidence and spectral distribution. Moreover, some hard to predict factors also affect the efficiency of the PV cells: ageing, mismatch, soil, dirt, snow and shading [1].

Furthermore, manufacturers provide only basic parameters of their products, for instance the open circuit voltage, the short circuit current and nominal efficiency. All these data are available at standard test conditions, where the irradiance is 1000 W/m^2, the cell temperature is 25°C and spectral distribution equivalent to air mass is 1.5. In reality, PV systems often work under higher temperatures or a lower value of solar radiation. Therefore, efficiency of photovoltaic panels is lower than given by the manufacturer.

On the other hand, photovoltaic modules are characterized by their current versus voltage curve (*I–V* curve) (Fig. 1). The shape of the *I–V* curve is largely dependent on irradiance and temperature [2]. Besides, technology of the solar cell (mono-crystalline, poly-crystalline, thin film or triple junction amorphous) also has influence on electrical characteristics.
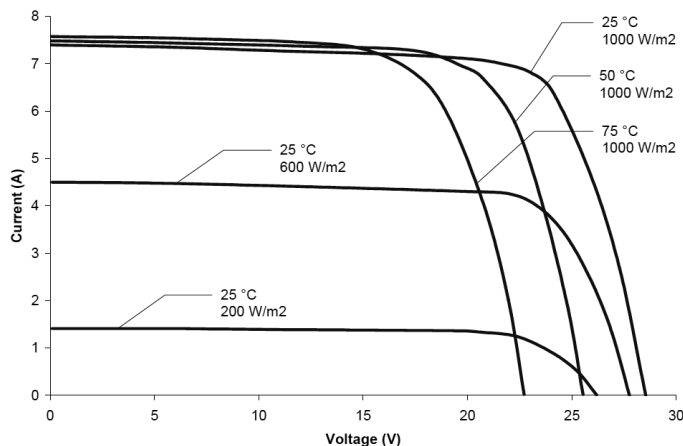
Fig. 1. *I–V* curve characteristic for PV model [1]

1.2. Computational methods

Many different computer programs were developed in order to estimate renewable energy produced from photovoltaic. Methods used to determine photovoltaic conversion can be more or less complex, according to the purpose of its use. Some simple methods take into account constant efficiency of energy conversion to estimate electrical power produced by photovoltaic cells. Others are characterized by very complex approach considering the dependence of conversion efficiency from temperature and intensity of solar radiation. These sophisticated methods include many factors such as cell temperature, radiation, shading as well as the heat exchange with adjacent surfaces and surrounding.

2. The ESP-r PV model

Building integrated photovoltaic components was implemented into ESP-r as a multi-layered construction model. A photovoltaic panel integrated into building facade consists of four layers of material: outer glazing, PV material, resin binder and inner glazing. PV material is formed as a middle layer consisted of a number of solar cells and determine in form of a 'special material'. Moreover, the PV material is a hybrid thermal/electrical component, because solar radiation absorbed by the photovoltaic material is converted simultaneously into heat and electrical energy [3].

A layer of PV material is represented by three thermal control volumes: two outer, mixed-property control volumes and one central, homogenous control volume. The thermophysical properties of each control volume are defined in individual nodes. Central thermal control volume is augmented with electrical control volume due to an additional calculation of the power produced by the PV material. Electrical characteristics of each solar cell, assigned as the electrical control volume, are determined by an equivalent circuit model. The electrical properties for each solar cell are defined as individual node *i* [3].

114

Into ESP-r are implemented three models of photovoltaic systems. Two of them were developed by Kelly (1998): a simple efficiency-based model and a one-diode equivalent model (Fig. 2). The second one is a basic ESP-r model. The calculation of power output are made using short circuit current and open circuit voltage without consideration of the temperature-dependence of these two variables. Hereafter, the basic equations characteristic to one-diode equivalent model describing the amount of power generated by the solar cell are presented.
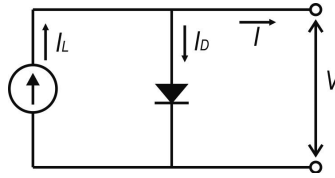
Fig. 2. Simple equivalent one-
-diode circuit [1]

The current balance equation for a solar cell is calculated from Kirchhoff's current law [3]:

$$I = I_L - I_D \tag{1}$$

$$I = \frac{q_{sw}}{a} - I_g \left(\exp\left[\frac{eV}{\lambda kT} \right] - 1 \right) \tag{2}$$

The power output from the individual solar cell can be defined by equation (3), [3]:

$$P = VI = \frac{Vq_{sw}}{a} - VI_g \left(\exp\left[\frac{eV}{\lambda kT} \right] - 1 \right) \tag{3}$$

Third model, applied in 2005 is developed on the more complete equivalent circuit model which contains representation of the series resistance (Fig. 3) [4]. Moreover, it is based on the WATSUN-PV model and considers the dependence of the short circuit current, open circuit voltage and the maximum power point on the temperature [5].

Simulation results for both ESP-r's models were compared with monitored data [4]. It was found that both of them correctly predict the shape of the power versus time curve. However, they over-predict the amount of direct current (DC) power generated at mid-day.

3. The TRNSYS PV model

Power generated by photovoltaic array in TRNSYS can be calculated using 4-parameter or 5-parameter PV model. The 4-parameter model was mostly developed by Townsend

in 1989 and implemented by Eckstein (1990) [6]. The name of the method indicates four independent parameters used in equation of the equivalent circuit: light current (I_L), diode reverse saturation current (I_o), series resistance (R_s) and ideality factor (a_T). The required parameters are generally available from the PV modules producers. Afterwards, the model was improved and developed into a 5-parameter model. Main properties of this model were presented by de Soto (2005) [7, 8]. The power provided by a PV panel is calculated based on a more complex equivalent one-diode circuit model containing shunt resistance (Fig. 3). In the 5-parameter model, in addition to four parameters from previous model, the fifth parameter used to calculate power output is shunt resistance (R_{sh}).
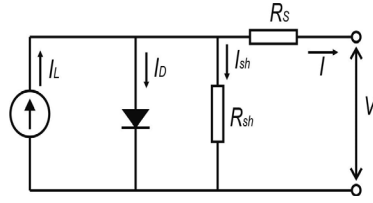
Fig. 3. Equivalent, one-diode circuit
including series of resistance [8]

The current generated in the presented circuit is expressed in equation (4) and more detailed in equation (5), [7].

$$I = I_L - I_D - I_{sh} \tag{4}$$

$$I = I_L + I_o \left(\exp\left[\frac{V + IR_s}{a_T} \right] - 1 \right) - \frac{V + IR_s}{R_{sh}} \tag{5}$$

The power output can be defined by equation [7]:

$$P = VI = V \left(I_L + I_o \left(\exp\left[\frac{V + IR_s}{a_T} \right] - 1 \right) - \frac{V + IR_s}{R_{sh}} \right) \tag{6}$$

Five parameters, used to evaluate the current and voltage in equation (5), are functions of the cell temperature and the solar radiation incident on this cell. Calculation of them is based on parameters obtained from manufacturers, properties of the I–V curve and the derivative of the power at the maximum power point.

Comparison of the 4-parameter and the 5-parameter models carried out in [6] follows that the second model, in contrast to the previous one, is able to calculate the electricity produced by amorphous photovoltaic systems. However, for single crystal and polycrystalline modules, the equations employed in the 5-parameter model reduce to those in the 4-parameter model.

4. Conclusions

Photovoltaic panels are commonly used as integrated systems in new, low energy modern office buildings. However, appropriate design and calculation of their efficiency is very difficult and requires advanced models and simulation techniques. In this paper, the methods implemented in the most popular simulation programs: ESP-r and TRNSYS. Both methods are based on the one-diode equivalent circuit model and correctly predict the power generated by photovoltaic systems.

R e f e r e n c e s

[1] Thevenard D., *Review and recommendations for improving the modelling of biulding integrated photovoltaic systems*, paper presented at the 9th International IBPSA Conference, Montreal, Canada, August 15–18, 2005.

[2] Heim D., *The simultaneous effect of the operating temperature and solar radiation of the efficiency of photovoltaic panels*, Archives of Civil Engineering, LVII, 3, 2011.

[3] Kelly N., *Towards a design environment for building-integrated energy systems: the intergation of electrical power flow modelling with building simulation*, PhD thesis, University of Strathclyde, Glasgow, UK, 1998.

[4] Mottillo M., Beausoleil-Morrison I., Couture L., Poissant Y., *A comparison and validation of two photovoltaic models*, Solar Energy 80, 2006, 78-88.

[5] Thevenard D., Dixon S., Rueb K., Chandrashekar M., *The current-voltage model for PV modules in the WATSUN-PV simulation software*, Proc. 18th Annual Conference of the Solar Energy Society of Canada (SESCI), Edmonton, Alberta, Canada, July 4–8 1992, 39-42.

[6] Fry, Bryan A., *Simulation of Grid-Tied Building Integrated Photovoltaic Systems,* M.S. Thesis, University of Wisconsin-Madison, US, 1998.

[7] De Soto W., *Improvement and validation of a model for photovoltaic array model*, M.S. Thesis, University of Wisconsin-Madison, US, 2004.

[8] De Soto W., Klein S.A., Beckman W.A., *Improvement and validation of a model for photovoltaic array performance*, Solar Energy 80, 2006, 78-88.

MARCIN KOFIŃSKI, AGNIESZKA LEŚNIAK*

PREFABRICATION AS THE CONSTRUCTION SYSTEM OF PASSIVE HOUSE – COST ISSUES

PREFABRYKACJA JAKO SYSTEM BUDOWNICTWA PASYWNEGO – ZAGADNIENIA KOSZTOWE

Abstract

As a response to the growing need for cheaper and more energy-efficient buildings, this paper presents a building system based on a heavy timber frame. The cost analysis to build a wall which meets the requirements for a passive building concludes that a prefabricated heavy timber frame is at the forefront of cost minimization. The recognized advantages of prefabrication can prove that this method of constructing single-family homes, with a positive impact on temperature and humidity, may become an alternative to existing technologies.

Keywords: prefabrication, passive housing, cost analysis

Streszczenie

Prezentowany w artykule system budownictwa prefabrykowanego może być odpowiedzią na rosnące zapotrzebowanie na tańsze i energooszczędne budynki. Przeprowadzona analiza kosztowa wybudowania ściany spełniającej wymagania dla budynku pasywnego lokuje element prefabrykowany oparty na ciężkim szkielecie drewnianym w czołówce pod względem najniższych kosztów. Istniejące zalety prefabrykacji mogą sprawić, że ten sposób budowy domów jednorodzinnych może stać się alternatywą dla istniejących technologii.

Słowa kluczowe: prefabrykacja, domy pasywne, analiza kosztowa

* Marcin Kofiński, student, Ph.D. Eng. Agnieszka Leśniak, Institute of Building and Transport Management, Faculty of Civil Engineering, Cracow University of Technology.

1. Introduction

The ongoing years of active promotion of the idea of passive construction continually bring in new solutions in building systems. The essence of passive construction is to reduce energy consumption as well as pollution. For a building to be considered passive, a number of certain criteria must be met. Consumption of end-use energy at 15 kWh/m²year, consumption of primary energy at 120 kWh/m²year; the U value for walls $U < 0.15$ W/m²K (for detached houses in Poland the recommended $U = 0.1$ W/m²K) and the air-tightness of the building at $n50 = 0.6$ 1/h [2].

Many Polish publications refer to aspects of passive construction [1, 3–6], however, despite intense promotion, numerous subsidies, grants and assistance in design, relatively few people decide to build their houses in a passive standard. Multiple problems, the level of complexity and the cost of construction increased by approximately 15–20% does not convince potential investors, even if the building will use minimal amounts of energy to function during the next 20 years [7].

It is for those reasons that the search for solutions to allow for reduced construction costs continues. One possibility is the use for prefabrication. Financial aspects of using prefabrication in passive construction is the subject of this paper.

2. Prefabrication technology

Prefabrication involves an earlier fabrication of finished building elements in a particular factory and their subsequent transport and assembly at the building site. The greatest developments in prefabrication took place in Poland in the 60s and 70s of the last century [10]. What was valued then was minimalism, high functionality of the building and the simplicity of structure. Prefabrication seemed an ideal solution, due to the capability of producing modular elements which allowed to construct a symmetrical and uniform-looking building. In Poland, despite good designs, execution failed.

The article presents wooden prefabrication which can be used in passive buildings. This solution is relatively new on the Polish market and the technology was imported from Austria and Germany which, in turn, followed the trends in the American building industry.

3. Prefabrication technology based on heavy timber frame [9, 10]

The basis of this prefabrication are wooden beams glued together longitudinally or transversely. The completed wooden frame is boosted from inside with OSB panels and then filled up with hard and heavy mineral wool. The total thickness of insulation amounts to 16 cm, as beams of this thickness are used for prefabrication. Having filled the frame up with mineral wool, the structure is closed by another OSB panel. The outer side of the wall is covered with vapour-proof membrane ensuring air-tightness which is required for every passive building. Plasterboard panels make up the inside first layer which secures the membrane and gives an aesthetic finishing to the interior. The finished construction of the wall has to be appropriately insulated. Such a finished wall (Fig. 1), covered with plaster on

the outside and plasterboard on the inside, is stored vertically with the rest of the partitions of similar size.

Finished walls and ceilings are transported to the building site, where foundations have already been constructed. The outer and inner wall lines are drawn and marked with washers which fit the washers placed on wall elements. Additionally, a separation layer is placed under the walls to prevent contact between wood and concrete. Subsequently, ceilings have to be attached to the finished walls of a particular storey. The ceilings are, like the walls, prefabricated elements brought to the building site. Finished ceiling panels arrive in the form of the constructional layer consisting of beams and mineral wool closed between OSB panels. The remaining layers of the floor are assembled on the site. The indispensable tightness of the partitions is ensured by the continuity of the vapour-proof membrane in the walls and ceilings. The membrane is folded on the edges of all window openings and doorways and its edges are glued to the reveal. 20–30 cm of the membrane are left at the edge of each partition, which is then glued to the membrane of the neighbouring partition. This solution ensures high air-tightness of the building.

The last element of the building is the roof or flat roof. The flat roof is produced like inter-storey ceilings. However, the most frequent solution in Poland is the classic double- or multi-sloping roof. A simple shape of the building, that is rectangular or similar to rectangular, allows to use a prefabricated roof construction, in which the ready-made structure is then laid with roof covering.

1. Drywall
2. Vapor barrier
3. OSB
4. Load-bearing timber construction
5. Mineral wool
6. OSB
7. External insulation glue
8. External insulation
9. Mesh-reinforced plaster base
10. External plaster
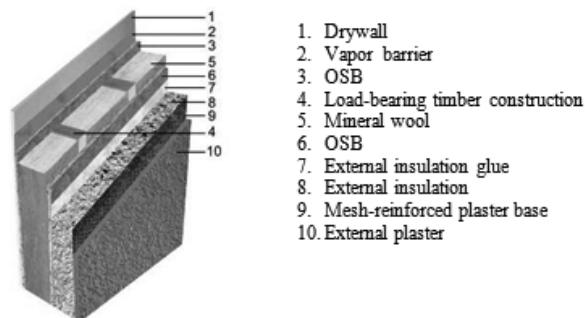
Fig. 1. Cross-section of the prefabricated heavy timber
frame wall construction. Source: [9]

4. Cost analysis

The aim of the economic analysis was to compare the costs of constructing a prefabricated vertical partition with other solutions. For this purpose, various construction layers of the wall and thermal insulation layers were used. The following materials were utilized:

- for the constructional layer: prefabricated timber frame and aerated concrete, slag concrete, silicate, ceramic,
- for thermal insulation layer: polystyrene and mineral wool. For insulation with mineral wool vapour-proof membrane had to be added to ensure appropriate insulation by the material.

To make cost comparison for 1 m² of a wall possible, it was necessary to set such thickness of the insulation layer that the partition received an appropriate U coefficient. Three various values of the coefficient for the partitions were studied: $U = 0.1$; $U = 0.15$; $U = 0.3$ [W/m^2*K]. To determine thermal insulation layer thickness, the formula for R_T – total thermal resistance according to PN-EN ISO 6946: 2008 "Building components and building elements – Thermal resistance and thermal transmittance – Calculation method" is used. The necessary technical parameters of materials have been adopted from the manufacturer's Technical Cards.

The calculated thickness of a thermal insulation layer necessary for the constructional material to provide the appropriate U coefficient is presented in Table 1.

T a b l e 1

The calculated thickness of a thermal insulation

The thermal insulation	The constructional material					
	Prefabricated heavy timber frame wall*	Aerated concrete block Thermalica 36.5	Silicate block Silka E24	Silicate block N24	Ceramic block MAX 220	Slag block Alfa 1/1
The thickness of thermal insulation [m] necessary to provide $U = 0.1$ [W/m^2*K]						
Polistyrene	0.13	0.26	0.41	0.41	0.39	0.40
Mineral wool	0.12	0.24	0.39	0.39	0.37	0.38
The thickness of thermal insulation [m] necessary to provide $U = 0.15$ [W/m^2*K]						
Polistyrene	0.00	0.11	0.27	0.26	0.24	0.25
Mineral wool	0.00	0.10	0.25	0.25	0.23	0.24
The thickness of thermal insulation [m] necessary to provide $U = 0.30$ [W/m^2*K]						
Polistyrene	0.00	0.00	0.12	0.12	0.09	0.11
Mineral wool	0.00	0.00	0.11	0.11	0.09	0.10

* prefabricated wall element presented in chap. 2.1. includes 16 cm thermal insulation (mineral wool).
Source: own study

The table 1 reveals that, in the case of the prefabrication analysed, an additional layer of insulation is necessary only to ensure $U = 0,1$ [W/m^2*K]. Considering the remaining types of walls, the smallest thickness of insulation is required for the wall constructed from Aerated concrete block Thermalica 36.5. On the other hand, in comparison to other solutions, the silicate walls need the thickest insulation layers to meet the parameters assumed.

In the next step of the analysis, the financial data planned were used to calculate the direct costs of wall construction (without plaster). The cost calculation involves only direct costs, that is: labour, materials and the work of the equipment needed to construct 1 m² of a wall.

The standards of material consumption, labour and equipment are in accordance with the books on standard expenditures: KNR, KNNR, KNNR.

Financial basis adopted for the estimate calculation: labour – 16.25 zł/r-g; prices of materials and required equipment taken from the market and the publication ''The prices of factors of production RMS'', Sekocenbud for the fourth quarter of 2013. Costs of purchases of materials are included in the prices of materials.

Table 2 summarizes the costs of constructing a 1 m² wall for the variants adopted previously.

T a b l e 2

The cost of the walls in different variants [PLN/1 m²]

The thermal insulation	The constructional material					
	Prefabricated heavy timber frame wall*	Aerated concrete block Thermalica 36.5	Silicate block Silka E24	Silicate block N24	Ceramic block MAX 220	Slag block Alfa 1/1
Costs [PLN] of a 1 m² wall with the $U = 0.1$ [W/m^2*K]						
Polistyrene	193.74	208.98	280.37	273.35	292.86	253.57
Mineral wool	225.10	300.07	449.68	441.05	449.04	415.80
Costs [PLN] of a 1 m² wall with the $U = 0.15$ [W/m^2*K]						
Polistyrene	155.07	175.38	198.54	192.52	219.14	173.11
Mineral wool	155.07	239.22	301.49	294.67	315.52	275.52
Costs [PLN] of a 1 m² wall with the $U = 0.30$ [W/m^2*K]						
Polistyrene	155.07	96.66	108.32	102.29	128.91	85.88
Mineral wool	155.07	96.66	138.09	131.26	152.11	112.11

* prefabricated wall element presented in chap. 2.1. includes 16 cm thermal insulation (mineral wool).
Source: own study

The analysis of the results presented in Table 1 and 2 reveals that the prefabricated heavy timber frame wall requires the lowest construction costs. Additional wall insulation is necessary only when the U coefficient is to reach the 0.1 [W/m^2*K] value. The greatest difference in costs in relation to the prefabricated heavy timber frame wall is shown by the wall constructed from silicate blocks Silka E24.

The construction costs of the walls when the U coefficient is to reach the 0.1 [W/m^2*K] value are shown in Fig. 2.
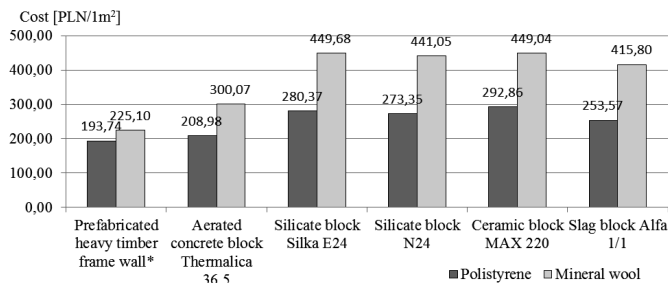
Fig. 2. The costs of constructing a 1 m² wall for the variants when
$U = 0.1$ [W/m^2*K]. Source: own work

5. Conclusions

The economic analysis of outer walls in the single-family house proves that, in comparison to various variants that had been proposed, the prefabricated heavy timber frame wall involves relatively low costs.

The prefabricated construction on a heavy wooden structure is worth considering by the potential investors who would like to build passive houses, as it ensures the required high value of the U coefficient with relatively low costs.

The other advantages of the prefabricated heavy timber frame system are: short construction time resulting from utilizing ready-made prefabricated elements and high air tightness of the building achieved by the vapour-proof membrane in every partition, end-joined and glued with a binder.

R e f e r e n c e s

[1] Dudzińska A., *Komfort cieplny w pasywnym budynku hali sportowej w Słomnikach*, Czasopismo Techniczne z. 3, Budownictwo z. 2-B, 2012, 66-73.

[2] Feist W., Schlagowski G., Munzenerg U., Thumulla J., Darup B.S., *Podstawy budownictw pasywnego*, *Polski* Instytut Budownictwa Pasywnego, 2006.

[3] Firląg S., *Szczelność powietrzna budynków pasywnych i energooszczędnych – wyniki badań*, Czasopismo Techniczne z. 3, Budownictwo z. 2-B, 2012, 105-113.

[4] Gintowt J., *Ekologiczne aspekty budownictwa pasywnego na przykładzie realizacji inwestycji*, Czasopismo Techniczne z. 11, Architektura z. 2-A, 2011, 97-103.

[5] Kisilewicz T., *Budynki pasywne jako ważne ogniwo zrównoważonego rozwoju*, Spraw. Pos. Komis. Nauk. PAN Krak., t. 45, nr 2, 2003, 156-157.

[6] Radoń J., Wąs K., Flaga-Maryańczyk A., Antretter F., *Thermal performance of slab on grade with floor heating in a passive house*, Technical Transactions i. 8, Civil Engineering i. 3-B, 2014, 405-413.

[7] Schlagowski G., *Budownictwo pasywne – Budynki na cztery pory roku*, http://www. surowce-naturalne.pl.

[8] Stopa M., *Wielka płyta nie do ruszenia*, http://www.muratorplus.pl.

[9] http://www.multicomfort.pl

[10] http://www.gebco.pl

KRISTIÁN KONDÁŠ[*]

ILLUMINANCE OF THE WORKING PLANE IN ATTIC SPACES UNDER DIFFERENT EXTERIOR DAYLIGHT CONDITIONS

NATĘŻENIE OŚWIETLENIA NA PŁASZCZYŹNIE ROBOCZEJ W PODDASZU POD RÓŻNYMI ZEWNĘTRZNYMI WARUNKAMI ŚWIATŁA DZIENNEGO

Abstract

The assessment of interior daylight conditions, under the current Slovak standards, is based on the Daylight Factor concept. It means that the worst exterior daylight conditions are reflected in calculations, represented by the CIE overcast sky. Since this evaluation criterion was adopted, several decades have passed. Because the overcast sky is not the only sky type observable in nature, the development of a new criterion, based on photometric variables, e.g. illuminance in lux, became necessary. This article presents a study which investigates the relation between relative and absolute illuminance, in specified points on the working plane illuminated by the standard overcast and clear sky.

Keywords: daylighting, attic room, illuminance, overcast sky, clear sky

Streszczenie

Ocena oświetlenia wnętrz światłem dziennym, w ramach obowiązujących słowackich standardów, opiera się na koncepcji współczynnika oświetlenia dziennego. Oznacza to, że najgorsze warunki oświetlenia światłem dziennym występują przy zachmurzonym niebie, co znajduje odzwierciedlenie w obliczeniach. Od przyjęcia tego kryterium za obowiązujące minęło kilka dekad. Ponieważ niebo zachmurzone nie jest jedynym, obserwowanym w przyrodzie rodzajem nieba, rozwój nowego kryterium opierającego się na zmiennych fotometrycznych, takich jak natężenie oświetlenia w luksach, stał się konieczny. W artykule przedstawiono badania, które określają związek między względną i bezwzględną iluminacją oświetlenia, w określonych punktach na płaszczyźnie roboczej, przy standardowo pochmurnym i bezchmurnym niebie.

Słowa kluczowe: światło dzienne, pokój na poddaszu, natężenie oświetlenia, zachmurzone niebo, jasne niebo

[*] Ing. Kristián Kondáš, Institute of Architectural Engineering, Civil Engineering Faculty, Technical University of Košice.

Denotations

a_v – luminous extinction coefficient
E_v – extraterrestrial illuminance
$E_{v,d}$ – diffuse external illuminance
$E_{v,g}$ – global external illuminance
$E_{v,o}$ – luminous solar constant, 133800 lux
$E_{v,s}$ – direct external illuminance, recalculated on the horizontal plane
J – day of the year
m – relative optical air mass
T_v – luminous turbidity factor
γ_s – solar altitude
ε – factor of eclepticity

1. Introduction

Sunlight plays a very important role in our daily lives. In addition to being associated with the basic processes of the contemporary life on the Earth, as a natural factor it has a significant impact on the physiological functions of the human organism and thus on the quality of the environment in which we are living and working. On the other hand, the uncontrolled amount of direct sunlight may cause thermal or visual discomfort, in some cases both at the same time.

According to the currently applicable standards, all kinds of spaces with permanent occupancy (i.e. work-, school-, residential spaces) have to be illuminated by daylight [1–3]. Daylight in buildings is assessed according to light conditions represented by overcast sky conditions, respecting the CIE overcast sky model. Recently, several models of the sky luminance distribution have been developed. They allow simulating conditions of the clear and also cloudy daylight situations [4–6]. Hence interiors are illuminated by each of them during the 365 days of the year, the Daylight Factor method seems to be at least a non-representative criterion.

The aim of this study is to provide a discussion about the differences of the working plane illuminance levels after CIE overcast- and subsequently CIE clear sky pattern. For this purpose a sample attic room with South orientation has been chosen and the time 12 a.m. on 21st March has been set as default for demonstration of sunlight penetration.

2. Methodology

The task was performed with a simple computer program Velux Daylight Visualizer. Unfortunately the program calculates only the diffuse illuminance under both – overcast and sunny sky condition, so the direct component has to be determined additionally. For this purpose the formulas were used – working on the solar altitude, diffuse ratio $E_{v,d}/E_v$ and luminous turbidity factor.

Generally, the horizontal illuminance on the ground can be expressed as:

$$E_{v,g} = E_{v,s} + E_{v,d} \tag{1}$$

where:

$E_{v,g}$ – global external illuminance,
$E_{v,s}$ – direct external illuminance, recalculated on the horizontal plane,
$E_{v,d}$ – diffuse external illuminance.

To calculate the direct component of the external illuminance the next exponential formula should be used:

$$E_{v,s} = E_v \cdot e^{\left(-a_v \cdot m \cdot T_y\right)} \tag{2}$$

where:

E_v – extraterrestrial illuminance,
a_v – luminous extinction coefficient,
m – relative optical air mass,
T_v – luminous turbidity factor, for clear sky ISO/CEI Type12 can be used value: $T_v = 4$.

The extraterrestrial illuminance represents a solar illuminance incident on the outer limit of the Earth's atmosphere, and in order to calculate its value, the luminous solar constant (illuminance produced by the extraterrestrial solar radiation on a surface perpendicular to the Sun's rays at mean Sun-Earth distance), the factor of eclepticity and the value of the solar altitude are needed.

$$E_v = E_{v,o} \cdot \varepsilon \cdot \sin \gamma_s \tag{3}$$

where:

$E_{v,o}$ – luminous solar constant, 133800 lux,
ε – factor of eclepticity,
γ_s – solar altitude.

The factor of eclepticity can be calculated after the [ISES, 1984] as follows:

$$\varepsilon = 1 + 0.034 \left[360 \cdot \frac{(J - 2°)}{365} \right] \tag{4}$$

where:

J – day of the year.

Thus, to determine the direct component of the external illuminance only two unknowns are left. The first is the luminous extinction coefficient (of the atmosphere) a_v (Clear, 1982) after the formula (5), which expresses the attenuation of the direct illuminance when the sun rays cross vertically the pure and dry atmosphere (Rayleigh atmosphere).

$$a_v = \frac{1}{(9.9 + 0.043 \cdot m)} \tag{5}$$

The second one is the relative optical air mass m (Kasten–Young, 1989) weighed to take account of the relative spectral transmittance characteristics of the atmosphere.

$$m = \frac{1}{\sin \gamma_s + 0.50272 \left(\gamma_s + 6.07995° \right)^{-1.6364}} \qquad (6)$$

Now, the last step, in order to determine the internal illuminance on the working plane, is to sum up the reduced direct component of the external illuminance (by the factor of light transmission, dirt reduction and directional light transmission) and the indirect component of internal illuminance obtained by means of VELUX computer program.

3. The tested room and the location

A sample room was designed as follows: rectangular floor plan, whose dimensions are 4.0 × 6.0 m, where the first measure corresponds to the windows wall (see Fig. 1). The height of the room was adjusted to 2.6 m, whereas the height of the 45° pitched roof's "roofwall" is 0.6 m. The floor has the reflectance of 30%, the ceiling 80% and the average reflectance of the walls is 50%.
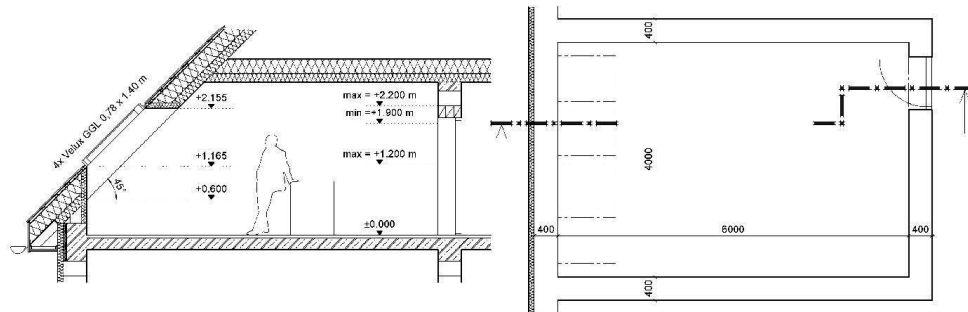
Fig. 1. The section and the floor plan of the tested room

The room is illuminated from one side by four roof windows with dimensions 0.78 × 1.4 m, the glazed area of each window is 0.69 m². The position of the windows was proposed in accordance to the current architectural rules and Slovak standards [4–6]. Thus, the total area of the window glazing is approximately equal to 1/10 of the floor area and their bottom and top edges were proposed within the allowable limits (see Fig. 1).

To calculate the required values of illuminance, the information about the location of the investigated room is also needed. For this purpose the city of Košice with the geographical coordination: latitude 48°43´ N, longitude 21°15´ E was chosen. The best study of sunlight influence on the interior illuminance levels is in an orientation where windows are placed towards the sun, i.e. along the solar meridian. Therefore the time 12 a.m. on 21st March and the orientation of the windows to South was chosen.

4. Test calculations and results

The levels of illuminance for both overcast and clear sky (without the direct component) were calculated by means of the computer program as it is shown in Fig. 2. Spacing between the points of the grid is generated automatically by the program. In our case it is created by the group of 24 points (4 points along the window wall and 6 points along the side wall).
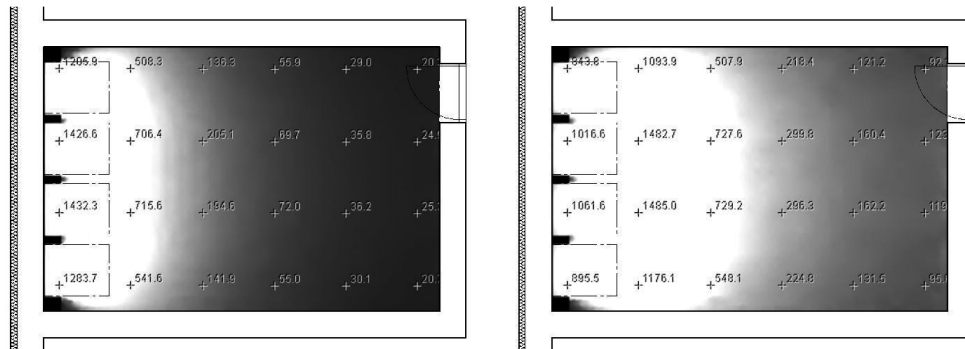
Fig. 2. Values of illuminance for overcast and clear sky (without the direct component)

The levels of global illuminance under clear sky conditions, including the direct component, have to be additionally determined. The positions of points, which are directly illuminated, were determined by calculations (basing on solar altitude) and subsequently by simulation. Fig. 3 leads to a conclusion that considerations were correct, and only the 2nd row of the points is directly illuminated by sunlight.
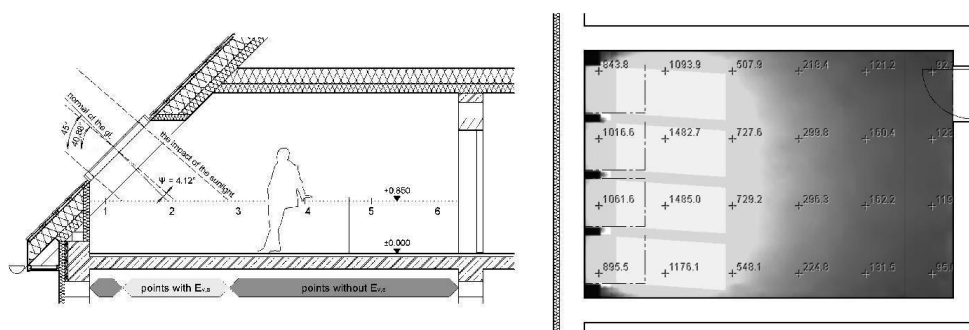
Fig. 3. The positions of directly illuminated points (calculated from the section and simulated in the floor plan)

The value of the factor of light transmission in normal direction for the double glazed window is 0.92^2, the factor of dirt reduction for the outer side of the glass is 0.7 for semi-polluted exterior air and 0.95 for the inner side of the glass for light-polluted interior air.

All results are summarized in the Table 1.

Values of illuminance E[lux] on the working plane

	Points	1	2	3	4	5	6
Overcast sky	1	1205.9	508.3	136.3	55.9	29.0	20.3
	2	1426.6	706.4	205.1	69.7	35.8	24.9
	3	1432.3	715.6	194.6	72.0	36.2	25.3
	4	1283.7	541.6	141.9	55.0	30.1	20.7
Clear sky without $E_{v,s}$	1	843.8	1039.9	507.9	218.4	121.2	92.1
	2	1016.6	1482.7	727.6	299.8	160.4	123.6
	3	1061.6	1485.0	729.2	296.3	162.2	119.9
	4	895.5	1176.1	548.1	224.8	131.5	95.6
Clear sky with $E_{v,s}$	1	843.8	27961.0	507.9	218.4	121.2	92.1
	2	1016.6	28403.8	727.6	299.8	160.4	123.6
	3	1061.6	28406.1	729.2	296.3	162.2	119.9
	4	895.5	28097.2	548.1	224.8	131.5	95.6

5. Conclusions

Sunlight has a significant effect on the human well-being and on the work productivity. In interiors it can also cause disability glare and overheating. The aim of this contribution was to provide a study about the effects of using different sky pattern on interior daylight conditions. The main finding is that the levels of illuminance in points illuminated by direct sunlight are an order of magnitude greater than in other points of the grid, which are illuminated only by diffuse skylight. This finding demonstrates the fact that in nature not only overcast sky conditions occur, but also other sky situations, which should be taken into account in the daylight design.

R e f e r e n c e s

[1] STN 73 4301: 2005, *Budovy na bývanie (Dwelling buildings)*, SÚTN, Bratislava 2005.

[2] STN 73 0580-1: 1987, *Denné osvetlenie budov. Časť 1: Základné požiadavky* (*Daylighting in buildings. Part 1: Basic requirements*), ÚNM, Praha 1987.

[3] STN 73 0580-2: 2000, *Denné osvetlenie budov. Časť 2: Denné osvetlenie budov na bývanie (Daylighting in buildings. Part 2: Daylighting of residential buildings)*, SÚTN, Bratislava 2000.

[4] Perez R., Seals R., Michalsky J., *All weather model for sky luminance distribution – preliminary configuration and validation*, Solar Energy, vol. 50, no. 3, 1993, 235-245.

[5] Kittler R., Darula S., Perez R., *A new generation of sky standards*, Proc. LuxEuropa Conf., Amsterdam 1997, 359-373.

[6] ISO 15409:2004/ CIE S 011/E:2003. *S*patial distribution of daylight – CIE Standard General Sky, 2004.

KATARZYNA KRAJEWSKA, MAJA ŚLIWIŃSKA, JOLANTA GINTOWT*

DESIGNING OF PASSIVE RESIDENTIAL BUILDINGS – CASE STUDY

PROJEKTOWANIE PASYWNYCH BUDYNKÓW MIESZKALNYCH – STUDIUM PRZYPADKU

Abstract

This paper describes the process of designing the passive residential buildings. The analysis is carried out on the basis of the Mannheim project, created as an entry for the Isover competition – Multi-Comfort House. Particular steps of the design process are analyzed for meeting the requirements of passive standard building. The specific solutions adopted in the Mannheim project are presented as an example.

Keywords: passive, residential, design, Mannheim, low-energy, passive house

Streszczenie

W artykule opisano proces projektowania pasywnych budynków mieszkalnych. Analizę przeprowadzono na podstawie projektu stworzonego w Mannheim do konkursu Isover Multi-Comfort House. Poszczególne etapy procesu projektowania są analizowane pod kątem spełniania wymogów określonych w standardzie budynku pasywnego. Szczegółowe rozwiązania przyjęte w projekcie Mannheim przedstawiono jako przykład.

Słowa kluczowe: pasywny projekt mieszkaniowy Mannheim, energooszczędny, dom pasywny

* Eng. Katarzyna Krajewska, Eng. Maja Śliwińska, M.Sc. Eng. Jolanta Gintowt, Institute of Building and Materials and Structures Management, Faculty of Civil Engineering, Cracow University of Technology.

Symbols

λ – heat conductivity coefficient
G – solar energy transmittance of glass
R – thermal resistance
U – overall heat transfer coefficient

1. Introduction

A passive building is an ultra low-energy building, where heat losses are minimized to the extent, when additional heat source is no longer necessary [1]. The annual heat requirement is equal to or less than 15 kWh/m²/year and the primary energy requirement is less than 120 kWh/m²/year. The standard is not confined to residential properties; several office buildings, schools, kindergartens and sports facilities have also been developed to the passive standard.

The project described in this paper was created as an entry for the Isover Multi-Comfort House competition. The main scope of the competition was to design residential buildings on the given site in Mannheim (Germany), while fulfilling the passive buildings' requirements. The features taken into account – apart from energetic requirements – included sound insulation, ease and time of construction, fire protection, architectural design and landscaping of the area. The assignment was to create a project of four buildings, accommodating 150 or less apartments and having the gross floor area of approximately 10440 m². The orientation of the site is North-East, the site has a triangular shape, with the longest side of triangle facing North.

2. Analysis of site and location

The process of designing every building starts with the analysis of site's orientation and possible building's location [3]. In case of passive buildings, the orientation is crucial, in terms of heat gains through the solar energy. If there is a possibility of choosing the site's shape and location, the most efficient is a flat or South-sloping site, free of obstructions to the South. The shape of the site should allow accommodating a relatively large southern wall. The principle is that the majority of windows should be located on the southern façade – it will maximize the heat gain through the solar energy and therefore its year-round temperatures and comfort. On the other hand, the number of transparent openings on the northern façade should be minimized or not used at all in order to maintain the highest wall insulation possible. The leaning walls were oriented South and the shorter base South-West, which was much more efficient in terms of solar energy, than the rectangular shape. The form of trapeze had to be modified in order to obtain a shape with no acute angles, which are disadvantageous in terms of insulation.
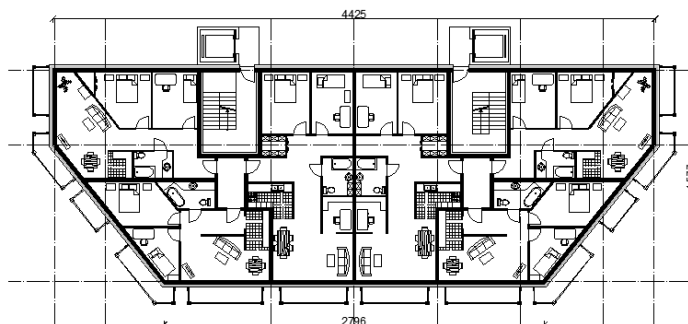
Fig. 1. First floor plan of the Mannheim building

3. Building layout

In the Mannheim project the residential building had to be planned with ca. 6 flats on each floor, which meant the need to provide as much daylight to every flat as possible, while maintaining the northern wall of the building with as little window openings as possible. In addition the vertical transport zone with the elevator shaft had to be planned. Such task led to several problems – first, the transport zone had to be placed. The simplest solution in terms of delivering daylight to all apartments would be to place the core in the center of the building. However, such solution is not acceptable for passive building – the elevator shaft does not fulfill the air-tightness regulations, therefore it has to be placed outside of the insulated part of the building. Due to space restrictions placing the elevator shaft along with the staircase outside of the mass of the building was not possible. The solution applied in the project consisted of the heated staircase placed within the building and non-heated elevator shaft placed outside. Such design allowed maintaining a simple line of the thermal insulation and was space-efficient, however required heating the staircase, which could generate additional costs.

4. Thermal insulation

Thermal insulation is one of the most important features of a passive building. Obtaining the correct U-value of exterior walls and ceilings is essential for controlling heat loss and gain. The most important principle is that the thermal insulation must be of highest quality and must form a closed and continued building envelope. The form of a passive building should be as compact as possible. Required and recommended values of λ are shown in Table 1. In case of Mannheim project, the prefabricated concrete system VST was used as a structure of whole building. The insulation of the exterior walls was designed as a 25 cm layer of Isover Multimax. On the flat roof, a 32 cm layer of Isover Export was used. Such solution allowed obtaining the U-factor equal to 0.10 W/m²K for both flat roof and exterior walls (Table 1). The occurrence of thermal bridges has significant influence on the performance of the building

envelope [1, 2, 4–9]. The problem of thermal bridges has been solved using typical solutions for passive buildings. Separate steel supporting structure for balconies allowed to get rid of cold bridges in connection between walls and balcony slab. To assure correct connection between insulation of vertical walls and slabs, the insulation blocks with heat conductivity as low as 0.2 W/mK were used.

T a b l e   1

U-value [W/m²K] for non-transparent exterior partitions in Mannheim building

Partition type	U-value [W/m²K]	Thickness and type of insulation	Total partition thickness
Exterior wall	0.105*	25 cm Isover MULTIMAX 30 $\lambda = 0.03$ W/mK	53.5 cm
Flat roof	0.10*	32 cm Isover EXPORIT $\lambda = 0.035$ W/mK	51.5 cm
Slab above unheated basement	0.127*	15 cm Isover TOPDECK $\lambda = 0.032$ W/mK	46 cm
* Required value: 0.15 W/m²K recommended value: 0.10 W/m²K of U-value.			

5. Windows and glazing

Windows and doors can account for more heat gain or loss than any other element in an insulated building envelope. A well designed glazing system can improve internal daylight levels, reduce glare, and help maintain thermal comfort by reducing heat gain and loss. This contributes to energy efficiency by reducing the need for artificial heating, cooling or lighting.

By considering the transmission of heat and light through the glazing system at the design stage of the project, the window performance can be significantly improved.

Maintaining the heat loss through windows and glazing as low as possible is essential for obtaining good results in thermal calculations of the building. Windows used for passive buildings are required to have low heat conductivity (low U-value), as well as high solar energy transmittance of glass. Special types of windows are produced with insulated frames, as well as double or triple glazing and argon filling. Such solution assures excellent performance of windows (U-value even as low as 0.6 W/m²K) and maintains the temperature of interior surface close to the air temperature in the room. Apart from type, the windows size plays significant role in heat gains and losses. On the southern wall, the area of glazing should be as big as possible, as the windows deliver more energy than they cause heat losses. The optimal glazing area for south facing façade is 60% of whole wall area, however the quality of glazing is far more important than quantity.

The windows used in Mannheim building are double glazed, argon filled VADB Plus 550+ windows with glazing of U_g-value of 0.7 W/m²K, fixed in insulation layer. The approximate area of the southern wall glazing is 50% of wall surface. Initially windows with less effective features have been assumed, however after performing the calculations in PHPP package it turned out, that the results were not sufficient. Only changing the type of the windows had a significant effect on the results, while enlarging the area of glazing did not change the results in a meaningful way. The calculations proved that the type of the window is the key feature in glazing design.

6. Analysis of shading

Shading should be designed to take into account the sun's path in summer and winter. Diversity of sun shades, blinds and eaves should be used in order to control the transfer of solar energy into the building. In order to avoid the possibility of over-heating the rooms in summer – when the sun position is high – the system of sun protection should be used. On the other hand, during winter – the solar energy is desired and helps to heat the room. System of sun protection should be designed after carrying out shading analysis of the building, including such factors as sun position, as well as possible surrounding obstacles shading the building. Vegetation could be helpful in shading design – it causes shading in summer, when the leaves are growing and passes the sunlight in winter.

The shading in Mannheim building has been assured by balconies – placed on the southern wall – which served as eaves in summer, and in winter did not block the sun in its lower position. Additionally, the moving, fixed on rollers sun blinds have been used to allow users of flats to control the quantity of sunlight coming through to the rooms. Climbing plants – such as clematis or vine – planted on balconies serve as 'vegetative' blinds in summer.

7. Airtightness

Building envelopes under the passive standard are required to be extremely airtight compared to conventional constructions. Airtightness is achieved through air barriers, careful sealing of every construction joint in the building envelope and sealing of all service penetrations. In airtight building the air flow is easier to control. The building is also more resistant to humidity – its acoustic parameters are not influenced by gaps in structure and heat losses are smaller. Airtightness is controlled by blower door test, in passive buildings the requirement of airtightness 0.6 h⁻¹ has to be kept.

In Mannheim building, the airtightness has been assured by variety of means. In residential buildings of more than 4 floors an elevator is required, however it cannot be used in a passive airtight building – since elevator shaft is not possible to insulate. That issue was solved by designing the building layout with elevator on the outside of the building. Every joint and connection in the structure have been analyzed and designed with precision regarding airtightness and thermal bridges. Additionally, the chosen window type also fulfilled the passive standards. Blower door test produced the result of result of 0.6 h⁻¹, which is a required value for building developed to a passive standard.

8. Heat recuperation and ventilation

As passive buildings are exceptionally airtight, the use of mechanical ventilation is required in every design. Ventilation serves mostly as a source of fresh air – essential for well-being and health of building's users. Recommended plan of ventilation comprises possibly short and not branched ventilation ducts. Air speed at normal usage must not exceed 3 m/s in any duct. Heating of passive house is dependent on climate zone – in temperate climate, a heat recovery system is necessary, as insulation alone would not be sufficient to warm the house in winter. There are several types of heat recovery systems, all of which however, have to meet the requirement of minimum 75% heat recovery rate.

The system assumed in calculations for Mannheim building is an internal heat recovery ventilation system, with 75% heat recovery rate and easy reach to every flat.

9. Conclusions

Designing a passive building involves multiple tasks and problems, which have to be solved in order to obtain a passive standard building. Designing a residential building raises even more complex issues, which have to be faced. However – with materials and solutions available today – every residential building can be a passive standard building.

R e f e r e n c e s

[1] Feist W., Munzenberg U., Thumulla J., Darup S.B., *Podstawy budownictwa pasywnego*, Polski Instytut Budownictwa Pasywnego, Gdańsk.

[2] Feist W., Pfluger R., Kaufmann B., Schneiders J., Kah O., *Pakiet do projektowania budynków pasywnych 2007. Wymagania dotyczące budynków pasywnych sprawdzanych pod względem jakościowym*, Passivhaus Institut, Darmstadt.

[3] Klemm K., *Wpływ zmian w układzie zabudowy na przepływ powietrza,* Fizyka Budowli w Teorii i Praktyce, Wyd. Politechniki Łódzkiej, Tom VI, Zeszyt 2, 2011.

[4] Jurkiewicz P., *Dom pasywny. Budowa domu pasywnego z zastosowaniem popularnych rozwiązań budowlanych,* Murator plus.pl.18/10/2012.

[5] Feist W., *Passive House in Darmstadt-Kranichstein*, 1998/2nd International Passive House Conference in Düsseldorf.

[6] *Energy Balances with the Passive House Planning Package*; Protocol Volume No. 13 of the Research Group for Cost-efficient Passive Houses, 1st Edition, Passive House Institute, Darmstadt 1998.

[7] Ebel W., Feist W., *Ergebnisse zum Stromverbrauch im Passivhaus Darmstadt-Kranichstein* in "Stromsparen im Passivhaus"; Protokollband Nr. 7 zum Arbeitskreis Kostengünstige Passivhäuser; PHI; Darmstadt 1997.

[8] *Energy balance and temperature characteristics*, Protocol Volume No. 5 of the Research Group for Cost-efficient Passive Houses, 1st Edition, Passive House Institute, Darmstadt 1997.

[9] Feist W., Loga T., *Comparison of measurements and simulation,* in "Energy balance and temperature characteristics", Protocol Volume No. 5 of the Research Group for Cost-efficient Passive Houses, PHI, Darmstadt, January 1997.

JULITA KRASSOWSKA[*]

EFFECT OF FIBERS REINFORCEMENT ON SHEAR CAPACITY OF DOUBLE SPAN REINFORCED CONCRETE BEAMS

WPŁYW DODATKU ZBROJENIA ROZPROSZONEGO NA NOŚNOŚĆ STREF ŚCINANIA W DWUPRZĘSŁOWYCH BELKACH ŻELBETOWYCH

Abstract

Fifteen double-span reinforced concrete beams (RC) with the addition of dispersed reinforcement were examined to determine the effect of the reinforcement on the shear resistance at the support area. Asalt fibers, whose mechanical properties (especially high tensile strength) have a beneficial effect on the behavior of components under load were used. Beams were subjected to a constant load forces gathered in the middle of the span of each bay. The study aimed to determine the deflection of beams, measuring the crack width perpendicular and diagonal capacity and determination of shear and/or bending. Almost all the beams have reached a shear failure mode. The addition of basalt fiber in each of a series of research results in diverse growth destructive force beam and a corresponding increase in the lateral force on the supports. The maximum strength increase of at 54%, as compared to the reference beam without the fibers was observed for the beam A-III 50/50.

Keywords: *basalt fiber reinforced concrete, BFRC beams, steel stirrups, shear capacity*

Streszczenie

Zbadano piętnaście żelbetowych belek dwuprzęsłowych z dodatkiem zbrojenia rozproszonego w celu określenia wpływu tego zbrojenia na nośność na ścinanie stref przypodporowych. Wykorzystano włókna bazaltowe, których właściwości mechaniczne (głównie wysoka wytrzymałość na rozciąganie) wykazują korzystny wpływ na zachowanie elementów pod obciążeniem. Belki poddano stałemu obciążeniu siłami skupionymi w środku rozpiętości każdego przęsła. Badania miały na celu określenie ugięcia belek, pomiar szerokości rys prostopadłych i ukośnych oraz określenie nośności na ścinanie i/lub zginanie. Niemal we wszystkich belkach osiągnięto model zniszczenia poprzez ścinanie. Dodatek włókien bazaltowych w każdej z serii badawczych powoduje zróżnicowany przyrost siły niszczącej belkę i odpowiedni przyrost siły poprzecznej na podporach. Maksymalny przyrost siły wynoszący 54%, w porównaniu do belki referencyjnej bez włókien zaobserwowano dla belki typu A-III 50/50.

Słowa kluczowe: *fibrobeton, włókna bazaltowe, belki żelbetowe, nośność na ścinanie*

[*] M.Sc. Eng. Julita Krassowska, Department of Building Structures, Bialystok University of Technology.

1. Genesis of fiber reinforced concrete

A long time ago, cut straw or hair calf were added to the manufacturing process of clay, then there were already-banned asbestos fibers. In 1910, the idea of adding small steel wires which were to improve the homogeneity of thick reinforced concrete rods. After more than 50 years, Romuldi and Batson seriously took up the addition of steel fibers [1]. Their argument for improving the properties of concrete with the addition of steel fibers holds true and has been confirmed in a number of test results. We know that the fibers prevent initiation of cracks and prevent their propagation, increase tensile strength and toughness of concrete. The development of materials technology has allowed for the production of fibers with new materials, such as synthetic (polypropylene, aramid fibers), glass, carbon and basalt. Depending on the characteristics of the fibers, they fulfill different functions and have an extensive range of applications. Most relevant to the construction industry are steel fibers. They are affordable and have good material parameters (high tensile strength, high modulus of elasticity). Modern basalt fibers coated with polymers may also work effectively in building construction. The modulus of elasticity is greater than the cement matrix and the tensile strength is three times greater than the steel fibers [2].

Numerous studies have shown that the use of steel fibers in RC beams can enhance their shear and flexural capacity. In support regions of the beams the presence of fibers can resist diagonal tensile stresses and bridging tensile diagonal cracks. Some previously undertaken studies concerned simply supported SFRC beams showed that steel fibers can be used in RC beams as a replacement of shear diagonal or vertical shear reinforcement.

In Poland, there are many studies on the use of extruded fiber. Silesian University of Technology has been tested reinforced concrete flat slabs, in which fiber supplement showed a significant increase in capacity [3]. Research conducted by J. Katzer indicates that fibers have a beneficial effect on fatigue and shock [4]. Pogan found that the addition of fibers in concrete construction leads to a reduction of longitudinal steel reinforcement bars, as well as the transverse reinforcement stirrups [5]. Studies on the reduction of shear reinforcement by the addition of steel fibers for concrete have been carried out in the USA by Dinh and others [6] and last time in Canada in the McGill University [7].

However, only very few experimental tests have been conducted on the RC two span beams with non-metallic fibers, especially with basalt fiber reinforced polymers BFRP, having very high resistance against corrosion.

It should be noted that the behavior of BFRP beams with steel flexural and shear reinforcement is not fully understood due to a very complex mechanism of failure, depending on several material and load factors, such as fiber properties and content in the concrete mix and also on the ratio of steel longitudinal and shear reinforcement. Therefore, for the structural use of BFRP in the RC beams, proper tests are required to clarify the effects of basalt fibers on the shear and flexural response of two span beams.

2. Assumptions for the experimental studies

A two-span beam with fiber reinforcement as an alternative to traditional reinforcement stirrups was used as the research case study. Five test series, based on the spacing of stirrups (Fig. 1), were designed. In the first series of A-I 100/100 stirrup spacing, designed in

accordance with PN-EN, each subsequent series of stirrups amount was reduced by 50%, until the last series of A-V 0/0, which is without stirrups [8]. All beams have the same structure of the longitudinal reinforcement and dimension $80 \times 160 \times 2000$ mm The research program assumed concentrated load in the middle of each span. Shear ratio is a/d = 2.89. The concrete contains two different amounts of fibers: the first type of concrete contained 2.5 kg/m^3 basalt fibers tested for compressive strength $f_{c,\text{cube}}$ = 30.80 MPa and tensile strength of f_{ctm} = 4.65 MPa, the second 5 kg/m^3 of $f_{c,\text{cube}}$ = 31.90 MPa and f_{ctm} = 5.89 MPa. In addition, the reference beam (without fibers) is tested for compressive strength $f_{c,\text{cube}}$ = 28.0 MPa and tensile strength of f_{ctm} = 4.01 MPa. Fiber reinforcement was finally added to the concrete and mixed for a few minutes until a uniform distribution of fibers could be seen. Even though good workability was obtained for all mixtures, fiber congestion was observed along the flexural reinforcement if the clear spacing between reinforcing bars was substantially less than the fiber length. Basalt fibers had a diameter of 20 μ and a length of 50mm. The fiber density is 2.65 t/mm^3. High tensile strength and Young's modulus 1680 MPa 90 GPa was observed. Basalt fibers are resistant to corrosion and acid and also to alkaline environment. They are characterized by resistance to high and low temperatures from –260°C to +750°C. They are coated with a polymer affecting the optimum adhesion to concrete. An additional advantage of fiber is its high hardness (8.5 Mosh), which greatly affects the increase in concrete's resistance to abrasion. Material is 100% organic. The big advantage of basalt fiber, as compared to steel fiber, is its low weight (3 times lighter than steel).

The overall behavior of the test beams was evaluated based on their crack distribution, average shear stress (load) versus displacement response, ultimate strength, failure mode, and strain field in the critical shear span. At each load level, deflection, deflection in the compression zone and the layout and width of the opening figure were measured.
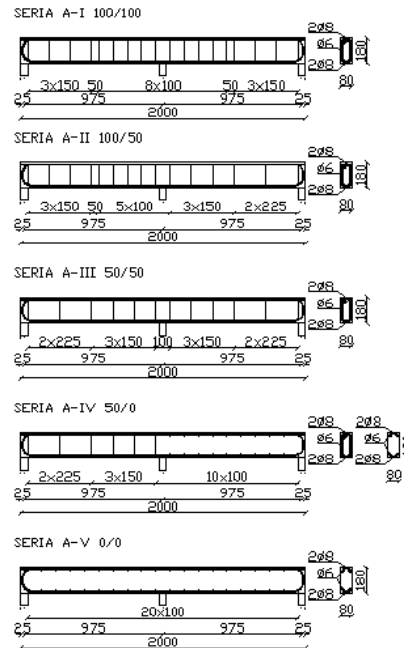
Fig. 1. Schematic of the reinforcement bars research

3. The test results

Table 1 shows the experimental braking forces and their growth. While short-term studies measured stress reactions at the supports, internal and total failure load,the presence of basalt fibers in each series showed an increase of destructive forces, and the according reaction. Table 1 shows the results of the destructive forces and their growth compared to the values obtained for the destructive forces of the reference beams Maximum increase the critical load is 54% for a series of A-III 50/50 5 kg/m^3 fiber content. The increase in shear strength was significant when basalt fibers were added in a 5 kg/m^3 fraction compared to the beams with no fibers.

T a b l e 1

Ultimate forces and their percentage increase for each test series

SERIES	AMOUT OF FIBRE [kg/m^3]	ULTIMATE FORCE [kN]	INCREASE IN FORCE [%]
A-I 100/100	0.0	80.6	–
	2.5	95.3	18.2
	5.0	106.7	32.4
A-II 100/50	0.0	57.8	–
	2.5	70.2	21.5
	5.0	75.3	30.3
A-III 50/50	0.0	60.7	–
	2.5	69.3	14.2
	5.0	93.5	54.0
A-IV 50/0	0.0	29.9	–
	2.5	33.5	12.0
	5.0	44.1	47.5
A-V 0/0	0.0	33.1	–
	2.5	37.9	14.5
	5.0	49.4	49.2

Beams of each series were destroyed by shear. Diagonal crack appeared with section where a smaller amount of stirrups at higher shear strength was used. Figure 2 shows a model of the destruction of the beams. There are three types of damage to beams: diagonal tension, a combination of diagonal tension and shear-tension and a combination of shear-

compression and shear-tension. For the failure mode that was considered: a combination of shear-compression and shear-tension failures, the widening of the critical crack started at the reinforcement level and extended upwards, toward the loading point. Beam failure was triggered by the crushing of the concrete in the beam compression zone adjacent to the loading point, accompanied by a significant splitting along the top layer of longitudinal tension reinforcement.

The crack patterns for the RC and BFRC beams were distinctly different. While the RC beams without transverse reinforcement exhibited a single inclined crack followed by a brittle shear failure, all BFRC beams showed at least two diagonal cracks. The presence of fibers, however, allowed the development of multiple diagonal cracks and the widening of at least one of them prior to a shear failure, which provided some warning about the imminence of failure. Even for these beams the failure was rather sudden.
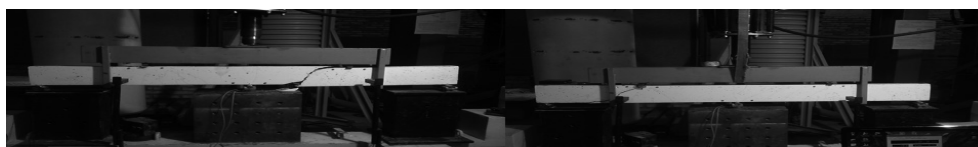
Fig. 2. Shear failure of the beams

4. Conclusions

The following conclusions can be drawn from the results of this experimental investigation. The use of basalt fibers in a mass fraction greater than or equal to 5 kg/m^3 led to an enhanced inclined cracking pattern (multiple cracks) and improved shear strength in beams without stirrup reinforcement. The increase in shear strength associated with an increase in fiber content beyond 2.5 kg/m^3 by mass, however, was relatively small. A comparison of the behavior of the BFRC beams with that of the RC beam with stirrup reinforcement satisfying the minimum requirement indicates that basalt fibers evaluated in this investigation, when used in a mass fraction greater than or equal to 2.5 kg/m^3, can be used in place of the minimum stirrup reinforcement.

Pilot studies conducted on the model: BFRC two span beams with different steel stirrups, clearly showed a beneficial effects of basalt fibers on BFRC beam behavior under short time loads. The addition of basalt fibers in each of a series of tested beams visibly influenced destructive forces and the corresponding values of support reactions. The maximum increase of ultimate load, equal to 54% compared to the reference beam without basalt fibers, was observed for the beam of Series A-III 50/50 with fiber content of 5 kg/m^3.

Further experimental and numerical studies are planned to clarify the use of BFRC double spans beams on full scale.

References

[1] Jamroży Z., *Drutobeton,* skrypt dla studentów wyższych szkół technicznych, Politechnika Krakowska, Karków 1985.

[2] http://www.fiberbet.eu/fiberbet.html

[3] Hulimka J., *The support zone of reinforced concrete flat slab with increased capacity to raise*, Silesian University of Technology Press, Gliwice 2009.

[4] Katzer J., *Shaping properties of selected fibro cement composites*, Bialystok University of Technology Publishing House, Białystok 2010.

[5] Pogan K., *Wzmacnianie konstrukcji kompozytami*, FRP, Inżynier Budownictwa 2010.

[6] Dinh H.H., Parra-Montesinos G.J., Weght J.K., *Shear Behavior of Steel Fiber – Reinforced Concrete Beams without Stirrup Reinforcement*, ACI Structural Journal, September–October 2010, 597-607.

[7] Aoude H. et all., *Response of Steel Fiber- Reinforced Concrete Beams with and without Stirrups*, ACI Structural Journal, May–June 2012, 359-367.

[8] PN-EN 1992-1-1 Design of concrete structures. Part 1-1: General rules and rules for buildings, 2004.

MICHAŁ MARCIN KRÓWCZYŃSKI*

INNOVATIVE ANALYSIS METHODS OF REINFORCED CONCRETE STRUCTURES:THE STRUT AND TIE METHOD

NOWOCZESNE METODY ANALIZY KONSTRUKCJI ŻELBETOWYCH: METODA STRUT AND TIE

Abstract

The paper is devoted to the strut-and-tie method (STM) which is used for analysis and design of reinforced concrete structures. The most important and valuable information about the STM has been gathered and the example that applies to the method has been presented.

Keywords: strut-and-tie method, corbels, reinforced concrete structures

Streszczenie

Metoda strut-and-tie służy do lokalnych analiz konstrukcji żelbetowych dla obszarów z silnymi nieciągłościami, w których założenie o liniowym rozkładzie naprężeń nie jest spełnione. Innowacyjność metody polega na wykorzystaniu zasad teorii plastyczności oraz założeń odnoszących się do transferu sił z prętów zbrojeniowych na beton. W artykule zaprezentowano aspekty teoretyczne metody oraz przedstawiono przykład jej zastosowania do wymiarowania krótkich wsporników. Otrzymane rezultaty porównano z wynikami analizy alternatywną metodą belkową.

Słowa kluczowe: metoda strut-and-tie, krótkie wsporniki, konstrukcje żelbetowe

---

* M.Sc. Eng. Michał Marcin Krówczyński, Ph.D. student, Cracow University of Technology..

1. Introduction

The strut-and-tie method (STM) is nowadays considered to be a powerful tool for the analysis by the limited stages of reinforced concrete structures with non-linear stress distribution. Although STM can be applied to all parts of reinforced concrete structures, it is usually applied to regions of stress discontinuities (*D*-Regions). *D*-regions which are not governed by Saint-Venant's principle are located near abrupt changes in geometry, openings, concentrated forces, anchorage zones etc.
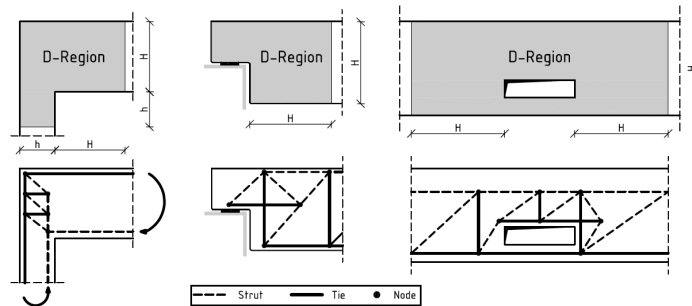
Fig. 1. Typical D-Regions and corresponding strut-and-tie models

The innovation of the method is the usage of plasticity principles and assumptions regarding the flow of forces in reinforced concrete structures. The STM is based on the lower-bound theory of the limit analysis. The strut-and-tie model is a statically admissible stress field in lower bound (static) solutions. The total capacity of a strut-and-tie model is always smaller or equal to the real capacity of the construction and, as a result, ensures a certain safety margin.

The essence of the method is changing the stress trajectories in an element into compressive or tensile forces and linking them in nodes. The strut-and-tie model is a truss-analogy of the construction in which following elements can be identified: struts, ties and nodes.

The role of the struts is bearing the compressive stresses. The struts are modelled as straight axial-compressed bars, although the real stress state is multi-axial. On the basis of the flow of the compressive strains, we can define three strut shapes: bottle-, fan- or prismatic-shaped. The natural tendency of struts to extend between the nodes can be suppressed by creating a reinforcement in the perpendicular line distributed over the length, as well as by the reduction of the compressive strength of concrete in struts.

Ties are modelled as linear axial tension elements which represent reinforcement that is smeared in layers. The centroid of the reinforcement corresponds to the center of the tie. It is crucial to ensure adequate anchorage of reinforcement out of the nodal zones, where it is not required.

Nodes can be classified according to the type of the forces which meet in the node, where *C* (compression) and *T* (tension) are as follows: CCC, CCT, CTT.

To develop strut-and-tie models, several methods, like elastic stress distribution or load path, can be used. When choosing the ST model, the practical aspects of the reinforcement location should be taken into consideration. If the location of the struts varies significantly

from the tension stress trajectory, it can cause the initial cracking of the construction. Another criterion that should be taken into account when choosing the model is whether it fulfils the optimization problem of minimum strain energy for linear elastic behavior of the struts and ties after cracking.

The strut-and-tie method has a vast range of usages. It can be applied in constructions such as: single corbel from column, half joint in beam, corners in a frame structures, deep beams, shields etc. The strut-and-tie method is recommended by Eurocode 2 [1] in the [2–4] numerous examples of the applications have been presented.

2. Design of corbels

One of the most popular usages of the STM is in designing corbels. In short corbels, the location of the vertical force (F_{Ed}) from the face of the supporting element (a_c) is smaller than the total height of the corbel (h_c). Through the corbels the load is transferred from beams (crane girders or joists) to columns. Apart from the vertical force, the corbel bears the horizontal load which results from non-mechanical influences (shrinkage, thermal effect) or mechanical (e.g. braking of gantry crane). When analyzed, the horizontal force (H_{Ed}) cannot be smaller than $0.2F_{Ed}$.

2.1. Beam analogy method

The main stage of the design of a corbel is calculating the requirements of reinforcement in the top part of the element. To achieve this, the beam analogy method has been commonly used. In this model, the effective span of the beam equals $0.15b_w$, where b_w is the width of the cross-section.
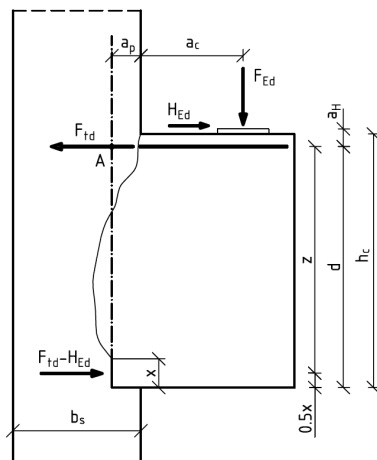
Fig. 2. Schematics to measure
reinforcement in corbel using beam
analogy method

Stresses in the compression area in concrete are assumed to be equal to f_{cd} (design value of concrete compressive strength). From the condition of equilibrium: the sum of the moments of all external forces in the point A is zero; the following formula (1) for the dimensions of the compressive area is obtained:

$$x = d - \sqrt{d^2 - \frac{2M_A}{b_w \cdot f_{cd}}} \, , \qquad (1)$$

where:

$$M_A = F_{Ed} \cdot \left(a_c + a_p\right) + H_{Ed} \cdot a_H \, .$$

2.2. Truss analogy method (STM)

According to the European standard – Eurocode 2, short corbels may be designed using strut-and-tie model which is shown in the following figure (Fig. 3). Apart from the main tension reinforcement, by using STM, the requirement for additional reinforcement (closed horizontal stirrups) can be obtained.
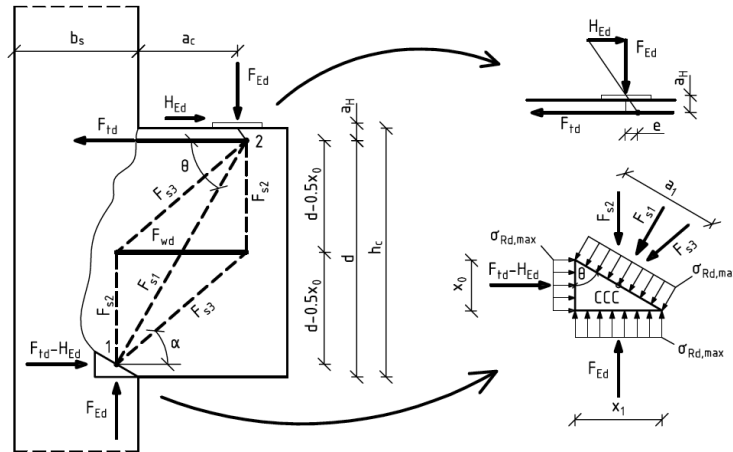
Fig. 3. The strut-and-tie model of the short corbel

The inclination of the strut (θ) is limited by $1.0 \leq \tan\theta \leq 2.5$.

In the recommended strut-and-tie model, node 2 is located in the point where the sum of moments of the vertical and horizontal forces is zero. Consequently, the distance equals

$$e = a_H \cdot \frac{H_{Ed}}{F_{Ed}} \, . \qquad (2)$$

Forces in the bars of the strut-and-tie model can be calculated in accordance with the following formulas (3)–(7).

$$F_{Td} = \frac{F_{Ed}(a_c + 0.5x_1) + H_{Ed}(d + a_H - 0.5x_0)}{d - 0.5x_0} \qquad (3)$$

$$F_{s1} = \frac{2(F_{Td} - H_{Ed})\sin\alpha - F_{Ed}\cos\alpha}{2\cos\theta\sin\alpha - \cos\alpha\sin\theta} \qquad (4)$$

$$F_{s3} = \frac{F_{Ed}\cos\theta - (F_{Td} - H_{Ed})\sin\theta}{2\cos\theta\sin\alpha - \cos\alpha\sin\theta} \qquad (5)$$

$$F_{s2} = F_3\sin\alpha \qquad (6)$$

$$F_{wd} = F_3\cos\alpha \qquad (7)$$

The formula (3) is obtained through the equilibrium condition: the sum of moments of the forces in the point one is zero. Dimensions of the nodal zone – x_1 and x_0 are calculated by taking into account limited stresses in the CCC node and geometrical relationships (similarity of triangles). Formulas (4), (5), (6) and (7) are derived from the system of equilibrium equations of forces in the nodes of the truss.

2.3. Example

In this paragraph, the short corbel which is shown in the following figure (Fig. 4) has been analyzed. The vertical load F_{Ed} from 200 kN to 1000 kN with 50 kN step, and horizontal force equal $0.2F_{Ed}$ have been established. According to these assumptions and formulas (3)–(7), the change of forces in bars of the strut-and-tie models is linear.
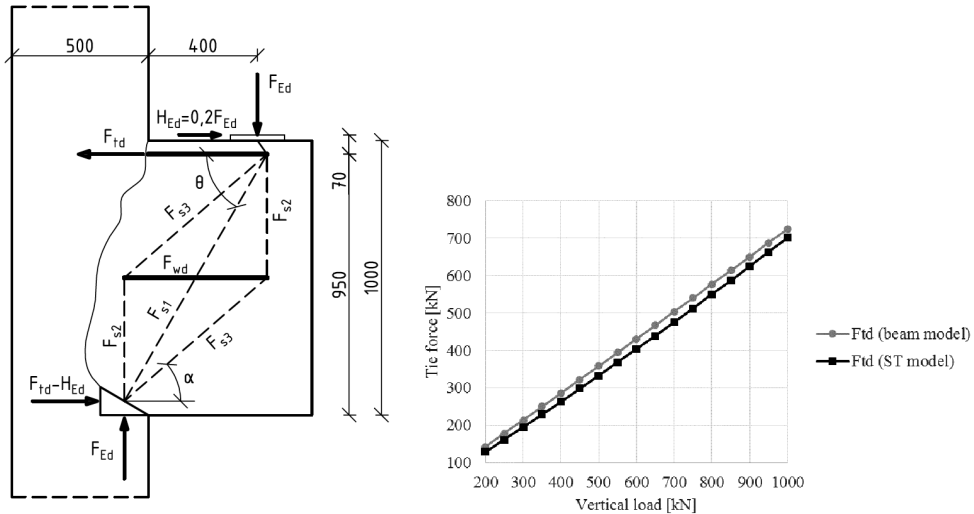
Fig. 4. The geometry of the corbel and the change of forces in the main reinforcement of the corbel for both of the methods

In the analysis, two of the methods have been employed: beam analogy method and STM. In the following graph (Fig. 5), the change of the force in the main reinforcement, which has been obtained from both of the methods for every load case, has been shown.

The results of the two methods are similar. However, those from the beam analogy method are higher in every load case. In the context of the lower bound theory in the limit analysis, the safety margin of the traditional beam analogy method is considerable.
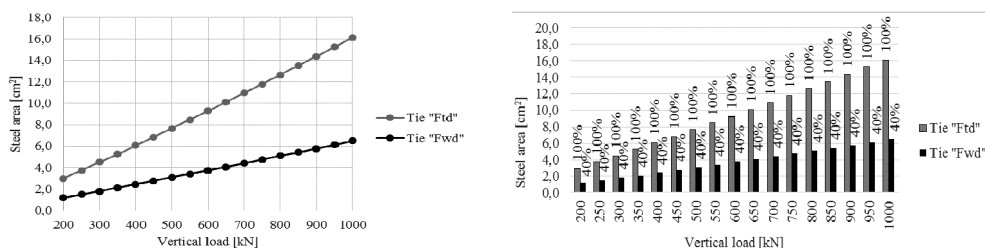
Fig. 5. The graph of requirement area of the main and additional reinforcement of the corbel

Short corbels, which satisfy the additional condition: $a_c < 0{,}5h_c$, work similarly to a shield. This is necessary to provide closed horizontal links that carry significant loads and are distributed over the height of the corbel. According to the recommendation in the original Eurocode 2 [1], the area of horizontal stirrups should not be smaller than 25% of the main tension reinforcement. This restriction was corrected in the Polish National Annex to 50%, which gives an impression to be proper, based on the analyzed example. In every case, the force in the horizontal tie equals 40% (Fig. 5) of the force in the main tie (F_{Td}).

The innovative approach to the analysis of reinforced concrete structures and usage rules of plasticity, expand design fields to the regions with non-linear stress distribution. For elements that are commonly designed using alternative methods, the results from the strut-and-tie method are similar which unveils its accuracy and effectiveness.

References

[1] PN-EN 1992-1-1:2008 Eurokod 2: Projektowanie konstrukcji z betonu. Część 1-1: Reguły ogólne i reguły dla budynków.

[2] Foster S., Kuchma D., Tjhin T., *Practitioners' guide for finite element modelling of rein-forced concrete*, International Federation for Structural Concrete (fib), Lausanne 2008.

[3] Knauff M., *Obliczanie konstrukcji żelbetowych według Eurokodu 2*, Wydawnictwo Naukowe PWN, Warszawa 2012.

[4] Starosolski W., *Konstrukcje żelbetowe według Eurokodu 2 i norm związanych*, Tom 3, Wyd. 4, Wydawnictwo Naukowe PWN, Warszawa 2012.

[5] Kubica J., *Krótkie wsporniki i belki podcięte*, w: *Podstawy projektowania konstrukcji żelbetowych i sprężonych według Eurokodu* 2, Sekcja Konstrukcji Betonowych KILiW PAN, Dolnośląskie Wydawnictwo Edukacyjne, Wrocław 2006.

[6] Urban T., *Przykłady projektowania żelbetowych wsporników*, Wydawnictwo Politechniki Łódzkiej, Łódź 2012.

MARIA KURAŃSKA, ALEKSANDER PROCIAK[*]

ENVIRONMENTALLY FRIENDLY POLYURETHANE--POLYISOCYANURATE FOAMS FOR APPLICATIONS IN THE CONSTRUCTION INDUSTRY

PRZYJAZNE ŚRODOWISKU SZTYWNE PIANKI POLIURETANOWO-POLIIZOCYJANUROWE DO ZASTOSOWAŃ W BUDOWNICTWIE

Abstract

In this paper, the influence of raw materials from renewable sources in the form of rapeseed oil-based polyols on thermal conductivity and the cell structure of rigid polyurethane--polyisocyanurate foams was presented. Bio-polyols were prepared by the following methods: transesterification, transamidization and two-steps method of epoxidation and oxirane rings opening.

Keywords: polyurethane-polyisocyanurate rigid foams, rapeseed oil-based polyols, thermal conductivity

Streszczenie

W artykule przedstawiono wpływ surowców ze źródeł odnawialnych w postaci polioli z oleju rzepakowego na współczynnik przewodzenia ciepła oraz strukturę komórkową sztywnych pianek poliuretanowo-poliizocyjanurowych. Poliole z oleju rzepakowego były otrzymywane następującymi metodami: transestryfikacja, transamidyzacja oraz dwuetapowa metoda epoksydacji i otwarcia pierścieni oksiranowych.

Słowa kluczowe: sztywne pianki poliuretanowo-poliizocyjanurowe, poliole z oleju rzepakowego, współczynnik przewodzenia ciepła

[*] Ph.D. Eng. Maria Kurańska, D.Sc. Ph.D. Eng. Aleksander Prociak, prof. CUT, Department of Chemistry and Technology of Polymers, Faculty of Chemical Engineering and Technology, Cracow University of Technology.

1. Introduction

Rigid polyurethane (PUR) and polyurethane-polyisocyanurate (PUR-PIR) foams have excellent properties such as low thermal conductivity, low apparent density, good mechanical resistance and low permeability. Such foams play an important role in buildings as insulating materials and in other industrial uses such as transportation, refrigeration, packaging, and automotive industry. The rigid PUR foams have the lowest thermal conductivity among heat-insulating materials which are commercially available.

Currently in the industry, there is an increasing interest in modern technologies, which are based on renewable raw materials. The introduction of vegetable oil-based polyols components to PUR-PIR systems meets all the requirements of sustainable development [1]. Natural oil-based polyols made from vegetable oils such as soybean, castor, palm and rapeseed oil are under intensive development and available on the small scale [2, 3].

In literature, different methods of the synthesizing polyols from natural oils such as hydroformylation, ozonolysis, transesterification, amidization [4] and epoxidation and opening oxirane ringare described. In this work, the three latter methods were used to prepare rapeseed oil-based polyols, which were next applied in the synthesis of PUR and PUR-PIR foams.

2. Experimental part

The rigid PUR and PUR-PIR foams were obtained by mixing two components (*A* and *B*). The reference chemical compositions of component *A* (REF) consisted of a petrochemical polyol, catalyst, water (as a chemical blowing agent) and surfactant. The mixture was stirred for 7 s. The isocyanate indexes were 110 and 250.This formulation was modified by replacing the petrochemical polyol with a rapeseed oil-based polyol in the amount of 70 wt. %. Three different rapeseed oil-based polyols were prepared using the following methods: epoxidation with opening oxirane rings (P_{epox}), transesterification with triethanolamine (P_{tr-est}) and transamidization with diethanolamine (P_{tr-am}). The most important properties of obtained bio-polyols (hydroxyl number and water content) are shown in Table 1.

T a b l e   1

The characteristic of polyols used in the synthesis of foams

	Petrochemical	P_{epox}	P_{tr-est}	P_{tr-am}
Hydroxyl number [mg KOH/g]	490.0	259.0	365.1	395.4
Water content [wt. %]	0.10	0.49	0.05	0.13

The foams were conditioned at 22°C and 50% relative humidity for 24 hours, before being cut to analyze their cellular structures and thermal conductivity. The initial (after 24 hours) thermal conductivity – λ values (mW/m·K) were measured using Laser Comp Heat Flow Instrument Fox 200. The measurements were also carried out after 7 days. The average temperature of measurements was 10°C (temperature of cold plate 0°C and warm plate 20°C).

The morphology of cells was analyzed using a scanning electron microscope (HITACHI S-4700). The samples were sputter coated with graphite before testing to avoid charging.

3. Results and discussion

The modifying reference formulation (based only on petrochemical polyols) with rapeseed oil polyol slightly increases the thermal conductivity of foams FP_{epox} and FP_{tr-est} (Fig. 1). Much higher deterioration of thermal conductivity was observed in the case of foam FP_{tr-am}. This is due to overly high reactivity of the polyol P_{tr-am} with the participation of diethanolamine, which causes processing problems and the considerable increase of apparent density of final foams.

More beneficial heat insulating properties of reference foam are an effect of more regular cellular structure of this material in comparison to the foams modified with bio-polyols (Fig. 2).
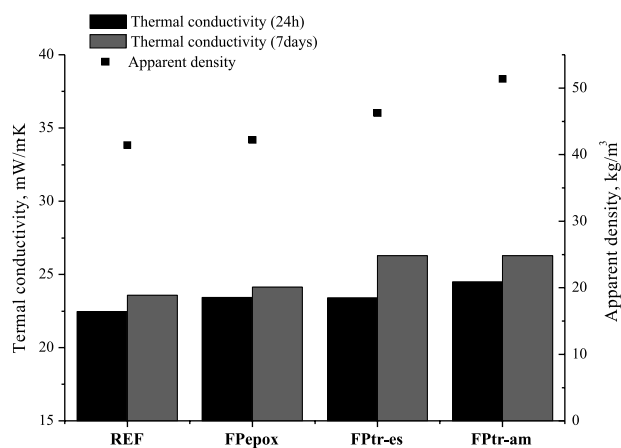
Fig. 1. The influence of different type of bio-polyols on thermal conductivity (after 24 hours and 7 days) and apparent density of rigid PUR foams
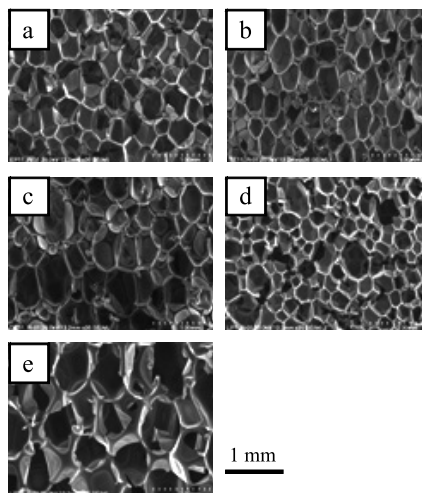
Fig. 2. SEM images of PUR foams (a – FP_{epox}, b – FP_{tr-est}, c – FP_{tr-am}, and d – REF); e – PUR-PIR foam. Magnification x35 in case of all images

The impact of the cellular structure on the thermal conductivity of foams was confirmed in the case of PUR-PIR foam. The cells of this material are considerably much larger compared with REF foam and affect the high value of thermal conductivity ca. 24.5 mW/m·K.

The results of thermal conductivity measured after 7 days showed that the smallest changes occur in the case of FP_{epox} foams, which is very important taking into account the long-term application of such materials.

4. Conclusions

The investigations have shown that rapeseed oil-based polyol as, the renewable raw material, can be used in obtaining of rigid polyurethane foams of low density. Two types of oil-based polyols synthesized by epoxidation with opening oxirane rings (P_{epox}), transesterification with triethanolamine (P_{tr-est}) make production of good quality PUR foams possible. The replacement of petrochemical polyol with the amount of 70 wt. % of rapeseed oil derivatives allows to obtain PUR foams with comparable thermal conductivity after 7 days, as in the case of reference foam.

References

[1] Kurańska M., Prociak A., Kirpluks M., Cabulis U., *Porous polyurethane composites based on bio-components*, Composites Science and Technology, 75, 2013, 70-76.

[2] Zhao Y., Yan N., Feng M., *Polyurethane foams derived from Liquefied mountain pine beetle-infested barks, Journal of Applied Polymer Science*, 123, 2012, 2849-2858.

[3] Pawlik H., Prociak A., Pielichowski J., *Synteza polioli z oleju palmowego przeznaczonych do otrzymywania elastycznych pianek poliuretanowych*, Czasopismo Techniczne, 1-Ch/2009, 111-117.

[4] Stirna U, Fridrihsone A, Lazdina B, Misane M, Vilsone D., *Biobased polyurethanes from rapeseed oil polyols – structure, mechanical and thermal properties*, J Polym Environ, 21, 2013, 952-962.

KAROLINA KWAPIŃSKA[*]

REVITALISATION OF DEGRADED AREAS AS EXEMPLIFIED BY THE ARCHITECTURAL DEVELOPMENTS IMPLEMENTED WITHIN THE FRAMEWORK OF THE LEED CERTIFICATION PROGRAMME

REWITALIZACJA TERENÓW ZDEGRADOWANYCH NA PRZYKŁADZIE INWESTYCJI ARCHITEKTONICZNYCH REALIZOWANYCH W PROGRAMIE CERTYFIKACYJNYM LEED

Abstract

Revitalisation of degraded areas fits in perfectly within the strategy of sustainable development in modern construction industry and architectural design. Basic principles of sustainable architectural design make all due allowances for, as well as address at some depth the overall need for respecting natural environment and natural resources. On the basis of the two select architectural developments sited within the ecologically degraded areas, i.e. Foshan Lingnan Tiandi Development estate, China and The Yard Redevelopment in Washington, DC, USA an evaluative study was undertaken, with a view to assessing the specific actions aimed at enhancing the prospective development sites. All three development projects were implemented within the framework of the LEED assessment programme for the sustainably built buildings, devised and developed by USGBC, a US non-profit organisation of global stature.

Keywords: revitalisation, degraded areas, urban sprawl, sustainable development, LEED certificate

Streszczenie

Rewitalizacja terenów zdegradowanych w znaczący sposób wpisuje się w strategię zrównoważonego rozwoju na polu współczesnego budownictwa i architektury. Podstawowe zasady projektowania zrównoważonego uwzględ-niają w sposób szczegółowy szeroko pojęte zagadnienia dotyczące ochrony środowiska i zasobów naturalnych. Na podstawie wybranych obiektów architektonicznych zrealizowanych na terenach zdegradowanych ekologicznie: kompleksu Foshan Lingnan Tiandi Development w Chinach oraz projektu urbanistycznego The Yard w Waszyng-tonie w USA przeprowadzono analizę działań podjętych w celu poprawy jakości wybranej przestrzeni. Omawiane obiekty były realizowane w programie do oceny budynków zrównoważonych LEED (*The Ledership in Energy and Enviromental Design*), opracowanym przez amerykańską organizację USGBC.

Słowa kluczowe: rewitalizacja, tereny zdegradowane, urban sprawl, zrównoważony rozwój, certyfikat LEED

[*] M.Sc. Arch Karolina Kwapińska, Faculty of Architecture, Cracow University of Technology (Ph.D. Student).

1. Introduction

The rapid growth of world population in recent years has had a marked influence on the quantity and quality of developed areas. According to prognoses for up to the year 2050, the percentage of developed areas will increase by two-thirds as compared to the present state. The design and realization of future urban architecture significantly affects our planet, the quality of natural environment and people's lives.

The design of an urban space has a direct effect on the quality of the natural environment and the lives of inhabitants. Examples of badly developed urban spaces can be found across the world, where their uncontrolled development has led to the degradation of many areas. The need for redevelopment of such spaces poses a challenge to the architects, urban planners and inhabitants, to which the principles of sustainable development may provide a solution. There are many global and local programmes promoting the redevelopment of such degraded, brownfield areas [1]. The multi-criteria building assessment system created by USGBC (*US Green Building Council*), an American non-profit organization, is one of them. It features guidelines for the designing and implementation of investments undertaken to improve the quality of urban spaces in accordance with the new regulations for reurbanisation and urban space redevelopment.

One of the major concerns for the degraded urban spaces is their segmentation. Observations show that in the last fifty years, urban areas divided by motorways have become the dominant model of all inhabited areas in the USA as well as Europe and Asia. Mechanical transport is responsible for one-third of greenhouse gas emission, the bulk of which is produced by cars. As a result of fossil fuels burning, there has been a significant increase in air pollution and environmental pollution. Distant urbanized areas seem to be falling short of the sustainable development principle, which naturally puts them in opposition to the wholesome traditional pattern of mixed architectural development whereby all necessary facilities such as shops, schools, cafes or hospitals are situated within walking distance.

Urban architecture scattered over many square kilometers also plays a part in the ground and water supplies pollution, the segmentation of valuable arable land and the precious green areas such as forests or woods. It also puts a marked strain on the urban infrastructure, increasing the costs of its construction and everyday use [3].

The degradation of urban spaces resulting from improper use has led to a change in the approach to future and existing urban architecture. The new designs take into consideration the redevelopment of urban areas as well as the protection of areas not yet developed [6]. The urban planning that places residential areas in the vicinity of working spaces and recreational areas can reduce the amount of mechanized transport and the subsequent greenhouse gas emissions and toxic waste production; it can also reduce the costs of construction and operation of the infrastructure. Concentrated, mixed architecture improves the quality of life and environment and functions better [4, 9]. It provides easy access to all necessary facilities such as banks, parks or schools; it encourages walking, bonding with other people and taking care of one's physical and mental health. A balanced urban environment is a chance to alleviate the results of natural environment exploitation, diminish air and water pollution or cut down on the natural resources consumption as well as protect the priceless green areas [5, 10].

2. The objective of this paper

The objective of this paper is to prove that rigorous compliance with programme framework in the designing and implementation of redevelopment projects for degraded urban areas using the tool like e.g. LEED Certification Programme has a positive influence on the environment and life quality.

3. LEED certification programme and its role in architectural and urban planning

The LEED (Leadership in Environmental and Energy Design) Certificate is a multi-criterion building assessment system that rates the compliance of buildings with the sustained development principles. It was created by an American non-profit organization, US Green Building Council (USGBC) with the purpose of rating the most environment-friendly buildings based on high ecological standards. Since 1998, investments worldwide have been carried out based on the requirements of the LEED certificate. It is also applicable in the already existing developments: housing, offices, hotels or hospitals. USGBC endorses projects that are guided by the sustainable development principles in their implementation. New constructions in the urbanized areas with good access to public transport and to basic services are likely to rate higher than buildings located haphazardly and thus contributing to the urban sprawl phenomenon.

As to the redevelopment of degraded urban areas, the LEED-ND (LEED Neighborhood Development) Certificate is of particular importance. It comprises architectural design assessment as well as infrastructure, neighborhood, natural environment and local and regional contexts that all contribute to the urban area project [6].

The LEED-ND Certificate comprises four credit categories: Smart Locations & Linkages, Neighborhood Pattern & Design, Green Infrastructure & buildings and Innovation in Design.

The Smart Locations & Linkages credits are awarded for the project's location and its compatibility with the existing urban space. The focus is on aspects of location such as the availability of public transport, access to basic services, distance from residential areas, protection of surface water and brownfields redevelopment.

The Neighborhood Pattern & Design credits concern the reduction of parking spaces in the streets, the creation of pedestrian-friendly spaces such as the streets and the easy access to public spaces as well as recreational and green areas.

Credits in the Green Infrastructure & Buildings category apply to buildings situated in urbanized areas. At least one building in the project area is required to be LEED-certified. The credits are awarded based on water economy, rainwater collection for the watering of green areas, the use of already existing buildings, urban heat island reduction and light pollution.

The Innovation & Design category is an opportunity for additional credits for outstanding achievements and the inclusion of LEED-AP in the project team.

The role of programmes like LEED-ND is setting an example of good practice and norms necessary in the designs of new urban developments and the redevelopments of already existing ones [7]. They enable a responsible and deliberate redevelopment process.

The LEED system emphasizes the importance of local aspects resulting cultural, geographical and legal differences which furnishes the possibility of objective comparison with similar implementations worldwide. Based on the already implemented LEED-ND-compliant redevelopments, a significant improvement in the quality of urban spaces has been noted.

4. Examples of urban brownfields redevelopments designed and implemented in compliance with LEED-ND certificate

According to the USGBC data of September 2013, there are 101 sites worldwide that have received a positive opinion and have subsequently been LEED-ND-certified. Of these, 83 are located in the United States, 12 are in China and 6 in Canada. Further 57 sites have been entered into the assessment programme in recent years (see Table 1).

T a b l e 1

Projects submitted to the LEED-ND and those who received a certificate in numbers

No.	Country	Projects awarded LEED-ND	Projects registered in the LEED-ND
1	USA	83	51
2	China	12	0
3	Canada	6	5
4	S. Korea	0	1
5	Poland	0	0
	SUM	101	57

(The table on the basis of statistics derived from the USGBC: http://www.gbci.org/GBCICertifiedProjectList.aspx)

Interesting examples of a LEED-ND programme brownfield redevelopment can be found in Foshan Lingnan Tiandi Development in China and The Yard Washington Redevelopment in the USA.

Located in the center of Foshan, a city in Guandong Province in southern China, Foshan Lingnan Tiandi is an example of a redeveloped urban space of mixed functionality that was degraded by years of improper use, the absence of a comprehensive urban development plan and the devastation of the city's historic architecture typical for the cities in the region. The primary project objectives were to restore the historical and cultural heritage of the site as well as the city's individual character while at the same time usher it into the 21th century through comprehensive redevelopment. The design and implementation team of the Foshan Lingnan Tiandi project has succeeded in enabling modern lifestyle in the redeveloped site and creating a balanced, modern urban space that blends in with its surroundings and matches the historical and cultural context. In the Foshan Lingnan Tiandi Development project, the site's negative impact on the environment was minimized. The designers focused on the reduction of greenhouse gas and other toxic emissions as well as on water economy and energy conservation. Owing to the site's location in the center of a highly urbanized area, the creation of a mixed functionality development was possible, providing the site's future inhabitants with access to residential areas, offices, shops, industrial areas and entertainment. The project combines not only different functionalities, but also different styles: as a part of the redevelopment plan, the designers have placed

the modern residential, commercial and industrial spaces within the historic architecture. This enabled the preservation of as much as 80% of the traditional Chinese buildings while simultaneously creating an urban area that encourages a new, active and dynamic society. In the project, 50% of the buildings of more than ten different functions have been located within 800 m of one another, which is a distance easily covered on foot. Thanks to the preservation of the existing grid of alleys, streets and squares, the place also encourages outdoor activity. The project's compliance with the sustainable development principle has been pursued further with the introduction of technologies reducing the consumption of non-renewable energy sources. Solar panels for water heating have been installed e.g. in the hotel in the redeveloped area, and photovoltaic panels have been used to power the urban lighting. To reduce energy costs, zone heating systems have been introduced in smaller buildings. A system of rainwater collection has also been designed, which reduced the use of drinking water. As a means of using the space to the utmost, over 50% of roofs and walls have been covered with plants, thus forming horizontal and vertical city gardens. The adherence to the sustainable development principle in the design and implementation process has resulted in the successful redevelopment of a degraded urban area, leading to a Gold-level LEED-ND Certificate awarded to the project in 2010.

Another good example of how the quality of an urban brownfield can be improved is The Yard, a redevelopment design for the wharf area situated by the Anacosti River in the southern part of Washington, DC. In 2009, a project was prepared for 170 ha of land, where 167.000 square meters' worth of offices, 38,000 square meters of commercial and entertainment areas, 2.500 square meters of housing and a surrounding park with waterfront boulevards are to be created. In spite of its opportune location in the center of Washington, The Yard project area has long been neglected and degraded, which resulted from long years of industrial use as a US Navy shipyard and an ammunition production site. The main objective of the project team that includes, among others, the developer, urban planners, architects, engineers and a LEED certification expert, was to convert the former military base into a modern multifunctional developed site that would constitute a valid part of Washington. According to the project, as a new district, The Yard would provide a residential area with a well-developed lattice of roads and sidewalks that would propagate a healthy lifestyle through its urban grid. All the necessary facilities, such as schools, shops or the underground station are to be located in buildings situated in an area that does not exceed 800 m in diameter. In the course of the project works, the designers have decided to redevelop many of the site's typical post-industrial buildings but respected their unique character. Seeing as the city of Washington has so far lacked in recreational waterfront areas, the project team has used the site's location to design a park by the harbor with general-access boulevards. Ground quality improvement has also been an issue in the project, which was resolved by purifying the ground of all oil-related pollution from post-industrial use of the land. The project team has also suggested a plan for the purification of ground water that would protect it from pollution; the plan also features rainwater collection scheme to conserve drinking water, intelligent irrigation and the reuse of greywater. The Yard urban redevelopment has been under construction since 2009 in compliance with LEED-ND, with the project team aspiring to obtain a Gold-level LEED-ND Certificate.

5. Sumary

The instances of urban redevelopment presented here are a good example of investments compliant with the principle of sustainable development. Based on the material presented, a conclusion has been reached that urbanized areas have a significant influence on the environment, economy, health and development. Owing to organizations like USGBC (*US Green Building Council*) and their sustainable building assessment systems such as *LEED* (*Leadership in Environmental and Energy Design*) Certificate, a wholesome and controlled redevelopment of degraded urban areas worldwide is possible. An important element of the transformation is a comprehensive consideration of the local aspects resulting cultural, geographical and legal differences of chosen area. The compliance with sustainable architecture and construction principles is an opportunity to slow down, or even altogether stop, the degradation of the spaces we live in [8]. The cooperation of architects and other urban planning specialists with local authorities and prospective users of the spaces is the basis of the movement for the sustainable development of new urban spaces as well as existing ones.

6. Conclusions

Based on the analysis of chosen examples, it has been proved that the rigorous adherence to the project requirements compliant with a certification programme such as LEED-ND has resulted in a high quality of the implemented architectural investments, an improved quality and status of a former degraded area, a socio-economic boost, the minimization of the urban sprawl effect, the restoration of natural resources and the improved quality of the ground.

R e f e r e n c e s

[1] Strzelecka E., *Rewitalizacja Miast w Kontekście Zrównoważonego Rozwoju*, scientific publication, 2011.

[2] Congress for the New Urbanism, Natural Resources Defense Council, and the U.S. Green Bulilding Council, *LEED 2009 for Neighborhood Development*, USA 2012.

[3] Rembeza M., *Rewitalizacja Zdegradowanych Centralnych Obszarów Mieszkaniowych w Aspekcie Ekonomizacji Kultury*, Technical Journal, Published by University of Cracow, Cracow, 2007.

[4] Bać Z. (ed.), *Habitaty Pro-Eko-Logiczne*, Publishing House of Wroclaw University of Technology, 2010.

[5] Pęski W., *Zarządzanie Zrównoważonym Rozwojem Miast,* Arkady Publishing, Warsaw 1999.

[6] Congress for the New Urbanism, Natural Resources Defense Council, and the U.S. Green Bulilding Council, *LEED 2009 for Neighborhood Development*, USA 2012.

[7] Kronenberg J., Bergier T., *Wyzwania Zrównoważonego Rozwoju w Polsce*, published by the Foundation Sendzimir, Kraków 2010.

[8] Ryńska D.E., *Architekt w Procesie Tworzenia Harmonijnego Środowiska*, University of Warsaw, Cracow 2004.

[9] Bać Z. (ed.), *Habitaty – Zrównoważony Rozwój Środowiska Mieszkaniowego*, Publishing House of Wroclaw University of Technology, 2010.

[10] GTZ Gesells chaftfur Technische Zusammenarbeit, Institutfur Wohnenund Umwelt Darmstadt, *Podręcznik Rewitalizacji, Zasady, Procedury i Metody Działania Współczesnych Procesów Rewitalizacji,* Książka, Published by the TRANSFORM program, Warsaw 2003.

ANNA MACHNIEWICZ, DARIUSZ HEIM[*]

MODELLING OF LATENT HEAT STORAGE IN PCM MODIFIED COMPONENTS

MODELOWANIE AKUMULACJI CIEPŁA UTAJONEGO W KOMPONENTACH MODYFIKOWANYCH MFZ

Abstract

Due to latent heat storage potential, phase change materials can be implemented in building materials to improve energy performance and thermal comfort. Nevertheless, the phase change effect is quite a complex phenomenon for numerical modelling and different methods can be used to estimate the results of latent heat storage. This paper presents a brief overview of the existing numerical methods and a short description of two most frequently used ones. Authors also investigated the capabilities of phase change modelling by three simulation tools. This work is a part of a wider research project which aims to find optimal solution of façade construction with the implementation of PCM. The choice of a proper numerical method was considered the first step to achieve this goal.

Keywords: phase change material, latent heat, thermal simulation

Streszczenie

W artykule przedstawiono skrócony przegląd metod modelowania numerycznego zjawisk przemiany fazowej oraz możliwości oceny akumulacji ciepła utajonego w komponentach modyfikowanych materiałami fazowo zmiennymi (MFZ). Scharakteryzowano również metody obliczeniowe trzech programów symulacyjnych umożliwiających modelowanie MFZ. W wyniku analizy oceniono zasadność wykorzystania poszczególnych metod do realizacji szerszego projektu mającego na celu znalezienie optymalnego rozwiązania fasady.

Słowa kluczowe: materiały fazowo zmienne, ciepło utajone, symulacje energetyczne

---

[*] M.Sc. Eng. Anna Machniewicz, Ph.D. D.Sc. Eng. Dariusz Heim, Department of Environmental Engineering, Faculty of Process and Environmental Engineering, Lodz University of Technology.

Nomenclature

C – heat capacity [J/kgK]
H – enthalpy [J/kg]
k – thermal conductivity [W/mK]
L – latent heat [J/kg]
ρ – density [kg/m³]
t – time [s]
T – temperature [K]
Subscripts:
eff – effective
M – melting
S – solidification

1. Introduction

Nowadays, incorporation of phase change materials (PCMs) within construction components and building elements is increasingly being considered and tested. Heat storage systems and heat capacity of construction materials are the main factors that determine energy efficiency of building envelopes which are highly exposed on solar radiation. Thermal capacity of such components can be increased with phase change materials impregnated in wallboard, microencapsulated or placed in the interspace between two glass sheets. Latent heat energy storage depends mainly on the amount of PCM, its position, melting point and heat of fusion.

During the last decade, the number of simulations and tests were carried out to investigate the performance of PCMs incorporated into building materials. The evaluation of phase change materials performance is a very complex phenomenon and necessitates the implementation of numerical methods to calculate non-linear thermal properties of PCM. Nevertheless, since it was stated that convective heat transfer in PCMs can be neglected [1], governing equations can be reduced to the energy conservation equation:

$$\frac{\partial(\rho H)}{\partial t} = \nabla(k\nabla T) \tag{1}$$

The classification of numerical algorithms for phase-change phenomena description proposed by Idelsohn [2] presupposes a division into two groups: front tracking methods (fixed mesh, variable mesh, moving mesh, moving boundary element) and fixed domain methods (apparent heat capacity, enthalpy based formulation, fictitious heat flow, freezing index, discontinuous integration). The former group of methods is usually used to solve Stefan problem, while methods from the second group give the possibility to model mushy zone (region with solid and liquid phase).

On the other hand, Verma [3] classified numerical models of latent heat thermal energy storage as based on first or second law of thermodynamics. First law models do not include the temperature at which the heat is supplied and the time of the heat storage and release. Nevertheless, second law models should complement – not replace – first law models [4].

Despite the selection of a specific numerical algorithm, the choice of a numerical method for approximating the solution is also crucial for the accuracy of the results. The most commonly used method is the finite-difference method which allows to approximate derivatives by Taylor Series expansion. It can be achieved by explicit, implicit or Crank-Nicholson method, using forward, backward or central difference at time, respectively. Due to non-linear dependence of heat capacity on temperature, which is used to estimate the latent heat storage during phase change, the application of the explicit scheme can cause errors. One of the recommendations leading to increased accuracy of the results is to reduce the calculation time step [5]. Moreover, rapid changes in thermal properties of PCMs can be calculated more precisely by the implicit method. It involves in solution both the current and the previous state of the system in each calculation step.

The most commonly known and used methods are effective heat capacity, enthalpy method and the combination of both.

2. Numerical methods

2.1. Effective heat capacity method

Latent heat storage during phase change can be evaluated using effective heat capacity method. In that method, enthalpy is represented by effective heat capacity – temperature dependence:

$$H = \int_{T_M}^{T_S} C_{eff} \, dT \tag{2}$$

It can be assumed that density change is negligible with time, thus the equation (1) can be expanded as:

$$\frac{\partial(\rho H)}{\partial t} = \rho \frac{\partial(H)}{\partial T} \frac{\partial(T)}{\partial t} = \rho C_{eff} \frac{\partial T}{\partial t} \tag{3}$$

which implies, the governing equation for PCM can be expressed as:

$$\rho C_{eff}(T) \frac{\partial T}{\partial t} = \nabla(k \nabla T) \tag{4}$$

where:

$$C_{eff}(T) = \begin{cases} C_p & T_S < T < T_M \\ \dfrac{L}{T_S - T_M} + C_p(T_M) & T_M \leq T \leq T_S \end{cases} \tag{5}$$

As stated before, calculation can be proceeded using explicit or implicit method of solution. Due to sharply changing function of effective heat capacity, proper assumption of the time step size is crucial while using explicit method. Calculation step has to be small to avoid the situation when the temperature "jumps" past the solidification point in one step

and latent heat is ignored [6]. Nevertheless, effective heat capacity method allows us to use implicit discretization scheme which, in that case, is unconditionally stable [7]. Through the use of DSC method for measuring effective heat capacity, in the equation (4) the only unknown variable is the temperature.

2.2. Enthalpy method

The second method for latent heat storage evaluation is enthalpy method, which estimates heat capacity in form of its integral form $H(T)$ with respect to temperature. This method assumes that enthalpy is a sum of sensible and latent heat [8]:

$$H(T) = h(T) + Lf(T) \tag{6}$$

where:

$$h(T) = \int_{T_M}^{T_S} C_p \, dT \tag{7}$$

and liquid fraction is given as:

$$f(T) = \begin{cases} 0 & T < T_M \\ \dfrac{T - T_M}{T_S - T_M} & T_M \leq T \leq T_S \\ 1 & T > T_S \end{cases} \tag{8}$$

One of the main advantages of that method is the applicability of the above equations directly to the three phases. There is no need to track over moving phase front and mushy zone can be easily modelled. The temperature is evaluated in each time step and values of thermo-physical properties can be determined precisely.
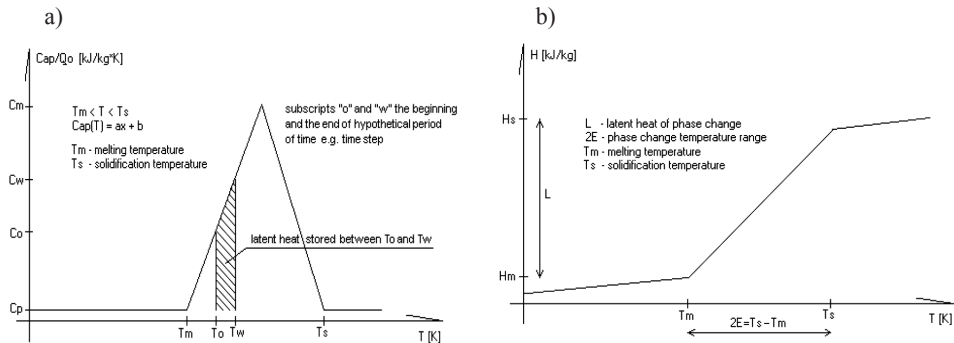
Fig. 1. Graphical representation of a) effective heat capacity method, b) enthalpy method [14]

3. Simulation tools

3.1. EnergyPlus

Latent heat storage in EnergyPlus can be evaluated by modified version of the enthalpy method. The implemented algorithm allows us to calculate heat capacity on the basis of enthalpy-temperature function in each time step [9]:

$$C_{eff} = \frac{H_{i,new} - H_{i,old}}{T_{i,new} - T_{i,old}} \tag{9}$$

Solution of one-dimensional conduction finite difference (CondFD) algorithm can be proceeded using Crank-Nicholson or fully implicit scheme [10]. Despite the fact that the model includes both phase-change enthalpy and temperature dependent thermal conductivity, it is not possible to take into account the effect of hysteresis on the heat capacity [11].

3.2. TRNSYS

TRNSYS is a modular simulation software consisting of many subroutines, which allows to implement different calculation methods. It is possible to implement new module TRNSYS Type [12, 13] or use the active layer tool in TRNSYS Type 56. As investigated by Klimes [8], both enthalpy and effective heat capacity methods are applicable in TRNSYS software. Nevertheless, it is necessary to implement numerical model of PCM in MATLAB (in case of the former method) or in the form of a stand-alone module in the C++ programming language.

3.3. ESP-r

Energy performance of PCM modified components can be evaluated using an active materials subroutine implemented in ESP-r software [14]. Through the definition of the special material properties latent heat storage is estimated on the basis of the effective heat capacity method. Despite the highly non-linear dependence of heat capacity and temperature, this function can be substituted by a linear one:

$$C_{eff}(T) = aT + b \quad T_M < T < T_S \tag{10}$$

where:

$$b = \frac{L}{\Delta T}$$

4. Discussion and further work

In this paper, three simulation tools calculating non-linear thermal properties of PCMs have been described and discussed. Authors also presented and compared two numerical

methods of assessing the effect of phase change and latent heat generation: effective heat capacity method and enthalpy method. The former method allows us to determine the temperature change on the basis of heat capacity measured through differential scanning calorimetry, while the second one describes enthalpy by integrating the heat capacity with respect to temperature. The main assumptions and limitations of both methods were pointed.

This study is a part of a wider research project devoted to optimization of the energy-efficient construction of the façade. Effectiveness of PCM is quite sensitive to external weather conditions and indoor temperature. Hence, the assessment of specific solution should be made taking into account all variables and using appropriate simulation tools. Furthermore, the accuracy of obtained results should match the scope of the analysis – analysis of a particular element, entire façade or whole building analysis. Authors investigated the possibilities of application mentioned numerical methods and concluded that further experimental investigations are necessary to confirm the accuracy and applicability of presented methods.

References

[1] Zalba B., Marin J.M., Cabeza L.F., Mehling H., *Review on thermal energy storage with phase change: materials, heat transfer analysis and application*, Applied Thermal Engineering, 23, 2003, 251-283.

[2] Idelson S.R., Stori M.A., Crivelli L.A., *Numerical methods in phase-change problems*, Archives of Computational Methods in Engineering, 1994, 49-74.

[3] Verma P., Varun, Singal S.K., *Review of mathematical modelling on latent heat thermal energy storage systems using phase-change material*, Renewable & Sustainable Energy Reviews, 12, 2008, 999-1031.

[4] Dutil Y., Rousse D.R., Salah N.B., Lassue S., Zalewski L., *A review on phase-change materials: Mathematical modeling and simulations*, Renewable & Sustainable Energy Reviews, 2011, 15 112-130.

[5] Almeida F., Zhang D., Fung A.S., Leong W.H., *Comparison of corrective phase change material algorithm with ESP-r simulation*, 12th Conference of IBPSA, Sydney 2011.

[6] Pham Q.T., *A fast, unconditionally stable finite-difference scheme for heat conduction with phase change*, Heat Mass Transfer, 28, 1985, 2079-2084.

[7] Klimes L., Charvat P., Ostry M., *Challenges in the computer modeling of phase change materials,* Materials and technology, 46, 2012, 335-338.

[8] Sharma A., Tyagi V.V., Chen C.R., Buddhi D., *Review on thermal energy storage with phase change materials and applications*, Renewable & Sustainable Energy Reviews, 13, 2009, 318-345.

[9] Pedersen C.O., *Advanced zone simulation in EnergyPlus: Incorporating of variable properties and phase change material (PCM) capability*, Proceedings: Building Simulation 2007.

[10] Tabares-Velasco P.C., Christensen C., Bianchi M., *Verification and validation of EnergyPlus phase change material model for opaque wall assemblies*, Building and Environment 54, 2012, 186-196.

[11] Evola G., Marletta L., Sicurella F., *A methodology for investigating the effectiveness of PCM wallboards for summer thermal comfort in buildings,* Building and Environment, 59, 2013, 517-527.

[12] Ibanez M., Lazaro A., Zalba B., Cabeza L F., *An approach to the simulation of PCMs in building applications using TRNSYS*, Applied Thermal Engineering, 25, 2005, 1796-1807.

[13] Kuznik F., Virgone J., Johannes K., *Development and validation of a new TRNSYS type for the simulation of external building walls containing PCM*, Energy and Buildings, 42, 2010, 1004-1009.

[14] Heim D., Clarke J.A., *Numerical modeling and thermal simulation of PCM-gypsum composite with ESP-r*, Energy and Buildings, 36, 2004, 795-805.

JAROSŁAW MALARA[*]

RESEARCH ON WORKING TIME IN THE CONSTRUCTION SECTOR

BADANIE CZASU PRACY W BUDOWNICTWIE

Abstract

The article describes the nature and the significance of research on working time of workers in the construction sector for the improvement of technology and organization of works. The author refers to the basic research methods and discusses the factors contributing to the performance of various works in the construction sector. Then, the research done on one of the construction sites in Warsaw, consisting of terrazzo tiling in stairways is discussed and the possible ways of interpreting the collected results is specified. The summary describes the benefits of proper observation and interpretation of research regarding working time of construction workers.

Keywords:working time, efficiency

Streszczenie

Artykuł opisuje istotę i znaczenie badania czasu pracy pracowników budowlanych dla doskonalenia technologii i organizacji robót budowlanych. Autor odnosi się do podstawowych metod badawczych czasu pracy oraz omawia czynniki składające się na wykonywanie poszczególnych robót w budownictwie. Następnie omówione zostały badania wykonane przez autora na jednej z warszawskich budów podczas wykonywania okładzin lastrykowych na klatkach schodowych wraz z określeniem możliwości interpretacji zebranych wyników. W podsumowaniu zostały opisane korzyści wynikające z prawidłowej obserwacji i interpretacji badań dnia roboczego pracownika budowlanego.

Słowa kluczowe:czas pracy, wydajność

[*] M.Sc. Eng. Jarosław Malara, Institute of Building and Transport Management, Faculty of Civil Engineering, Cracow University of Technology.

1. Introduction

The continuous development of the construction forces the participants of the construction process to constant improvement of technologies and organizational solutions during different works. An essential element of the construction industry is the physical work of people performing different works. Due to the high organizational and executive complexity and plurality of the attendant factors, the situation needs to be constantly monitored in order to draw proper conclusions that contribute to the optimization of the process.

Work measurement is one of the methodological concepts of work study that allows to measure the time required to perform the analyzed activities and to measure the level of disturbance in the factors accompanying the execution, necessary to determine the amount of time needed to effectively perform a task and determine the basis of the technical standards of time [1]. Determining the correct standards which take into account all the key factors affecting the working time allows for a reliable assessment of the construction being led. The conslusions drawn from the observation of working time are needed for the proper scheduling of works.

2. The Components of executed work research

For proper research of working time, it is necessary to isolate different aspects. Most general division of work distinguishes the three main research areas of work: quality of work, quantity of work and work organization (Fig. 1).
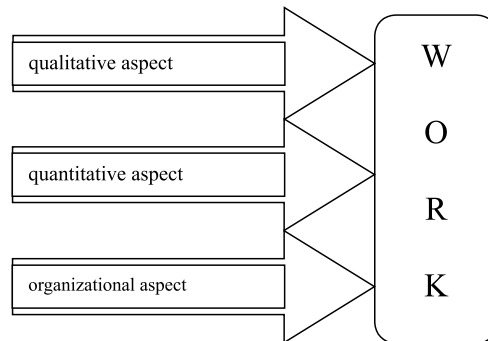
Fig. 1. Areas of work research (own description)

The proper and complete assessment of working time of construction workers should include possibly the largest number of factors affecting the performance of tasks on the site. The difficulty lies not in recording all components, but in their investigation. In order to analyze the work, the following factors need to be measured: physical and psychological effort, worker's qualifications, work ergonomics, existing legislation (eg. labor law), the wage system, macro and microeconomic situation, day of the week, distance from the date of completion of the works. Each of the factors mentioned above has a significant impact

on work, but it can't be examined with the same method of analysis. In order to accurately analyze the work of construction workers, interdisciplinary knowledge from the humanities (psychology), across economics (wage rate and the economic situation), finally, to the mathematical models (i.a.: quantitative aspect) should be used. Due to the complexity of the argument, it is necessary to perform research using practically all methodologies, since none of them in separation gives the feasibility of collecting the full amount of data for a complete description of the problem.

At present, working time in the construction sector is analyzed in several aspects. Very great importance is attached to an appriopriate balance between work and time spent at home (work-life balance) [2]. Balance maintained in this aspect increases productivity and employee satisfaction, which is beneficial for the investment. Besides, the influence of temperature and humidity on work of the construction workers is thoroughly investigated. As a result, China has developed a model [3] that takes into account the weather conditions. The effects of calculations can be used directly to correct the construction schedules. Currently, from the group of psychophisical factors, the effect of stress and diseases is being analyzed [4, 5].

In the qualitative aspect of the research on work, it is necessary to analyze all the factors related to the work evaluation. Work evaluation is a process that aims at an accurate assessment of the factors affecting the difficulty and complexity of individual work components execution in the whole work. Within this area, it is essential to extract two types of research methods:
– summary (statistical, estimating, comparative),
– analitycal (computational, investigative, simplified).

The study of the organizational aspect of work is based on one of the following methodologies:
– standard predetermined time,
– timing,
– sampling method,
or uses complementary methods such as photography of a working day or analytical estimation technique [6].

3. Completed research

The research on working time of the construction workers was performed on one of the sites in Warsaw during the realization of a part of the Eco-Park settlement at Chodkiewicza street. The whole observation concerned terazzo tiling. The construction owner of the whole development was Sobiesław Zasada JSC Group, while the general executor was Krakow Re-Bau LLC.

That part is a set of five residential buildings connected by an underground garage. The height of each building is five floors above ground and one underground level. The buildings are each composed of two staircases. On the ground floor, a retail- service surface is located, while floors 1–4 are dedicated for living.

With the purpose of executing research, the observation of terrazzo lining in the staircases was carried out. The stairwells were stacked with prefabricated measured stairs consisting of treads and risers in a single element. The dimensions of every element were: length – 140÷145 cm, width – 34 cm, height – 17 cm, thickness – 4 cm. The stairwells were made

T a b l e   1

Summary of execution times for each activity Zestawienie czasów trwania poszczególnych czynności

Number of staircase	Auxiliary and preparatory works	Execution of lining	Preparation of landings and corridors	Terrazzo lining on landings and in the corridors	Installation of stair plinths	Installation of plinths on landings and in the corridors	Grouting	Silicone application
	[h]	[h]	[h]	[h]	[h]	[h]	[h]	[h]
A1	71.77	233.1	86.85	131.15	22.73	26.98	44.3	24.28
A2	69.93	152.72	73.51	112.1	23.5	24.47	38.01	22.92
B1	41.4	131.06	52.23	95.27	24.18	25.34	37.91	22.83
B2	44.1	112.97	51.65	78.83	23.31	22.73	35.5	21.57
C1	61.9	113.45	64.71	100.98	30.18	26.4	30.37	23.41
C2	66.83	127.86	71.48	101.36	26.21	23.41	39.75	23.02
D1	48.65	108.13	62.58	79.41	24.18	24.28	35.21	23.7
D2	58.52	112.68	62.96	85.69	23.5	23.5	44.1	28.05
E1	52.13	133.76	64.9	92.37	22.63	28.53	36.56	21.28
E2	56.77	136.18	78.05	100.78	24.28	25.63	38.2	24.18

with the traditional method by using semi-dry cement mortar. Landings of staircases and corridors were laid with terrazzo tiles measuring 30 cm × 30 cm and with thickness of 2.8 cm, with the adhesive mortar, after having aligned the ground with a cementtious surface filler. After cleaning and preparing the ground for tiling, workers started to prepare semi-dry cement mortar. Ready, prefabricated steps, immediately after transportation to the place of incorporation, have been incorporated. When the stairwells were ready, workers started to align the ground of the landings and corridors in order to prepare it for terrazzo tiling. Once flat surfaces were ready, the workers tiled the plinths in the staircases, corridors and landings and they performed final termination activities, such as grouting and silicone application.

To conduct the research, the timing method was used [7]. Cards of daily worker observation were prepared, in which, to the nearest one minute, individual activities related to the execution of lining were described. The unit adopted for the presentation of the data was an hour, with the decimal expansion to second digit after decimal point.

The following components, performed by the workers were separated: auxiliary and preparatory works, execution of lining, preparation of landings and corridors, terrazzo lining on landings and in the corridors, installation of stair plinths, installation of plinths on landings and in the corridors, grouting and silicone application. Activities performed by workers were each time classified in an appropriate group, which allowed the researchers to extract the exact time for processes execution in every single staircase. Table1 presents the results.

Using the timing method, the degree of influence of the workers' habituation to the new working conditions (new building) on the efficiency of works can be determined. Over the course of time, construction workers perform various tasks and, consequelntly, the whole job faster, more efficiently and effectively. For the realization of a single element they need less time, as it is presented in Fig. 2.
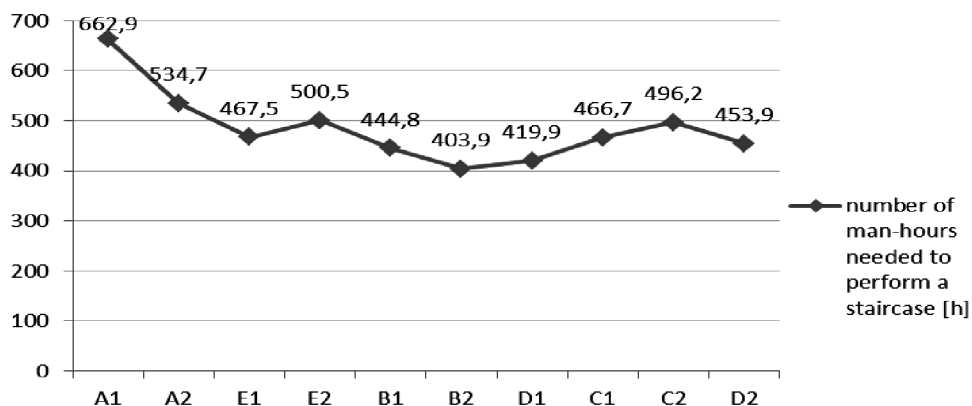
Fig. 2. Number of man-hours needed to perform a staircase

Basing on the timing method, the influence of days of the week on effectiveness of the construction workers can also be specified (Table 2). After analyzing the collected material, two variants of work on Friday were calculated:
– before working Saturday (Friday*),
– not before working Saturday (Friday**).

Employees achieve the greatest performance in the middle of the week, while the weakest at the beginning and at the end of the working week.

Performance of workers on each day of the week Wydajność pracowników w poszczególnych dniach tygodnia

	Monday	Tuesday	Wednesday	Thursaday	Friday*	Friday**	Saturday
Stairs installation [m/h]	1.09	1.24	1.24	1.25	1.09	1.01	0.91
Preparation of landings [m²/h]	1.25	1.7	1.76	1.58	1.92	1.72	1.28
Formation of landings [m²/h]	1.19	1.17	1.24	1.23	1.19	0.87	1.07

The studies presented above are an introduction to the analysis of working time of construction workers. Their objective is the determination of the impact of several factors on time and efficiency of construction workers. After analyzing all the factors and aspects that affect working time, it is possible to build a mathematical model of working time of construction workers. The presented results are only the beginning of a thesis and will be continued.

4. A comprehensive study of working time

In order to realize the full research, that would present the widest image of working time of a construction worker and impact of each factor on its effectiveness, a multidisciplinary research using most of described research methods should be performed. Only a focus on the aspect of quantity, quality and organization analyzed together allows for an objective assessment.

Continuous development of the construction sector, implementation of new technologies and increasingly sophisticated mechanization of works impose the need for a constant monitoring of workers and the drawing of correct conclusions. Modern construction should not be based on old, outdated standards as, in any type of work, equipment manufacturers and materials suppliers aim to facilitate people's work. It increases the productivity and efficiency of every single worker. Keeping constant observation ended with the right conclusions increases optimalization of the whole process, expense redundancy and faster turnaround time.

R e f e r e n c e s

[1] Stabryła A., Trzcieniecki J., *Organizacja i zarządzanie. Zarys problematyki*, Akademia Ekonomiczna w Krakowie, Kraków 1986.

[2] Townsend K., Lingard H., Bradley L., Brown K., *Complicated Working Time Arrangements: Construction Industry Case Study*, Journal of construction engineering and management – ASCE, 138, 2012, 443-448.

[3] Zhao J., Zhu N., Lu S.L., *Productivity model in hot and humid anvironment based on heat tolerance time analysis*, Building and environment, 44, 2009, 2202-2207.

[4] Bowen P., Edwards P., Lingard H., *Workplace Stress Experienced by Construction Professionals in South Africa*, Journal of construction engineering and management – ASCE, 139, 2013, 393-403.

[5] Hermanowski T., *Absencja chorobowa pracowników a funkcjonowanie przedsiębiorstw i rynku – wyniki analizy z użyciem symulacyjnego modelu wieloagentowego*, [In:] T. Hermanowski, *Szacowanie kosztów społecznych choroby i wpływu stanu zdrowia na aktywność zawodową i wydajność pracy*, Wolters Kluwer Polska SA, Warszawa 2013, 48-70.

[6] Martyniak Z., *Metody organizowania procesów pracy*, Państwowe Wydawnictwo Ekonomiczne, Warszawa 1996.

[7] Pasieczny L., *Encyklopedia organizacji i zarządzania*, Państwowe Wydawnictwo Ekonomiczne, Warszawa 1981.

MAGDALENA MIKOŁAJCZYK[*]

DYNAMIC COMPACTION OF COHESIVE SOILS – THEORETICAL ASPECTS AND MODELING

DYNAMICZNE ZAGĘSZCZANIE GRUNTÓW SPOISTYCH – ASPEKTY TEORETYCZNE I MODELOWANIE

Abstract

The principles of dynamic compaction of soils are presented in the paper, along with a short description of its usefulness for cohesive soils. The main topic of the article is the description of ways of modeling the phenomenon related to dynamic compaction. This is based on experimental data and on recently developed computer models using the Finite Element Method. Existing simplified 'perfectly flexible plastic' model is presented and used for computer modeling. The model does not capture the highly plastic and nonlinear behavior of cohesive soils under dynamic compaction. Additionally, a modified Cam-Clay constitutive model will be briefly described, which can address the above mentioned issues. Computer modeling method of the phenomenon will be discussed, together with a short description of the dynamic characteristics of the process.

Keywords: dynamic compaction, cohesive soils, Final Elements Method

Streszczenie

W artykule przedstawiono podstawy zagęszczania dynamicznego wraz z krótkim opisem jego stosowalności dla gruntów spoistych. Podstawowym tematem artykułu jest jednakże opis modelowania tego zjawiska. Jest on oparty na danych doświadczalnych oraz, ostatnio rozwiniętych, metodach opartych na Metodzie Elementów Skończonych. Przedstawiono podstawy modelu doskonale plastycznego (stosowanego w modelowaniu komputerowym). Model ten nie odzwierciedla jednak wysoce plastycznego i nieliniowego zachowania gruntów spoistych pod wpływem dynamicznego zagęszczania. Zmieniony model konstytutywny Cam-Clay został krótko opisany, może on do pewnego stopnia rozwiązać powyższe problemy. Zostaną przedstawione sposoby praktycznego modelowania zjawiska, a także podstawy komputerowego modelowania zjawiska, wraz z dyskusją dynamiki procesu.

Słowa kluczowe: zagęszczanie dynamiczne, grunty spoiste, metoda elementów skończonych

[*] M.Sc. Eng. Magdalena Mikołajczyk, Ph.D. student, Institute of Geotechnics, Faculty of Environmental Engineering, Cracow University of Technology.

Notation

c – cohesion [kPa]
C_c – wave velocity [m/s]
d – crater depth [m]
D – tamper diameter [m]
E – elastic modulus [kPa]
f – wave propagation frequency [Hz]
F – force [MN]
G – shear modulus [kPa]
H – tampering height [m]
M – constrained modulus [kPa]
t – time [s]
W – tamper weight [Mg]
H – tampering height [m]
λ – wave length [m]
ρ – density [Mg/m^3]
υ – Poisson's ratio [–]
φ – friction angle [deg]
ψ – dilation angle [deg]

1. Introduction

Dynamic compaction (DC) is an engineering process used to increase structural bearing capacity of soils – for building purposes (in particular – foundation soils straightening).There are a few distinct types of that process, but only DC using heavy tampering issues is shortly discussed in this paper. It was invented a long time ago, but in modern practice it has been developed by Louis Mennard and his commercial company MENARD Corp [1–3].

The process can be described as follows: the tamper (usually a steel cylinder of 2–3 meters of diameter, several tons of weight) is raised up to a pre-calculated height using a special crane to be then released. It gains speed quickly (and thus kinetic energy) and then it hits the ground, compacting it. A crater forms, sometimes of a depth of 1m or more. The structural parameters of soils are then greatly improved (albeit only in the vicinity of actual impact site). The procedure is repeated for neighbouring places following a pre-planned regular pattern. Sometimes more than one hit of the tamper is required. The procedure is referred to as the "multiple passes" approach. The entire area is leveled afterwards, using bulldozers, and sometimes other materials (gravels) are introduced [3, 4].

The following parameters are of main interest: the tamper weight W, the tampering height H, the tamper diameter D of the bottom area, the crater depth d, the type of soil to be treated, including its actual layered structure.

This technology is used for improvement of foundations for large-scale projects, where no other known technology can be used in an economical way. It has been successfully utilized for granular soils, where its functioning is quite well understood. It can be used for fine soils as well, but the physics behind this is far more complicated [4].

From an engineering point of view, there are three main differences between Dynamic Compaction of granular and fine soils. Firstly, there are water-pore pressure issues. In coarse, granular soils after tampering, water is filtered away through small pores between the grains. The water pressure slowly decreases after that. This process can take a few months to complete. In fine soils it is, however, hardly possible. Water will not filter through soils that easily. When the pore water pressure is high enough, it creates cracks in the body of soil around the point of tampering, so that water may escape. Sometimes this flow is so intensive that shallow marshes or puddles are visible on the surface after tampering [2, 4, 5].

Secondly, the situation with compressed gas bubbles is different for fine and coarse soils. In fine soils a large part of air trapped in the soil pores does not escape during dynamic compaction, and while this will not crack the soil body, it is being compressed, thus the overall volume of pores can be decreased, resulting in some soil compaction [2].

Thirdly, there is a difference between fine and coarse soils regarding remoulding issues. With great stresses caused by DC the internal structure of the soil may be destroyed, so at that point the soil may behave like a liquid. This happens when the stresses overcome the forces holding the grains together. This phenomenon is called a "soil liquefaction". After some time, however, the soil "remoulds" as it returns to the solid state, albeit with different parameters. This may lead to a general improvement of the soil condition (as it gets compacted that way), but if fine soils are surrounded by significant inlets of coarse material (that is fine soils are "supported" by a coarse "skeleton") liquefaction of the fine part will be of no use, as it shall "remould" into the same shape as before the treatment. Because of that, DC must be performed in such a way that liquefaction of coarse material happens before, or nearly at the same time, as of the fine one [2].

Dynamic Compaction can thus be utilized for both granular, and fine soils, or a combination of both, but there is a need for good modeling tools and guidelines. Louis Mennard has proposed some rough estimations [2, 3], based on actual engineering practice, but a more refined approach is needed, because not all soils can be effectively treated that way. The other problem is that DC is an efficient, though costly technology. Excess tampering may be unnecessary representing wasted time and money, or even counterproductive, since a poorly designed DC process may even weaken the soil. A lot of energy is put into the ground in a dynamic way. This may cause serious problems for neighbouring buildings which poses a risk of cracking or even failing. An estimation of the allowable distance from the nearest structure is therefore very important.

2. Common modeling approaches

The described phenomenon has been studied extensively. Some of the main findings and theories used are summarized below. In most cases the calculations are done using the Finite Element (FE) method.

As a first step for modeling of dynamic consolidation of soils, some models based on the linear equivalent viscous-elastic theory are introduced and implemented. However, they are not realistic for a medium like soils characterized by complicated behavior under dynamically changing pressures, among other issues. Some parameters however, may be extracted from that models for further use. Models based on the elastic principle are much

better as they can capture the nonlinear behavior under changing and variable stress paths. There is still a serious problem with capturing and modeling of dynamic processes, including Dynamic Compaction [6].

The linear viscoelastic model, yet only partially useful, has one big advantage: only one stiffness matrix is needed for each time step. The equivalent for elasto-plastic models are much more complicated. Moreover, their implementation is more difficult [6].

To be able to solve these problems simultaneously, a new approach was referred to as the hypo-plasticity model. It was developed for stress-strain under simple loading. Then it was extended to more complicated loadings.

The model is based on dividing an effective stress tensor so that the spherical and the deviator stress which determine the behavior are seen. The theory was implemented into the FE code, and some reasonable results were obtained [6], but only for saturated sand foundations (although the authors of the method have stated that the model had also been verified using triaxial tests on silty clays).

Another widely used model is a Cam-Clay plasticity model. It was developed only for deformation and strain analysis of partially or fully saturated granular soils, using three-phase continuum theory [7].

Firstly, the energy expressions for the constitutive models are given. They are then related to effective stresses and deformations of the soil matrix, the pressures and the volume changes. Also, perhaps most importantly, they are linked to the seepage forces and the corresponding pressure gradients. The dissipation inequality is then calculated as well as condition of convexity of the yield function [7]. Next, conditions describing deformation bands for drained and undrained states are given. Finally, specific constitutive models for partially saturated soils have been developed, taking into account the calculated plasticity of the media. An interesting point is that the matrix suction is treated as another strain-like variable. Again, the model can only be partially used for fine soils, or for a mixture of different types of soils, under dynamic loads.

3. Force – load function

Another approach was proposed in [8]. Here, to overcome the general problem of dynamic loads, a different modeling tool has been developed. A specially constructed force-time function was superimposed on a fairly classic elastic model. This has led to a hybrid model, which was then introduced into the widely used Finite Element Method (FE) software. This approach is especially interesting for the author, although another software is to be used, named Z_SOIL v13.09 2d. This software is widely used for various tasks involving foundations analysis in different conditions. It has become an industrial standard for FE analysis. Being able to model DC that way, shall greatly increase the usefulness of the software referred to [8]. This is, however, a model for coarse soils.

The proposed function [8] consists of two parts: The left (ascending) part and the right (descending) part. Both are chosen to provide the composite characteristics of the phenomenon. The shapes of the two parts of the plot were based on both experimental and analytical data.
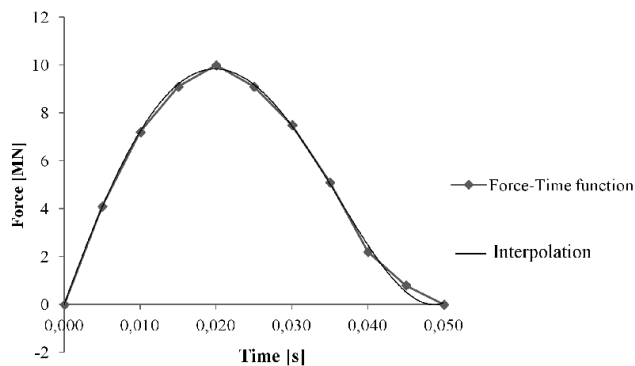
Fig. 1. Force-time function, along with the interpolation plot

To simplify the analysis an interpolation function is proposed (Fig. 1), using the following polynom:

$$F(t) = 10000000t^4 - 747786t^3 - 8715.6t^2 + 873.15t + 0.0042 \qquad (1)$$

where:

t – denotes the time [s].

The function was based on regeresion analysis of the available data.

The figure shows that main differences between the lines (original data and interpolation) occurs in the very last part (about 0.045s). This can be easily rectified by using a more complicated polynominal function, or another type of interpolation, but it seems to have no big impact on the results.

4. FE model

To build a working model, boundary conditions must be specified. The Figure 2 shows the original plot [8] together with the author's implementation of this plot using Z_SOIL. (Fig. 2). The model is axi-symmetric.
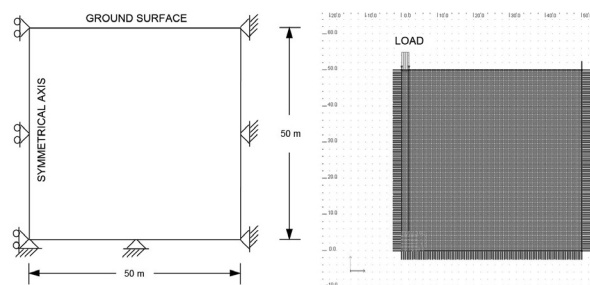
Fig. 2. Boundary conditions for modeling [8] (left), as used in
Z_SOIL software suite (right)

This is a provisional model, based on [8], for coarse soils. The soil parameters used are: $E = 5000$ kPa, $\varphi = 25$ deg, $\psi = 5$ deg, $c = 5$ kPa, $\nu = 0,35$, $\rho = 1.8$ mg/m^3. Some other data were calculated: $M = 8025$ kPa, $G = 1852$ kPa, $Cc = 66.8$ m/s, wave propagation frequency for $f = 10$ Hz, $\lambda = 6.7$ m. They were used for determination of the size of FE mesh and mesh density identification.

5. Conclusions

Dynamic compaction technology has been known for some time now. It has been successfully used for different conditions, however an advanced tool for a correct design of the process is needed, especially for fine soils.

A proposed polynominal force-time function in its current form can be a meaningful step for formulating better modeling tools for dynamic loads assessment.

The results obtained by the Z_SOIL model differ from the expected deformations and settlements. This may mean that the model will have to be modified taking into account the highly nonlinear behavior of soils. The next step will be the improvement of the Z_SOIL model and its implementation for cohesive soils. It is emphasized, however, that much more work is required to attain a useful model for fine soils under dynamic loads, including the multiple-passes case.

References

[1] Gaszyński J., Pabian Z., *Modeling research of dynamic compaction of cohesive soils. Badania modelowe udarowego zagęszczania gruntu spoistego*, Czasopismo Techniczne 3-Ś/2011, Kraków 2011, 28-50.

[2] Menard L., Broise Y., *Theoretical and practical aspects of dynamic compaction*, 1975, Geotechnique, 25, 3-18.

[3] Menard Soltraitementi Freyssinet Polska, *Means of foundations enchencing. Metody wzmacniania podłoża gruntowego*, Materiały reklamowe, 2011.

[4] Mostafa K., *Numerical modeling of dynamic compaction in cohesive soils*, disstertation for the phd title, University of Akron, Akron 2010.

[5] Pabian Z., *Experimental research of cohesive soils deformation process under dynamic loads. Proces deformacji gruntów spoistych wywołany obciążeniem udarowym w świetle badań eksperymentalnych,* praca doktorska, Politechnika Krakowska, 2005.

[6] `Zhou Ch., Shen Z.J., Yin J.H., *Biot dynamic consolidation finite element analysis using a hypo-plasticity model*, 13th World Conference on Earthquake Engineering, Vancouver, Canada, 2004, Paper No.351.

[7] Borja R.I., *Cam-Clay plasticity. Part V: a mathematical framework for three-phase deformation and strain localization analyses of partially saturated porous media,* Comput. Methods. Appl. Mech. Engineering 193, 2004, 5301-5338.

[8] Pan J.L., Selby A.R., *Simulation of dynamic compaction of loose granular soils*, Advances in Engineering Software, 33, 2002, 631-640.

ANNA MŁYŃSKA[*]

EXPERIMENTAL ANALYSIS OF BIELANY WASTEWATER TREATMENT PLANT HYDRAULIC LOAD VARIABILITY

EKSPERYMENTALNA ANALIZA ZMIENNOŚCI OBCIĄŻENIA HYDRAULICZNEGO OCZYSZCZALNI ŚCIEKÓW W BIELANACH

Abstract

In the performed research, the variability of sewage inflow to the Wastewater Treatment Plant in Bielany during dry and wet weather in different years and months in the period of 2008–2012 was analyzed. Particular attention was paid to the problem of accidental water which inflows to the sewage system in Bielany. Considering the period of observation, the hydraulic capacity of wastewater treatment plant was most frequently exceeded in 2010 (172 cases), least frequently in 2012 (54 cases). The probability of the appearance of daily sewage inflows, which exceed the hydraulic capacity of wastewater treatment plant in the period between 2008 and 2012 was 42%. The performed research has shown that, after eliminating the inflow of accidental water to the sewage system, the average-daily hydraulic load would not exceed 78.1% of the designed hydraulic capacity.

Keywords: hydraulic capacity, sewage, wastewater treatment plant

Streszczenie

W wykonanych badaniach przeanalizowano zmienność dopływu ścieków do oczyszczalni ścieków w Bielanach podczas pogody suchej i mokrej w poszczególnych latach i miesiącach 2008–2012. Szczególna uwaga została poświęcona problemowi wód przypadkowych dopływających do systemu kanalizacji w Bielanach. W całym okresie obserwacji najczęściej przepustowość hydrauliczna oczyszczalni ścieków była przekraczana w 2010 roku (172 przypadki), a najrzadziej w 2012 roku (54 przypadki). Prawdopodobieństwo pojawienia się dobowych dopływów ścieków, przekraczających przepustowość hydrauliczną oczyszczalni ścieków w latach 2008–2012, wyniosło 42%. Wykonane badania wykazały, że po wyeliminowaniu dopływu wód przypadkowych do systemu kanalizacji średniodobowe obciążenie hydrauliczne nie przekraczałoby 78,1%.

Słowa kluczowe: przepustowość hydrauliczna, ścieki, oczyszczalnia ścieków

[*] M.Sc. Anna Młyńska, Ph.D. student, Institute of Water Supply and Environmental Protection, Faculty of Environmental Engineering, Cracow University of Technology.

1. Introduction

Proper design of wastewater treatment plant and its further exploitation requires the knowledge of characteristic changes of quantitative sewage inflow. The inequality of sewage outflow from sewage systems appears both in daily, weekly and yearly cycle [1]. The most important factors, which determine the quantitative characteristics of sewage produced in settlements are dependent primarily on the quantity of households equipment with sanitary facilities and its condition, the method of water supply, the method of sewage disposal, the price of water and the cost of sewage drainage, people's lifestyle, the number of people living in the area, different types of manufacturing present, service and administration facilities which are not equipped with their own sewage disposal systems, and the degree of influence the infiltration and accidental water has on sewage systems [2].

Objects which are affected by improper dimensioning, by incorrectly defining the reliable flow can have problems with hydraulic underload. In this case, the challenge is to maintain the activated sludge in good condition with very low, or even evanescent, sewage inflow. Small amounts of sewage inflows to wastewater treatment plant cause the increase of the time of their retention in different technological objects of a wastewater treatment plant [3, 4]. Apart from the objects which have problems with hydraulic underload, one can also meet objects which even several times exceed the designed capacity. On such state, the uncontrolled inflows of foreign water – accidental and infiltration water – has influence. These waters cause dilution of pollutants contained in the sewage and cause reduced sedimentation ability of sludge as a result of too high sewage flow speed and the reduction of organic substance content susceptible to biodegradation in raw sewage [5]. Increasing sewage inflows to wastewater treatment plant contributes to the reduction in the efficiency of the equipment such as sand traps, and initial and secondary clarifiers. They can also cause flushing of the activated sludge from the biological reactor [6] and can increase the financial expenses of transportation and sewage aeration [7].

2. Research purpose

The main purpose of the executed research was the analysis of hydraulic load of Wastewater Treatment Plant in Bielany in terms of design capacity in specific years and months of period between 2008 and 2012 for the dry and wet weather. Very important was also to show the frequency and probability of sewage inflows appearance, the values of which exceeded the design capacity of the object. Particular attention was paid to foreign waters, mostly accidental water, which inflows to the sanitary sewage system in Bielany. Knowledge of the real quantity and the inflow inequality of wastewater to the sewage system is important due to the choice of a suitable method of their disposal and the proper exploitation of technological objects of the wastewater treatment plant.

3. Characteristics of the research object

The Wastewater Treatment Plant in Bielany is located in the southern part of the Bielany settlement, located in District VII "Zwierzyniec" in the western part of Cracow. It is estimated

that this wastewater treatment plant is used by about 1500 inhabitants. It is a mechanical – biological treatment plant, purifying domestic wastewater. The design capacity of this object is equal to 225.0 $m^3 \cdot d^{-1}$. To the sanitary sewage system in Bielany, the length of which is 10 km, 330 buildings are connected. The length of the storm water drainage in this area equals 1 km.

4. Research methodology

Based on the measurement results of daily sewage inflows to the Wastewater Treatment Plant in Bielany in the period from 1.01.2008 to 31.12.2012, the analysis of hydraulic load variability were conducted. The basis for the study was to determine the maximum, average, and minimum daily sewage inflows to the wastewater treatment plant. To measure the inflows, the measuring system installed in measuring recess, located in the wastewater treatment plant area was used.

In addition, this study took into account the daily precipitation. Knowledge of this parameter was necessary to determine which of the days of the period between 2008 and 2012 were dry, which were wet, and what was the degree of influence the foreign waters had on sewage system in the days with rainfalls. The amount of daily precipitation was measured by sensor trough, which was installed in the wastewater treatment plant area.

5. Research results and analysis

The first stage of research focused on the presentation of the shape of the average daily sewage inflow to the wastewater treatment plant in days with rain and days without rainfall, in each year of the period between 2008 and 2012 (Fig. 1). Inflows of sewage in days with rain in all years were much higher than in days without rainfall. The analysis showed that the average amount of daily sewage inflow to the wastewater treatment plant in the days of rainless weather in the study period was 175.8 $m^3 \cdot d^{-1}$ and was lower than the design capacity of the object (225.0 $m^3 \cdot d^{-1}$) by 21.9%. In the period between 2008 and 2012, accidental water caused the increase in the average daily sewage inflow by 37.1%, compared to the average daily inflow sewage during dry weather. The largest average daily sewage inflow to the wastewater treatment plant in the days of rain was recorded in 2010 (average 278.6 $m^3 \cdot d^{-1}$), while the lowest average daily inflow was recorded in 2012 (average 218.4 $m^3 \cdot d^{-1}$). Considering the values of the average daily sewage inflows in days without precipitation, there was no excess of design capacity of the wastewater treatment plant in any year of the analyzed period.

In the next stage of the study it was shown (Fig. 2) that the average daily inflow of the proper sewage to wastewater treatment plant in the period between 2008 and 2012 reaches the level 186.4 $m^3 \cdot d^{-1}$ and is lower than the design capacity of the object by 17.2%. In a multi-year period, accidental water caused an increase in the average daily sewage inflow in relation to the average daily proper sewage inflow by 19.5% which was probably primarily caused by precipitation. Annual total precipitation increased from 609 mm in 2008 to 895 mm in 2010 and then decreased to about 500 mm in the next years of the analyzed period. In turn, the average
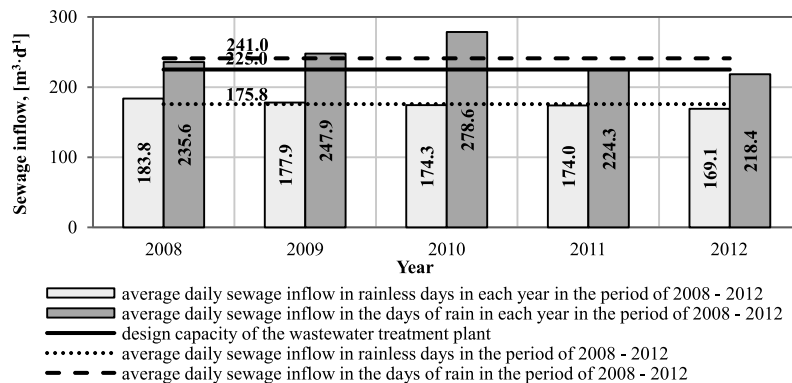
Fig. 1. The average daily sewage inflow to Wastewater Treatment Plant in Bielany
in the days of rain and in rainless days in each year in the period between 2008 and 2012

annual total precipitation in the period between 2008 and 2012 was about 650 mm. The largest average daily sewage inflow, equal to 260.3 m³·d⁻¹ and the largest part of accidental water was recorded in 2010. Accidental water were 27.4% of the average daily sewage inflow. The lowest average daily sewage inflow equaled 196.6 m³·d⁻¹ and the lowest part of accidental water was recorded in 2012. Accidental water was only 10% of the average daily sewage inflow.

Considering the rate of the hydraulic load the object in each month in the period between 2008 and 2012, the largest average daily sewage inflow to wastewater treatment plant in the days of rain was usually observed in May (average 309.4 m³·d⁻¹) and was higher than the design capacity of Bielany Wastewater Treatment Plant by 37.5% and in June (average 251.8 m³·d⁻¹) when the design capacity was exceeded by 11.9%. The lowest average daily sewage inflow in the days of rain was recorded in January (average 225.8 m³·d⁻¹) and November (average 221.8 m³·d⁻¹). Based on the average daily sewage inflows in days without precipitation, the design capacity was not exceeded in any month of the analyzed period (Fig. 3).
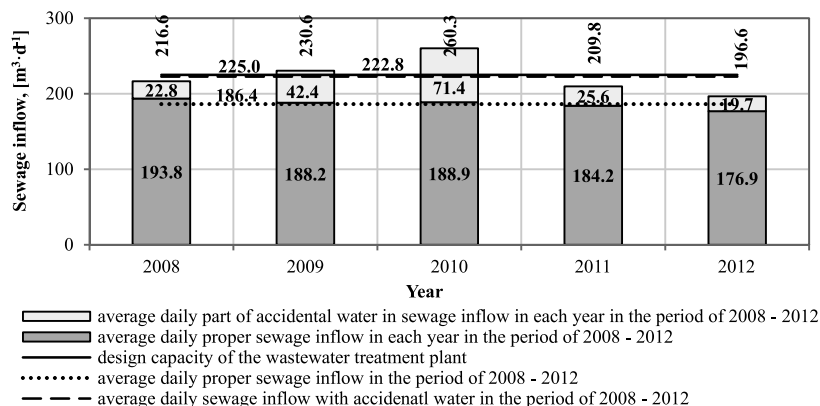
Fig. 2. The fraction of accidental water in average daily sewage inflow to
Wastewater Treatment Plant in Bielany in each year in the period of 2008–2012
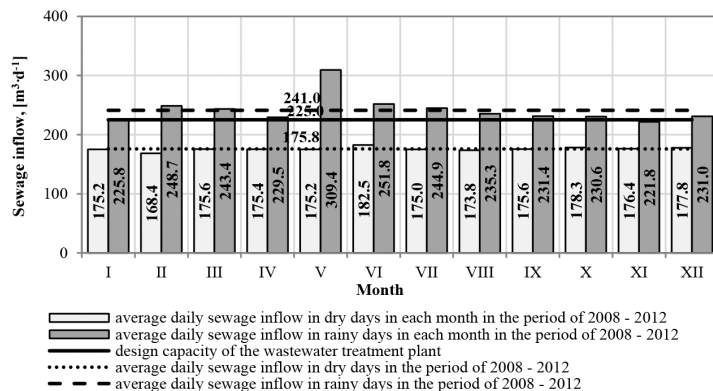
Fig. 3. Average daily sewage inflow to Bielany Wastewater Treatment Plant
in the days of rain and in rainless days in each month of period 2008–2012

The final stage of the research was to determine the frequency and probability of the appearance of sewage inflows of specified sizes. From 2008 to 2010, an increase in the number of cases when the object design capacity has been exceeded was noted. In 2010, 172 cases of exceeding the design capacity of the wastewater treatment plant were reported, while the smallest number of these events was reported in 2012 (54 cases). Over the five years of research, 534 cases of exceeding the design hydraulic capacity were reported, so the probability of this event was 42%.

6. Conclusions and statements

1) Throughout the research period the design capacity of wastewater treatment plant was not exceeded only in days of rainless weather.
2) In the period between 2008 and 2012, accidental water caused an increase in the hydraulic load of the wastewater treatment plant in comparison to the rainless period by 37.1%.
3) Performed research has shown that, from 2008 to 2010, there was a gradual increase in the number of cases in which the design capacity (225.0 $m^3 \cdot d^{-1}$) was exceeded. After 2010, the number of cases exceeding the hydraulic capacity decreased.
4) The design capacity of the wastewater treatment plant was most frequently exceeded in 2010 (172 cases), while in 2012 (54 cases) it was least frequently exceeded. In the period between 2008 and 2012 the total amount of events exceeding the design capacity was equal to 534.
5) In the analyzed multi-year period of 2008–2012, the probability of exceeding the design capacity of the object was 42%. The high probability of this event shows that it is necessary to eliminate inflowing of accidental water to the sanitary sewage system in Bielany, the large amounts of which appear during heavy rain or spring snowmelt. The completed research has shown that after eliminating accidental water inflow to the sanitary sewage system, daily average hydraulic load would not exceed 78.1%.

R e f e r e n c e s

[1] Myszograj S., Panek E., *Bilansowanie ilości ścieków dopływających do oczyszczalni*, Gaz, Woda i Technika Sanitarna, 5, 2007, 9-12.

[2] Osmulska-Mróz B., *Lokalne systemy unieszkodliwiania ścieków*, Instytut Ochrony Środowiska, Warszawa 1995.

[3] Pawełek J., Kaczor G., *Dobowe ilości ścieków w systemach kanalizacyjnych wsi Kluszkowce i Maniowy*, Zeszyty Naukowe Akademii Rolniczej w Krakowie, 17, 1997, 13-23.

[4] Kaczor G., *Prognozowanie dobowych dopływów ścieków do oczyszczalni wiejskich na podstawie wybranych miejscowości*, Acta Scientiarum Polonorum, 2002, 1-2, 7-20.

[5] Kaczor G., Wałęga A., *Wstępne badania nad wpływem wód przypadkowych na aktywność osadu czynnego oraz podatność ścieków na biodegradację*, Gaz, Woda i Technika Sanitarna, 2, 2012, 100-102.

[6] Kaczor G., *Wpływ wiosennych roztopów śniegu na dopływ wód przypadkowych do oczyszczalni ścieków bytowych*, Acta Scientiarum Polonorum, 10 (2), 2011, 27-34.

[7] Kaczor G., Satora S., *Problem wód przypadkowych w wiejskich systemach kanalizacyjnych województwa małopolskiego*, Inżynieria Rolnicza, 2 (3), 2003, 35-46.

IZABELA J. MURZYN[*]

DYNAMIC RESPONSE OF A PEDESTRIAN BRIDGE TO TRAFFIC LOAD

ODPOWIEDŹ DYNAMICZNA KŁADKI DLA PIESZYCH O ROZPIĘTOŚCI 120 M NA OBCIĄŻENIE DYNAMICZNE GENEROWANE PRZEZ ŚRODKI TRANSPORTU

Abstract

In the paper, a detailed analysis of the dynamic response of the pedestrian and cyclist footbridge to traffic loads typical for trucks, trains, metro and trams was presented. The representative time histories registered in the further cases were used as ground motion data in calculations of the dynamic response of the footbridge. The results of numerical analysis were checked with the criteria of vibration comfort for footbridges. The ABAQUS software was used for the dynamic calculations.

Keywords: footbridge, dynamics, footbridge vibrations

Streszczenie

W artykule zaprezentowano wyniki analizy dynamicznej kładki dla pieszych i rowerzystów w Pcimiu poddanej oddziaływaniom komunikacyjnym przenoszonym przez grunt. W tym celu wykonana została analiza modalna w pakiecie ABAQUS. Do przyczółków kładki zostało przyłożone obciążenie kinematyczne zarejestrowane dla oddziaływań komunikacyjnych. Wyniki analizy zostały porównane z kryteriami komfortu wibracyjnego kładek dla pieszych.

Słowa kluczowe: kładki dla pieszych, komfort wibracyjny, dynamika budowli

[*] M.Sc. Eng. Izabela J. Murzyn, Institute of Structural Mechanics, Faculty of Civil Engineering, Cracow University of Technology.

1. Introduction

1.1. Footbridges – definition, task and basic requirements

Footbridges are constructions, whose main task it is to carry pedestrians over a physical obstacle [2, 6, 9]. Currently, in addition to the safe conduct of traffic on the other side of the obstacle, pedestrian bridges are – for their users – a kind of an opportunity to enjoy the advantages of the environment with which they are associated.

Footbridges differ significantly from conventional bridges in how they influence the users. Footbridges' users are located directly on the object deck, staying there longer than when traveling by car across the bridge and feel its behavior directly. Users are exposed to a greater feeling of structural behavior [2, 6].

The application of advanced solutions makes the currently designed footbridges longer, lighter and more slender than the older ones [4, 11]. The new approach has a contrary effect on the dynamic properties of these objects. Sometimes, the lowest natural frequency of a structure coincides with the frequency of pedestrian steps (while walking or running). This situation may cause a resonance phenomenon and contribute to the failure of the structure. It should be noted that not only the pedestrians are the source of a dynamic load for footbridges. These structures can also be exposed to kinematic excitation originating from seismic or paraseismic phenomena, like mining tremors and traffic load [9].

In the paper, the comparison of the maximal acceleration obtained for the following types of traffic loads was presented. The results were summarized for loads generated by trucks, trains, metro and trams.

1.2. Traffic load [8]

The development of means of transport is the cause of an increase in the number of sources of vibration. This type of a load is transmitted via the ground [7]. They are outside of the construction. In particular, the effect of dynamic impact generated by traffic should be emphasized. One of the major conditions of sustainable development is also ensuring the safe, efficient and as rapid as possible movement between different places. The development of urban space causes the quality of people's life in cities to be disrupted by noise and vibrations. In the city space, the most common and troublesome source of vibration are movements of different vehicles. An interesting and poorly recognized issue is the effect of traffic loads which are source of vibration on footbridges [10].

This type of vibration is outside of the analyzed object. The vibrations are transmitted to the foundations of the structure by the ground. It should also be noted that the vibration which are generated by traffic have its own specific characteristics: during their lifetime their accretion and then decrease takes place [10]. It is shown in Fig. 1.
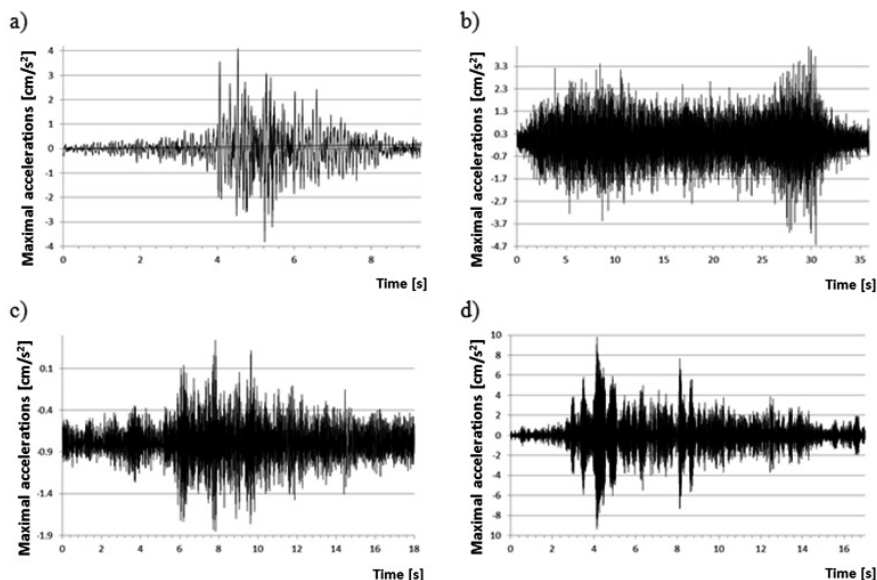
Fig. 1. Time histories of ground motion accelerations [cm/s²] registered in the urban space in az (vertical) direction for transit: a) truck, b) train, c) metro and d) tram [10]

2. Dynamic response of a pedestrian and a cyclist footbridge to traffic load

2.1. Main data and the numerical model of the footbridge

The calculations of the dynamic response of a pedestrian and cyclist footbridge to traffic load were performed for an existing footbridge located in Pcim, Southern Poland [1]. The primary purpose of the structure is to carry pedestrians and cyclists across the Raba river [8, 9].

In the work the model (see Fig. 2) presented in [9] has been used. The model was created in the ABAQUS software on the basis of the existing technical documentation [8]. The suspended structure of the footbridge consists of three spans: the middle one is 60.00 m long, whereas two extreme ones are 25.50 m long. The total theoretical length is 120 m. The footbridge's plat is composite with steel girders. The modulus of elasticity of steel girders and cross-bars was taken as 210 GPa. The Poisson's ratio was assumed as 0.29. The superstructure has been suspended from steel pylons 11.80 m high. The pillars and abutments are founded on reinforced concrete piles with a diameter of 100 cm [8, 9].

The footbridge is equipped with elastomeric bearings as linking elements between the deck and the piers. Usually, a two-coefficient Mooney-Rivlin model is used as a constitutive model of hyperelastic nonlinear elastomeric material of bearings. However, the parameters of the Mooney-Rivlin material: C_{10} and C_{01} can be replaced with equivalent elasticity modulus: $E = 6 (C_{10} + C_{01})$. In this work, the parameters of the Mooney-Rivlin model, assumed as $C_{10} = 0.292$ MPa and $C_{01} = 0.177$ MPa [3], were replaced with the equivalent elasticity modulus of 2.814 MPa. Such simplification is commonly used in calculations of bridges with elastomeric bearings [3, 5]. The Poisson's ratio of elastomeric material was taken as 0.49.

2.2. Dynamic response of the footbridge to traffic loads

Firstly, the natural frequencies of the footbridge were evaluated. The first natural frequency $f_1 = 1.94$ Hz is associated with vibrations in the vertical direction, whereas the second natural frequency, $f_2 = 2.29$ Hz, corresponds to the horizontal mode of vibrations.

Then, for the assessment of the influence of dominant frequencies of the traffic loads on the dynamic response of the structure, full time history analysis (THA) was carried out. The time history analysis (THA) was carried out with the Hilber-Hughes-Taylor time integration algorithm provided in the ABAQUS software. Modal dynamic analysis was implemented for the solution, since the problem was assumed to be linear-elastic. The calculations of the dynamic responses were performed using time histories of the selected vibration generated by traffic load registered in three directions in the urban space. Rayleigh model of damping was introduced in the calculation. Rayleigh damping coefficients were determined based on: $\alpha = 0.1862$, $\beta = 0.00113$ [8].
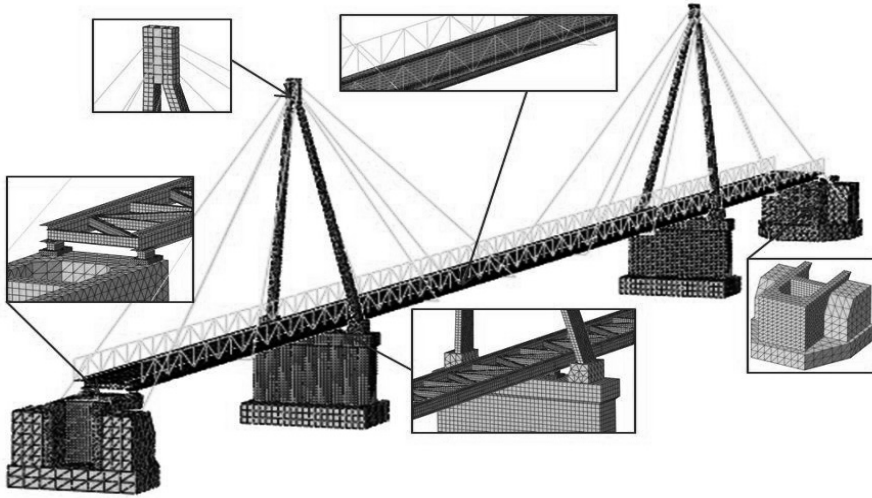
Fig. 2. The FE model of the footbridge [9]

The dynamic response of the footbridge to the selected traffic loads were evaluated for the whole model, but in the comparative analysis of the obtained responses, maximal acceleration was compared only for a point in the middle span of the footbridge (see Fig. 3). The relation between maximal acceleration and different type of traffic load obtained from the THA methods for traffic load from urban space is presented in Fig. 3. Taking into account the results of the numerical analysis, the vibration comfort criteria were checked for the footbridge. The results are summarized in Table 1, and compared with the selected comfort criteria (according to the literature). In all types of traffic load (truck, train, metro and tram), the vibration comfort criteria are met.

a) $a_{max} = 3.32$ [cm/s^2]

b) $a_{max} = 4.55$ [cm/s^2]

c) $a_{max} = 1.50$ [cm/s^2]
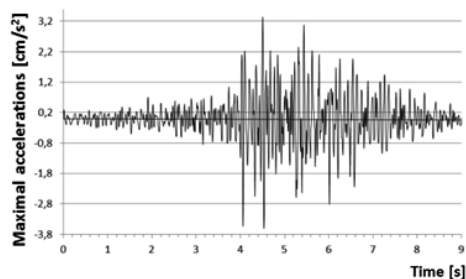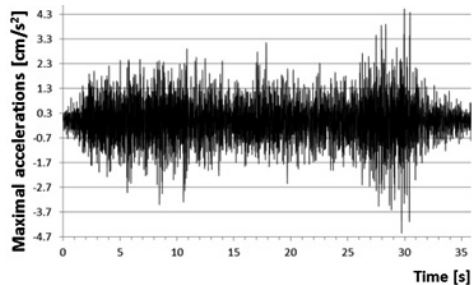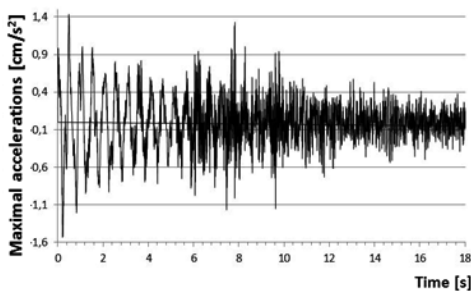
d) $a_{max} = 8.21$ [cm/s^2]
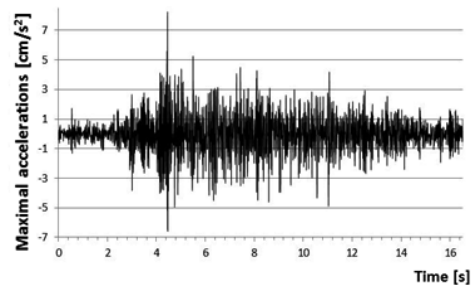
Fig. 3. The maximum accelerations [cm/s^2] in the middle span of the footbridge in a_z (vertical) direction for transit: a) truck, b) train, c) metro and d) tram

Table 1

The vibration comfort criteria for the footbridge

Standard	Acceptable acceleration [m/s^2]
BS 5400 [10]	0.63
The paper [4]	0.70–1.0
The paper [9]	0.65
SETRA [2]	0.50
PN-EN 1990/A1 [11]	0.70

3. Conclusions

The numerical analysis showed that the vibrations generated by the traffic load and transmitted via the ground (abutments) on the footbridge do not disturb the comfort of its use. For all checked cases of traffic loads: truck, train, metro and tram, the vibration comfort criteria which are summarized in Table 1 are met. What is more, the vibrations are practically imperceptible by the users of the footbridge.

194

R e f e r e n c e s

[1] Bilszczuk J., Szymczyk O., *New footbridges in Poland*, Modern Building Engineering, January–February 2012, 40-43.

[2] Bilszczuk J.W., Barcik et al., *Design of steel footbridges*, Lower Silesia Educational Publisher House (DWE), Wrocław 2004.

[3] Buckle I., Nagarajaiah S., Ferrell K., *Stability of Elastomeric Isolation Bearings: Experimental Study*, Journal of Structural Engineering 128, 1, 3-11.

[4] Charles P., Hoorpah W. et al., *Technical Guide: Footbridges – Assessment of vibrational behaviour of footbridges under pedestrian loading.* SÉTRA/AFGC, 2006.

[5] Dulińska J., Szczerba R., *Simulation of dynamic behaviour of RC bridge with steel-laminated elastomeric bearings under high-energy mining tremors*, Key Engineering Materials, 531-532: 662-667.

[6] Flaga A., *Mosty dla pieszych*, WKŁ, Warszawa 2011.

[7] Kawecki J., Stypuła K., *Zapewnienie komfortu wibracyjnego ludziom w budynkach narażonych na oddziaływania komunikacyjne*, Wydawnictwo PK, Kraków 2013.

[8] Murzyn I.J., Pańtak M., *The vibration comfort criteria assessment for the cable-stayed pedestrians and cyclists footbridge in Pcim*, Engineering and Construction, 9, 493-496.

[9] Murzyn I.J, *Dynamic characteristics of a cable-stayed pedestrian and cyclists footbridge 120 m long, International journal of earth sciences and engineering*, Vol. 07, No. 01, 313-319.

[10] Murzyn I.J, *Dynamic response of pedestrian and cyclist footbridge to communication load*, 9th Cracow Conference of Young Scientists, 2–4.10.2014, Kraków, Poland.

[11] Nowak A.S, *Live Load Model for Pedestrian Bridges*, 4th International Conference Proceedings, 2011.

[12] Pańtak M., *Analiza komfortu użytkowania stalowych kładek dla pieszych podatnych na wpływy dynamiczne*, praca doktorska, Politechnika Krakowska, Kraków 2007.

[13] British Standards Institution, BS 5400, Part 2, Appendix C: Vibration Serviceability Requirements for Foot and Cycle Track Bridges, 1978.

[14] PN-EN 1990:2004/A1:2008 Eurocode: Basis of structural design.

KATARZYNA NOWAK-DZIESZKO, MAŁGORZATA ROJEWSKA-WARCHAŁ[*]

MEASUREMENTS OF THE THERMAL COMFORT IN THE W70 PANEL BUILDING

POMIARY KOMFORTU CIEPLNEGO W BUDYNKU WIELKOPŁYTOWYM W SYSTEMIE W70

Abstract

It is estimated that about 4 million flats in Poland are made of prefabricated elements in different systems. Moreover, at present more than 10 million Poles live in system buildings. Despite the commonness of those buildings the analyses of the microclimate of the interior space are very rare. The paper presents the results of the thermal comfort measurements conducted in different flats of multi-family panel building made in W70 system. It appears there is a problem with the overheating effect during the summer months in all parts of the building.

Keywords: panel building, W70 system, thermal comfort measurements, PMV (Predicted Mean Vote), PPD (Predicted Percentage of Dissatisfied)

Streszczenie

Szacuje się, że w Polsce około 4 milionów mieszkań wykonanych jest w technologi wielkiej płyty w różnych systemach. Co więcej, obecnie ponad 10 milionów Polaków mieszka w budynkach systemowych. Pomimo powszechności tychże budynków analizy mikroklimatu wnętrz jest bardzo rzadkie. W artykule przedstawiono wyniki pomiarów komfortu cieplnego przeprowadzonych w różnych mieszkaniach wielorodzinnego budynku wzniesionego w systemie W70. Okazuje się, że we wszystkich analizowanych mieszkaniach występuje problem przegrzania w miesiącach letnich.

Słowa kluczowe: budynek wielkopłytowy, system W70, pomiary komfortu cieplnego, PMV (Predicted Mean Vote), PPD (Predicted Percentage of Dissatisfied)

[*] M.Sc. Eng. Katarzyna Nowak-Dzieszko, M.Sc. Eng. Małgorzata Rojewska-Warchał, Institute of Materials and Building Structures, Faculty of Civil Engineering, Cracow University of Technology.

1. Prefabricated panel buildings

In the fifties of the twentieth century the erection of panel system buildings began in Poland. For the several dozen years about 4 millions flats have been adjusted to use. At present more than 10 million Poles live in system buildings. It makes the problems connected with the proper usage and thermal insulation very important and common. The thermal insulation of those buildings is low and the seasonal heating energy demand is usually 50% higher than the national requirements [1]. The most important aspect is the improvement of the building energy certificate of those buildings. It is connected with the thermal modernization of the building envelope and change of windows.

Unfortunately at the stage of considering and designing the thermal modernization no-one takes into account the thermal comfort and overheating issues in summer which seem to be very important from the occupants' point of view.

The W70 System is the "opened" system used for the erection of multi-family buildings, in which, contrary to the "closed" system, all construction walls within the flats were eliminated. It allowed the changes of the partition wall pattern and at the same time enabled designing of flats with different areas and room arrangements. It is estimated that about 15% of all system buildings were erected this way.

2. Thermal comfort

Thermal comfort is related to the thermal balance of the body which is affected by different parameters: personal and environmental. The microclimate of the interior space is the combined effect of the design process, erection and the utilization of particular rooms. Thermal comfort is affected by human activity, clothing insulation and the environmental parameters such as air temperature, average radiation temperature, air flow speed and relative humidity. The evaluation of thermal comfort is based on the PMV (Predicted Mean Vote) and PPD (Predicted Percentage of Dissatisfied) indices.

The international standard PN-EN ISO 7730 "Ergonomics of the thermal environment. Analytical determination and interpretation of thermal comfort using calculation of the PMV and PPD indices and local thermal comfort criteria" [4] uses Fanger's method to estimate thermal comfort.

The Fanger's PMV method combines the following environmental features: air temperature, air velocity, mean radiant temperature and relative humidity and two personal variables: clothing insulation and activity level into the index that can be used to predict the average thermal sensation of a large group of people. The thermal sensation 7-level scale with values between −3 and 3 describes the thermal sensation between "hot" and "cold".

In this model, all major modes of energy losses from the human body are taken into account and the person is assumed to be at the steady state condition.

3. Flats analyzed

The aim of the field measurements was to analyze the thermal comfort in the particular parts of the W70 panel dwelling building, built in 1974 (Fig. 1). The tests were conducted using the digital thermal comfort measurement device (Babuc), Fig. 2 Infogap program to analyze test data.

a)

b)
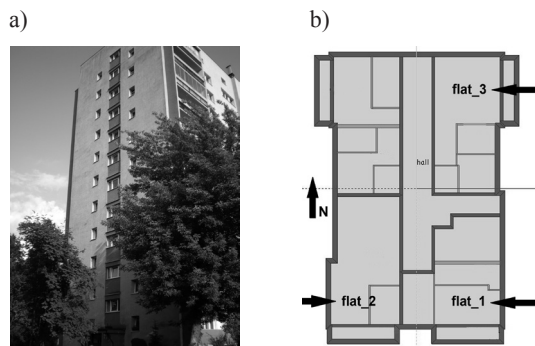
Fig. 1a) South elevation of the analyzed building,
b) location of flats at building floor

Fig. 2. BABUC – device used to measure
thermal comfort

Building plan area 21.5 × 13.2 m; usage building area – 2279 m², 25 m high with 11 levels. Basement below the entire building, flat roof.

Building with the natural ventilation, central heating system with convection heaters.

Communication area located in the center part of each building level. Four flats at every story located in the corners of the building.

The field tests were conducted in three flats at different levels and with different window orientation:

1) Flat number 1 – ground floor, South-East orientation,
2) Flat number 2 – fifth floor, South-West orientation,
3) Flat number 3 – seventh floor, North-East orientation.

Exterior walls made of prefabricated panels in W70 system, insulated with 10 cm of styrofoam with plasters at both sides: $U = 0.25$ [W/m²K], double glazing windows: $U = 1.7$ [W/m²K].

4. Test results

The main aim of the field tests was to analyze the microclimate conditions of the particular flats at different elevations during summer. Measurements allowed to determine the internal operative temperatures, and therefore – based on the measurement data – calculate the values of PMV index and PPD index.

The measurements were conducted in three days between 29th July and 31st July, for 24 hours in every flat referenced above, starting at seventh floor, next of the fifth floor and finally at ground floor. In each case the measuring device was located in the living room where the percentage of glazing at exterior walls is the highest.

The average external temperatures during those days were even above 30°C and were measured continuously, the results are presented in Fig. 3. The electronic device used for temperature measurements was located at the balcony of each flat.
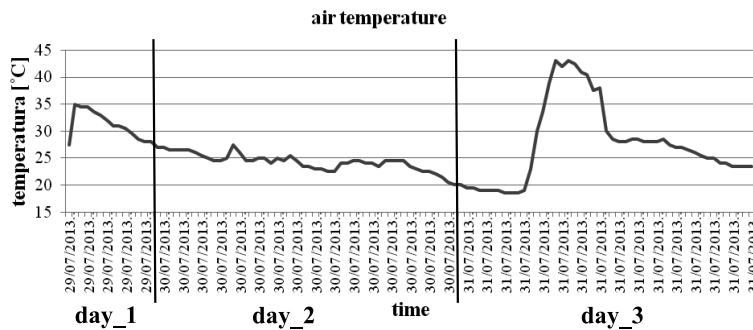
Fig. 3. External temperature between 29th and 31st July in Cracow

In all dwellings the operative temperature in the analyzed period of time is considerably higher than 25°C. The daily maximum interior operative temperature is 29.17°C. Those negative flat conditions continue for the entire day and do not change significantly at night. The flats can be cooled down during the night through the open windows. However, in case of such high external temperatures, it doesn't change the operative temperature much. All data are presented in Fig. 4.
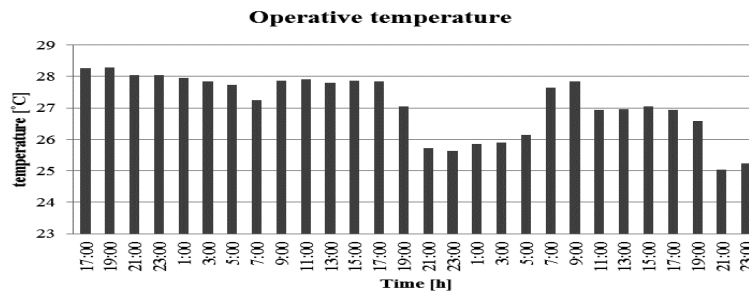
Fig. 4. Internal operative temperatures between 29th and 31st July in the analyzed flats

The thermal comfort conditions are closely related with the human activity and clothing insulation. The parameter *clo* = 0.5 describing clothing insulation, based on standard [3], was assumed in the calculations of PMV index. Regarding human activity, two cases were calculated: first one for a person having a rest and the second one for a person doing the cleaning.

Figure 5 presents the PMV values with the assumption that flat users have a rest. For most of the time the PMV value is between –0.5 and 0.5, for the rest of the time it's higher than 0.5 but not more than 1.
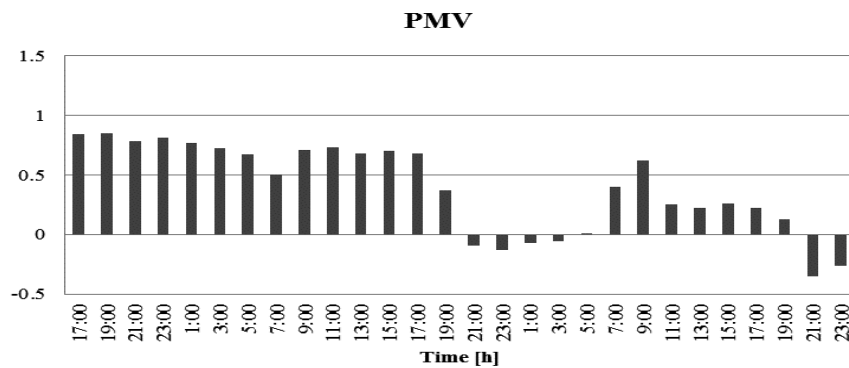
Fig. 5. PMV index – users having a rest

The results are much different when we assume different activity level of people staying inside the flats. Figure 6 presents the results. The PMV values are much higher than 1.5 almost for the entire period of time. Those are not comfortable conditions for users.

The predicted percentage of dissatisfied, described by PPD index in the analyzed period of time is between 50% and 80% (Fig. 7).
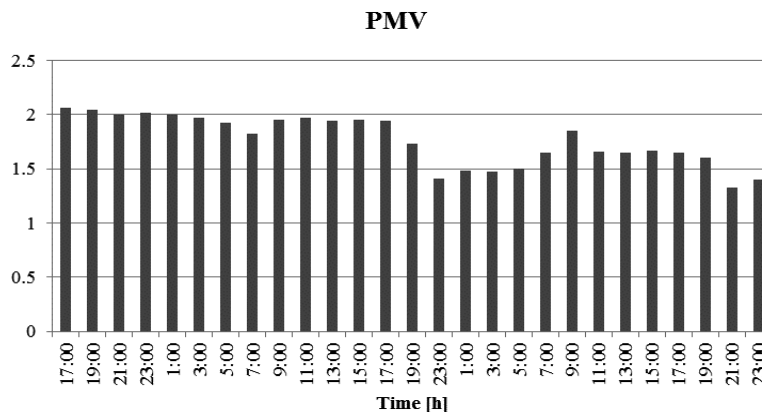
Fig. 6. PMV index – users cleaning the room

PPD
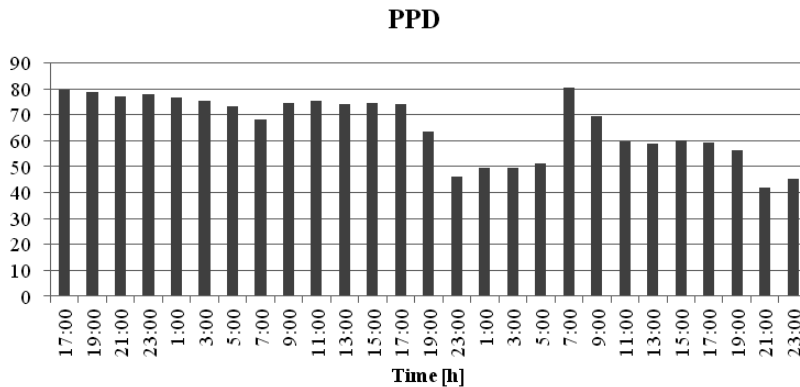
Fig. 7. PPD index – users cleaning the room

5. Conclusions

The results of conducted analysis show that the overheating problem in summer occurs in all flats of the panel building. Windows in the prefabricated panel buildings in most cases are poorly shaded from solar radiation. Glazing is the source of the excessive heat gains and results in overheating of the dwellings. The microclimate conditions in all flats are very uncomfortable and the parameters describing thermal comfort exceed the acceptable values. The operative temperatures are much higher than 25°C and the PMV values for most of the time are between 1.5 and 2 and the percentage of dissatisfied people for all the time is higher than 50%.

In case of all flats the internal or external shadings should be used to improve the microclimate conditions and reduce the internal operative temperatures.

R e f e r e n c e s

[1] Rozporządzenie Ministra Infrastruktury w sprawie warunków technicznych, jakim po-winny odpowiadać budynki i ich usytuowanie z dnia 12 kwietnia 2002.

[2] Ostańska A., *Wpływ dotychczasowych termomodernizacji budynków mieszkalnych na oszczędność energii i planowanie programów rewitalizacji na przykładzie jednego z lubelskich osiedli* Budownictwo i Architektura 7, 2010, 89-103.

[3] PN-EN ISO 7730 Ergonomics of the thermal environment. Analytical determination and interpretation of thermal comfort using calculation of the PMV and PPD indices and local thermal comfort criteria.

[4] Nowak K., *Modernizacja budynków a komfort cieplny pomieszczeń*, Energia i Budynek, 11 (54), 2011.

[5] Dębowski J., *Cała prawda o budynkach wielkopłytowych*, Przegląd budowlany 9/2012.

KATARZYNA NOWAK-DZIESZKO, MAŁGORZATA ROJEWSKA-WARCHAŁ[*]

THRMAL COMFORT OF THE INDIVIDUAL FLATS OF MULTI–FAMILY PANEL BUILDING

KOMFORT CIEPLNY MIESZKAŃ W BUDYNKU WIELKOPŁYTOWYM

Abstract

The paper presents the results of the annual computational simulations conducted for the W70 panel building. The calculations were carried out in the Design Builder program which allows preparing the simulation of the building envelope as well as the separate parts of the building interior. It is very rare to considerate the requirements connected to the overheating effect in the panel buildings. This issue is closely related to the thermal comfort in the building, especially during the summer months. Based on the conducted simulations, authors indicated the influence of building orientation, individual flat location and thermal insulation on the thermal comfort in the different flats of prefabricated panel building.

Keywords: panel building, W70 system, thermal comfort of the panel buildings, PMV (Predicted Mean Vote), PPD (Predicted Percentage of Dissatisfied)

Streszczenie

W artykule zostały przedstawione wyniki symulacji komputerowych przeprowadzonych dla budynku wielkopłytowego wzniesionego w systemie W70. Symulacje wykonano w programie Design Builder, który pozwala symulować obudowę budynku, a także poszczególne części wnętrza budynku. Problematyka przegrzania pomieszczeń jest bardzo rzadko analizowana w przypadku budynków wielkopłytowych. Problem ten jest ściśle związany z komfortem cieplnym budynku, szczególnie w miesiącach letnich. W oparciu o przeprowadzone symulacje autorzy określili wpływ termomodernizacji oraz orientacji poszczególnych mieszkań w budynku wielkopłytowym na komfort cieplny.

Słowa kluczowe: budynek wielkopłytowy, system W70, komfort cieplny w budynkach wielkopłytowych, PMV, PPD

[*] M.Sc. Eng. Katarzyna Nowak-Dzieszko, M.Sc. Eng. Małgorzata Rojewska-Warchał, Institute of Materials and Building Structures, Faculty of Civil Engineering, Cracow University of Technology.

1. Panel buildings in Poland

It is estimated that about 4 million flats in Poland are made of prefabricated elements in different systems. Moreover, at present more than 10 million Poles live in system buildings. It makes the problems connected with the proper usage and thermal insulation very important and common. The most important aspect is the improvement of the building energy certificate of those buildings. It is connected with thermal modernization of the building envelope and change of the windows.

Unfortunately, at the stage of considering and designing thermal modernization no-one takes into account the thermal comfort and overheating issues which seem to be very important from the occupants' point of view.

2. Thermal comfort

Thermal comfort is related to the thermal balance of the body which is affected by different parameters: personal and environmental such as human activity, clothing insulation and the environmental parameters (air temperature, average radiation temperature, air flow speed and relative humidity). The evaluation of thermal comfort is based on the PMV (Predicted Mean Vote) and PPD (Predicted Percentage of Dissatisfied) indices.

The international standard PN-EN ISO 7730 „Ergonomics of the thermal environment. Analytical determination and interpretation of thermal comfort using calculation of the PMV and PPD indices and local thermal comfort criteria" uses Fanger's method to estimate thermal comfort. This method combines the following environmental features: air temperature, air velocity, mean radiant temperature and relative humidity and two personal variables: clothing insulation and activity level into the index that can be used to predict the average thermal sensation of a large group of people.

3. Building description

The aim of the building simulations was to analyze the influence of thermal insulation and flat location on the thermal comfort in the particular parts of the panel building. The simulations were conducted for the W70 panel dwelling building, built in 1974. Plan area of 21.5 m × 13.2 m; usage building area – 2279 m^2, 25 m high with 11 stories. Basement below the entire building, flat roof. Thermal modernization of external walls was conducted in 2006. The picture and visualization of the building are presented in Figure 1.

Building with the natural ventilation, central heating system with convection heaters. Communication area located in the center part of each building level. Four flats at every story located in the corners of the building. Exterior walls made of prefabricated panels in W70 system, insulated with 15cm of styrofoam with plasters at both sides: $U = 0.20$ [W/m^2K] (before thermal modernization $U = 0.75$ [W/m^2K], double glazing windows: $U = 1.7$ [W/m^2K].

The percentage share of glazing areas at the elevations is as follows: N – 7.3%, S – 40%, E – 26%, W – 26%.

Fig. 1. West building elevation and visualization of the analyzed building

The calculations were carried out in the Design Builder v.3. The program has been specifically developed around Energy Plus allowing the simulation of the building envelope and building interiors. It provides extensive databases of building materials, constructions, window panes, glazing units, shadings and blinds. The simulations conducted for the Polish climatic conditions (building located in Cracow, Krowodrza district) allowed the evaluation of the thermal comfort of the entire building and of the particular rooms.

4. Simulation settings

The main aim of simulations was to determine the temperature and PMV index of the particular flats at different stories during summer months (Fig. 2).

Every single flat is the separate thermal comfort zone. Orientations of the flats are as follows: flat number 1 – East and South with the balcony at South side, flat number 2 – West and South with balcony at South, flat number 3 – West and North – balcony at West, flat number 4 – East and North – balcony at East side.

The analysis of the microclimate of particular rooms in the separate flats will be the subject of the further research.
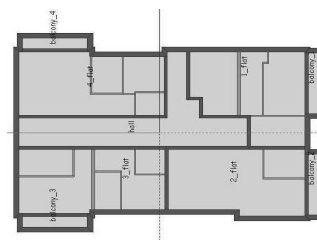
Fig 2. Visualization of typical zones at every building level

The simulations were conducted for the building model before thermal modernization (base case) and next compared with the current service conditions (after the thermal modernization). The Authors compared data for flats located at four different levels: ground

floor, third floor, seventh floor and tenth floor. The period of time between 15th May and 15th September was chosen as there may be a risk of overheating at this time in Poland.

The assumptions for the simulations:
1. Heating system on from September to March (22°C), 7 days a week, 24 hours a day.
2. Occupancy density: flats – 0.08 person per m^2.
3. Operating schedule: flats – 3 people per flat between 4 pm and 7 am, 5 days a week; at the weekends 3 people – all inside between 6 pm and 9 am; 50% reduced occupancy between 9 am and 6 pm.
4. Metabolic activity: factor 0.9, winter clothing – clo = 1.0, summer clothing clo = 0.5.
5. Ventilation requirements per Polish national standards PN-83/B-03430 [2] , in every flat: 70 m^3/hour for kitchen and 50 m^3/hour for bathroom.

5. Test results

All simulation results presented below have shown that during a few days between 15th May and 15th September the average interior air temperatures of different dwellings exceed 30°C and the PMV factor is higher than 2. Those microclimate building conditions exceed the optimal internal summer temperature of 25°C and recommended value –0.5 < PMV < +0.5.

Taking the orientation of the flats into account, in the first step of simulations the results for flat 2 – South-West orientation (the worst thermal conditions) and flat 4 – North-East orientation were compared. Figures 3a and 3b present the number of discomfort hours for South-West flat (number 2) and North-East flat (number 4) at four different levels in the building before thermal modernization. Comparing the diagrams the highest number of discomfort hours is noticeable at third floor. The values are slightly lower for North-East flat orientation. Overheating problem is noticeable in all analyzed months, both before and after the thermal modernization in flats at all levels. The worst conditions are observed during July and August at third floor. At ground level the number of overheating hours is the lowest.

In the dwelling located at the South-West building side, on the third floor, the operative temperature for most of the time is significantly higher than 25°C. The daily maximum interior temperature is 34.70°C and the PMV value is above 3. The number of discomfort hours in the assumed period of time is 2079. Those negative flat conditions continue almost for the entire day and do not change significantly at night. The flats can be cooled down during the night through the open windows.

In case of flats at the third floor temperatures above 32°C are higher than for other levels. It is connected with the direction of solar radiation during summer months and presence of balconies at southern building elevation.

Figures 4a and b present similar results but for the building after the thermal modernization. The number of discomfort hours is much higher and for temperatures above 32°C has almost doubled. The daily maximum interior temperature is 35.80°C and the number of discomfort hours in the taken period is 2532.

Figures 5a and b compare the results for flats with different orientations before and after the thermal modernization but located at the same, third floor. There are only slight differences between dwellings at the same level. The number of overheating hours is much higher after the modernization, for temperatures above 32°C increased from about 350 hours

to almost 600 hours. Figure 6 presents a diagram with the comparison of PMV index for South-West flat at different stories, after the thermal modernization. PMV index in all cases exceeds the value of 2 and in July it is even higher than 3.
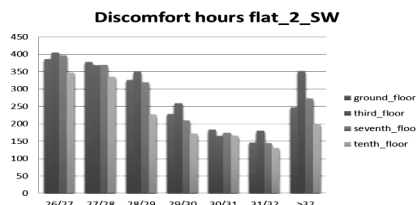
Fig. 3a. Number of overheating hours for flat 2 (South-West) at four levels – base case
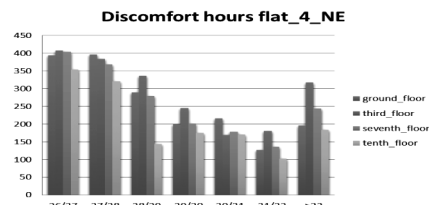
Fig. 3b. Number of overheating hours for flat 4 (North-East) at four levels– base case
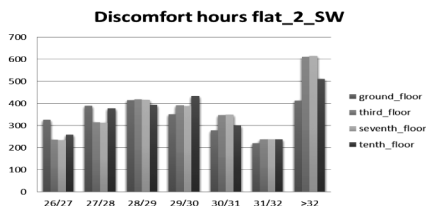
Fig. 4a. Overheating hours for flat 2 (South-West) at four levels – after thermal modernization
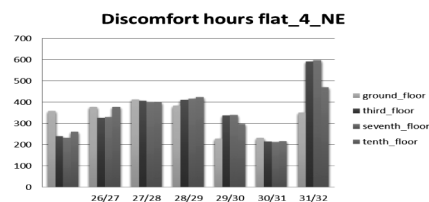
Fig. 4b. Overheating hours for flat 4 (North-East) at four levels – after thermal modernization
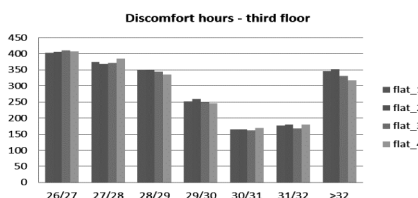
Fig. 5a. Number of discomfort hours for different flats at third floor – base case
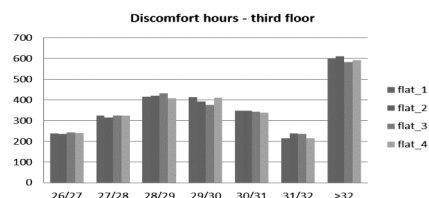
Fig. 5b. Number of discomfort hours for different flats at third floor – after thermal modernization
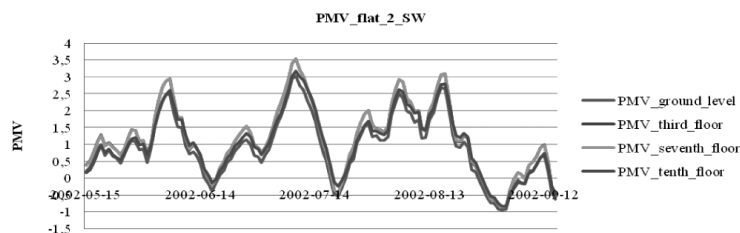
Fig. 6. PMV comfort index for South-West flat at different levels – after thermal modernization

6. Conclusions

The results of conducted analysis show that the overheating problems in summer months occur in panel buildings, both before and after the thermal modernization. Windows in the prefabricated panel buildings in most cases are poorly shaded from solar radiation. Glazing is the source of the excessive heat gains and results in the overheating of the dwellings. The microclimate conditions in all flats are very uncomfortable and the parameters describing thermal comfort exceed the acceptable values.

The modernization of the building should be preceded by the extensive analysis of how the changes influence the thermal comfort of the particular flats. The priority aim is reduction of heating costs in the winter season. The conducted analyses show that improving only the building envelope thermal insulation can unfavorably affect the internal conditions during summer season. In the process of thermal modernization of panel buildings, using internal or external shadings to reduce summer overheating should be considered. Those solutions are the subject of authors' further research.

R e f e r e n c e s

[1] PN-EN ISO 7730 Ergonomics of the thermal environment. Analytical determination and interpretation of thermal comfort using calculation of the PMV and PPD indices and local thermal comfort criteria.

[2] PN-83/B-03430 Wentylacja w budynkach mieszkalnych zamieszkania zbiorowego i użyteczności publicznej – Wymagania.

[3] Nowak K., *Modernizacja budynków a komfort cieplny pomieszczeń*, Energia i Budynek, 11 (54), 2011.

[4] Dębowski J., *Cała prawda o budynkach wielkopłytowych*, Przegląd budowlany, 9/2012.

[5] Nowak K., Nowak-Dzieszko K., Rojewska-Warchał M., *Thermal comfort of the rooms in the designing of commercial buildings*, Research and Applications in Structural Engineering, Mechanics and Computation. SMEC Cape Town 2013, 651-652.

KATARZYNA NOWAK, ANNA ZASTAWNA-RUMIN[*]

ANALYSIS OF TEST STUDIES OF THE BUILDING BARRIER CONTAINING PCM

ANALIZA BADAŃ TESTOWYCH PRZEGRODY ZAWIERAJĄCEJ PCM

Abstract

This paper presents the results of experimental tests of a wall barrier containing a layer with the addition of phase-change material. The study was performed in a climatic chamber for a light frame wall in two versions: with inner lining made of plaster-cardboard panel and of panel containing PCM. Temperature measurements were made on the surface of panels for non-stationary conditions in a climatic chamber. Research stand was prepared, in which heating of coat layers was effecting from an increase of the room's air temperature rather than from direct heating of the layers. The influence of the PCM was analyzed for faster and slower pace of air heating.

Keywords: phase-change material, experimental test, heat capacity, heat accumulation

Streszczenie

W artykule przedstawiono wyniki badań eksperymentalnych przegrody zawierającej warstwę z dodatkiem materiału fazowo-zmiennego. Badania wykonano w komorze klimatycznej dla lekkiej ściany szkieletowej w dwóch wariantach: z okładziną wewnętrzną wykonaną z płyty gipsowo-kartonowej oraz płyty zawierającej materiał fazowo-zmienny. Przeprowadzono pomiary przebiegu temperatury na powierzchniach płyt dla niestacjonarnych warunków panujących w komorze klimatycznej. Przygotowano stanowisko badawcze, w którym nagrzewanie płyt okładzinowych następowało poprzez wzrost temperatury powietrza w pomieszczeniu, a nie poprzez ich bezpośrednie nagrzewanie. Analizowano wpływ PCM podczas nagrzewania powietrza w szybkim i wolniejszym tempie.

*Słowa kluczowe: materiał fazowo zmienny, badania eksperymentalne, pojemność cieplna, aku-
mulacja cieplna*

[*] Ph.D. Katarzyna Nowak, M.Sc. Eng. Anna Zastawna-Rumin, Institute of Building Materials and Structures, Faculty of Civil Engineering, Cracow University of Technology.

1. Introduction

Preventing heat loss in a building is one of the many aspects taken into consideration during its design. The required result can be obtained by the application of a heat-insulation of a specific thickness. Unfortunately, there is not much attention paid to the microclimate of the buildings that do not actually fulfill the thermal comfort requirements. The situation occurs more often in modern buildings, especially based on a light-frame construction. The technology allows for sophisticated architectonic forms and is easy and fast at the same time (another popular trend uses glass surfaces). They both influence the architecture and make it more interesting, however, they also gain a lot of heat (mainly from insolation) that cannot be accumulated by the building's envelope. The result is seasonal overheating of a building and large temperature oscillations of internal air, due to temperature variation of external air.

The phase-change materials accumulate considerable amounts of heat thanks to high latent heat of phase-change of organic compounds, e.g. paraffins, fatty acids or inorganic salt hydrates. During their phase transition, accumulation or emission of large amount of heat occurs and is accompanied with a small temperature variation of a specific PCM. Hence, the application of PCM in a building increases its heat capacity.

Since the 1980's, one can notice the involvement of scientists in the integration of PCM with the elements of construction wall barriers. To this end, various types of materials and methods of their use were implemented. Applications, in the form of plasterboards with the addition of PCM have been the subject of numerous studies [1–3, 5, 8]. Research by teams of L.V. Shilei, A.K. Athienitis [1, 2] were conducted on plaster panels impregnated with PCM intended for the heating period. Research by S. Scalata team [3] was carried out in a laboratory simulating conditions of both summer and winter, and analysis was made solely on the basis of air temperature in the test room (also for PCM impregnated panels). Due to concerns about durability of these materials (PCM directly in contact with traditional materials, may cause leakage and corrosion), a solution in the form of microcapsules filled with PCM is preferred. Research on plasterboard with PCM microcapsules was carried out by C. Voelker and P. Schossig [6, 8]. These analyses were made only on the basis of air temperature after application of PCM lining, but without analyzing heat flux density and amount of accumulated energy. The tests were performed on real buildings. At the same time, the studies [6] indicate a low efficiency in case of high heat load of a room and of rapid temperature increase resulting from sun exposure. They show an increase in efficiency of the application, as a result of room shading, and a very important role of sufficient cooling of the material.

Despite numerous studies on plasterboards with the addition of PCM, there are no sufficient and reliable data that can serve as a comparison of effectiveness in relation to use of other types of PCM materials. The studies are carried out with different parameters of materials and the environment, and the results relate to parameters non-comparable with each other (e.g. air temperature changes, the surface of walls and shifts during peak temperatures, the number of hours when the temperature exceeds a given amount); there is also insufficient data based on the analysis of the heat flow, and the actual amount of stored energy determined with respect to traditional solutions. The presented results of the experiment show one of the stages, which is a part of the analysis of various applications efficiency. The aim of the study on plasterboard with PCM is also to use them as a comparison element for further work on other solutions.

2. The purpose of this article

The aim of this experiment is to analyze the influence of dynamics of change rate of ambient temperature on the efficiency of the phase-change material. The results may be helpful in the process of optimizing the use of these materials in relation to the likely thermal conditions in various buildings. Effectiveness was determined primarily based on the difference between the indications of heat meters placed above and below the tested panels which makes it possible to determine the amount of stored energy, compared to conventional panel. Analysis has been performed both on the basis of the temperature curve on the inner surface of the building partition, and of the heat flux density course. Amount of energy stored and donated in different phases of the energy cycle was compared.

3. Description of the measuring stand

A measuring stand consisted of two climatic chambers (called: hot and cold chambers) separated by the investigated building partition. The chambers were equipped with heating, cooling and ventilation units with automatic controls which allowed to maintain required temperature in both chambers. Controlling the internal air humidity following the required scheme was also possible.

The investigated wall was built as a light structure and it consisted of a wooden grid filled with 15 cm layer of mineral wool. The finishing layer in the hot chamber consisted of a plaster board. There were also two 1 m^2 boards fixed to the finishing layer: the ordinary plaster board (12.5 mm) and the board containing phase change material (12.5 mm), BASF brand – SmartBoard 26. The organic material used in PCM board was Micronal–its melting point is 26°C and the heat of phase transition is 110 kJ/kg (according to the manufacturer's data). 30% of the board mass was PCM. Both panels had similar densities and thermal conductivities. Parallel placement of the boards ensured identical external conditions during measurements and allowed the direct comparison of the measured parameters.

4. Measuring equipment

Temperature and heat flux were the parameters measured both at the surface and between the layers of the wall. 4 sensors Pt 1000 and 2 heat meters (the first one was round with a radius of 33 cm, and the second one was rectangular with dimensions 120 × 120 cm) were placed on the surface of each board. Four temperature sensors Pt 1000 and one circular heat meter were also placed below the surface of each board. The air temperature inside chambers was measured by temperature sensors Pt 100 and Pt 1000. The measured parameters were recorded by the Ahlborn Almejo data collecting system connected to a computer. All measured data were collected by the system Data-Control 4.2.

5. Tests in the climatic chamber

The tests were carried out in several stages. The article analyzes two cycles that vary in terms of rate of ambient temperature change. The experiment was conducted under conditions of constant temperature in the cold chamber, and of changing conditions in the hot chamber. In this chamber, dynamic changes in air temperature were observed from 18°C to 30°C. In the first cycle, these changes consisted of the rapid temperature rise in 1 hour and then equally rapid cooling of the air to the starting temperature of 18°C.
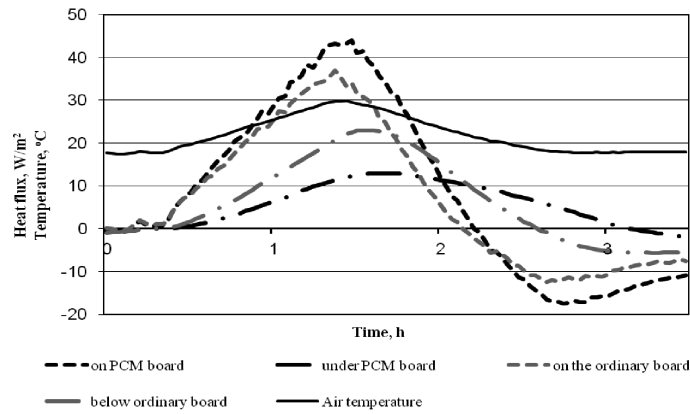
Fig. 1. Course of heat flux, according to the indications of heat meters placed on and under the surface of a regular panel and a panel with addition of PCM, and of the temperature inside the chamber for CYCLE II (with the rapid pace of change)
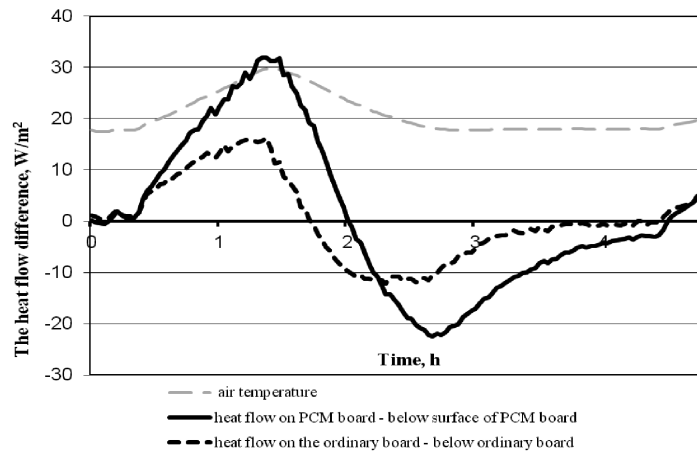
Fig. 2. Course of changes in time of indications difference between heat meters located on and under the surface of the tested panels in CYCLE II (showing the amount of energy accumulated in different phases of the cycle)

In the second cycle, heating to the temperature of 30°C occurred within 3 hours, then the temperature was maintained constant for 3.5 hours, to drop to 18°C within the period of 4 hours. Both the first and the second cycle were preceded by the 11-hour period with constant temperature of 18°C. After each cycle, the temperature was kept constant at 18°C (in the first cycle for two hours, in the second cycle for 10 hours).

During the measurements, both plasterboards were subject to the same conditions.

This stage of the study was to observe changes in the temperature on the surfaces of the panels and the heat flux density on and under the analyzed panels, in case of dynamically changing indoor environment while, on the other side of the partition, the temperature conditions are stable.
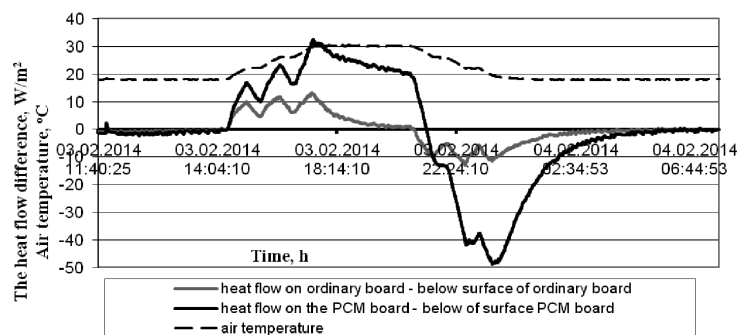
Fig. 3. Course of changes in indications difference between heat meters and located on the surface of the tested boards in CYCLE I (showing the amount of energy accumulated in the different phases of the cycle)

Table 1

Comparative analysis of energy stored in different stages of the cycle CYCLE I and CYCLE II

Time	Phase of the cycle	The amount of stored energy		Comparison	Balance of stored energy	
		Regular panel	Panel with PCM			
	CYCLE I	OB	PCM	OB/PCM	OB	PCM
3 [h]	from 18 [°C] to 30 [°C]	3250	6930.7	2.13	3250	6930.7
3.5 [h]	30 [°C]	1145	9206.4	8.04	4395	16137.1
4 [h]	from 30 [°C] to 18 [°C]	−3803.7	−13288.4	3.49	591.3	2848.7
2 [h]	18 [°C] (2 [h])	−396.2	−2189.2	5.53	195.1	659.5
8 [h]	18 [°C]	−198.2	−621.4	3.14	−3.1	38.1
	CYCLE II					
1 [h]	from 18 [°C] to 30 [°C]	1514.4	2579.08	1.70	1514.4	2579.08
1 [h]	from 30 [°C] to 18 [°C]	−954.4	−54.4	0.06	560	2524.68
2 [h]	18 [°C]	−496.44	−1942.96	3.91	63.56	581.72

The results of integrated difference of heat flow for both cycles demonstrate that plasterboard panels with PCM are more efficient for slower heating process (in case of heating time of 3 hrs. the panel with PCM accumulated 2.13 times more energy than a conventional panel; for the faster cycle it was 1.7 times more). In the course of a further maintenance of 30°C temperature inside the chamber, the panel modified with PCM accumulated over 8 times more energy than a traditional panel. The amount of stored energy has a direct impact on the difference between the surface temperature of the two panels in different cycles during the heating process ÷ in the first cycle it is up to 1.35 K (when the temperature of 30°C is maintained, it rises to 1.65 K), in the second cycle it is 0.93 K. Studies show the need for a longer cooling time for the partition containing PCM, than the second cycle allowed (energy balance shows only negligible (approx. 2%) loss of energy when lowering the temperature inside the chamber, and at the end of the cycle there is still more than 22% of previously accumulated energy). During the slower (4 hour) rate of ambient temperature decrease, over 82% of the stored energy is released. Two hours of maintaining a constant temperature at 18°C results in almost complete discharge of the panel (there is only approx. 4% of previously stored energy).

6. Conclusions

The case study demonstrates an increased efficiency of PCM for a slower rate of ambient temperature changes. It is also preferred due to its longer cooling time. The study shows that the rapid reduction in the temperature, a PCM panel−as opposed to a regular panel−does not allow for enough time to emit the stored energy to its ambient, which is likely to result in the lower efficiency in subsequent cycles. There are also plans for the further analysis involving different PCM materials and various heating and cooling rates, which will contribute to the optimal selection of the PCM material (e.g. for use on surfaces not exposed directly to sunlight, or with a low probability of very rapid temperature fluctuations).

R e f e r e n c e s

[1] Athienitis A.K., Liu C., Hawes D., Banu D., Feldman D., *Investigation of the thermal performance of a passive solar test-room with wall latent heat storage*, Building and Environment, 32 (5), 1997, 405-410.
[2] Shilei L.V., Neng Z., Guohui F., *Impact of phase change wall room on indoor thermal environment in winter*, Energy and Buildings, 38, 2006, 18-24.
[3] Scalat S., Banu D., Hawes D., Paris J., Haghighata F., Feldman D., *Full scale thermal testing of latent heat storage in wallboard*, Solar Energy Materials and SolarCells, 44 (1), 1996, 49-61.
[4] Shilei Lv, Guohui Feng, Neng Zhu, Li Dongyan, *Experimental study and evaluation of latent heat storage in phase change materials wallboards*, Energy and Buildings, 39, 2007, 1088-1091.
[5] Eddhahak-Ouni A., Colin J., Bruneau D., *On an experimental innovative setup for the macro scale thermal analysis of materials: Application to the Phase Change Material (PCM)wallboards*, Energy and Buildings, 64, 2013, 231-238.

[6] Schossig P., Henninga H.M., Gschwandera S., Haussmann T., *Micro-encapsulated phase-change materials integrated into construction materials*, Solar Energy Materials and Solar Cells, 89, 2005, 297-306.

[7] Kuznik F., Virgone J., *Experimental assessment of a phase change material for wall building use,* Applied Energy, 86, 2009, 2038-2046.

[8] Voelker C., Kornadt O., Ostry M., *Temperature reduction due to the applicationof phase change materials*, Energy and Buildings, 40, 2008, 937-944.

[9] Arranz Arranza B., Vega Sáncheza S., Neila Gonzálezba F.J., *Influence of the use of PCM drywall and the fenestration in building retrofitting*, Energy and Buildings, 65, 2013, 464-476.

[10] Oliver A., *Thermal characterization of gypsum boards with PCM included: Thermal energy storage in buildings through latent heat*, Energy and Buildings, 48, 2012, 1-7.

[11] Tatsidjododoung P., Le Perries N., Luo L., *A review of potensial materials for thermal energy storage in building application,* Renewable and Sustainable Energy Reviews, 18, 2013, 327-349.

[12] Kuznik F., David D., Johannes K., Roux J., *A review on phase change materials integrated in building walls*, Renewable and Sustainable Energy Reviews, 15, 2011, 379-391.

[13] Wnuk R., Jaworski M., *Badania charakterystyk cieplnych elementów budowlanych akumulujących ciepło zawierających materiały PCM (Phase Change Materials)*, Polska Energetyka Słoneczna, 2 4/2010, 1/2011 5-11.

[14] Wnuk R., *Magazynowanie ciepła, pozyskanego z energii promieniowania słonecznego, z wykorzystaniem materiałów fazowo-zmiennych, w budownictwie*, II Konferencja SOLINA 2008, Innowacyjne Rozwiązania Materiały i Technologie dla Budownictwa.

[15] Soares N., Costab J.J., Gasparb A.R., Santosc P., *Review of passive PCM latent heat thermal energy storage systems towards buildings' energy efficiency*, Energy and Buildings 59, 2013, 82-103.

[16] Wnuk R., *Bilans energetyczny pomieszczenia ze strukturalnym, funkcjonującym w cyklu dobowym, magazynem ciepła z materiałem fazowo-zmiennym*, Czasopismo Techniczne 1-B/2009, 269-277.

[17] Berrouga F., Lakhala E.K., Omaria M.El, Faraji M., Qarniac H.El., Thermal performance of a greenhouse with a phase change material north wall, Energy and Buildings 43, 2011, 3027-3035.

[18] Nowak K., Zastawna-Rumin A., *Badanie i analiza przegrody z dodatkiem materiałów fazowo-zmiennych w warunkach niestacjonarnych*, Fizyka Budowli w Teorii i Praktyce, 2013, 291-296.

[19] Nowak K., Zastawna-Rumin A., *Badanie przegrody zawierającej materiał fazowo--zmienny w komorze klimatycznej*, materiały konferencyjne 1st World Multi-Conference on Intelligent Building Technologies & Multimedia Management, Kraków 2013.

AGATA PAWŁOWSKA[*]

ECOLOGICAL AND ECONOMIC ANALYSIS OF A BUILDING HEATING SYSTEM THERMOMODERNIZATION EFFICIENCY

ANALIZA EKOLOGICZNA I EKONOMICZNA EFEKTYWNOŚCI TERMOMODERNIZACJI SYSTEMU GRZEWCZEGO BUDYNKU

Abstract

The paper presents a project of a building heating system thermomodernization. Currently, the building is not insulated which results in great heat losses and, consequently, high maintenance costs. The essential calculations performed by the Audytor OZC 4.8 Pro programme enable to estimate the range of a thermomodernization and payback period of thermomodernization. The report contains ecological analysis showing the annual reduction of the pollutants released into the atmosphere.

Keywords: thermomodernization, heat pump

Streszczenie

W artykule przedstawiono projekt termomodernizacji systemu grzewczego budynku. Aktualnie budynek nie jest ocieplany, co wiąże się z dużymi stratami cieplnymi, skutkującymi wysokimi kosztami ogrzewania. Wykorzystanie programu Audytor OZC 4.8 Pro umożliwiło określenie zakresu działań termomodernizacyjnych oraz wyznaczenie prostego okresu zwrotu nakładów inwestycyjnych. Analiza ekologiczna wykazuje roczne zmniejszenie emisji substancji zanieczyszczających.

Słowa kluczowe: termomodernizacja, pompa ciepła

[*] M.Sc. Agata Pawłowska, Ph.D. student, Institute of Water Supply and Environmental Protection, Faculty of Environmental Engineering, Cracow University of Technology.

1. Introduction

Constant social and economic development in the world is associated with an increased demand for energy. Due to the increase in the cost of generating energy in a conventional manner, the limited resources of fossil fuels, as well as concerns about the environment, there has been a growth in interest in thermomodernization. Thermomodernization is an action that lowers the heat demand which results in the reduction of the maintenance costs [1]. Apart from the economic benefits, there is an important aspect of ecological effects that can be visible in the reduction of pollutants released into the atmosphere.

In general, thermomodernization includes insulation of walls and ceilings, doors and windows weatherstripping, adaptation of heating system to the reduced demand for heat, and the replacement of conventional energy sources with renewable ones [1].

2. Methodology and the Characteristics of the Research Object

In this paper, the Audytor OZC 4.8 Pro programme was used to determine the range of the thermomodernization and to select a heat pump with appropriate power.

The analyzed building is not insulated and it is heated by a coal stove. The heated area of the building equals 1171.6 m² and the volume equals 5340.3 m³.

In order to perform the calculations in the Audytor OZC 4.8 Pro programme, the basic data concerning the location of the building, the thickness and kinds of materials of the walls and the dimensions of the rooms were entered. Another parameter that must be taken into account in the assessment was orientation relative to cardinal directions.

The defined barriers with thickness of the components were as follows:
– Exterior wall: plaster 1.5 cm, ceramic brick 75 cm, plaster 1.5 cm,
– Interior wall type 1: plaster 1.5 cm, ceramic brick 75 cm, plaster 1.5 cm,
– Interior wall type 2: plaster 1 cm, ceramic brick 38 cm, plaster 1 cm,
– Floor: terracotta 1 cm, concrete – 1900 22 cm,
– Ceiling: plaster 1.5 cm, reinforced concrete 22 cm,
– Roof: roofing paper 0.5 cm.

3. Thermomodernization

The first step to determine the range of the thermomodernization is to check whether the overall heat transfer coefficients (*U*-values) of the barriers fulfill the requirements included in the PN-EN ISO 6946 norm. The *U*-value is a measure of heat loss in an analyzed building element. The higher the *U* value, the worse the thermal performance of the building envelope.

Taking into account the thickness of the building materials *d*, characterized by a coefficient of thermal conductivity λ, the total thermal resistance R_T is calculated. Finally, the *U*-value is calculated as the reciprocal of the total thermal resistance of the building materials in the constructional element.

$$R = \frac{d}{\lambda}$$

where:

    R – thermal resistance of a homogeneous layer [m²K/W],

    d – thickness of a layer [m],

    λ – coefficient of thermal conductivity [W/mK].

$$R_T = R_{SI} + R_1 + R_2 + \ldots R_n + R_{SE}$$

where:

    R_T – total thermal resistance [m²K/W],

    R_{SI} – the heat transfer resistance on the inner surface [m²K/W],

    $R_{1,} R_{2,} \ldots, R_n$ – the heat transfer resistances of particular layers [m²K/W],

    R_{SE} – the heat transfer resistance on the outer surface [m²K/W].

$$U = \frac{1}{R_T}$$

where:

    U – the heat transfer coefficient [W/m²K],

    R_T – the total thermal resistance [m²K/W].

    As there were no data concerning doors and windows available, the maximum values were entered and they were not analyzed later. For that reason, its weatherstripping was not a part of this project.

Table 1

Comparison of the Umax-value form the PN-EN ISO 6946 norm with the current values

Kind of barrier	U_{max} [W/m²K]	U [W/m²K]
Exterior walls (temperature inside building >16°C)	0.3	0.847
Floor	0.45	0.449
Roof (temperature inside building > 16°C)	0.25	1.420
Windows (temperature inside building > 16°C)	1.8	1.8
Doors in exterior walls	2.6	2.6

    According to the obtained results, it can be said that the roof and the external walls should be insulated, as the defined U-values exceed the values from the norm.

    In both cases (the roof and the exterior walls), it was decided to perfrom the insulation by using a panel of mineral wool with the following specifications: thermal conductivity $\lambda = 0.045$ [W/mK], a density $\rho = 130$ [kg/m³], and specific heat capacity $c_w = 0.75$ [kJ/kgK]. The main advantage of mineral wool is waterproofing and breathability, as well as, dimensional stability, elasticity and mechanical strength [2].

    In order to choose the appropriate thickness of the mineral wool insulation of the roof, different thicknesses were taken into consideration. The minimal thickness that fulfills the requirements (the U-value lower than the U-value from the norm) was 14 [cm]. The other options of 16 and 18 [cm] were also examined. Thee variants presented in a table below have

numbers 1, 2, 3. Assuming heating by coal, the annual savings resulting from the reduced demand for heat were calculated. Then, the payback time (SPBT) was found.

The roof area equals 584 [m²] and it was assumed that the net calorific value of coal was 23 [MJ/kg] and its price was 720 [zł/t].

Table 2

The basic results of the roof thermomodernization

	Unit	Actual state	Variants		
			1	2	3
Thickness of the mineral wool d:	[m]		0.14	0.16	0.18
Growth in thermal resistance ΔR:	[m²K/W]		3.333	3.810	4.286
Thermal resistance R_t:	[m²K/W]	0.704	4.038	4.514	4.990
Overall heat transfer coefficient U:	[W/m²K]	1.42	0.248	0.222	0.200
The unit price of mineral wool:	[zł/m²]		100	103	106
The cost of improvement Nu:	[zł]		58400	60152	61904
Heat demand Q:	[GJ/year]	1679.27	1226.22	1216.70	1209.12
The amount of coal used for heating B:	[t/year]	73.01	53.31	52.90	52.57
The cost of heating K:	[zł/year]	52568.44	38386.13	38088.08	37850.67
Annual saving ΔK:	[zł/year]		14182.31	14480.36	14717.76
SPBT:	[years]		4.12	4.15	4.21

The same calculations were done in case of exterior walls. The total area of exterior walls (without the area of windows and doors) equals 800 [m²]. The results of the payback period were similar, so it was decided to use the thickness layer of mineral wool.

Table 3

The Basic results of the exterior walls thermomodernization

	Unit	Actual state	Variants			
			1	2	3	4
Thickness of the mineral wool d:	[M]		0.1	0.12	0.14	0.16
Growth in thermal resistance ΔR:	[m²K/W]		2.381	2.857	3.333	3.810
Thermal resistance R_t:	[m²K/W]	1.181	3.562	4.038	4.514	4.990

Overall heat transfer coefficient U:	[W/m²K]	0.847	0.281	0.248	0.222	0.200
The unit price of mineral wool:	[zł/m²]		94	97	100	103
The cost of improvement Nu:	[zł]		75200	77600	80000	82400
Heat demand Q:	[GJ/rok]	1226.22	778.09	756.70	739.82	726.18
The amount of coal used for heating B:	[zł/year]	53.31	33.83	32.90	32.17	31.57
The cost of heating K:	[zł/year]	38386.13	24357.46	23687.89	23159.63	22732.6
Annual saving ΔK:	[zł/year]		14028.66	14698.24	15226.5	15653.52
SPBT:	[years]		5.36	5.28	5.25	5.26

The obtained results indicate that there is a small difference in the payback time when various thicknesses of mineral wool are taken into consideration. Nevertheless, in both cases, the shortest payback time occurs when the mineral wool has a thickness of 14 cm. It is practical to buy the same thickness of mineral wool for both the roof and the exterior walls.

Thanks to the roof and exterior walls thermomodernization, the actual annual energy consumption is lower by more than 50 [%] and was reduced from 1680 [GJ/year] to 740 [GJ/year].

4. Selection of the heat pump

Due to an investor suggestion, only the brine/water and water/water heat pumps were taken into consideration. In the first one, the energy accumulated in the ground can be captured by a horizontal or vertical heat exchanger [3]. As there is not enough area, the option with the horizontal heat exchanger was rejected. Using the Ochsner technical specification [4], the brine/water and the water/water heat pumps were compared. The pumps that provide the appropriate heat demand are water/water OWWP 96 and two pumps brine/water (OSWP 56) (cascade connection).

The total heat load considering the heat load calculated in the Audytor OZC 4.8 Pro programme and the heat load for the hot water preparation equals 125 192 [kWh/year].

Considering this value, efficiency of heating by the coal stove (0, 61), the real heat load for generating heat by the coal stove was calculated. Then, assuming the net coal calorific value of 6.4 [kWh/kg], its price 720 [zł/t], and the service charge 2000 [zł/month] the annual operating cost was determined. It is equal to 48107.80 [zł/year].

Similar calculations were done to compare two types of heat pumps. Power consumption includes the power needed for heating and for preparing hot water. The electricity price was assumed as 0.6 [zł/kWh].

Comparison of the OWWP 96 and OSWP 56 heat pumps

	Unit	Heat pump Ochsner OWWP 96	Heat pumps 2x Ochsner OSWP 56
Heat demand	[kWh/year]	125192	125192
Coefficient of Performance	–	4.1	3.2
Power consumption	[kWh/year]	41528	50841
Annual operating cost	[zł/year]	24916.8	30504.6
Annual saving in comparison with the coal stove	[zł/year]	23191	17603.2
The cost of buying	[zł]	148222	349524
SPBT	[year]	6.4	19.8

It can be seen that the cost of buying the heat pump water/water OWWP 96 is more than 2 times lower than in case of heat pumps brine/water OSWP 56 in a cascade connection. What is more, the coefficient of performance of OWWP 96 is higher and the payback time is more than 3 times lower than in case of OSWP 56.

5. Economic analysis

The total cost of thermomodernization was calculated as a sum of the costs of exterior walls and roof thermomorednization, the costs of exchange of the actual heaters for the heaters adapted to the new operating parameters and the costs of buying and installing the heat pump. The total cost of thermomodernization equals 313497 [zł]. Thanks to this action, the annual cost of heating was lowered from 76568.44 [zł] to 24916.8 [zł]. The payback period of the whole enterprise is about 6 years.

$$SPBT = \frac{313497}{76568.44 - 24916.8} = 6.1\,[\text{year}]$$

6. Ecological analysis

The best way to estimate the ecological effect is to calculate the reduction of the emissions of pollutants into the atmosphere. Currently, each year, 33.48 [t/year] of coal is used in the coal stove to heat the building. In order to calculate the reduction of the emissions, it was necessary to determine the amount of the pollutants released during the production of electricity in the power plant. As the annual heat pump energy consumption equals 41528 [kWh/year] it was calculated that 19.12 [t] of coal has to be used to generate electricity. The

table below shows that the thermomodernization contributes significantly to the reduction of pollutants released into the atmosphere.

<div align="right">T a b l e 5</div>

Emission of pollutants released to the atmosphere in [kg/year]

	Coal stove (before thermomodernization)	Power plant (electricity for the heat pump. after thermomodernization)	The difference
SO_2	803.52	458.88	344.64
NO_2	73.66	19.12	54.54
CO	1506.6	860.4	646.2
CO_2	61938	38240	23698
dust	334.8	191.2	143.6

7. Conclusions

The first step of the thermomodernization concerns building insulation. Thanks to this action, by using 14cm–mineral wool, the actual annual energy consumption is lowered by more than 50 [%] from 1680 [GJ/year] to 740 [GJ/year] and the payback period is shorter than 5,5 year. The second one concerns the selection of a heat pump. The Ochsner pump chosen is OWWP 96, as it has the payback time more than 3 times lower than the OSWP 56. The thermomodernization results in a decrease of the annual cost of heating from 76568.44 [zł] to 24916.8 [zł] with the payback time of about 6 years. Apart from the economical benefits, there is an important ecological aspect present. The emissions of the pollutants into the atmosphere is reduced significantly. There is a reduction of 23698 [kg/year] of carbon dioxide released into the atmosphere which is especially important as the carbon dioxide is one of the greenhouse gases.

To sum up, it can be said that the action of thermomodernization is reasonable, as the payback time period found to be short. What is more, better barriers insulation and the use of a heat pump as an energy source will increase thermal comfort in rooms and it will add to the value of the building.

<div align="center">R e f e r e n c e s</div>

[1] Koczyk H., *Ogrzewnictwo praktyczne*, Systemtherm D. Gazińska s.j., Poznań 2009.
[2] Murat R., *Ocieplenie pod lupą*, Murator, 9/2010.
[3] Rubik M., *Pompy ciepła* Poradnik, Ośrodek Informacji Technika Instalacyjna w Budownictwie, Warszawa 2006.
[4] Ochsner: Technical specifications, unpublished materials.

RAFAŁ POLAR, JOLANTA GINTOWT*

EFFECT OF REVERBERATION ON SPEECH INTELLIGIBILITY, LOGATOM TEST "IN SITU"

WPŁYW POGŁOSU NA ZROZUMIAŁOŚĆ MOWY, BADANIA LOGATOMOWE „IN SITU"

Abstract

The influence of acoustic parameters of lecture halls is essential for the quality of reception and the understanding of the content. One of the basic acoustic parameters is the reverberation time in the room. The study demonstrates that the room which is not properly designed for acoustics, causes difficulty in understanding the delivered text. Selected acoustic parameters were analyzed, such as reverberation time, acoustic background, and delivered text intelligibility. A possible solution was proposed, using reflecting and absorbing surfaces appropriately positioned in the room.

Keywords: acoustics, reverberation time, logatom test, quality of teaching

Streszczenie

Wpływ parametrów akustycznych sal, w których odbywają się wykłady, ma zasadnicze znaczenie dla jakości odbioru i zrozumienia treści. Jednym z podstawowych parametrów akustycznych jest czas pogłosu pomieszczenia. W pracy wykazano, iż sala nie będąca odpowiednio zaprojektowana pod kątem akustyki powoduje trudności w zrozumieniu wygłaszanego tekstu. Analizowano wybrane parametry akustyczne, takie jak: czas pogłosu, tło akustyczne, zrozumiałość czytanego tekstu. Zaproponowano dopuszczalne rozwiązanie przy zastosowaniu powierzchni odbijających i pochłaniających odpowiednio usytuowanych w pomieszczeniu.

Słowa kluczowe: akustyka wnętrz, czas pogłosu, logatomowy test, jakość nauczania

* Eng. Rafał Polar, M.Sc. Eng. Jolanta Gintowt, Institute of Building Materials and Structures, Faculty of Civil Engineering, Cracow University of Technology.

Designations

V	–	total volume of the room [m³]
S	–	total surface of the faces limiting the room [m²]
Sx, Sy, Sz	–	total surface perpendicular to the axes
aśr	–	average sound absorption coefficient [m²]
aśr.x, aśr.y, aśr.z	–	average sound absorption coefficient in the direction of the axes
α	–	Fitzroy-sound absorption Fitzroy coefficient,
f	–	frequency [Hz]
T	–	reverberation time [s]

1. Introduction

The influence of acoustic parameters of the halls where lectures are held, is essential for the quality of reception and understanding of the content, and for listeners' concentration [1–5, 8]. One of the basic parameters is the reverberation time in the room [6, 7]. The reason for choosing this particular topic in the field of acoustics, was the concentration difficulties of students during long speeches and lectures held all day, due to designers' and users' ignorance in the field of acoustics, which negatively impacted the teaching effects.

2. The subject of investment

The investment subject is a project of acoustic adaptation for the room 209H in the "Houston" building of Cracow University of Technology. It is a hall which hosts lectures and presentations. The room is a cuboid of a rectangular base, it is long and relatively narrow, the outer wall is covered with windows. The room is located on the second floor of the building, there are similar classrooms above it and below it, and it is separated from the hallway by wooden door and from the outside by PVC windows.

3. Measuring devices and methods and calculation methods.

According to the [1, 4–7, 11] are used formulas: Sabine, Fitzroy, Eyring (formula 1) as below:

$$T_{60.Fitzroy} = (0.161*V)/(S*\alpha_{Fitzroy}) \quad \alpha_{Fitzroy} = -S*(S_x/\ln(1-\alpha_x) + S_y/\ln(1-\alpha_y) + S_z/\ln(1-\alpha_z))$$

$$T_{60.Sabine} = (0.161*V)/(S*\alpha_{sr}) \quad T_{60.Eyring} = (0.161*V)/(-S*\ln(1-\alpha_{sr})) \tag{1}$$

After the analysis [7–11], a range of measuring instruments and methods led to the use of simple methods and basic measuring equipment. Mobile phone – with integrated microphone (used for the initial analysis) with frequency: 20 Hz ~ 20 kHz, frequency range –6 dB,

THD+N (total harmonic distortion plus noise) 1.0% ± 0.2%, high sensitivity – up to 10 m, sensitivity of the comparative microphone 2 mV/Pa. Sound level meter – a device with a sensitive microphone, used to measure the background noise and reverberation time. The sensitivity of the loudspeaker SPL 2.83 V/1m 1 W was 94 dB. The meter gives the volume in dB. In background noise measurements an A-weighting was used. The study for speech intelligibility was carried out using the logatom test [12].

Logatom test was developed in accordance with [12–14]. Example of logatom is illustrated in Fig. 1.

dufcze	cze	teń	jo	czalmy	chfypa	dy	pa	gruto	słynej
ajtes	wać	foli	es	ny	ca	zjaiech	piestma	ke	jentuś
Wesk	niacko	delak	gapysz	nij	czniesa	wyzo	fa	todzi	jos
Pi	wespa	szo	tyr	dnaf	szaźmo	żam	żnota	ply	bep

Fig. 1. Part of 100-logatom list for the Polish language

4. Results

The results of the in situ reverberation time measurements and calculations are shown in Fig. 1. The results of logatom test are shown in Fig. 2. The study (for logatom test) was carried out successively at 9.15 am, 10.40 am, 12.20 pm, 6.00 pm. The graph shows the results of the three measurements, due to the fact that one of the tests was considered to be invalid.
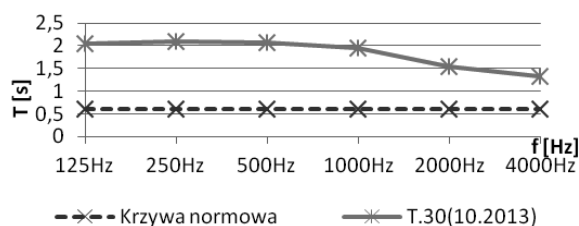
Fig. 2. Measured reverberation time
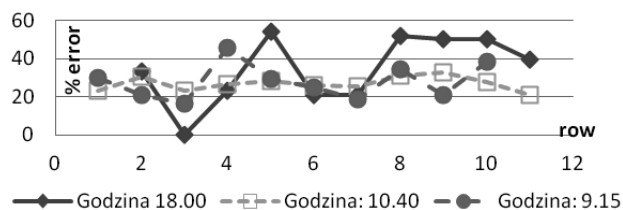
Fig. 3. Intelligibility test: the error % to row number

5. Analysis of the results

In terms of 1000 <f> 4000 Hz, both in May and October, the reverberation time was in the range 1,55–1,33 s. It corresponds to a value of preferred in sites such as an opera hall. In terms of 125 to 1000 Hz, the measured reverberation time was 2,34–1,95 s. This value exceeded the value preferred even for concert halls. The results of logatom test: in the morning on average 25–38% of the students made mistakes. In the afternoon percent of errors ranged from 40 to 58. This means that more than half of the students did not understand more than half of the content of the lecture. The worst speech intelligibility showed in the research is for rows 5 and 8, and the effect of time of day on the logatom test results is noticeable (Fig. 2). The results: auditorium can be classified into groups of rooms that require the improvement of acoustics.

6. Acoustic adaptation

In order to obtain better acoustic parameters, the use of materials was proposed as follows: the ceiling – 60 m² of drywall and 20 m² of Ecophon Master Rigid, plus two Extra Bass panels; the side wall with the door – 25 m²of drywall and 12 m² of Rockfon Verti Q as one strip alongside the ceiling; the back wall – 15 m² of Rockfon Verti Q (on both, opposite side wall). The proposed arrangement is shown on the next page (Fig. 4). The calculation result of future application of these materials is shown in the Fig. 3 and, because not always all the seats are occupied in the classroom, an additional analysis with 50% of seats being occupied (Fig. 5) was carried out. The results of theoretical calculations (reverberation time 0,49–0,59 s) correspond to the values preferred for voice-recording studio (reverberation time of 0.3–0.5 s) and did not exceeded the normalized value (Fig. 3, 5).
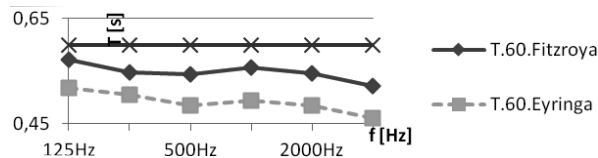
Fig. 4. Reverberation time after acoustic adaptation
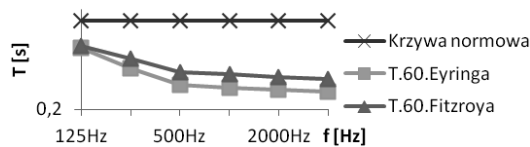
Fig. 5. Reverberation time after acoustic adaptation
for 50% of seats being occupied
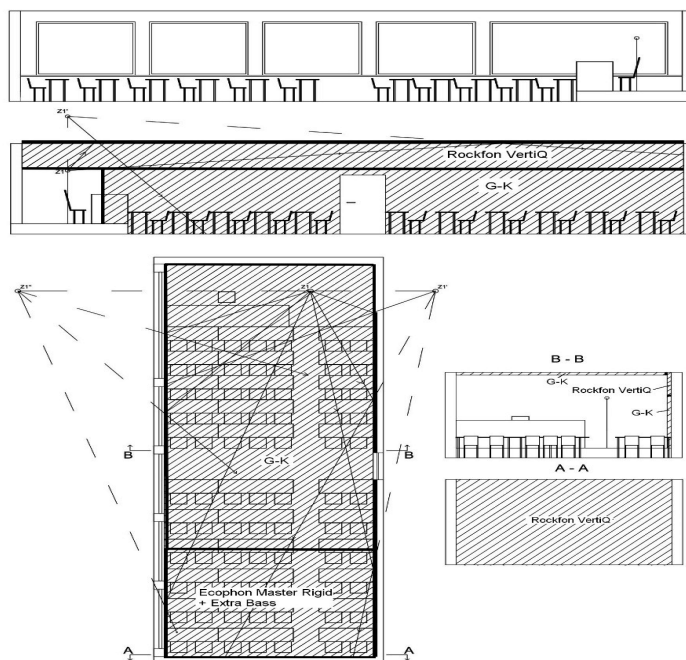
Fig. 6. Design of arranging acoustic materials. Z1 – the source of sound

7. Conclusions

It seems that, at the stage of preliminary assessment of acoustic lecture halls (without the need for lengthy and complicated measurements), measuring two basic parameters such as reverberation and speech understanding as a logatom study, is sufficient in the two cases. First: their categorization. Second: the decision what kind of material should be applied to improve the quality of understanding. However, in order to obtain precise results one should run more tests with a constant number of students in each group. it may depend on the location of the door, which carried the sounds of the corridor (in this case study). Use of the logatom test to assess the acoustic quality of rooms is a very good method. It allows us, under real conditions, to check the actual ability of listeners to understand the transmitted content. Even more importantly, in classrooms the teaching effect directly depends on understanding the teacher's speech, and this directly and strongly depends on the reverberation time. Before the acoustic-renovation of the auditorium, the logatom test should be repeated using an intelligibility measurement method in rooms (classrooms) together with its automated version called modified intelligibility test with forced choice (MIT-FC), according to the [15] measurement, and subsequently compared with previous research. After the acoustic-renovation of the auditorium, in order to assess the actual effect, a control logatom test according to the [15] must be carried out.

R e f e r e n c e s

[1] Bukowski B., *Dźwięk i budowa – podręcznik akustyki budowlanej*, nakł. Instytut Badawczy Budownictwa, Warszawa 1947.

[2] Sadowski J., *Akustyka w urbanistyce, architekturze i budownictwie*, Arkady, Warszawa 1971.

[3] Sadowski J., *Akustyka architektoniczna*, PAN, Warszawa–Poznań 1976.

[4] Kowal A., *Zagadnienia akustyki budowlanej,* Politechnika Krakowska, Kraków 1969.

[5] Barron M., *Auditorium Acoustics and Architectural Design*, E & FN Spoon, New York 1993.

[6] Rossing T.D., *Springer Handbook of Acoustics*, Sturtz AG, Wurzburg 2007.

[7] Leizer I.G., *Applicability of the Methods of Geometric Acoustics for the Calculation of Sound Reflection from Plane Surfaces*, Soviet Physics – Acoustics, 12 (2), 1966.

[8] Long M., *Architectural Acoustics*, Elsevier Academic Press, chapter 7, 2006.

[9] Rindel J.H., *Design of New Ceiling Reflectors for Improved Ensemble in a Concert Hall*, Applied Acoustics 34, 1991.

[10] Skålevik M., *Low frequency Limits of Reflector arrays*, Institute of Acoustics IOA conference on Auditorium Acoustics, Copenhagen 2006.

[11] Kamisiński T., Szeląg A., Rubacha J., *Sound reflection from overhead stage canopies depending on ceiling modification*, Archives of Acoustic, 37 (2), 2012, 213-218.

[12] Meisenbacher K., *Development and evaluation of an adaptive Logatom test to determine consonant understandability;* [in German] Graduate thesis, Fachhochschule Oldenburg, 2008.

[13] ISO/TR 4870, *Acoustics – The Construction and Calibration of Speech Intelligibility Tests*, International Organization for Standardization, 1991.

[14] ITU-T Recommendation P.800, *Method for Subjective Determination of Transmission Quality,* International Telecommunication Union, Geneva, Switzerland 1996.

[15] Brachmańsk S., The Subjective Measurements of Speech Quality in Rooms, *Proc. of Subjective and Objective Assessment of Sound*, Poznań, September 1–3, 2004.

ALEKSANDRA PRZEWOŹNIK[*]

POLYURETHANE – ALTERNATIVE TO MINERAL WOOL AND POLYSTYRENE

POLIURETAN – ALTERNATYWA DLA WEŁNY MINERALNEJ I STYROPIANU

Abstract

Polyurethane was discovered in 1937. It is a common name for material which can be hidden under many forms, such as, rigid foam, flexible foam, coatings, sealants, adhesives and elastomers. The main constituents are isocyanate and polyol. Depending on the components and proportions it can have different properties. Polyurethane is widely used in industry and has a variety of uses in everyday life. Rigid foam is used in building construction as a thermal insulation. It is produced by the so-called polyurethane system. This material is light and durable. Besides, it has closed-cell structure and a low thermal conductivity.

Keywords: polyurethane, isocyanate, polyol, thermal insulation, thermal conductivity, foam

Streszczenie

Poliuretan został wynaleziony w 1937 roku. Jest to popularna nazwa dla materiału, który może być ukryty pod wieloma formami, między innymi sztywnej pianki, elastycznej pianki, powłok, substancji łączących, past uszczelniających i elastomerów. Jego głównymi składnikami są izocyjanian i poliol. Zależnie od ich proporcji i użytych dodatków może on mieć różne właściwości. Poliuretan ma wiele zastosowań w przemyśle i życiu codziennym. W budownictwie do izolacji cieplnej używana jest sztywna pianka. Jest ona produkowana w procesie zwanym systemem poliuretanowym. Jest to materiał przede wszystkim lekki i wytrzymały na wiele czynników zewnętrznych. Ponadto cechuje się zamkniętą strukturą i niską przewodnością cieplną.

Słowa kluczowe: poliuretan, izocyjanian, poliol, izolacja cieplna, przewodność cieplna, piana

[*] Aleksandra Przewoźnik, student, Faculty of Civil Engineering, Cracow University of Technology.

1. History of polyurethane

Production of polyurethane (PU) from other substances was discovered and patented by the German chemist Otto Bayer in 1937. At the beginning of World War II there was a deficit of rubber and it reached high prices. This led to a situation that the rubber began to be replaced with PU. One example of such an application is the use of rigid polyurethane foam to seal the aircraft and protective coating of metal, wood and stone. During the war, PU has become more and more popular because of its properties and began to be produced on a global scale. In the fifties it was available on the commercial market in the form of elastomers, adhesives and rigid foam. At the end of the decade, the widespread use also introduces flexible polyurethane foam similar to the one that is currently very popular in many areas. Over the next years, the research was ongoing on the development of PU applications mainly in the automotive industry, construction, clothing and medical equipment. In the 70s PU began to be used as a thermal insulation of buildings in the form of spray. In the 80s it was used in the production of cars as a material which absorbs impact energy and thereby improves the safety of the passengers. In the 90s the first medical tubing was made with polyurethane elastomer. In 2001 the car tires started to contain PU in order to increase their efficiency. Nowadays, most people are not familiar with the use of PU because it is often hidden in various forms in everyday products [1–3].

2. Types of polyurethanes

PU is hidden under many forms. Its composition is characterized by two main components. Namely: an isocyanate and a polyol derived from petroleum. By mixing them along with presence of various catalysts, stabilizers and other additives, PU of different properties may be created. Different proportions and components can influence the composition, flexibility, rigidity, insulation and other properties needed for a particular use. PU can be found in several forms. One of them is the flexible foam that can be easily shaped. This material is characterized by lightness, durability and resistance to deformation. Rigid foam has a very good insulation. There are two kinds of rigid foam: polyurethane rigid foam (PUR) and polyisocyanurate rigid foam (PIR). Their compositions are similar, but in the second one there is more isocyanate at the extense of polyol. This difference causes the PIR to have better fire resistant properties, but because of the higher cost and difficulty of production it is less often produced. PU can also be present in coatings, adhesives, sealants, and elastomers. The coatings enhance the appearance and durability of the products. Adhesives are durable and strong. Sealants layer does not have to be thick in order to fulfil its function and elastomers are resistant to environmental influences and adapt well to the variable stress. One of the types of PU is thermoplastic polyurethane which can be processed in many ways, for example, by extrusion, injection, blow and compression molding equipment. It is also highly flexible, resistant to abrasion, impact and influence of weather. PU is also used as a binder, for example in the manufacture of oriented strand board. Not only to join fibres and particles to each other, but also to impart flexibility and improve endurance [1, 3–5].

3. The use of polyurethane

The use of PU depends on the form in which it is produced and specific properties related to this. Flexible foams are used mainly in the furniture and upholstery as supplementary filling material. PUR and PIR are primarily used in construction as insulation. It is also available in a number of devices as an insulator. PU is exploited in the automotive industry because of its light weight, durability and insulation. It is used in the production of many parts, such as, car body, bumpers and seats. In medicine PU can be found in hospital bed sheets, curtains and also in short-term implants. PU is exploited in the manufacture of paints, lacquers, glues, composite wood, clothing, footwear and many accessories used in everyday life [3, 4].
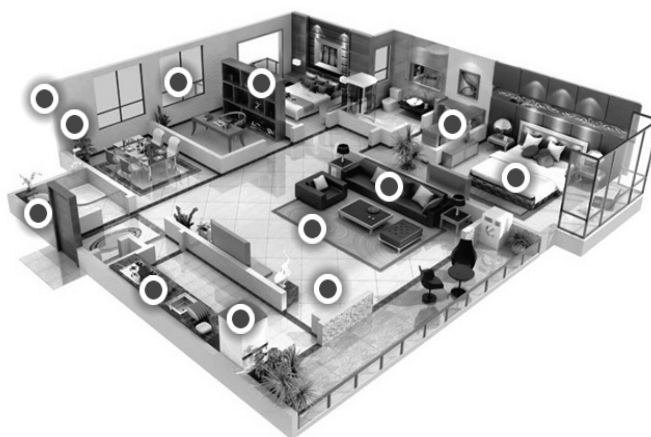
Fig. 1. The variety of polyurethane applications [2]

4. Characteristics of rigid polyurethane foams

As thermal insulation in construction, PUR is mainly used. It is produced by the so-called polyurethane system. It consists of polyol chemically reacting with toluene diisocyanate (TDI) or diphenylmethane diisocyanate (MDI) with the presence of suitable catalysts and additives. As a foaming agent, pentanes or low-boiling, inert solvents may be used, usually derived from halogens. During the reaction there is an increase of temperature, evaporation of the blowing agent starts and the volume of the foam expands. The obtained PU foams must be in a closed cell structure in order to be used as thermal insulation material. This process, simplified to the laboratory conditions, is shown in Fig. 2. For the industrial production of PUR equipment is needed, which includes storage, metering, heating, dosing and mixing ingredients. Depending on the application of the final product, mixing unit can be low or high pressure or in the form of spray using special spray guns. Some manufacturers also practise hand-mixing that, along with the right experience, ensures good quality of the material.
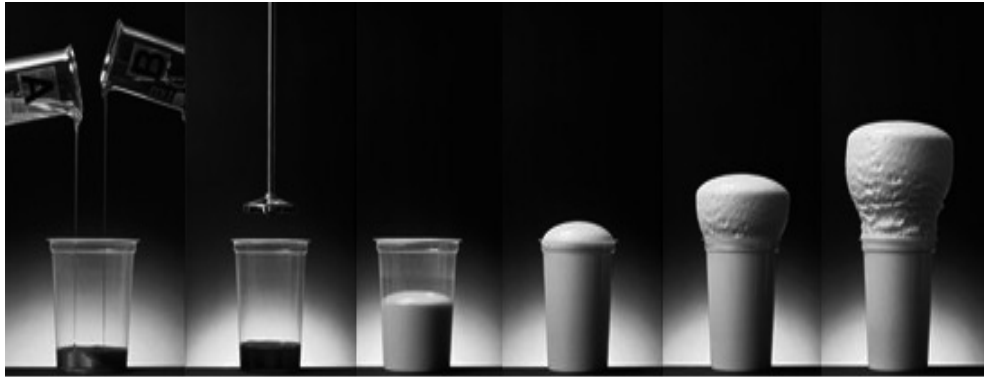
Fig. 2. The formation of polyurethane foam [2]

PUR has a closed cell structure, which is 90% filled with gas. The density is in the range of 24–60 kg/m^3. Noticeable is the fact that with increasing density, the water absorption decreases and the compressive strength increases. The level of water absorption is in the range of 0.3–0.4% by volume of the material. The thermal conductivity is about 0.024 W/(m·K) and is not dependent on humidity. The water vapour permeability of PUR is very low due to the closed structure and is 70 g/m^2/24 h. PUR is resistant to the biological effects of the environment and does not react with grease, organic solvents and diluted acids and alkali. However, it is susceptible to the negative effects of UV radiation. Because of this, it is covered with a special paint or plaster to protect the foam from the radiation. PUR is a slow burning and self-extinguishing material which can withstand temperatures up to 150°C [1, 3, 5–7].

5. Comparison of insulation: polyurethane rigid foam, mineral wool and expanded polystyrene

The most common insulating materials are mineral wool (MW) and expanded polystyrene (EPS). Comparing the thermal insulation obtained using these materials and PUR, clear differences can be seen. One of them is the thickness of insulation needed to achieve the same heat transfer coefficient when other layers are the same. In order to achieve the heat transfer coefficient of $U = 0.25$ W/(m^2·K) 14 cm of EPS should be used, 13cm of MW and 9 cm of PUR. The combination of these data and the thermal conductivity of materials can be found in Table 1.

While choosing the insulation, attention is mainly paid to thermal conductivity, but other properties are also important. The EPS is the lightest. However the weight of material with the thickness needed to achieve the same heat transfer coefficient is comparable to the weight of the required PUR. The MW is incomparably heavier than EPS and PUR and is characterized by non-flammability and fire resistance. The PUR has worse fire properties but PIR allows to overcome the problem [8–11].

Comparing thickness of the thermal insulation obtained using expanded polystyrene, mineral wool and polyurethane rigid foam

$U = 0.25 \ [W/(m^2 \cdot K)]$		
Heat insulating material	Thermal conductivity	Thickness of insulation
Expanded polystyrene	0.038 [W/(m·K)]	14 [cm]
Mineral wool	0.037 [W/(m·K)]	13 [cm]
Polyurethane rigid foam	0.024 [W/(m·K)]	9 [cm]

6. Conclusions

The most common thermal insulating materials on the market in Poland are MW and EPS. However, the PUR and PIR insulation is gaining attention due to its superior thermal performance and decreasing costs of production. These are important advantages in the increasingly stringent thermal requirements of buildings because the traditional insulation materials must increase its already considerable thickness to about 20 cm. In addition, research to improve the properties of the PU is ongoing and it makes this material more attractive on the construction market.

R e f e r e n c e s

[1] www.polyurethanes.org, access: 19.08.2013.
[2] www.puhse.com, access: 19.08.2013.
[3] www.polyurethane.americanchemistry.com, access: 19.08.2013.
[4] www.polyurethanes.basf.de, access: 20.08.2013.
[5] Połyga M., *Poliuretan-materiał dla budownictwa*, Izolacje 7-8/2010, Dom Wydawniczy Medium, Warszawa 2010.
[6] Wrona M., *Uszczelnienie, wypełnienie, wygłuszenie – pianki poliuretanowe w budownictwie*, Izolacje 5/2009, Dom Wydawniczy Medium, Warszawa 2009.
[7] Szycher M., *Szycher's handbook of polyurethanes*, CRC Press, 2013.
[8] www.termoorganika.com.pl, access: 12.02.2012.
[9] www.rockwool.pl, access: 12.02.2012.
[10] Pałasz J., *Pianki poliuretanowe PUR/PIR a inne materiały termoizolacyjne*, Izolacje 11–12/2010, Dom Wydawniczy Medium, Warszawa 2010.
[11] Dreger M., *Izolacje z pianki poliuretanowej a wyroby z wełny mineralnej*, Izolacje 4/2011, Dom Wydawniczy Medium, Warszawa 2011.

MICHAŁ REPELEWICZ, DAWID ŁĄTKA*

USE OF FOAM GLASS AS A SLAB ON GRADE THERMAL INSULATION

SZKŁO PIANKOWE JAKO TERMOIZOLACJA „PODŁOGI NA GRUNCIE"

Abstract

This paper describes the results of simulation and calculation of heat loss through a slab on grade to the ground. Calculations are performed for a single-family house. The effect of using foam glass as insulating material is analyzed.

Keywords: foam glass, slab on grade, heat losses

Streszczenie

Artykuł opisuje wyniki przeprowadzonych symulacji i obliczeń strat ciepła przez podłogę na gruncie. Obliczenia przeprowadzono dla budynku jednorodzinnego. Przeanalizowano efekt zastosowania szkła piankowego jako materiału termoizolacyjnego.

Słowa kluczowe: szkło piankowe, podłoga na gruncie, straty ciepła

* M.Sc. Eng. Michał Repelewicz, M.Sc. Eng. Dawid Łątka, Institute of Building Materials and Structures, Faculty of Civil Engineering, Cracow University of Technology.

Symbols

ψ_e – linear thermal transmittance associated with wall/floor junction [W/mK]

L_{2D} – linear thermal feedback coefficient [W/mK]

U_1 – thermal transmittance of basement walls and doors [W/m²K]

U_2, U_m – thermal transmittance of slab on grade (U_2) – mean value (U_m) [W/m²K]

H_{tr} – stationary thermal coupling coefficient for the slab on grade [W/K]

q – heat flux [W]

Q – heat loss for the slab on grade [kWh]

1. What is foam glass?

Foam glass is formed from cullet, which is extracted in the process of glass recycling; among others, from conventional glass bottles. The cullet is mixed with glycerol and foaming agents and, in the form of such a mixture, it is subjected to high temperatures of up to 900°C. The result – a large-size foam glass block – can be rapidly cooled down and, due to this sudden change of temperature, the stress destroys the compact structure. This the way in which a foam glass in the form of aggregate is obtained.

2. The analyzed model

Simulations were carried out for a single-family building without a basement, founded on reinforced concrete strip footing and with the slab on grade.

For this building, the simulation involving the change in designed slab on grade layers to layers suggested by the company Geocell [1] was conducted. Compared solutions are shown

PD1
1. Finishing layer—e.g. tiles / PVC
2. Concrete floor on PE foil
3. Polystyrene foam
4. Damp proofing
5. Reinforced concrete slab
6. Lean concrete base
7. Sand and gravel mix
8. Natural soil

PD2
1. Finishing layer—e.g. tiles / PVC
2. Concrete floor
3. Damp proofing
4. Geocell foam glass (1:1.3 consolidation)
5. Geotextiles
6. Natural soil

SZ1
1. Inner thin-coat plaster work
2. Ceramic masonry wall
3. EPS 70 styrofoam
4. Outer thin-coat plaster work

Fig. 1. Stratification diagram for the analyzed building

in Fig. 1. Slab on grade with the use of foam glass PD2 suggested by the manufacturer [2] were examined in different variants:changing the layer thickness from 15cm to 50cm by 5 cm. The manufacturer recommends using 30 cm layer of foam glass for typical buildings, and 40 cm layer for passive buildings. Spaces with entrances to the building were also considered due to the fact that different thermal bridges are created in these places [3].

3. Simulation results

3.1. Properties of analyzed partitions

The heat loss calculations through the building partitions, computational schemes and values of heat transfer resistance were established based on Polish standard [2]. Thermal resistance for the different layers of materials was determined based on their thickness and thermal conductivity, and adopted depending on the material and in accordance to [4] and [1] for foam glass. From these data, the thermal transmittance coefficient was determined for wall SZ1 and floors PD1 and PD2 (in this case with a variable thickness of the heat insulating layer – from 15 to 50 cm); the obtained values are shown in Table 1.

T a b l e 1

Thermal transmittance

	SZ1	PD1	PD2							
			15 [cm]	20 [cm]	25 [cm]	30 [cm]	35 [cm]	40 [cm]	45 [cm]	50 [cm]
U [W/m^{2}K]	0.17	0.598	0.465	0.36	0.294	0.248	0.212	0.19	0.169	0.153

3.2. Analysis on thermal bridges level

Numerical calculations may be widely used in the analysis of thermal bridges as it is presented in [5]. Computational procedures for determining the building's heat demand which are in force in Poland, allow us to evaluate the effect of thermal bridges in three different ways. The article uses a method of heat flow simulation available in the Therm program. Based on the Polish norm, a computational scheme was adopted (Fig. 2) according to [6], where: l_w is the equivalent thickness for wall SZ1, and B` is a characteristic dimension of floor.

This model, adopted with the applied material properties according to [6], has been subjected to simulation. Due to high ampleness, only exemplary simulation results are hereby attached; they are presented by rendered maps. (Fig. 3) shows the simulation results for a thermal bridge located in places of the door woodwork (Fig. 3a, c, e) and of the junction of outer wall to foundation (Fig. 3b, d, f). The map of heat flux distribution (Fig. 3) presents thermal bridges simulation using 2D models for: floor layers of the finished building PD1 (Fig. 3a and b], PD2 with a 15 cm foam glass layer (Fig. 3c and d) and PD2 with a 50 cm foam glass layer (Fig. 3e and f).

238

In the simulation, the coefficient for 2D bridges was determined, using a method based on heat flux integration with the use of external dimensions. Subsequently, from the equation (1), the thermal bridge was determined. The results of all thermal bridges simulations described in the article are presented in Table 2.

$$\psi_e = L_{2D} - U_1 \cdot 1.41m - U_2 \cdot 3.30 \ m \tag{1}$$
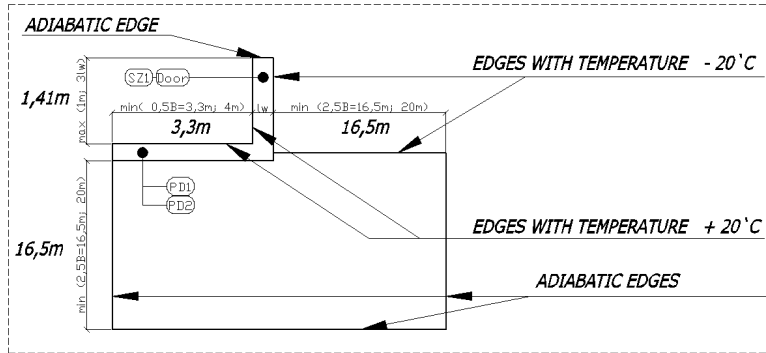
Fig. 2. Computational scheme and boundary conditions by [6]

a) Door, PD1

b) SZ1, PD1

c) Door, PD2 (15 cm)

d) SZ1, PD2 (15 cm)

e) Door, PD2 (50 cm)

f) SZ1, PD2 (50 cm)
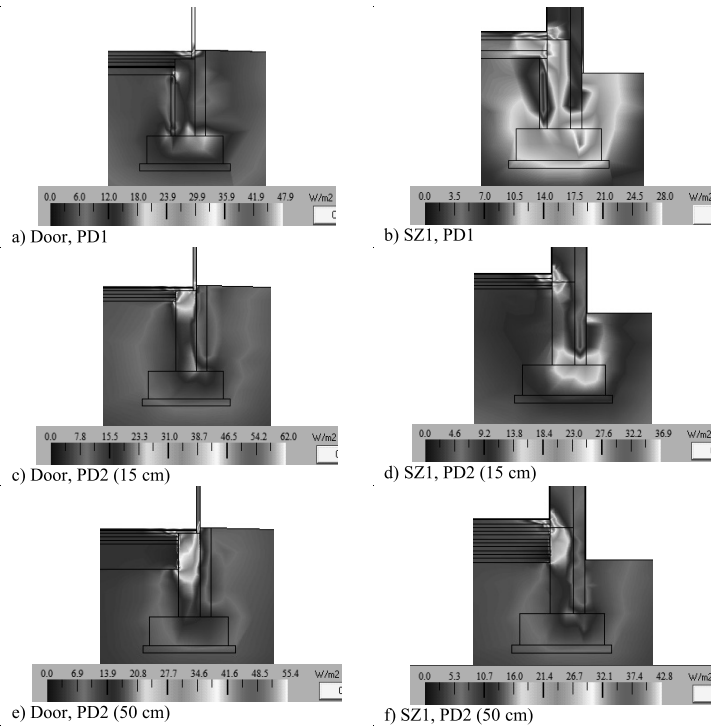
Fig. 3. Distribution of the heat flow

Linear thermal transmittance associated with wall/floor junction

$\psi_{e\,[W/mK]}$	PD1	PD2							
		15 [cm]	20 [cm]	25 [cm]	30 [cm]	35 [cm]	40 [cm]	45 [cm]	50 [cm]
Door	−1.91	−1.373	−1.01	−0.795	−0.651	−0.054	−0.465	−0.411	−0.346
SZ1	−1.417	−0.97	−0.63	−0.425	−0.29	−0.196	−0.13	−0.078	−0.037

3.3. Analysis of thermal bridges levels

Severe impact of thermal bridges can have unpleasant consequences [7]. Using practical solutions for the analysis of heat losses through the slab on grade according to [8] and sources previously cited, a heat flux was determined. That heat flux is lost at the junction of the wall and the ground surface through thermal bridges like door woodwork and between slab-outer wall connection. The results were averaged using a weighted average, dependent on the length of the bridge in the total perimeter of the building. Additionally, an average heat transfer coefficient for the slab on grade – U_m – was determined. Subsequently, a stationary thermal coupling coefficient was determined for the slab on grade H_{tr} of 160.88 m² area, which gives us the scope to estimate the actual heat loss q for the whole slab on grade, depending on the length of the analyzed period and on outdoor temperatures, which are determined by the location of the building. The results are shown in Table 3.

Calculations results as described above

	PD1	PD2							
		15 [cm]	20 [cm]	25 [cm]	30 [cm]	35 [cm]	40 [cm]	45 [cm]	50 [cm]
U_m [W/m²K]	0.219	0.206	0.187	0.173	0.165	0.152	0.144	0.137	0.131
H_{tr} [W/K]	35.17	33.18	30.15	27.84	26.54	24.49	23.12	22.00	21.04
q [W]	1406.74	1327.10	1205.89	1113.53	1061.64	979.63	924.60	880.07	841.46
Q [kWh] January	348.87	329.12	299.06	276.16	263.29	242.95	229.30	218.26	208.68

4. Conclusions

The use of foam glass as a thermal insulating leads to a significant reduction in heat loss for analyzed slab on grade. The analysis of the linear heat loss coefficient presented in Table 2 shows that with the thickness increase of the foam glass layer, the impact of the bridges

tends to zero, and the coefficient value for the PD2 layer (15 cm) is about 30 times smaller than for the PD2 layer (50 cm). The values summarized in Table 3 show that a change from traditional solutions to the solution recommended for typical buildings PD2 (30 cm) will reduce the heat loss through the floor by about 25%, while the use of solution for passive buildings PD2 (40 cm) will reduce the heat loss by about 35%. The analysis also shows that increasing the thickness of foam glass layer above 40cm does not yield such good results – that is approximately 40% less heat loss compared to the traditional layer.

References

[1] www.geocell-schaumglas.eu

[2] PN EN ISO 6946:2008 Komponenty budowlane i elementy budynku. Opór cieplny i współczynnik przenikania ciepła. Metoda obliczania.

[3] Pogorzelski J.A., *O mostkach cieplnych w przegrodach*, Materiały Budowlane, 1/2007, Wydawnictwo SIGMA-NOT.

[4] PN EN ISO 10456:2009 Materiały i wyroby budowlane – Właściwości cieplno-wilgotnościowe – Tabelaryczne wartości obliczeniowe i procedury określania deklarowanych i obliczeniowych wartości cieplnych.

[5] Steidl T., *Komputerowe wspomaganie obliczeń – mostki cieplne*, [w:] *Poradnik diagnostyki cieplnej budynków*, Praca zbiorowa, t. 1, Gliwice 2013, 113-124.

[6] PN EN ISO 13370:2008 Cieplne właściwości użytkowe budynków. Wymiana ciepła przez grunt. Metody obliczania.

[7] Szyszka J., Lichołai L., Starakiewicz A.A., *Skutki złej izolacji ścianki kolankowej*, http://www.izolacje.com.pl, access: 15.11.2010.

[8] Dylla A., *Praktyczna fizyka cieplna budowli, szkoła projektowania złączy budowlanych*, Uniwersytet Technologiczno-Przyrodniczy w Bydgoszczy, 2009.

KONRAD RODACKI*

ANALYSIS OF THE INFLUENCE OF WOOD FRAMED DOME JOINT RIGIDITY ON INNER FORCES DISTRIBUTION

ANALIZA WPŁYWU SZTYWNOŚCI WĘZŁÓW DREWNIANEJ KOPUŁY PRĘTOWEJ NA ROZKŁAD SIŁ WEWNĘTRZNYCH

Abstract

The aim of this paper is to show the unfavourable influence of simplifications we adopt in modelling real structures numerically. The simplest way to model joints is to treat them as either rigid or flexible. However, there are structures whose stability strongly depends on joints' stiffness, an example of which is the structure of a dome whose joints have been designed as semi-rigid. It has been shown that even minor underestimation of the real rigidity of supports or joints has a negative impact on the static inner forces distribution.

Keywords: rigidity, joint, wood structures, forces distribution

Streszczenie

Głównym celem artykułu było wskazanie niekorzystnego wpływu uproszczeń, które przyjmujemy podczas numerycznego modelowania konstrukcji. Najprostszym znanym sposobem modelowania połączeń jest przyjęcie ich jako całkowicie sztywne bądź całkowicie podatne. Istnieją jednak konstrukcje, których stateczność silnie zależy od sztywności węzłów. Doskonałym przykładem okazuje się prezentowana poniżej konstrukcja kopuły, której węzły przyjęto jako częściowo podatne. Ukazano, że nawet małe niedoszacowanie rzeczywistej sztywności połączeń negatywnie pływa na pracę statyczną konstrukcji.

Słowa kluczowe: sztywność, węzły, konstrukcje drewniane, dystrybucja sił

* M.Sc., Eng. Konrad Rodacki, Institute of Building and Physics of Structures, Faculty of Civil Engineering, Cracow University of Technology.

Notation

u	–	linear displacement [m]
ϕ	–	angular displacement [rad, –]
C, k, K	–	joints rigidity [kNm, kN/m]
E	–	Young's modulus [GPa]

1. Numerical model of the object

In order to verify if the influence of joints' rigidity is significant on the inner forces, the numerical model of the dome was created in RFEM 5 [9] on the basis of available material data following the currently valid norms. The dome was modelled as a system supported on columns, which represents the actual structure. The model consists of 1145 bars. The surface load is applied to the structure using the cell option, so that the program will transfer the surface load onto the bar immediately below the surface according to the generally accepted principles. There are 1035 wood bars and 110 steel bars. The steel columns are hinged based on rigid supports. It is an approximation of real case structures, since the real structure rests on a steel structure [2]. Wood and steel were modelled as linear elastic materials. Global view of the modelled structure is shown in Fig. 1.
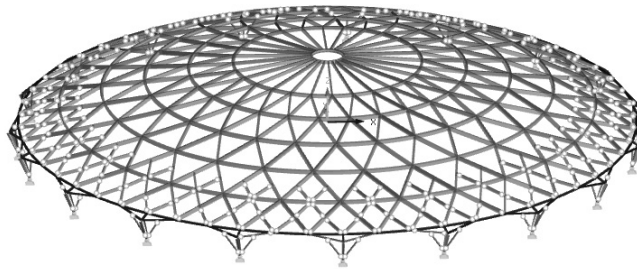
Fig. 1. Structure view form RFEM 5 program [9]

Plywood and glass roof was modelled and introduced as a constant load to the global model. There were two variants of the global model load varying in uniform or non-uniform snow distribution, adopting the basic load area per a dome quadrant, followed by connecting the quadrants with one another. The overall wind load operation was treated as suction.

The global structure was modelled as working linear, the stiffness matrix was calculated in the classical manner, followed by calculation of force results (without iteration). Initially the connections between the main bars were assumed as fully rigid and the secondary bars, with lower stiffness, as hinged joints operating in all directions. The minimal axial forces in Ultimate Limit State for this case are presented on Fig. 2. Next, an analysis of the joints stiffness of the structure was performed.
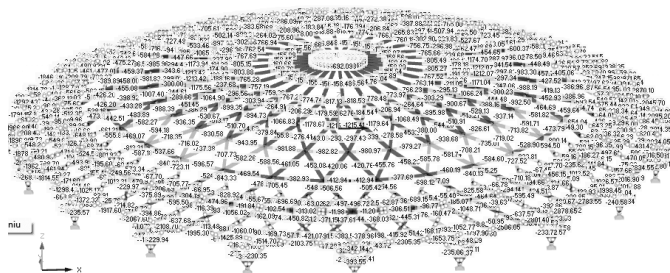
Fig. 2. Figure of minimal axial forces in Ultimate Limit State

2. Joints susceptibility designation

An analysis of the flexibility of the steel connector was carried in the most strained six-branched joint. The main goal of single joint analysis was the assumption of steel connectors stiffness. After that, calculated stiffness was put into the global model of the dome.

The single joint was modelled as panels of a constant thickness. The material of the joint was steel S 420. In order to check what the relationship between elements dimensions and joint rigidity is, six cases were taken under consideration:

Case 1 – the rotation stiffness for 20 mm thick sheets and pipe external diameter of 140 mm (without wood-bolt joint influence),

Case 2 – the rotation stiffness for 40 mm thick sheets and pipe external diameter of 170 mm (without wood-bolt joint influence),

Case 3 – the rotation stiffness for 40 mm thick sheets and pipe external diameter of 250 mm (without wood-bolt joint influence),

Case 4 – the joint rotational stiffness covering the stiffness of wood-bolt joint for the sheets dimensions from case 1,

Case 5 – the joint rotational and longitudinal stiffness covering the stiffness of wood-bolt joint for from case 1,

Case 6 – the joint rotational and longitudinal stiffness covering the stiffness of wood-bolt joint for from case 3.

In case of steel sheets, the joints panels were modelled as surfaces divided into tetragonal finite elements of 8×8 cm. The joint's central part was a pipe with wall thickness of 50 mm, divided into tetragonal finite elements of ca. 7×7 cm. The elements were made by program RFEM 5 [9] itself and, as a result, there were 432 finite elements for the connector shown on Fig. 3. The joint was loaded with forces derived from the global analysis to check the distribution of stresses. Loads were applied as point loads and point moments applied in the gravity centre of bolts configuration (Fig. 3). The values of these loads were taken from the dome model (from places where members were jointed) as axial and shear inner forces and moment in *XY* plane of sheets.

Detailed calculation of stresses in a single connector was carried out for case 2 in two steps. First, the forces were taken from the full rigid model of the dome, then the calculation of joint stiffness was made. After this, reduced stiffness of joints was applied to the global dome model, calculated once more, and than the inner forces were applied to the joint model once more.

Due to the fact that the connectors' metal components are situated between the rigid wood elements insensitive to rotation, they were supported on the entire plane, on the support of a given stiffness along the surface local axis z. The support stiffness was assumed as mean value of elasticity modulus perpendicular to the grains for timber [6, 7]. The angles of supporting timber surfaces are about 60 degrees, so this assumption was taken as a safety precaution.
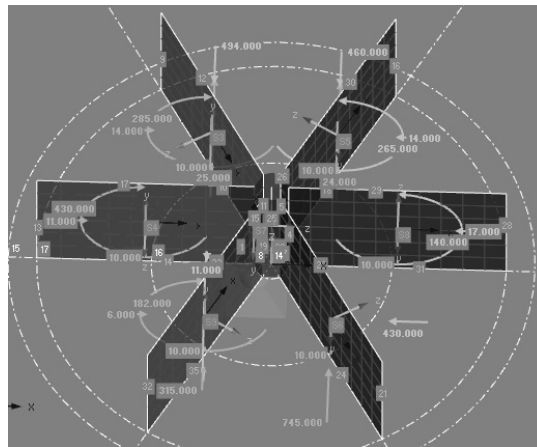
Fig. 3. Sheet joint's model loaded with maximum forces (axial forces, shear forces and moment in *XY* plane of the surface) for case 2
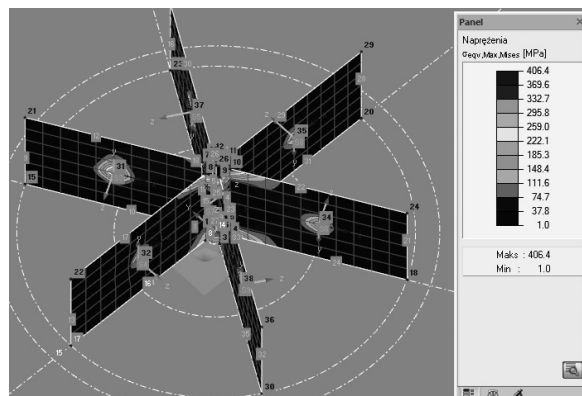
Fig. 4. Von Misses stresses in the most strained joint (case 2)

In order to maintain the stability of the model, a hinge support in one node was assumed, with the support receiving the entire vertical displacement.

As was mentioned before, the global model of the dome structure was modelled as linear. This assumption must have been made due to the size of the model. However, a single joint

(Fig. 3) was modelled as made of elastic-plastic material with a horizontal plasticity line. For a linear model, the stresses were too big for any available steel, so the plastic properties of steel were taken under consideration. The results of the calculation are shown as Von Misses Stresses in the Fig. 4.

In order to test the influence of joints rigidity on the structure's work, an analysis of the rigidity of a typical steel joint was carried out. This analysis was done separately for the deformation of the joint steel, as the most flexible part, and the deflection of the bolts, which are anchored in timber elements, due to the complexity of the calculations the following the PN-EN 1995-1-1 algorithm was determined [6, 8, 10]. The deformation of wood elements was not included due to their high flexural rigidity. The analysis was conducted by applying unit forces to the gravity centre of the bolts, with the displacements subsequently measured. It helps to give the final joints rotational and longitudinal stiffness.
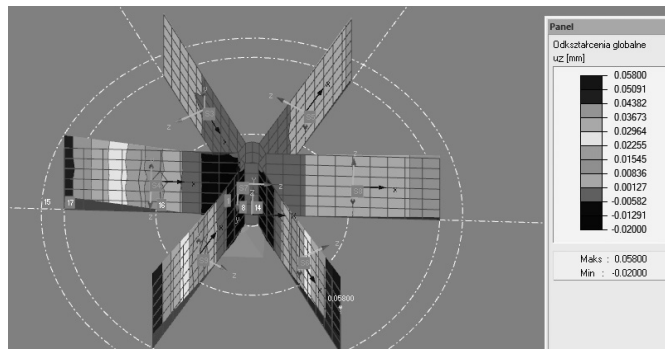
Fig. 5. Global element strain from unit moment

In a vector $\boldsymbol{u^T} = \begin{bmatrix} 0.001 & 0.014 & 0.017 & 0.020 & 0.004 & 0.003 \end{bmatrix} m$, displacements of points corresponding to gravity centres of a group of bolt connectors (Fig. 5), which were used to determine the average stiffness of the connector are shown.

In order to simplify calculations for joint rigidity, the mean value of the displacement was calculated as an arithmetical mean. The next step was the calculation of a mean angular displacement of a single joint as mean displacement divided by the distance between gravity centres of bolts configuration and gravity centres of the joint. Rotational stiffness ($C_{\phi,\gamma}$) was calculated as unit moment value divided by mean value of the angular stiffness.

Equations (1) (6) show the way of stiffness determination for the bolt connections – the wood element after PN-EN 1995-1-1 [4, 6, 8, 10].

Due to PN-EN 1995-1-1 [6] slip modulus on Ultimate Limit State (K_{ser}) was calculated according to the formula 1 and the value for single bolt was K_{ser} = 19.4 MN/m

$$K_{ser} = \frac{2}{3} \times \rho_m^{1,5} \times \frac{d}{23} \tag{1}$$

Angular stiffness of a single joint depending on the bolts connection with timber in Ultimate Limit State was calculated as a geometrical sum given in formula 2 [3, 6]. In this

246

formula, the long-term effects of loading and moisture content are taken under consideration by dividing it by $1+\psi_{2.1} \times k_{def}$. It equals 26.9 MNm.

$$k_{u_1} = \frac{2K_{ser}}{1+\psi_{2.1} \times k_{def}} \times \sum_{i=1}^{8} 4\left[x_{i.1}^2 + x_{i.2}^2\right] \tag{2}$$

$$C_{\phi,\text{.co}} = \left(\frac{1}{k_{u_1}} + \frac{1}{C_{\phi.y}}\right)^{-1}$$

The final stiffness of the joints was calculated according to formula 3 [3], and for case 4, it equals: $C_{\phi.\gamma.co}$ = 18.2 MNm, for case 5, it equals: $C_{\phi.\gamma.co}$ = 20.7 MNm and for case 6, it equals: $C_{\phi.\gamma.co}$ = 26.2 MNm.

Angular stiffness in Serviceability Limit State was calculated according to formula 4, similar to the angular stiffness for Ultimate Limit State.

$$k_{ser_1} = \frac{2K_{ser}}{1+k_{def}} \times \sum_{i=1}^{8} 4\left[x_{i,1}^2 + x_{i,2}^2\right] \tag{4}$$

Moreover, joints longitudinal stiffness and transversal stiffness were calculated for each case for a group of bolts in each wood-bolt connection, according to formulas 5 and 6. Longitudinal stiffness equals 134.1 MN/m and transversal stiffness equals 234.1 MN/m

$$K_{H_1} = \frac{n_{sz1} \times 2K_{ser}}{1+\psi_{2.1} \times k_{def}} \tag{5}$$

$$K_{V_1} = \frac{n_{sw1} \times 2K_{ser}}{1+\psi_{2.1} \times k_{def}}$$

3. Results based on static analysis of the dome structure

The resulting values of joints rigidity for six cases were introduced into the calculation model of the dome, and next re-calculated.

Cases analysed in the RFEM [9] program:

Case 0 – initial assumption of rigid joints,
Case 1 – the rotation stiffness of the joint steel sheet $C_{\phi y1}$ = 52.6 MNm,
Case 2 – the rotation stiffness of the joint steel sheet $C_{\phi y2}$ = 79.6 MNm,
Case 3 – the rotation stiffness of the joint steel sheet $C_{\phi y3}$ = 445.7 MNm,
Case 4 – the joint rotational stiffness covering the stiffness of wood-bolt joint for $C_{\phi y1}$ = 18.2 MNm,
Case 5 – the joint rotational and longitudinal stiffness covering the stiffness of wood-bolt joint for $C_{\phi y1}$ = 18.2 MNm,
Case 6 – the joint rotational and longitudinal stiffness covering the stiffness of wood-bolt joint for $C_{\phi y1}$ = 26.2 MNm.

The obtained results for all the above cases referred to the case 0.
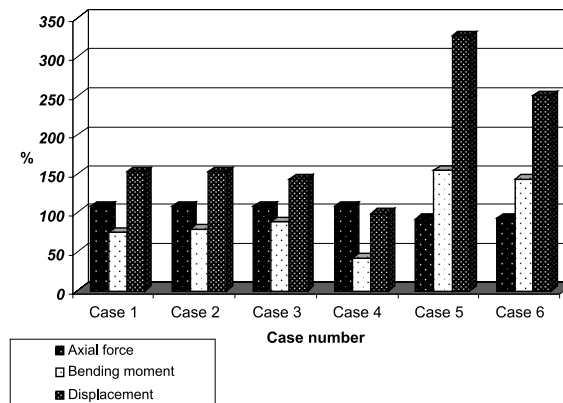
Fig. 6. Relationship between axial forces, bending
moments and displacement for each case related
to the case 0

As follows from the Fig. 6, the flexibility of joints does affect the forces distribution in both the bars and the joints. Whilst the rotational flexibility of joints reduced the joints moments, it increased the axial and shear forces. This phenomenon is favourable, since in moments transfer, the joints' work is non-symmetrical (only some joints are the most strained). On the other hand, assuming elastic strains of the connectors, on the transfer of axial and shear forces all joints are loaded uniformly. In wood-steel connections, the work in the connections is practically non-linear, the most strained joints are the extreme ones, even when purely axial forces are transferred.

What was initially considered was only the work of a steel joint in the form of a welded sheets pack which affected the forces redistribution only slightly (cases 1–3). After additionally taking into account the work of bolt connectors in the timber, there was another significant reduction in the rigidity of the joint (cases 4–6). What should be highlighted is the fact that the inclusion of longitudinal and transverse flexibility completely disturbed the distribution of forces in the structure (cases 5–6). It is generally believed that the global work of an element is affected mainly by flexural rigidity. In this case, also the reduction of compressive/tensile rigidity significantly affected the distribution of forces in the structure, which considerably changed the work quality (the reduction of the axial force in favour of the bending moment).

The impact of bolt connections in wood shear plate, adopted in the analysis, corresponds to the case 3, i.e. by analysing work most similar to rigid connections. When all the connections were assumed to be hinged, there was no convergence of calculations, unfortunately, and the displacement result was 13 m. From the above analysis, it can be concluded that the distribution of forces in the elements does not change significantly with the suggested variation of the rotational stiffness of the structure nodes analysed in this paper. Moreover, the moments M_z, transferred purely by the pressure of the wood members to each other decrease significantly when stiffness is reduced in this direction. Therefore, it can be stated that with some reserve for beam members carrying capacity, part of the moment will shift further away from the joint, which allows stresses to spread better in this direction.

The conspicuous change in the results of Serviceability Limit State is the only change that results directly from the reduction of the global stiffness of the structure. The design of a dome-shaped structure fortunately allows a large reserve in terms of displacements, which permits a partial loss of stiffness.

4. Conclusions

The analyses indicate that, as long as there are certain safety factors safeguarded in bar members design, assuming initially the joints as fully rigid, for more precise results it is possible to obtain less strained work of the joints. This phenomenon is favourable particularly in wood members, as the deformations in highly strained steel-wood connections are considerable and spoil the appearance of the structure. The aspect which was not analysed but may have a significant influence on the dome with a very small rise, is an equilibrium analysis which is shown in [1]. Domes with a small rise may be very sensitive to potential imperfections for a perfect structure. In the next stages of this analysis it should be verified.

References

[1] Chodor L., Bijak R., Kołodziej G., *Wrażliwość nośności konstrukcji nieliniowych*, XLIII Konferencja Naukowa Komitetu Inżynierii Lądowej i Wodnej PAN i Komitetu Nauki PZiTB, Poznań–Krynica 1997, 43-48, http://www.e-architect.co.uk/barcelona/las_are-nas_shopping_center.htm.

[2] Rodacki K., *Design for timber-steel dome structure including joint rigidity analysis*, Master diploma, Kraków 2013;

[3] Neuhaus H., *Budownictwo drewniane*, Polskie Wydawnictwo Techniczne, Rzeszów 2008.

[4] Nożyński W., *Przykłady obliczeń konstrukcji budowlanych z drewna*, WSiP, Warszawa 1994.

[5] PN-EN 1995-1-1, Projektowanie konstrukcji drewnianych. Część 1-1: Postanowienia ogólne i reguły dotyczące budynków, PKN, Warszawa 2010.

[6] PN-EN 338: 2011, Drewno konstrukcyjne – klasy wytrzymałości, PKN, Warszawa 2011.

[7] Porteou J., Kermani A., *Structural Timber Design to Eurocode 5*, Blackwell Publishing, Oxford 2007.

[8] Program RFEM 5. Spatial Models Calculated Acc. to Finite Element Method. Program Description, Dlubal Software GmbH, Tiefenbach 2013.

[9] Smitch I., Asiz A., Snow M., *Design Method for Connections in Engineered Wood Structures*, UNB, Brunswick 2006.

ALICJA SZNURAWA[*]

ANALYSIS OF PHOTOVOLTAIC SYSTEMS FOR FRENCH HOUSEHOLDS

ANALIZA PRZYDOMOWYCH SYSTEMÓW FOTOWOLTAICZNYCH WE FRANCJI

Abstract

The analysis, which has been conducted for four households in France, has shown that the use of photovoltaic panels for electric energy production has been economically effective. The analysis has been conducted using RETScreen® International software and compared with real data form system owners. The calculations were based on daily solar radiation and have been demonstrated using a simple payback period and internal rate of return. The majority of the photovoltaic system's necessary cost has been taken into account. The calculations have demonstrated that a simple payback time for systems set before 2012 is below 10 years, which is a half time of panels' life span. Moreover, the ecological effect on producing electric energy using analyzed systems has been calculated.

Keywords: photovoltaic, renewable energy source, solar energy

Streszczenie

Analiza przeprowadzona na czterech francuskich gospodarstwach domowych pokazuje, że stosowanie paneli fotowoltaicznych do produkcji energii elektrycznej jest ekonomicznie opłacalne. Analizę przeprowadzono w oparciu o program RETScreen® International, a wyniki porównano z rzeczywistymi wartościami przekazanymi przez właścicieli systemów fotowoltaicznych. Obliczenia oparte są na dobowym promieniowaniu słonecznym, a wyniki zobrazowane poprzez prosty okres zwrotu (SPBT) i wewnętrzną stopę zwrotu (IRR). Pod uwagę wzięto większość kosztów wzniesienia i utrzymania instalacji fotowoltaicznej. Wyniki obliczeń pokazują, że systemy zainstalowane przed 2012 rokiem charakteryzuje SPBT poniżej 10 lat, co jest połową okresu życia paneli. Ponadto wyznaczono efekt ekologiczny produkcji energii elektrycznej za pomocą systemów fotowoltaicznych.

Słowa kluczowe: fotowoltaika, odnawialne źródła energii, energia słoneczna

---

[*] M.Sc. Eng. Alicja Sznurawa, Ph.D. student, Cracow University of Technology.

1. Introduction

Photovoltaic systems (PV) may be the answer to the continuously rising energy prices. Installing them allows decreasing monthly households outcomes, due to selling energy produced by panels. Additionally, installing PV systems contributes into lessening CO_2 and other greenhouse gases emission, comparing with conventional power plants emission. In Poland, installing PV systems is mildly supported, as so they are rare. However, France strongly supports such projects.

2. Photovoltaic systems

The core element of photovoltaic system is the cell – it is made of silicon and semiconductors compound. Single cell provides power of 1–2 W. In order to gain greater power, it is necessary to combine them into modules and modules into panels or batteries [1–6].

Produced energy may be utilized by the recipient, accumulated or transmitted to the grid. Most often the law demands selling energy to the grid managing company.

The first step in calculating photovoltaic systems is to define its application (autonomic or connected to grid) and then select the panels of appropriate power. Unitary energy produced by 1 m² cell area during given time period equals:

$$E_j = N\eta_p [\text{kWh/m}^2] \qquad (1)$$

where:

N – insulation [kWh/m²] in given time period,
η_p – average efficiency of photovoltaic cell [%].

In order to calculate the amount of energy produced by all cells, their unitary energy have to be multiplied by the cells area.

PV cell efficiency depends highly on its temperature. As solar radiation increases the temperature of cell, its efficiency is dropping. New hybrid PV/T systems however, can be the answer to decreasing the temperature of panels [7].

3. Subject of analysis

The analysis has been set for four households located in the department of Isère, France. The systems had been installed between 2010 and 2012. Each system consisted of 16 panels installed on the roof and did not exceed 3 kW (owners of PV systems characterised by power output of over 3 kW are recognised as professional energy producers and as such are regulated by different laws). The analysis was conducted using RetScreem International software, which uses meteorological data provided by NASA [6].

The investments in photovoltaic are strongly encouraged in France. Companies that install PV systems hold agreements with banks, which grant them credits on preferential conditions. Those loans are paid off with money earned by selling electric energy produced

by PV system (it is assumed that the credit period will not exceed ten years, which is a half of the system's span life). Additionally, the government funds such investments with 4 K to 8 K € grants.

The object of analysis is to estimate the economical and ecological profitability of installing photovoltaic systems. The analysis is based on real electric energy production data. Calculations were conducted for the following systems.

T a b l e 1

Analysed systems. Own study

No	Location	Year of installation	System's power [kW]	Inclination [deg]	Azimuth [deg]	Installation cost [€]	Energy price [€/kWh]
1	Miribel-les-Echelles	2011	2.80	45	45	19 000	0.584
2	Miribel-les-Echelles	2010	2.88	45	45	24 300	0.584
3	Miribel-les-Echelles	2012	2.80	45	30	19 000	0.388
4	St Aupre	2011	2.96	24	30	16 000	0.584

Fig. 1. Photographs of analysed systems, from left 1, 2, 3, 4 (own study)

As mentioned earlier, all systems' power is lower than 3 kW, table 1. Almost all systems' cost was lower than 20 K €. As one could see, systems set before 2012 are characterised by more favourable energy price, than the one set in 2012.

4. Results

Analysis has shown that in most cases, the annual production was greater than, or similar to the predicted one (Table 2). Moreover, for systems set before 2012, simple payback time is lower than 10 years, which is caused by much lower energy price in 2012. SPBT of the 2nd system is a bit higher, as the cost of installation was over 25% higher. Furthermore, annual life cycle savings for all instalations but the 3rd are around 1 K euro. Nevertheless, the three credited systems' debt service coverage is between 0.6–0.9.

T a b l e 2

Analysis results. Own study

No.	Calculated annual production [MWh]	Real annual production [MWh]	SPBT [year]	IRR [%]	Annual life cycle savings [EUR]	Debt service coverage [–]	Annual GHG emission reduction [t_{CO_2}]
1	3.004	3.686	6.3	–	1336	0.9	0.2
2	3.089	3.410	9.1	–	1054	0.72	0.2
3	3.004	2.765	17.0	5.5	23	0.58	0.2
4	3.314	3.226	6.3	16.2	1141	–	0.3
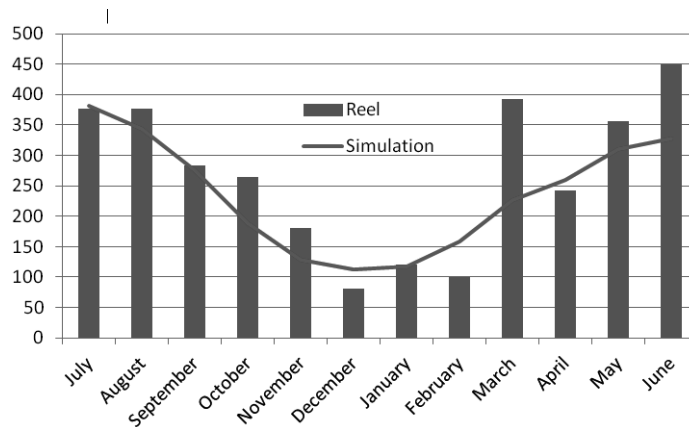
Fig. 2. Part of production history compared with the simulation
provided by the installer of system № 4 (2011/2012) (owner's study)
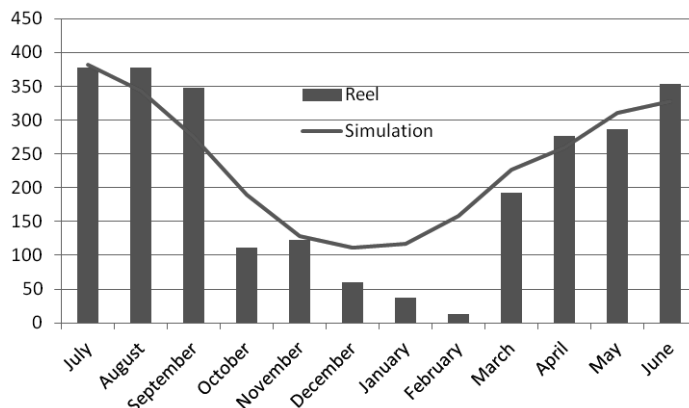
Fig. 3. Part of production history compared with the simulation
provided by the installer of system N° 4 (2012/2013) (owner's study)

The installation of photovoltaic systems reduced the GHG emmision by about 0.2 tonnes of CO_2 annualy, whitch equals 85.9 saved liters of gas or 0.5 acres of forests.

Simulations prepared for system N° 4 were comapred with real production history. They show that most of the time the production is higher than predicted, but in two years' time did not show any trend.

5. Conclusions

In conclusion, the analysis has shown, that two years ago the investment in photovoltaic systems in France was more profitable than nowadays, which is caused by the Government lowering the energy price. Additionally, the simple payback time for most of the installations is relatively short and therefore the investment appears to be profitable.

Moreover, the analysis has shown that one household with photovoltaic installation reduces CO_2 emission only slightly. However, if we consider the number of such households in one village, the resulting emission reduction becomes more vivid.

R e f e r e n c e s

[1] Kaiser H., *Wykorzystanie energii słonecznej*, Wydawnictwa AGH, Kraków 1995.
[2] Lorenzo E., *Solar Electricity. Engineering of photovoltaic systems*, Progensa, Sevilla 1944.
[3] Chwieduk D., *Eergetyka słoneczna budynku*, Arkady, Warszawa 2011.
[4] Sarniak M., *Podstawy fotowoltaiki*, Oficyna Wydawnicza Politechniki Warszawskiej, Warszawa 2008.
[5] Ewers W., *Solar energy: A Biased Guide,* Domus Books, Northbrook 1979.

254

[6] Zimny J., *Odnawialne źródła energii w budownictwie niskoenergetycznym*, Polska Geo-termalna Asocjacja, Kraków–Warszawa 2010.

[7] Tripanagnostopoulos Y., Nousia Th., Souliotis M., Yianoulis P. *Hybrid photovoltaic/thermal solar systems*, Solar Energy, vol. 72, issue 3, March 2002, 217-234.

[8] www.retscreen.net, access: 04.2013.

MATEUSZ SZUBEL, TOMASZ SIWEK[*]

THE APPLICATIONS OF NUMERICAL MODELING FOR THE OPTIMIZATION OF THE OPERATION OF ENERGY DEVICES ON THE EXAMPLE OF AN AIR DISTRIBUTION SYSTEM INSIDE THE BIOMASS BOILER

MOŻLIWOŚCI ZASTOSOWANIA MODELOWANIA NUMERYCZNEGO W PROCESIE OPTYMALIZACJI PRACY URZĄDZEŃ ENERGETYCZNYCH, NA PRZYKŁADZIE SYSTEMU DYSTRYBUCJI POWIETRZA KOTŁA NA BIOMASĘ

Abstract

The paper addresses the results of a numerical – based on experimental data – study of air distribution in the manifold responsible for air supply into a combustion chamber of a biomass boiler. An analysis of the possibilities of optimizing the air distribution system using a ommercial CFD program by changing the diameter of the feeding ducts was performed and described.

Keywords: Renewable energy; Straw combustion; CFD; Air distributor optimization

Streszczenie

Artykuł opisuje wyniki opartego na danych eksperymentalnych modelowania numerycznego kolektora powietrznego, odpowiedzialnego za dostarczanie powietrza do komory spalania kotła na biomasę. Przeprowadzono analizę możliwości optymalizacji systemu rozprowadzania powietrza z wykorzystaniem komercyjnego programu z grupy CFD poprzez zmianę średnic rur dolotowych.

Słowa kluczowe:energia odnawialna, spalanie słomy, obliczeniowa mechanika płynów, optymalizacja kolektora powietrznego

[*] M.Sc. Eng. Mateusz Szubel, M.Sc. Eng. Tomasz Siwek, AGH University of Science and Technology, Faculty of Energy and Fuels.

Designations

σ – standard deviation
N – total number of air feeding ducts
X_i – air mass flow of i duct

1. Introduction

1.1. The process of combustion of solid biomass in energy appliances

The growing interest in renewable energy resources and total pollution emissions reduction is raising the research efforts in the process of biomass combustion [1].

The oldest form of biomass, combusted in domestic devices is wood, but today the utilization of different biofuels, such as straw, many types of pellets, brickets or even sewage sludge [1, 2] is rising rapidly. Practices related to the use of biomass for electricity generation in large scale of co-combustion (power plants) have shown a lot of disadvantages of this form of biomass utilization, especially because of transport costs, energy density and difficulties related to the adaptation of the coal-fired boilers to new parameters of fuel [3].

The alternative way to utilize biomass effectively is gasification, pyrolysis or combustion in small heating and cogeneration systems, which are characterized by power equal maximally a few hundreds of kW. Most of popular small systems are based on the biomass batch or retort boilers with fixed bed or retort.

1.2. The energy appliances studies and optimization with use of numerical models, based on the computational fluid dynamics (CFD) tools

The application of CFD tools is a helpful method for the design and optimization of innovative concepts in power engineering. It is easy to find many examples of CFD simulations, which are directly related with the operation of some elements of heat generation systems or combustion and heat transfer processes.

Miltner et. al. used process simulation and computational fluid dynamics to achieve the maximization of the thermal efficiency and the reduction of gaseous and particulate matter emissions in an innovative baled biomass-fired combustion chamber [4].

Menghini et. al. described experimental and computational activities, which were performed to determine the possible improvements of total environmental impact of a wood-open fireplace. Results of experimental tests were used to validate the simulation model. Then, the simulation results have been adopted to hypothesize a new configuration of fireplace [1].

Many papers are devoted to the study of the air distribution process, into combustion chamber of fireplace or boiler. Bhasker discussed simulation of turbulent air flow distribution in a boiler furnace, where primary air is entrained through the inlet duct system called windbox [5]. Dong and Blasiak presented a numerical model, designed to analyze the advanced secondary/over fired air Ecotube system [6].

However, only small part of works is devoted to the air feeding systems of small-scale heating units. Therefore, it is reasonable to consider the example of such a type of system.

2. Experiments and simulations

2.1. The system of biomass boiler

The paper describes the results of numerical simulations, related to the function of air collector of the biomass boiler "EKOPAL RM40", which is intended for the combustion of straw. The boiler and manifold system is presented in Fig. 1. In the rest of the paper, mass air flows for individual ducts, which in Figure 1 are marked as $R1$-$R7$ (for front ducts) and $D1$, $D2$ (for side ducts) will be presented as X_i (i – the number of duct). The appliance which is studied and simulated is responsible for air distribution into the primary and secondary combustion chamber of the boiler.
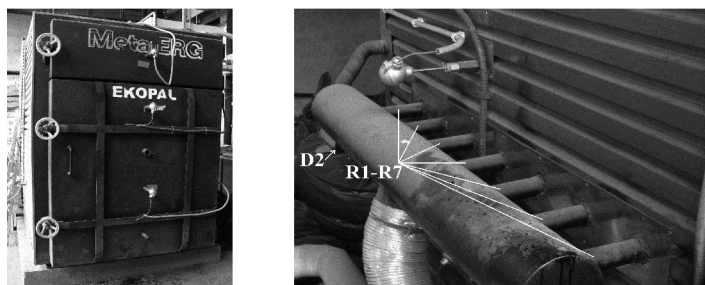
Fig. 1. View of the front of the biomass boiler "EKOPAL RM40" and air collector installed at the backside wall of the combustion chamber

The air flow distribution in the whole area of the primary chamber of boiler, affects the process of combustion. Various quantities of air (oxygen) in different areas of the chamber may cause incomplete combustion.

2.2. Results of experimental studies

The air collector is composed of seven front pipes and two curved side pipes, welded to the main duct. Pipes at the front of the main duct are numbered as $R1$–$R7$ (radius). The symbol of the pipe at the center of the main duct is $R4$. Two side curved pipes are numbered as $D1$ and $D2$ (diameter).

The results of the analysis with the use of a thermo-anemometer probe were used to characterize the distribution of air at the inlet pipe of the fan (diameter – 150 mm). Air velocity distribution inside the pipe was determined by measurements in 16 points along the radius. As a result of calculations, the air mass flow which is provided by fan was defined.

2.3. Numerical model

The air collector was analyzed with use of the 'ANSYS CFX' tool. The spatial geometry (3D) of the modeled object has been prepared in Autodesk Inventor Professional 2013.

The designed geometry was imported into the ANSYS Design Modeler environment, and then transferred to the ANSYS Meshing where discretization has been carried out automatically. Because of the relative simplicity of the manifold design and size, it was

decided that in the case of the domain interior it is not necessary to use advanced meshing options, but it was important to take into account the phenomenona near the boundary layer. A fine final grid was imposed by generating the inflation layer having the first element thickness of 0.0005 m and the growth rate of 1.2 for the next 6 sublayers. The total number of the computational grid elements was 61×10^4. The details of the applied computing grid are shown in Fig. 2.
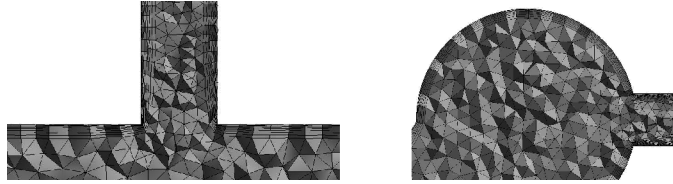
Fig. 2. The details of computing grid applied in the designed model

The SST (Shear Stress Transport|) model of turbulence was used. The air was assumed as an ideal gas (stationary domain). The air flow through the collector was solved by the commercial code ANSYS CFX, with the use of the finite volume method (FVM). The level of residues chosen for the simulation was 10^{-5}.

Because of certain details of the geometry of the secondary combustion chamber, the accurate measurement of the outlet air flow inside the boiler is difficult. Consequently, the distribution of air mass flows at the outlets of the collector ducts has been simulated by CFD.

The results of experiments show that the distribution of air along the outlets of feeding pipes, inside the chamber, is heterogeneous. To optimize (compensate) air distribution inside the combustion chamber, the objective function $\sigma(X)$ (Equations 1–3), that relates the diameter of the pipe with the air flow was defined. The function $\sigma(X)$, which is classic standard deviation of dispersion of the air mass flux X_i was chosen because, in the considered case, the standard deviation is a measure of divergence of individual mass flows. Minimization of the standard deviation means homogenization of the mass flow in the ducts along the manifold.

$$\sigma(X) = \sqrt{\frac{1}{N} \sum_{i=1}^{N} (X_i - X)^2} \tag{1}$$

$$X = \frac{1}{N} \sum_{i=1}^{N} X_i \tag{2}$$

$$\sigma(X) \rightarrow \min \tag{3}$$

The above mentioned function was implemented to the ANSYS CFX and results of standard deviation for all design points were displayed as a part of post processing.

3. Results and discussion

In the optimization process, the objective function $\sigma = 5^{-5}$kg/s was achieved. The air mass flow for the designed collector with new dimensions of feed ducts is equal to about 0.024 kg/s (for each pipe).
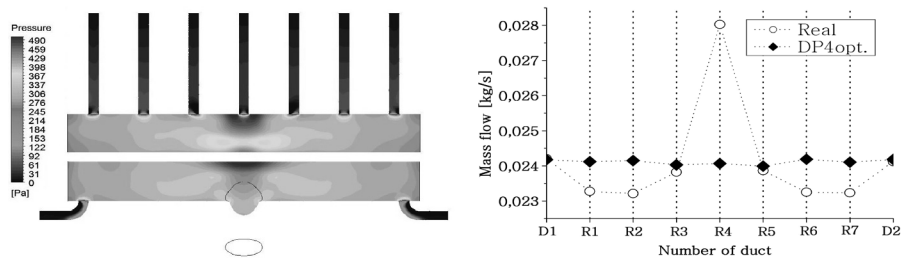
Fig. 3. Simulation of pressure distribution inside the optimized collector (left side) and chart, which presents the comparison of mass flow in pipes for real and optimized dimensions (right side)

Table 1

Presentation of the dimensions of ducts in given design points (DP) and major parameters of the device

Name	The radius (*R*)/diameter (*D*) of the given duct [mm]					Pressure [Pa]	Power [W]	σ [kg/s]
	*R*1 = *R*7	*R*2 = *R*6	*R*3 = *R*5	*R*4	*D*1 = *D*2			
Current	18.35	18.35	18,35	18.35	36.7	524	95.7	18•10⁻⁴
DP4	18.35	18.65	18.3	16.9	36.7	548	100.1	5•10⁻⁵

The comparison between the current and optimized air flow distribution is presented in Fig. 3. For the chosen air mass flow values, changes of pressure and fan power in function of air velocity were defined. It was found that both curves are described by a second degree polynomial function. Consequently, the loss of pressure inside the collector was calculated, according to the Darcy-Weisbach equation. Pressure loss inside air collector after optimization, for air mass flow 0.217 kg/s, rose from 523 to 548 Pa.

Because of it, the fan power which is required to overcome the increased flow resistance, is growing from 67 to 100W (Table 1). The distribution of pressure inside the optimized collector is showed on Fig. 3. Growth of pressure is particularly visible in the main duct, near to narrow inlets of ducts.

4. Conclusions

In the studies described in the paper, CFD model has been used to successfully simulate the physical properties of air inside the collector of the biomass boiler. The results of model

calculations allow to design a device, which provides homogeneous distribution of air inside the combustion chamber of a boiler.

Based on reference [7], it can be concluded that proper construction of the air collector avoids too high emission of carbon monoxide (CO), which is a product of incomplete fuel combustion. Confirmation of the effect should be the subject of further works. Numerical and experimental analysis of the impact of proposed air manifold design changes on the CO emission effect will be performed and described in the separate paper. Moreover, in the considered case, it is suggested to analyze the possibility of using a different type of a collector – for example a device with equal lengths of the profiled feed ducts.

It is always important to compare growth of efficiency of combustion process and energy generation to the financial aspects of design changes. In the simulated appliance, modification is related only to a change of the pipes' diameter, so the implementation of the presented solution seems to be reasonable.

R e f e r e n c e s

[1] Menghini D., Marchione T., Martino G., Marra F.S., C. Allouis, Berenta F., *Numerical and experimental investigations to lower environmental impact of an open fireplace*, Experimental Thermal and Fluid Science 31, 2007, 477-482.

[2] Szubel M., Sornek K., Robak B., Ciołek M., Filipowicz M., *Analysis of the possibility of co-combustion of sewage sludge in biomass boilers*, Archiwum Spalania, nr 4/2012, 263-271.

[3] Szubel M., *Fuel cells powered by hydrogen from biomass*, Zeszyty Naukowe Politechniki Rzeszowskiej, nr 283, Budownictwo i Inżynieria 2012, z. 59, nr 2, t. 2, 755-762.

[4] Miltner M., Miltner A., Harasek M., Friedl A., *Process simulation and CFD calculations for the development of an innovative baled biomass-fired combustion chamber*, Applied Thermal Engineering 27, 2007, 1138-1143.

[5] Bhasker C., *Simulation of air flow in the typical boiler windbox segments*, Advances in Engineering Software 33, 2002, 793-804.

[6] Dong W., Blasiak W., *CFD modeling of ecotube system in coal and waste grate combustion*, Energy Conversion and Management 42, 2001, 1887-1896.

[7] Rybak W., *Spalanie I współspalanie biopaliw stałych*, Oficyna Wydawnicza Politechniki Wrocławskiej, Wrocław 2006, 108-114.

GRZEGORZ ŚLADOWSKI*

MODELING TECHNOLOGICAL AND ORGANIZATIONAL VARIANTS OF BUILDING PROJECTS

MODELOWANIE WARIANTÓW TECHNOLOGICZNO--ORGANIZACYJNYCH PRZEDSIĘWZIĘĆ BUDOWLANYCH

Abstract

The paper addresses the possibility to utilize alternative-decision networks to model and analyze technological and organizational variants of building processes [1]. The undetermined structure of such networks makes it possible to simultaneously model any given number of variants of the scrutinized project and, as a result of the network's analysis, to select the solution (variant) which is optimal within the set criterion. The paper attempts to broaden thevertex set of the subject network by adding two logical formulas on the side of the peak entrance: namely „and" and „or" to make the modeling of certain technological and organizational relationships of a construction enterprise easier. Introducing new vertices into the network required extending the mathematical model used to determine the optimal technological and organizational variant of the analyzed enterprise.

Keywords: network models, technological and organizational structure, optimization

Streszczenie

W artykule zwrócono uwagę na możliwość zastosowania sieci alternatywno-decyzyjnych do modelowania i analizy wariantów technologiczno-organizacyjnych procesów budowlanych [1]. Niezdeterminowana struktura takich sieci umożliwia jednoczesne zamodelowanie dowolnej liczby wariantów realizacji rozpatrywanego przedsięwzięcia oraz w wyniku analizy takiej sieci, wybór rozwiązania (wariantu) optymalnego w sferze ustalonego kryterium. W artykule podjęto próbę poszerzenia zbioru wierzchołków przedmiotowej sieci poprzez dodanie dwóch form logicznych od strony wejścia do wierzchołków, a mianowicie „i" oraz „albo", aby uprościć modelowanie niektórych zależności technologiczno-organizacyjnych rozważanego przedsięwzięcia budowlanego. Wprowadzenie do sieci nowych wierzchołków, wymagało rozszerzenia modelu matematycznego służącego do wyznaczenia optymalnego wariantu technologii i organizacji rozważanego przedsięwzięcia

Słowa kluczowe: modele sieciowe, struktura technologiczno-organizacyjna, optymalizacja

* M.Sc. Eng. Grzegorz Śladowski, Institute of Building and Transport Management, Faculty of Civil Engineering, Cracow University of Technology.

Symbols

Y, U – sets

$[Y, U]$ – graphs

$\{\lambda_{i,j}\}$ – matrix elements

$\langle y_i, y_j \rangle$ – ordered pair: y_i – antecedent, y_i – consequent

Γ_y – set of direct consequents y

Γ_y^- – set of direct antecedents y

$\pi^+ r$ – output half-degree (the number of arcs originating from a node)

$\pi^- r$ – input half-degree (the number of arcs reaching the node)

1. Introduction

Each irregular process, which is commonly defined as an atypical – regarding structure and organization – individual project, should have its reflection in a delivery project. In such a project, to describe its technological and organizational structure (as well as the parameters of the process in question), graph-based mathematical objects of special nature are utilized. Such objects are commonly referred to as networks. Their broad scope makes it possible to effectively plan the process so that, as a consequence, we can obtain an optimal delivery project. Such networks are a convenient tool of creating correct schedules for the realization of processes.

The subject literature [e.g. 2–6] gives the opportunity to get acquainted with the basic issues of network planning, as well as grants the possibility to find multiple examples of their practical implementation.

The criteria for networks' division include a division based on their logical structure which can be determined or non-determined. Networks of a determined structure (i.e. canonic networks) are suitable for modeling processes for which technologies and organizational connections are univocally established. Non-determined structure networks, on the other hand, take into account variants of technological and organizational occurrences in the process being modeled. If it turns out that certain variants of such process will be coming into existence in a random manner, the network which models such a process will be called a stochastic network [e.g. 2, 5–7]. If it turns out that the aforementioned variants of the process will come into existence in deterministic conditions, the network which models such a process will be called an decision network [1, 5].

Research studies [1] which first proposed the concept of alternative-decision networks introduced a definition of such a network based on a special, network-specific graph which allowed modeling of both: technological and organizational variants of the project.

Objectives of the work: The author of this article introduces additional emitters and receptors into the structure of the subject networks. The application of such emitters and receptors facilitates modeling of certain technological and organizational relationships which are typical for construction projects. Introducing new nodes into the network required broadening the mathematical model used to establish the optimal technological

and organizational variant of the project in question by adding new, node-specific limiting conditions. Subsequently, their correctness was proven [8]. Additionally in the paper, practical examples of such networks' application in construction were presented.

2.1. Objectives with alternative-decision networks

a network is given whose graph $G = [Y, U]$ where Y stands for any finite set of elements (nodes); U: non-empty, two-segment relationship $U \subset Y \times Y$ and $|Y| \geq 2$, and meets the following requirements: it is consistent and acyclic – there exists exactly one initial node and at least one goal node in the graph. A node $y \in Y$ of the network is described as an event and is the element that expresses, from one side, the reaching of a certain state or goal manufactured by determined subsets of arcs, and from the other side, for other determined subsets of arcs acts as a condition for their realization. Based on the description presented above, the node can be divided into two parts:

– **receptor** that determines the conditions of reaching a given state (receptor activation),
– **emitter** that determines the conditions of the realization of certain actions that are symbolized by the arcs.

In the defined network, we can single out six possible, two-segment combinations (nodes) of the network, including the four newly introduced by the author of this paper, characterized by the following receptors and emitters that are presented in the table (Fig. 1).

RECEPTOR / EMITTER	and	or	either
Canonic	◯	◇	⬡
Decision	◖	⬠	◖⬠

Fig. 1. Nodes of an alternative-decision network (source: own work)

In the alternate-decision network under the question, we can also distinguish two subsets of arcs:

a) set $U_A \in U$ containing so-called alternative arcs, the interpretation of which is as follows: An alternative arc is an arc originating from the node with the decisive emitter. It is assumed that only alternative arcs originate in the node with the decisive emitter. In order for the previous assumption to make sense, we also assume that at least two of such arcs must originate from the aforementioned node. A situation where alternative arcs originate from the initial node should be excluded. For that reason, we assume that the initial node of the network in question should not hold a decisive emitter;

b) set $U_k \in U$ that contains so-called canonic arcs, the interpretation of which is as follows: A canonic arc is an arc originating from a node with a canonic emitter. We assume that only canonic arcs can originate from a node with a canonic emitter. A graphical interpretation of both an alternative arc and a canonic arc is presented in Fig. 2.

This last assumption pertains to the goal node of the defined network, which is preceded in the path by at least one node with a decision emitter. A path in a graph $G = [Y, U]$ should be understood as a sequence of arcs in which the end of each arc overlaps (through a node) with the beginning of the subsequent arc.

a)

b)

Fig. 2. Graphical interpretation of arcs:
a) alternative, b) canonic (source: [1])

2.2. Allowable structures (allowable sub-networks)

Non-determined logical structure of the decision-alternative network in question contains certain allowable structures (allowable sub-networks) which will represent selected technological and organizational variants of the modeled process. An allowable structure (allowable sub-network) in an alternative-decision network can be described as a sub-network based on a graph $G^* = \left[Y^*, U^*\right]$, where $Y^* \subset Y, U^* \subset U$ are non-empty. That graph has to meet the following requirements: it is consistent and acyclic. The initial node of graph, $G = [Y, U]$ of alternative-decision network is also the initial node of, $G = [Y^*, U^*]$ contains at least one goal node that belongs to graph $G = [Y, U]$ of the alternative-decision network. If a node with a canonic emitter in graph $G = [Y, U]$ of an alternative-decision network belongs to a graph $G = [Y^*, U^*]$, then all directly subsequent consequents of the node will also belong to it. If a node with a decision emitter in the graph $G = [Y, U]$ of the alternative-decision network belongs to the graph $G = [Y^*, U^*]$, then one and only one direct subsequent nod belongs to that graph. Consequently, following the second definition, each allowable structure (allowable network) of an alternative-decision network can be described by using a row vector characterized in the following way:

$$A = \left\{\lambda_{ij}\right\}, \quad \text{where} \quad \lambda_{ij} = \begin{cases} 0 & \text{for } y_i, y_j \notin U^* \\ 1 & \text{for } y_i, y_j \in U^* \end{cases} \text{which for} \quad r, s \in Y$$

3. Binary extreme issue

each alternative-decision network contains a finite number of allowable structures (allowable sub-networks) and it is known that it has to possess, as the properties of such networks dictate, at least two such structures. In the course of further analysis, we will be interested in the way of determining the allowable structure and making the determined allowable structure of the considered network such an allowable sub-network that will be also optimal in terms of the adopted section criterion.

In order to solve the above task, a binary extreme issue, presented in short by the symbol (BZE), must be formulated.

$$\sum_{i,j \in U} c_{ij} \lambda_{ij} = \mathbf{min} \left(\text{or } \mathbf{max}\right) \tag{2}$$

with limiting conditions:
for $s \in Y$ („canonic" emitter)

$$\sum_{r \in \Gamma s} \lambda_{sr} = \pi^+ s \tag{3}$$

for $r \in Y$ (receptor „and", „canonic" emitter)

$$\pi^+ r \lambda_{ir} - \sum_{j \in \Gamma r} \lambda_{rj} = 0 \ \text{ for } \ i \in \Gamma_r^- \tag{4}$$

for $r \in Y$ (receptor „or", „canonic" emitter)

$$\pi^+ r \lambda_{ir} - \sum_{j \in \Gamma r} \lambda_{rj} \leq 0 \ \text{ for } \ i \in \Gamma_r^- \sum_{j \in \Gamma r} \lambda_{rj} - \sum_{i \in \Gamma_r^-} \pi^+ r \lambda_{ir} \leq 0 \tag{5}$$

For $r \in Y$ (receptor „either", „canonic" emitter)

$$\sum_{i \in \Gamma_r^-} \pi^+ r \lambda_{ir} - \sum_{j \in \Gamma r} \lambda_{rj} = 0 \tag{6}$$

for $r \in Y$ (receptor „and", „decision" emitter)

$$\sum_{i \in \Gamma_r^-} \lambda_{ir} - \sum_{j \in \Gamma r} \pi^- r \lambda_{rj} = 0 \tag{7}$$

for $r \in Y$ (receptor **„or"**, **„decision"** emitter)

$$\sum_{i \in \Gamma_r^-} \lambda_{ir} - \sum_{j \in \Gamma r} \pi^- r \lambda_{rj} \leq 0 \quad \sum_{j \in \Gamma r} \lambda_{rj} \leq 1 \quad \sum_{j \in \Gamma r} \lambda_{rj} - \sum_{i \in \Gamma_r^-} \pi^+ r \lambda_{ir} \leq 0 \tag{8}$$

for $r \in Y$ (receptor **„either"**, **„decision"** emitter)

$$\sum_{i \in \Gamma_r^-} \lambda_{ir} - \sum_{j \in \Gamma r} \lambda_{rj} = 0 \quad \sum_{j \in \Gamma r} \lambda_{rj} \leq 1 \tag{9}$$

Limitation for variable λ_{ij}

$$\lambda_{ij} = \begin{cases} 0 \\ 1 \end{cases} \tag{10}$$

An objective function (commonly referred to as a criterion function) formulated for (BZE) is the most basic of all the possible functions where: c_{ij} is a constant value, the load of the graph arc $y_i, y_j \in U$ of an alternative decision network and λ_{ij} is a variable (decisive) determining if a given arc $y_i, y_j \in U$ belongs (or doesn't belong) to an optimal structure (that is the best one allowable within the accepted selection criterion) in an alternative-decision network. Additional conditions (4), (6), (7), (9) are the consequence of the author's introduction of the aforementioned additional nodes into the network structure.

4. Technological and organizational structures in construction

below, an example of modeling variants of technological and organizational of foundation works as a part of a construction project. Fig. 3 shows a fragment of an alternative-decision network that models the elevation of foundation for two buildings simultaneously. Table 1 contains data on the net cost of each task. Then the author has established a minimum cost as a criterion for selecting the optimal variant of technological and organizational of foundation works.

Table 1

Data on the net cost of each task within the foundation works (source: own work)

SYMBOL OF TASK	DESCRIPTION OF THE TASK	UNIT OF MEASURE	QUANTITY OF UNITS	UNIT PRICE	VALUE
A1	Groundworks for construction nr 1	[m³]	600	43	**25800**
A2	Groundworks for construction nr 2	[m³]	600	43	**25800**
B1	Foundation formwork traditional for construction nr 1	[m²]	140	60	**8400**
B2	Foundation formwork traditional for construction nr 2	[m²]	140	60	**8400**
C1	Assembly and disassembly of tower crane for construction nr 1	[Set]	1	2600	**2600**
C2	Assembly and disassembly of tower crane for construction nr 2	[Set]	1	2600	**2600**
D1	Foundation formwork system for construction nr 1	[m²]	140	41	**5740**
D2	Foundation formwork system for construction nr 2	[m²]	140	41	**5740**
E1	Reinforcement manual for construction nr 1	[T]	2.20	4022	**8848**
E2	Reinforcement manual for construction nr 2	[T]	2.20	4022	**8848**
F1	Prefabricated reinforcement for construction nr 1	[T]	2.20	4063	**8939**
F2	Prefabricated reinforcement for construction nr 2	[T]	2.20	4063	**8939**

G1	Reinforcement manual for construction nr 1	T	2.20	4022	**8848**
G2	Reinforcement manual for construction nr 2	T	2.20	4022	**8848**
H1	Task apparent for construction nr 1	–	–	0	**0**
H2	Task apparent for construction nr 2	–	–	0	**0**
I1	Concreting using ready-mixed concrete pump for construction nr 1	$[m^3]$	64	320	**20480**
I2	Concreting using ready-mixed concrete pump for construction nr 2	$[m^3]$	64	320	**20480**
J1	Concreting using a tower crane with container for construction nr 1	$[m^3]$	64	328	**20992**
J2	Concreting using a tower crane with container for construction nr 2	$[m^3]$	64	328	**20992**
K1	Concreting using ready-mixed concrete pump for construction nr 1	$[m^3]$	64	320	**20480**
K2	Concreting using ready-mixed concrete pump for construction nr 2	$[m^3]$	64	320	**20480**
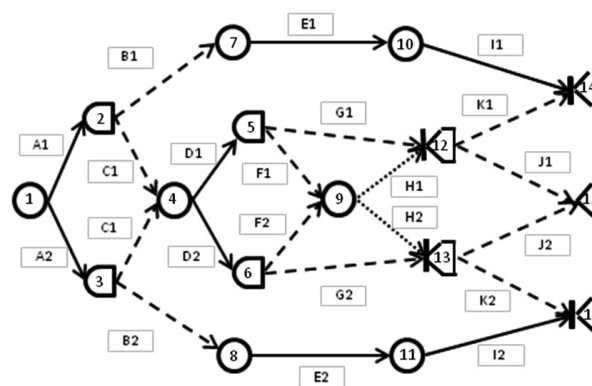
Fig. 3. A fragment of an alternative-decision network that models the elevation of foundation for two buildings simultaneously (source: own work)

Table 2 shows the result of optimization in the form of a vector of decision variables which defines the cheapest variant of technological and organizational the foundation works (optimal structure of the network model) (Fig. 4). Calculations were made using the application "Solver" in Microsoft Office.
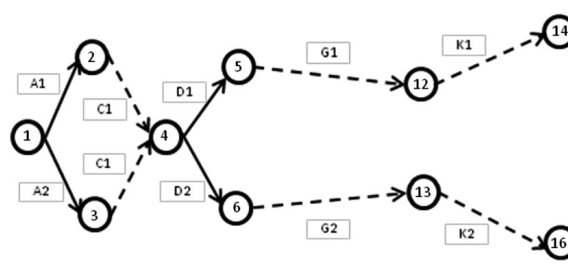
Fig. 4. The optimal network model, which showing
the dependencies technological and organizational of
foundation works whose execution cost is the lowest
(source: own work)

Table 2

Optimal solution to the extreme binary issue (source: own work)

Arcs	1–2	1–3	2–4	2–7	3–4	3–8	4–5	4–6	5–9	5–12	6–9	6–13	7–10	8–11	9–12	9–13	10–14	11–16	12–14	12–15	13–15	13–16			
	1	1																					2	=	2
	1		1	1																			0	=	0
		1			1	1																	0	=	0
			2				1	1															0	=	0
				1									1										0	=	0
					2		1	1															0	=	0
						1								1									0	=	0
							1		1	1													0	=	0
								1			1	1											0	=	0
									2						1	1							0	=	0
										1					1				1	1			0	=	0
																			1	1			1	≤	1
											2				1	1							0	=	0
												1		1		1					1	1	0	=	0
																					1	1	1	≤	1
													1				1						0	=	0
														1				1					0	=	0
																							0	=	0
cij	A1	A2	C1	B1	C1	B2	D1	D2	F1	G1	F2	G2	E1	E2	H1	H2	I1	I2	K1	J1	J2	K2	Σcijλij		
λij	1	1	1	0	1	0	1	1	0	1	0	1	0	0	0	0	0	0	1	0	0	1	126936		

4. Conclusions

In construction, networks of a determined structure of connections, which depict univocally a certain organization and technology used to deliver a planned project, are primarily used for planning construction projects. Analysis methods developed for these networks make it possible to effectively resolve the project's schedule regarding parameters determined for it, such as delivery time, delivery cost, or the availability of resources. Unfortunately, all attempts at creating variants of schedules with either partial or complete changes in technology or organization of the planned project, require the reformulation of a new network model and subsequently the repetition of the following stages of its analysis.

The concept to solve this issue can be using the properties of alternative-decision networks, the non-determined logical structure of relationships, makes it possible to create variants of projects regarding their technology and organization.

R e f e r e n c e s

[1] Ignasiak E., *Optymalne struktury projektów*, PWE, Warszawa 1977.
[2] Jaworski K.M., *Metodologia projektowania realizacji budowy*, PWN, Warszawa 2009.
[3] Jaśkowski P., *Metoda projektowania struktury systemu wykonawczego przedsięwzięcia budowlanego z zastosowaniem algorytmu ewolucyjnego*, Budownictwo i Architektura, 2, 2008.
[4] Kapliński O., *Metody i modele badań w inżynierii przedsięwzięć budowlanych*, PAN, Warszawa 2007.
[5] Biernacki J., Cyunel B., *Metody sieciowe w budownictwie*, Arkady, Warszawa 1989.
[6] Woźniak A., *Grafy i sieci w technikach decyzyjnych*, PAN, Kraków 2010.
[7] Głowacz L, Kołton A., *Analiza wariantów realizacji przedsięwzięcia na podstawie struktur algebraicznych sieci alternatywno-koniunkcyjnych*, Przegląd statystyczny, 2/1989.
[8] Śladowski G., *Kanoniczno-decyzyjne modele sieciowe oraz ich zastosowanie w planowaniu przedsięwzięć budowlanych*, Praca magisterska, PK, Kraków 2002.

PAULINA TABAK*, KINGA STANUSZEK, JOLANTA GINTOWT**

VISION & REALITY – GLÜCKSTEIN QUARTIER – CONCEPTUAL DESIGN OF A HOUSING ESTATE IN THE TECHNOLOGY OF PASSIVE HOUSE – PROJECT ANALYSIS

VISION & REALITY – GLÜCKSTEIN QUARTIER – KONCEPCYJNY PROJEKT OSIEDLA WIELORODZINNEGO W TECHNOLOGII BUDOWNICTWA PASYWNEGO – ANALIZA PROJEKTU

Abstract

The article is about the concept of a housing estate in Germany. The project was created as a part of a competition. The contest was organized by the ISOVER Company. The name of the contest is ISOVER Multi-Comfort House Students Contest Edition 2013 Vision & Reality – Glückstein Quartier. With reference to a historical place which belongs to our place, the development has been called "diamond apartments" Houses have a shape like the crystal of a diamond. The way of creation, location, and building shape assure the maximum usage of solar energy, so that there will by optimal thermal comfort inside. The project also includes a large scale service and entertainment building complex, located in the immediate vicinity planned residential development.

Keyword: housing estate, multi house, passive house

Streszczenie

Niniejsza praca przedstawia opis, koncepcji projektu energooszczędnego osiedla mieszkaniowego w Niemczech. Projekt powstał w odpowiedzi na konkurs ogłoszony przez firmę ISOVER, ISOVER Multi-Comfort House Students Contest Edition 2013 Vision & Reality – Glückstein Quartier. W nawiązaniu do historycznego kontekstu miejsca, osiedle zostało nazwane „diamentowym". Forma budynków bezpośrednio nawiązuje do kształtu diamentowego kryształu. Sposób posadowienia budynków na działce, oraz ich kształt pozwalają na maksymalne wykorzystanie energii słonecznej, celem zapewnienia optymalnego komfortu cieplnego wewnątrz mieszkań. Projekt zakresem obejmuje również duży kompleks usługowo-rekreacyjny znajdujący się w bezpośrednim sąsiedztwie projektowanego osiedla.

Słowa kluczowe: osiedle mieszkaniowe, budownictwo pasywne

* Eng. Arch. Paulina Tabak, Faculty of Architecture, Cracow Univesity of Technology.
** Eng.Kinga Stanuszek, M.Sc. Eng. Jolanta Gintowt, Institute of Building Materials and Structures, Faculty of Civil Engineering, Cracow University of Technology.

1. Introduction. Aim of the competition

People thinking in a different way about the use of non-renewable sources of energy that follows technological progress, is something that is reflected in the modern process of design and construction of buildings.

Therefore, engineers created effective solutions for improving energy efficiency of residential buildings [1, 3–5]. With the aim of popularizing energy-saving construction, the organizer of the contest has announced a multi-family housing project in the historic district of the city of Mannheim in Germany. The project scope of the Isover Multi-Comfort House Students Contest Edition 2013 Vision & Reality – Gluckstein Quartier project consisted of residential buildings with high energy systems.
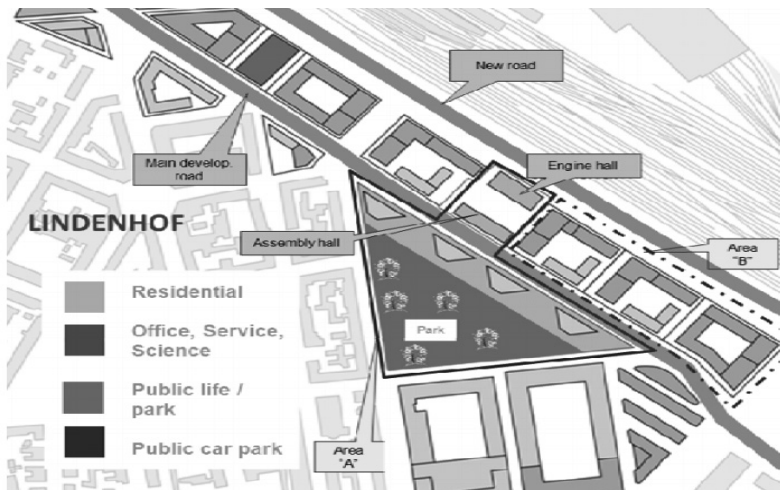
Fig. 1. Designed area, Mannheim

Glückstein Quartier is the north district of Mannheim. Situated directly opposite to the train station, between housing stock the Lindenhof and also Inner-City. The main aim of this project is create a new neighborhood planning system which connects different zone development parts. There are two areas: A and B where urban complex should be created. Area "A" is dedicated to residential functions. A maximum of 4 buildings with the maximum height level of ground floor + 4 floors shall be constructed in this area. The estimated number of flats is estimated at under 150 apartments. This area also contains historical buildings as well as the park. The task is to find a sustainable usage for both these spaces as well as a good link between the park area and the existing building stock of "Lindenhof" in the South-West and the two historic buildings and the new development to the North-Est.

"B" area is for both non-residential and residential usage. The task of the contest for this part is to create a master plan and a design for the building shapes, facades and the exterior green, taking into account office, service and scientific functions as well as residential functions. The height level for this area is: residential: ground floor + 5 upper floors, non-residential: ground-floor + 11 upper floors [1].

2. The concept of a passive building

The design for area "A" presented in our concept provides four multi-family buildings. The building is formed so as to take maximum advantage of solar energy. The name and the idea of new residential building comes from a diamond. The shape and the form of the buildings are similar to a diamond shape. The design is simple, transparent and excellently collaborates with the sun . Symmetrical shape, modular units of dwellings and the repeatability of used materials makes our investment quick and inexpensive. This factor provides a high class and energy-saving passive house that is economical both at the stage of formation and in operation.

Most of the windows are oriented south-east and south-west, which supplies maximum solar energy gains. In front of the elevation there are balconies, designed to eliminate the overheating of the housing during the summer. Their design is not connected to the the facade, so the thermal insulation is constant. The northern part of the building is a corridor. Designing the corridor as a separate structure saves us energy, which is needed to heat such a large area, and also is a buffer zone isolating from a busy, noisy street. All machinery and equipment, which use passive and active methods of saving and gaining energy, contributes to the low energy consumption on A++ level.

The most important part of the project is the optimally corresponding layer of thermal insulation. For vertical partitions, a double layer of Isover Sillatherm WVP 1–035 0.16 m (Fig. 3) is adopted, for the flat roof: Isover Metacam FLP 1 – DURATEC 2×0.18 m. (Fig. 4). There are solar collectors, located on the roofs of buildings at 45% of the surface, ceiling to roof. In addition, the operation of the building assumes the use of rain water, spin-off sites for waste segregation, and storage of rainwater to be used on private plots.

The existing parts of the city have been linked to park streets which lead to the other new urban neighborhood. This site is designed as a recreational services complex. It is composed of a modern office space, science facilities, high-quality living space and meeting places for social life. The district also offers a tremendous opportunity for investors who want to get involved in the development of an economically and ecologically valuable project of utmost importance. This zone consists of three similar building complexes. To help with the navigation around this district, each was named after a stone: Amber, Ruby, Gold.

Between the modern facilities, we can find two interesting historical buildings. The arrangement of Diamond buildings, trees and paths give us a perfect open view and connection from the Lindenhof. Renovated engine hall was adapted as an Independent Art Center, where residents will be able to learn a new craft that is film, music, theater, and present their work. In assembly hall, there are cafes and restaurants. Between the buildings, park with numerous small fountains for spending leisure time was designed.

All residential and recreational complex service is designed to raise the standard of living and working, as well as minimizing the need for non-renewable energy in the city center.

Buildings meet the requirements for passive certification: usable energy of less than 10 kWh /m^2 per year, primary energy below 60 kWh/m^2 per year. Linear heat transfer coefficient $\Psi = 0.01$ W/mK. Calculations were performed according to [2, 6–9] and the procedure laid down by the competition organizer.
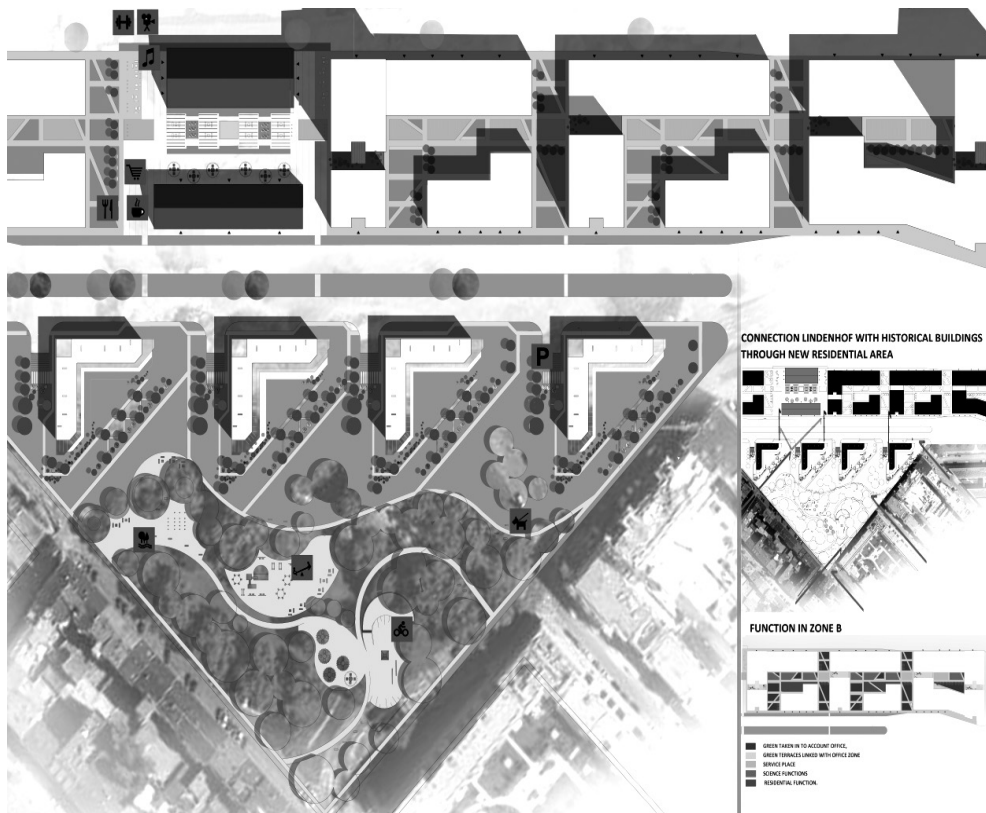
Fig. 2. Project diamond apartments's development

Exterior wall in cocntact with air [cm]
U-value: 0.10 W/m2K

1.5   Lime cement rendering
25.0 Perforated brick
16.0 ISOVER Silatherm WVP 1-035
16.0 ISOVER Silatherm WVP 1-035
      Water vapour permeable wind protection
3.0   Ventilation area
3.0   Cladding with precast concrete bloks
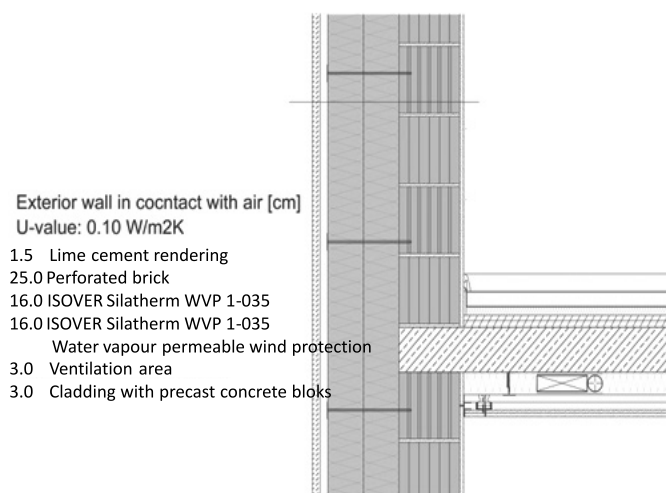
Fig. 3. Exterior wall in contact with air

5. Conclusions

This design of a multi-family residential complex may be an example of combining modernity and innovative solutions with historic buildings. It is one example that can be in harmony with the psychological habits of future users to design buildings with high energy efficiency while blending them in with the tissue of a historical urban area.

SCALE 1:20

1,9	OSB board
10,0	ISOVER Integra ZKF 1-032
1,9	OSB board

Warm roof [cm]
U-value: 0.10 W/m2K

8.0 Pebbles
0.8 Double layer and sealing sheeting, bonded or scorched
18.0 ISOVER Metac FLP 1 Duratec
18.0 ISOVER Metac FLP 1 Duratec
     Vapour retarder
     Lvelling layer, bitumen perforated glass-mat sheeting
     Preliminary coat at inclination of at leat 2 %
20.0 Reinforced cocrete ceiling
1,5 Interior plaster

Fig. 4. Warm roof

R e f e r e n c e s

[1] Feist W., Munzenberg U., Thumulla J., Darup S.B., *Podstawy budownictwa pasywnego*, Polski Instytut Budownictwa Pasywnego, Gdańsk.
[2] Feist W., Pfluger R., Kaufmann B., Schneiders J., Kah O., *Pakiet do projektowania budynków pasywnych 2007. Wymagania dotyczące budynków pasywnych sprawdzanych pod względem jakościowym*, Passivhaus Institut, Darmstadt.
[3] Klemm K., *Wpływ zmian w układzie zabudowy na przepływ powietrza*, Fizyka Budowli w Teorii i Praktyce, Wyd. Politechniki Łódzkiej, Tom VI, Zeszyt 2, 2011.
[4] Jurkiewicz P., *Dom pasywny. Budowa domu pasywnego z zastosowaniem popularnych rozwiązań budowlanych*, Murator plus.pl.18/10/2012
[5] Feist W., *Passive House in Darmstadt-Kranichstein*, 1998/2nd International Passive House Conference in Düsseldorf.
[6] *Energy Balances with the Passive House Planning Package*; Protocol Volume No. 13 of the Research Group for Cost-efficient Passive Houses, 1st Edition, Passive House Institute, Darmstadt 1998.
[7] Ebel W., Feist W., *Ergebnisse zum Stromverbrauch im Passivhaus Darmstadt–Kranichstein* in "Stromsparen im Passivhaus"; Protokollband Nr. 7 zum Arbeitskreis Kostengünstige Passivhäuser, PHI, Darmstadt 1997.

276

[8] *Energy balance and temperature characteristics*, Protocol Volume No. 5 of the Research Group for Cost-efficient Passive Houses, 1st Edition, Passive House Institute, Darmstadt 1997.

[9] Feist W., Loga T., *Comparison of measurements and simulation*, "Energy balance and temperature characteristics" Protocol Volume No. 5 of the Research Group for Cost-efficient Passive Houses, PHI, Darmstadt, January 1997.

MICHAŁ TOPOLSKI, JAKUB ŻUREK, JOLANTA GINTOWT[*]

COLLATION OF QUALITATIVE RESEARCH WITH QUANTITIVE FEM RESEARCH IN TERMS OF TWO DIMENSIONAL HEAT FLOW

PRÓBA KORELACJI BADANIA JAKOŚCIOWEGO IN SITU Z ANALIZĄ ILOŚCIOWĄ MES W ASPEKCIE DWUWYMIAROWEGO PRZEPŁYWU CIEPŁA

Abstract

The paper concerns an attempt to collate qualitative research with quantitative FEM research in terms of two dimensional heat flow. It shows the accuracy of both methods, according to in situ researches with a thermal camera and models – done with software Therm 5, Therm.

Keywords: simulations, heat transfer, thermal bridge, in situ, modeling

Streszczenie

Artykuł dotyczy próby zestawienia badań jakościowych z badaniami ilościowymi w zakresie MES dwuwymiarowego przepływu ciepła. Próba korelacji obu metod, według badań *in situ* przy użyciu kamery termowizyjnej i modeli – wykonane z oprogramowaniem Therm 5, Therm.

Słowa kluczowe: symulacje, przepływ ciepła, mostek termiczny, badania in situ, modelowanie

[*] Michał Topolski, student, Jakub Żurek, student, M.Sc. Eng. Jolanta Gintowt, Institute of Building Materials and Structures, Faculty of Civil Engineering, Cracow University of Technology.

1. Introduction

Due to the existing legal and formal rules, regulations resulting from the NFOŚ programs relating to subsidies to the newly-erected buildings nearly zero energy, the problem of verification and modeling of thermal bridges has become an important issue from the point of view of both the investor the verifier of projects. From the scientific point of view, the matter could seem simple. On the other hand, the task sounded like an easy way to correlate the design assumptions with their verification on a real object. Typically, verification of the numerical model is associated with laboratory testing or an in situ examination. In general, the measurement (whether in the laboratory or in the experimental object or an existing object) is treated like a check on the theoretical results. In addition, verification and accuracy of measurement of heat flow through the building's envelope is important, both for determining the energy balance of the building, as well as diagnosing the causes of the destruction of construction joints.

The subject of the paper focuses on the combination of the two methods of testing and analysis of two-dimensional heat flow – a qualitative in situ research executed using an infrared camera and a quantitative research performed with FEM software. Its aim is to attempt to correlate the results, assess the accuracy and to show the advantages and disadvantages of *p*/*m* methods.

2. Subject of analysis

The subject of analysis were buildings located in south part of Poland, Małopolska, in the fourth climatic zone. Buildings, taken into account, are located in Wieliczka, Brzesko, Tarnów, Radłów (as it is showed in Fig. 1). A qualitative study was performed in February and March of 2013. The construction of outer walls is described in Table 1.

Fig. 1. Brzesko, Radłów i Wieliczka houses subjected to research

3. Methods of analysis

A comparative analysis of *in situ* measurements of real objects is described above (computer modeling using MES). Measurement of *in-situ* (in-) was used as a verification

of both models and the temperature distribution and the boundary conditions such as the temperature at the surface of the partition.

T a b l e 1

**External partitions, thermal characteristics
of the examined objects**

Thermal characteristics of the examined objects			
No.	Type of material	thickness [cm]	1 [W/mK]
Object 1	hollow block Porotherm	25	0.88
	thermal insulation EPS	5	0.042
Object 2	solid brick	30	0.77
	thermal insulation EPS	8	0.042
Object 3	hollow block MAX	28.8	0.43
Object 4	reinforced concrete	25	1.7
	thermal insulation EPS	10	0.042

The analysis of *p/m* buildings in terms of two-dimensional heat flow were done using: situ measurement and a computer modeling method of MES. For the measurement, the following measuring equipment was used:
– for qualitative research, an infrared camera VIGOcam v50 bolometer detector with resolution of 384 × 288, the measured wavelength ranging from 8 to 14 mm, and the detector sensitivity of two 2 degrees Celsius;
– for the quantitative study – software integrated with VIGOcam: Therm, and to model the selected calls Therm 5 – a program that uses finite element method algorithm;
– Hygrometer VOLTCRAFT PL-100TRH probe Type *K*, Temperature range: 0 to + 60°C; Type *K*: from – 200 to 1372°C. Temperature measurement accuracy: ±1°C, Humidity measuring range: 0–100% RH, Humidity accuracy: ± 2.5%,
– VIDEO THERMOMETER IR-pyrometer model: 7550, Range: –50 ... + 1600°C, Optics: 50: 1, 1% accuracy +/–, Adjustable emissivity: 0.10–1.00. For the modeling models – done with software Therm 5, Therm.

For comparison, critical, the most neglected, points, where there have been the most intense heat transmission were selected. These include (listed by type of node design) a combination of the cantilever with the outer wall, ring beams, window frames, door (lintels, sills, sides), a connection of foundation walls to the ground, corners of external walls, reinforced concrete columns placed in the exterior walls, such as building ceramics, identified and defined bridges "internal" resulting from the discontinuity of insulation and its misalignment.

For modeling the finite element method [1–3, 11, 12] was used. The verification of the thermal resistance partitions calculations was also carried out in accordance with [20]. Still, in some studies, eg.: [7, 8, 0, 13], one can find references to the simple ways of determining the estimated thermal bridges [4–6] and the applicable provisions of [15, 16, 18, 19] consistent with the Regulation of the Ministry of April 7, 2004 [21 as amended]. To simulate and analyze the flow of heat through building components – in orderto be credible – into the modeling data external and internal environment in accordance with [19, 20, 21] was not accepted, but according to the measurement data *in situ*.

4. Results

The first case being discussed is the combination of cantilever with the outer wall. A faulty arrangement of the insulating layer for the support results in excessive heat transfer to the outside. Measurement data in situ: temperature 0.7°C, humidity 90.3%, pressure 980 hPa, dew point –0.5°C. According to the infrared camera survey (Fig. 2), the temperature on the surface is – 7.3 degree Celsius. FEM model of the same place, with set earlier environmental values indicates the temperature of 7.25 degrees Celsius. The difference 0.05 Kelvin corresponds to the expected correlation between the results of both methods, it`s 0.68% less then 1% acceptance for statistical error.
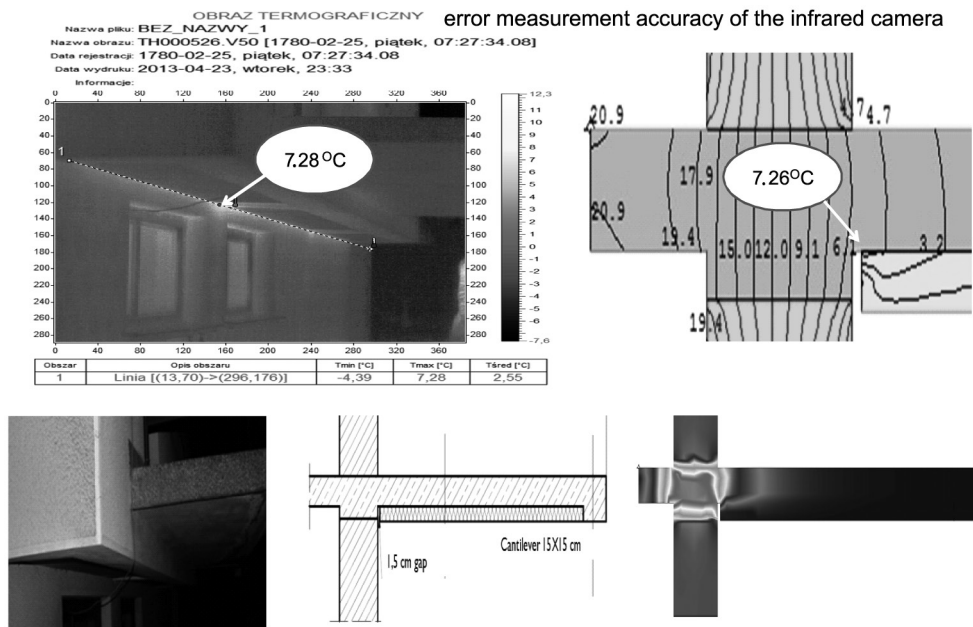
Fig. 2. Temperature distribution on the surface of constructional cantilever

In the latter case, the verification of the results of numerical simulation by comparison to the results of measurements on a real object, showed a difference of 14 Kelvin, which constitutes a significant mistake and is, of course, unacceptable. In this case, for the analysis, the gap between floor and construction wall was chosen (Fig. 3). The gap results from the lack of continuity of thermal insulation. Measurement data in situ: temperature 7.6°C, humidity 43.3%, pressure 980 hPa, dew point –3.4°C. According to the infrared camera survey, the temperature fluctuates in the slot limit – 8.16°C. After that, the FEM model observed the score of 6.8°C (Fig. 3). The difference of 14 Kelvins, does not coincide with the expected correlation between the results of both methods. The reason for this large difference is an error in specific environmental conditions during the thermal imaging inspection. The ambient temperature (accepted) was 22.5°C, the ambient temperature (measured by

a VOLTCRAFT PL-100TRH) was 7.6°C, which translates into a more accurate quantitative method in the test case.
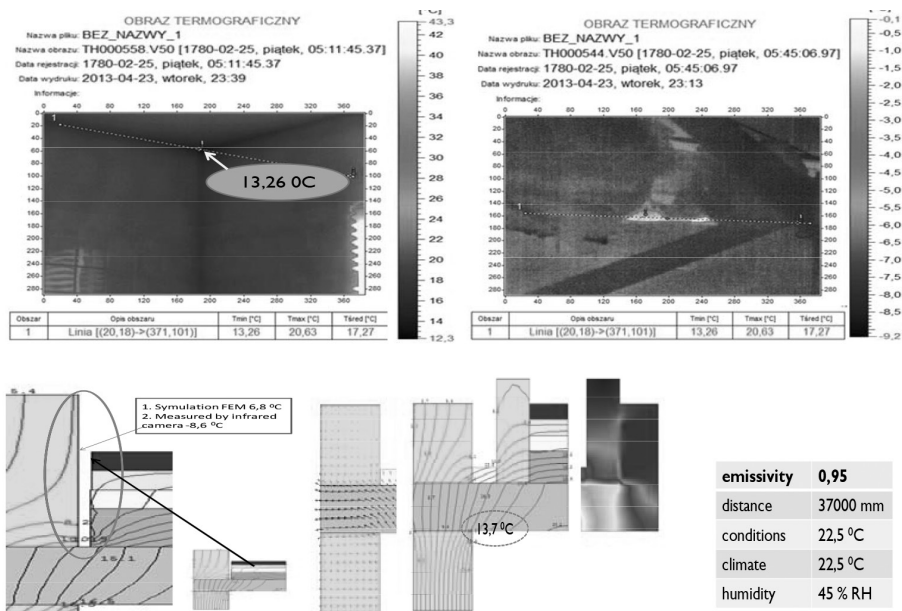
Fig. 3. Distribution of temperature, the gap between floor and construction wall

5. Conclusions

After an analysis of the extreme and most defective cases, conclusions have been drawn below. Thermal bridges were analyzed from a point of view of a cause-and-effect relationship. The two main reasons for the occurrence of weak spots, when it comes to thermal comfort is: design errors, mistakes in regulations resulting in air gaps, poor ventilation, increased heat loss, condensation-distance, fungus and mold, old-fashioned methods of the trade -increased heat loss, gaps in the insulation coating.

The correct analysis of thermal images is possible only with a report of environmental conditions such as temperature, humidity and the characteristics of the material such as a emissivity surface, the surface temperature. Sensitivity analysis should be carried out due to the performance of elements – aspects particularly crucial in view of the thermal conductivity coefficient.

It seems legitimate to accept an assumption that the analysis should be carried out in two ways, at the same time – the verification of the results – return ie., In exceptional cases, modeling can be a tool for the verification of measuring methods.

282

R e f e r e n c e s

[1] Rynowski P., Teleszewski T.J., *Modelowanie pola temperatury mostków cieplnych przy wykorzystaniu metody elementów skończonych*, Civil and Environmental Engineering. Budownictwo i Inżynieria Środowiska, 2, 2011, 85-90.

[2] Press W.H., Teukolsky S.A., VetterlIng W.T., Flannery B.P., *Numerical Recipes*, Cambridge University Press, Third ed., 2007.

[3] Heim D., Clarke J.A., *Numerical modeling and thermal simulation of PCM – gypsum composites with ESP-r*, wyd. ELSEWIER, Energy and Buildings 36, 2004, 795-805.

[4] Pogorzelski J.A., Awksientjuk J., *Katalog mostków cieplnych. Budownictwo tradycyjne*, Instytut Techniki Budowlanej, Warszawa 2003.

[5] Zbijowski K., *Świadectwo charakterystyki energetycznej budynku*, Studio Sto, 2009.

[6] Kowalczuk Z., *Charakterystyka Energetyczna Budynków* 2, Polskie Wydawnictwo Naukowo-Techniczne, 2010.

[7] Brzezińska S., *Obliczanie zapotrzebowania na ciepło*, Dashofer 2011.

[8] Dylla A., Pawłowski K., *Wady w procedurze obliczania współczynnika przenikania ciepła*, Czasopismo Techniczne 1-B/2007.

[9] Hołownia P., *Wpływ przestrzennych mostków termicznych na podstawowe parametry fizykalne jednowarstwowych zewnętrznych przegród budowlanych*, Czasopismo Techniczne 1-B/2007, 83-90.

[10] Wouters P., Schietecata J., Standaert P., Kasperkiewicz K., *Cieplno-wilgotnościowa ocena mostków cieplnych*, Instytut Techniki Budowlanej, Warszawa 2004.

[11] Rożek P., *Nowoczesne metody numeryczne w budowaniu katalogu mostków cieplnych w ścianach dwuwarstwowych*, praca dyplomowa nr 6855, UTP, Bydgoszcz 2007.

[12] Instrukcja programu komputerowego TRISCO.

[13] Pawłowski K, *Efektywność zewnętrznych przegród budowlanych i ich złączy w aspekcie cieplno-wilgotnościowym*, rozprawa doktorska, UTP, Bydgoszcz 2008.

[14] PN-EN ISO 6946:2008 Komponenty budowlane i elementy budynku. Opór cieplny i współczynnik przenikania ciepła. Metoda obliczania.

[15] PN-EN ISO 10211-1 Mostki cieplne w budynkach. Strumień cieplny i temperatura powierzchni. Ogólne metody obliczania.

[16] PN-EN ISO 10211-2 Mostki cieplne w budynkach. Obliczanie strumieni cieplnych i temperatury powierzchni. Liniowe mostki cieplne.

[17] PN-EN ISO 13788:2003 Cieplno-wilgotnościowe właściwości komponentów budowlanych i elementów budynku. Temperatura powierzchni wewnętrznej umożliwiająca uniknięcie krytycznej wilgotności powierzchni wewnętrznej kondensacji. Metody obliczania.

[18] PN-EN 12524:2003 Materiały i wyroby budowlane. Właściwości cieplno-wilgotnościowe. Tabelaryczne wartości obliczeniowe.

[19] PN-EN 12831:2006 Instalacje grzewcze w budynkach. Metoda obliczania obciążenia cieplnego.

[20] PN-82/B-02403 Ogrzewnictwo. Temperatury obliczeniowe zewnętrzne.

[21] Rozporządzenie Ministra Infrastruktury z dnia 7 kwietnia 2004 r. zmieniające rozporządzenie w sprawie warunków technicznych, jakim powinny odpowiadać budynki i ich usytuowanie (DzU z 2004 r. nr 109, poz. 1156).

MAŁGORZATA URBANEK, ALEKSANDRA PAWLAK-BURAKOWSKA[*]

COMPARISON OF EXPERIMENTAL AND NUMERICAL MODELS OF LONGASF RAILWAY FOUNDATION

WERYFIKACJA ZGODNOŚCI MODELU LABORATORYJNEGO Z MODELEM NUMERYCZNYM NAWIERZCHNI KOLEJOWEJ LONGASF

Abstract

This paper outlines the innovative concept of unconventional railway track on longitudinal sleepers and asphalt track bed. The authors presented a method for LONGASF numerical modeling. This paper describes the creation of the numerical model at the macro scale according to the behavior and interaction of analyzed laboratory sample in a micro scale.

Keywords: numerical modeling of railway track, LONGASF, unconventional railway track, model rescaling

Streszczenie

W artykule przedstawiono zarys koncepcji innowacyjnej niekonwencjonalnej nawierzchni kolejowej na podkładach wzdłużnych i podłożu asfaltowym. Autorzy zaprezentowali metodę modelowania numerycznego nawierzchni LONGASF. W niniejszej pracy opisano stworzenie numerycznego modelu w skali makro analizowanej nawierzchni uwzględniając zachowania i pracę nawierzchni w skali mik ro.

Słowa kluczowe: modelowanie numeryczne nawierzchni kolejowej, LONGASF, niekonwencjo- nalna nawierzchnia kolejowa, przeskalowanie modelu

[*] M.Sc. Eng. Małgorzata Urbanek, M.Sc. Eng. Aleksandra Pawlak-Burakowska, Faculty of Civil Engineering, Cracow University of Technology.

1. Introduction

Designing the railway track requires consideration of a large-size construction and repeatability of its components (slippers, fastening system, rail). The implementation of new methods for railway tracks for ballasted as well as slab track requires numerous experiments including numerical modeling as a basis for further design [4]. In such a case the problem of the transition between the size of laboratory sample occurs, as in laboratory conditions it must be short and the actual dimensions of the railroad truck is considerably longer. An important element in the design of a new rail track is numerical modeling.

This paper presents the implementation of finite element method for numerical analysis of the rail road. Such surveys were also performed by other researchers [5–10]. Numerical analyss and experimental tests of the compressed concrete slippers were carried out. In the next stage of experiments the slippers are stressed firstly in the laboratory and later on an experimental track. The set of aforementioned tests are called multilayer approach.

In order to develop a new method for design of the railway substructure using a multilayer approach, a set of Finite Element Models have been developed. To evaluate the accordance of the models with the real construction [11], a set of experiments were performed using a laboratory LONGASF construction sample. Bearing capacity of the construction was assessed and compared with the values obtained from numerical simulation. This method allows the transition from micro to macro scale. It also enables the designers to carry out additional simulations that require considerable distance along the track such as braking test.

Unconventional railway track called LONGASF, described in this paper, is designed on the foundation typical for roads. The mechanically stabilized aggregate layer is located on the ballast with sufficient capacity. At the top of it a layer of asphalt concrete without wear layer is placed. LONGASF construction consists of longitudinal slippers. The width of slippers is selected so that the load transferred to the surface of the asphalt is no higher than the heaviest load unit cars. Due to the fact that it is not possible to obtain higher accuracy of positioning the asphalt than ± 1 cm, the use of balancing layer was provided under the longitudinal slippers. Longitudinal slippers are connected transversely with steel fasteners and longitudinal elastic layers (Fig. 1).
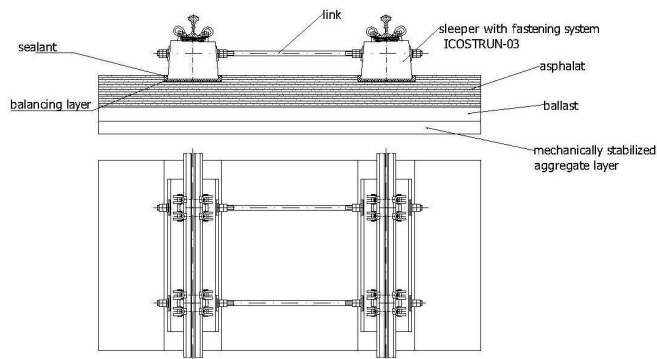
Fig. 1. General diagram of LONGASF railroad track [1]

2. Laboratory tests of the LONGASF sample

Laboratory tests (Fig. 2, 3) were carried out on the small size sample in relation to the dimensions of the actual railway structure. The dimensions of the asphalt surface were limited to the length of 1.5 meters and the width of 3.0 meters [1]. During the tests the vertical displacement of the rail has been measured.

Studies of the LONGASF railroad track with the fastening system ICOSTRUN-03 were carried out according to the standard PN- EN 13481-5:2004 Railway applications – Track – Performance requirements for fastening systems – Part 5 [2].

Fig. 2. LONGASF sample with ICOSTRUN 03 during stiffness tests [1]

Fig. 3. Sample with forcing element and measuring system during vertical stiffness test
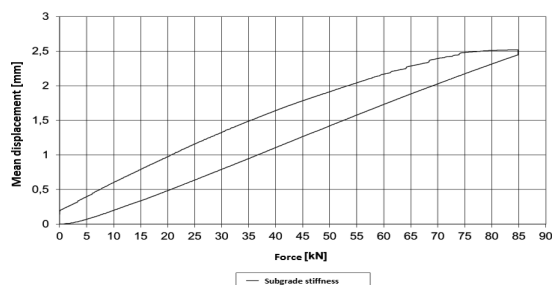
Fig. 4. Rail vertical displacement graph

The tests have shown that the maximum vertical displacement of the rail is 2.5 mm (Fig. 4). The results of preliminary laboratory tests, in which a ride on the curves was simulated, made it possible to carry out further computer simulations. This test shown that the maximum horizontal displacement of rail was about 4.6 mm. Such high value of displacement was caused by the lack of influence of neighboring fastenings.

3. Development and calculations of numerical sample

The three-dimensional model of the rail track LONGASF was created using Autodesk Simulation Multiphysics based on the laboratory model. It consists of a 3D placeholder (brick) and actuator, which were used in order to fix the fastening system as shown in Fig. 5.
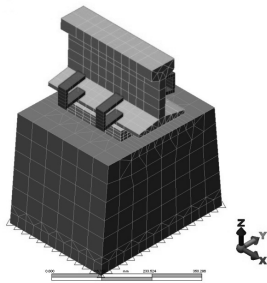
Fig. 5. Numerical model of fastening system ICOSTRUN 03

Subgrade (under the asphalt layer) was modeled by a spring element. During the computation a very weak subgrade, with C coefficient of 75 MN/m^3 was used. Similarly as in the laboratory, backfill was omitted in the numerical model (Fig. 6).
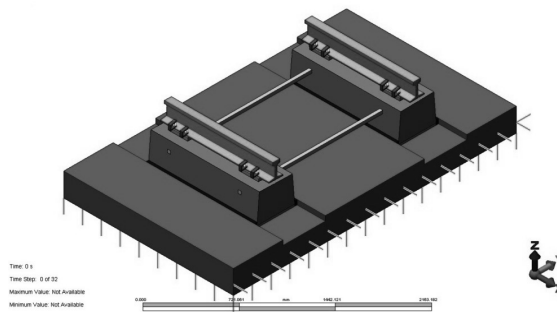
Fig. 6. Numerical model created in Autodesk Simulation Multiphysics

Force was applied at the contact point of the rail wheels, corresponding to the selected node.

For the purpose of model validation, the comparison of laboratory results and the numerical model was made. The obtained results of vertical displacement were similar to those laboratory ones and were equal to 2.5 mm.

In order to verify the influence on the sample of adjacent fastenings a 3D model was extended (Fig. 7). With such a method the behavior of the railway, the repetition of elements, and significant disparity dimensions were achieved, for example the width to the length ratio of the object.
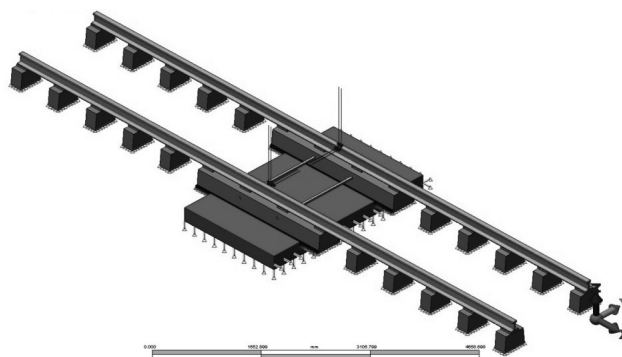
Fig. 7. Extended numerical model created in Autodesk Simulation Multiphysics
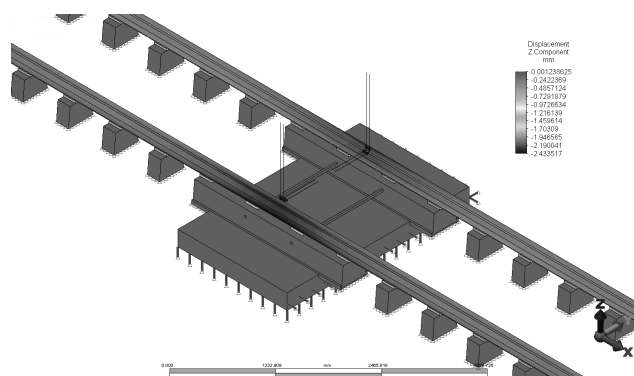
Fig. 8. Vertical displacements of LONGASF railway track

As a result of the extended model simulation, displacement of the rail was computed. The maximum vertical displacement was equal to 2.4 mm (Fig. 8). This result did not differ significantly from laboratory tests.

The simulation showed the maximum horizontal displacements as 2.4 mm (Fig. 9). This result was significantly different from the laboratory tests results, indicating the influence of the adjacent fastening. Maximizing dimensional model, its extension affects the results and illustrates the work of analyzed railway track.
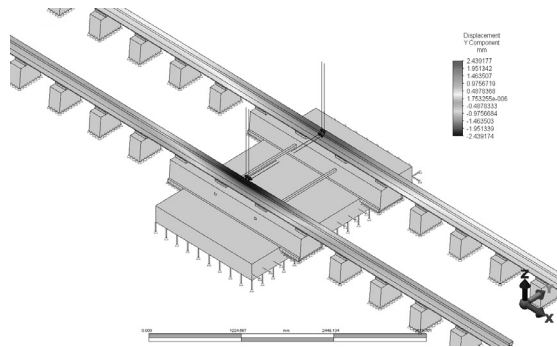
Fig. 9. Horizontal displacements of LONGASF railway track

4. Conclusions

This paper presents the comparison between micro and macro scale of the rail displacement in the LONGASF type of railway track. The displacement results were simulated in Autodesk Simulation Multiphysics and have shown that the vertical and horizontal displacement of the analyzed type of track didn't exceed the value of 2.5 mm. The results of the computer simulation were consistent with the results obtained from laboratory model. Accuracy of the results indicated that the appropriate parameters were chosen for numerical modeling of the sample. Therefore, such 3D modeling should be used to design such structures like railway tracks. The objective of these experiments was to propose a method of numerical modeling which allows the designer to obtain a variability of the mechanical and geometrical prosperities of a railway track. The recommendations are to adopt the presented methodology in order to decrease long computations.

References

[1] Czyczuła W. et al., *Report from Railway track with a higher standard and reduced impact on the environment, project number: NR10-0004-10/2010*, Kraków 2013.
[2] PN-EN 13481-5:2004 Railway applications – Track – Performance requirements for fastening systems – Part 5.
[3] BN-64/8931-02 Standard, Roads, modulus determination of susceptible subgrade to the load plate.
[4] Kukulski J., *Wybrane aspekty modelowania nawierzchni kolejowej, jej części składowych oraz podtorza, Problemy kolejnictwa*, Zeszyt 148, Instytut Kolejnictwa, 2009.

[5] Sakdirat K., Remennikov A.M., *Dynamic flexural influence on a railway concrete sleeper in track system due to a single wheel impact*, Engineering Failure Analysis, 2008.

[6] Sakdirat K., Remennikov A.M., *Field trials for dynamic characteristics of railway track and its components using impact excitation technique*, NDT&E International, 40, 2007, 510-519.

[7] Sakdirat K., Remennikov A.M., *Impact Capacity of Railway Prestressed Concrete Sleepers*, Engineering Failure Analysis, 2008.

[8] Sakdirat K., Remennikov A.M., *Nonlinear Finite Element Modeling Of Railway Prestressed Concrete Sleeper*, The tenth East Asia – Pacific c Conference on Structural Engineering and Construction, Bangkok, Thailand 2005.

[9] Shokrieh M.M., Meysam R., *On the reinforcement of concrete sleepers by composite materials*, Composite Structures, 76, 2006, 326-337.

[10] INNOTRACK Report Project No. TPI5-CT-2006-031415, Modeling of the track subgrade.

ANDRZEJ WOLAK, PIOTR PRZECHERSKI[*]

GENERAL-PURPOSE UNMANNED RESEARCH VESSEL USED FOR MEASUREMENT OF WATER DEPTHS IN RESERVOIRS AND THEIR DEPOSITS LAYOUT

BEZZAŁOGOWA UNIWERSALNA ZDALNIE STEROWANA PLATFORMA POMIAROWA SŁUŻĄCA DO BADAŃ NA ZBIORNIKACH WODNYCH

Abstract

Large artificial water reservoirs are one of the most valuable assets in flood protection. However, the overall volume of a reservoir can decrease over time. This happens mainly because of sediment accumulation, and that alluvia is "eating-up" an otherwise useful volume of water. It is therefore important to know the current volume of sediments accumulated in the reservoir. This way one is able to calculate the useful volume of the reservoir storage capacity, secondly, for assessment of future reservoir operation. The process of obtaining relevant data for this is normally partially automated but nevertheless, it is arduous, extremely time-consuming, and may be dangerous. To overcome those problems we have developed an unmanned vessel, which is able to perform the work much faster and easier. The vessel is a fully unmanned, integrated, nonetheless it is still under development (working prototype 1E), but it can be still easily used in its current state, albeit with some minor limitations.

Keywords: water reservoirs, sediment accumulation measurements, unmanned surface vehicles, echo sounder, anti-roll system for boats

Streszczenie

Duże sztuczne zbiorniki wodne są jednym z najważniejszych ogniw w systemie ochrony przeciwpowodziowej. Całkowita objętość zbiornika nie jest wartością stałą i zmniejsza się w miarę jego eksploatacji. Jako główny czynnik można tu wyróżnić gromadzenie się osadów nanoszonych przez rzekę. Proces pozyskiwania danych do oceny załadowania zbiornika jest częściowo zautomatyzowany, mimo wszystko jest to zadanie trudne i czasochłonne. Opracowane przez autorów pływające urządzenie pomiarowe sprawia, że pomiary wykonuje się o wiele łatwiej i szybciej. Jest to urządzenie bezzałogowe, zdalnie sterowane i w pełni zautomatyzowane. Prototyp będący w fazie udoskonalania może być z niewielkimi ograniczeniami wykorzystywany do wykonywania pomiarów na zbiornikach wodnych.

Słowa kluczowe: zbiorniki retencyjne, pomiary załadowania, bezzałogowe urządzenie pomiarowe, echosonda, system eliminacji wpływu falowania

[*] Ph.D. Eng. Andrzej Wolak, M.Sc. Eng. Piotr Przecherski, Ph.D. student, Institute of Water Engineering and Water Management, Faculty of Environmental Engineering, Cracow University of Technology.

1. Introduction

Large artificial water reservoirs are one of the most valuable assets in flood protection. Their value cannot be overestimated. They offer the cheapest and most effective tool against floods – water retention. They can significantly lower flood flow volumes in rivers, thus giving anti-flood protection to areas downstream. The other tools – like dikes, small "dry" reservoirs and polders are important as well, but nothing is equivalent to vast water retention reservoirs – concerning overall impact and the relative cost [see 1]. However, the overall volume of a reservoir can decrease in time. This happens mainly because of sediment accumulation, and that alluvia is "eating-up" useful volume of stored water. That is a rather slow process, which may speed up considerably during flood events. The yellow curve in the centre is a swollen Vistula River entering the reservoir, the water is firstly contained within the old flood protection dikes (see Photo 1 below).

It is very important to know the current volume of sediments accumulated in the reservoir, firstly to be able to calculate useful volume of the reservoir storage capacity (which is needed to plan flood protection and other purposes) and secondly for assessment of future reservoir operation. Sediment input into a large water retention reservoir (like Goczałkowice reservoir pictured above, with approx. 118 mln m³ of nominal capacity [see 2]) can go into the several thousands of cubic meters annually.

Fig. 1. Aerial photo of flood water entering Goczałkowice
reservoir in May 2010 (source: ZiZoZap Project)

Another, though related issue is the changing of riverbeds due to sediment accumulation and erosion. That can lead to dramatic changes in river cross-section geometry, thus alternating its hydraulics and making flood events much more likely and severe. Knowledge of the actual geometry of the river beds, especially for river segments inside towns and cities, is also very important for flood protection and planning [see 3].

2. Present measurement practice

Typically the measurements of the layout of bed of water reservoir are performed using the devive called the "echosounder" mounted on a boat. (like "UŚKA" pictured below). The device emits sound into the water and measures the time between emission and echo reception, thus allowing for distance calculation. It is attached to a boat and together with a GPS receiver (only for plane, or for XY, location) is used to record actual water depth at a given position. In order to complete a meaningful research, however, a lot of measurement points are required (hundreds of thousands or even more for medium-sized water reservoirs). The process is usually partially automated but nevertheless, it is arduous, extremely time-consuming and may be dangerous.

Fig. 2. Research vessel "UŚKA" used for measurements in Goczałkowice reservoir (source: ZiZoZap Project)

3. Our Invention

To overcome the above mentioned problems we have developed an unmanned surface water vessel (called UPP-1E), which is capable of doing that work much easier and faster. The vessel is a fully integrated device, consisting of following subsystems (see schematics in Fig. 1):
- Measuring subsystem: high-class echosounder consisting of the central unit (signal reception and formatting) and dual frequency heads (transducers). This device is a NaviSound 215 of Teledyne-Reson.
- GPS receiver – Garmin 18x unit. The signal from this unit is directly fed into the central unit of the echosounder for combining with the depth data and then transmitted further – into the central computer.
- Steering/propulsion and control system. Consisting of the central computer (with provisions for expanding into redundant double system in the future), and the switchboards (including associated firmware), electric motor and propeller. The power supply for all the systems is provided by a set of high energy density batteries (5 items, 12VDC) allowing for at least 6 hours of continuous operation. Communication with the shore station comes

through a GSM-based modem, allowing for almost clear and stable signal coverage throughout most of Europe.

• Auxiliary systems. As for now it is a surveillance/hazard avoidance camera, mounted on a small mast on the fore part of the boat (see Fig. 4). Adding a forward looking, short distance hazard avoidance radar is planned in the near future (funds allowing).

The use of two measurements frequencies allows us to perform two tasks simultaneously: the first frequency (200 kHz) is used for first-contact measurement, which is typically understood as "real lake bed" depth. This sound frequency reflects off first obstacles near the lake bed, sand, stones or vegetation. The other frequency (50 Hz) is a penetrating one, and can be used for direct deposit layer width determination. This must be carefully calibrated before any meaningful results can be presented.

A simple schematics of the system is presented on Fig. 3, below:
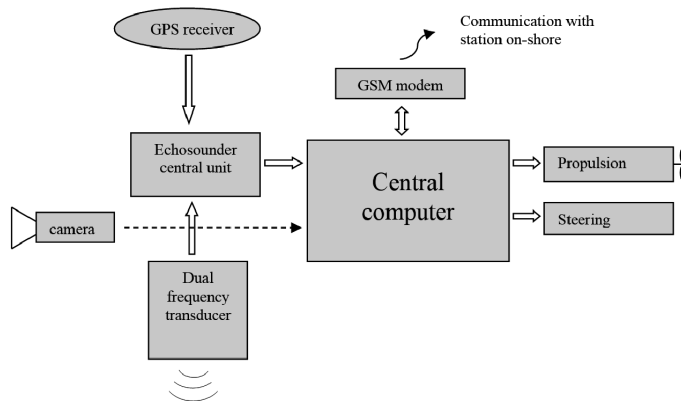
Fig. 3. Base schematics of the UPP-1E vessel. The UPP-1E vessel is pictured below

Fig. 4. General view of UPP-1E vessel (source Delta Prototypes)

Fig. 5. Steering mechanism

Fig. 6. Propeller, diameter 9 cm

Fig. 7. Control software screen shot

Fig. 8. Batteries compartment

In the Fig. 3 the whole vessel can be seen. It is 200 cm long (not counting the rudder) and 80 cm wide (including impact dampeners – grey tube around the hull). Its projected draft shall be no more then 10 cm. The echo sounder compartment is located between the camera and the tall mast. (First white cover). The other compartment is for batteries and propulsion (see Fig .7).

The Fig. 4 shows the details of the steering mechanism. A removable rudder will be utilized to allow for rapid replacement in case of expected rapid wear-and-tear.

In the next, (Photo 5), the propeller is shown just under the main hull. It is going to be the most exposed part of the entire vehicle. We expect it to be replaced fairly often (more then 6 times in a season). Currently a 9 cm diameter is being used. After the initial trials we may change it for a larger one.

In the last picture (Fig. 7) the batteries compartment can be seen. As for now only five units are used (for testing purposes). For a final use there is space provided for 15 more. Our aim is to be able to perform at least 8 hours of continuous operation. The maximum speed of the vessel is to be about 2 m per second, but for nominal measurement conditions it shall be no more then approx. 1 m per second (as the echo sounder gives up to 5 pings a second, it should be more then enough for most applications).

The UPP-1E vessel is meant to be able to replace the large boats (like UŚKA above) as bathymetric (depth measurements) platforms. Our vessel shall be much cheaper to procure, easier to maintain and able to perform much more research, even in adverse conditions. There shall be no crew on water, much longer measurement passes are possible, the draft will be minimal.

There is, however, a problem with boat stability. Larger vessels as a rule offer a much more stable platform against waves then smaller ones. It is a difficult problem for echo sounder measurements. If the sound beam emitted from the transducer is skewed (as happens when a wave rolls a boat) the resulting water depth value is incorrect – much higher (30% or even more then the "true" value).

The UŚKA vessel is 8 meters long, 2.5 meters wide with draft of 40 cm. It is possible to record bathymetric measurements (using a stabilized transducer firmly attached to its side) for up to approx. 20 cm of wave heights. Achieving the same with a much smaller boat is a challenge. To overcome that we are proposing a three-part solution:

1) Software. Using a white noise statistical function some impact of high wave can be eliminated during post processing of the obtained data.
2) Passive wave dampening. This will be done by using two additional hulls, attached to the sides of the main one, forming a trimaran configuration. The auxiliary hulls will be much smaller, but nevertheless shall offer some stabilization.
3) Active wave dampening. A device (under development) to actively dampen the rolling of the boat.

The anti-roll system – active and passive, integrated with steering and propulsion system is currently under development and in preparation for obtaining a Patent protection.

The entire system (even in its current configuration) is meant to be as rugged as possible. We are currently testing it to see what can be improved for the product to be able to work in the most adverse conditions. Trying to assess the progress of this new technology National Aeronautics and Space Administration (NASA) Technology Readiness Level can be utilized. Using this scale UPP-1E vessel in its current shape is on the TRL 6 – "Prototype demonstration in relevant environment" (see [4]).

The vessel is still under development (working prototype 1E), but it can easily be used in its current state, albeit with some limitations (mostly concerning surface wave impact dampening, man-machine interface and firmware issues). After it is completed it can be a game-changer for the industry.

References

[1] Bojarski A., Mazoń S., Wolak A., *Czasza zbiornika zaporowego Goczałkowice – jej przygotowanie i zmiany w dotychczasowej eksploatacji*, ZiZoZap 2010.

[2] Pasternak K., *Observations on the transformation of banks in the Goczałkowice Reservoir*, Acta Hydrobiol., nr 6, 1964.

[3] Czaja S., Degórska V., Leśniok M., *Naturalne i antropogeniczne zmiany biegu koryta Wisły od zbiornika w Goczałkowicach do ujścia Przemszy*, Geographia, Studia et disertationes, t. 17, Prace Naukowe UŚ, Katowice 1993.

[4] Mankins J.C., *Technology readiness levels*, A White PaperAdvanced Concepts Office, NASA, April 6, 1995.

ANNA ZASTAWNA-RUMIN[*]

THE INFLUENCE OF PHASE CHANGE MATERIALS ON ENERGY BALANCE AND THE RISK OF OVERHEATING

WPŁYW MATERIAŁÓW FAZOWO ZMIENNYCH NA BILANS ENERGETYCZNY I RYZYKO PRZEGRZEWANIA

Abstract

The paper presents the results of a computer simulation of a building under the assumption of the presence of a phase change material in wall elements. The influence on the cooling energy requirements and, also, the risk of overheating of the low-energy building (without HVAC systems) have been analyzed. The obtained results were compared with the ones of a low-energy building without a phase change material in walls. The comparison calculations were performed for a model of a service building located in Silesia, which is built according to an energy-efficient standard. It has a light-frame construction with light covering (external panels, heat-insulation, interior plasterboard). In the study, the presence of a 1 cm thick PCM board placed under the inner surface of plasterboard is assumed. Tests were conducted for organic materials that undergo phase transition in different temperatures, such as: 23°C, 25°C and 27°C. Based on the results of operative temperature measurements, it is possible to determine the influence of PCM on the risk of building's overheating.

Keywords: heat capacity, phase change material

Streszczenie

W artykule przedstawiono wyniki komputerowych symulacji budynku, zakładając wbudowanie w jego przegrody materiału fazowo-zmiennego. Analizowano wpływ zastosowania różnych materiałów fazowo--zmiennych na zapotrzebowanie energii do chłodzenia budynku i ryzyko przegrzewania wnętrza obiektu (nie wyposażonego w instalację chłodzącą). Wyniki porównywano do stanu wyjściowego (bez PCM). Przedmiotem porównawczych obliczeń jest model istniejącego budynku o charakterze usługowym, zlokalizowany w województwie śląskim. Budynek ma konstrukcję szkieletową z lekkim poszyciem (blacha elewacyjna, termoizolacja, blacha konstrukcyjna). W kolejnych wariantach pod powierzchnią blachy od strony wewnętrznej założono wbudowanie PCM w postaci mat o grubości 1 cm. Materiałem ulegającym przemianie fazowej jest materiał organiczny. Analizie poddano warianty z zastosowaniem PCM o różnej temperaturze przemiany fazowej, tj. 23°C, 25°C, 27°C. Na podstawie wyników obliczeń temperatury operatywnej można określić wpływ MFZ na ryzyko przegrzewania budynku.

Słowa kluczowe: pojemność cieplna, materiał fazowo-zmienny

[*] M.Sc. Eng. Anna Zastawna-Rumin, Institute of Building Materials and Structures, Faculty of Civil Engineering, Cracow University of Technology.

1. Introduction

The aim of introducing PCM into building elements is to increase the heat capacity of the building envelope. Too low heat capacity results in the deficiency of heat stability in a popular light-frame construction with light filling walls that causes seasonal overheating of the building and large temperature oscillations of internal air due to temperature variations of outdoor air.

The idea of using phase change materials to accumulate heat is based on energy saving process such as latent heat of organic compounds e.g. paraffins, fatty acids or inorganic salt hydrates. Accumulation or emission of large amounts of heat occurs during phase transition and is accompanied by a small temperature change of a specific PCM.

Nowadays, there are many building energy simulation tools for studies analyzing benefits from PCMs [11]. The most popular are EnergyPlus [13], ESP-r [14], and TRNSYS [12].

ESP-r is an advanced building energy simulation tool which allows for a detailed thermal description of buildings. The software discretizes the problem domain in a control volume scheme and solves the corresponding conservation equations for mass, momentum, energy, etc. It uses the effective heat capacity method for PCM solutions.

The TRNSYS software is used for building dynamic simulation based on transfer functions technique. It contains many subroutines. The storage and release effects of PCMs can be simulated using the active layer tool Type 56 or by the implementation of a new module.

Energy Plus PCM algorithm uses a one-dimensional conduction finite difference (CondFD) solution algorithm [9, 10]. The CondFD algorithm in Energy Plus uses an implicit finite difference scheme, where the user can select Crank-Nicholson or fully implicit. In the CondFD algorithm, all elements are divided or discretized automatically, which depends on a space discretization constant, the thermal diffusivity of the material, and the time step [9, 10, 11]. For the PCM algorithm, the CondFD method is coupled with an enthalpy temperature function that the user inputs to account for enthalpy changes during phase change. The enthalpy temperature function is used to develop an equivalent specific heat at each time step. The resulting model is a modified version of the enthalpy method. Here, the values of the specific enthalpy h for the PCM can be provided by the user as a function of the temperature T [9].

2. The aim of the article

The aim is to determine the influence of phase change materials on the internal temperature of examined building and on the energy demand for cooling. Both internal air temperature and internal surface temperature of the wall were tested. The study was performed with particular consideration of the thermal parameters influencing thermal comfort and the determination of building overheating risk.

The analysis refers only to a change in thermal parameters inside the building. The impact of other parameters (for example of humidity), which are important factors in the aspect of thermal comfort, is not taken into account. The analysis will show whether the use of PCM leads to significant changes and whether it is appropriate to carry out a more precise analysis using relevant indicators such as the rate of PPD (Predicted Percentage Dissatisfied). PPD will be treated as a quantitative parameter for the assessment of thermal comfort in the room.

3. The description of the calculation model

The calculations were performed for a model of a service building located in Katowice. It has a light-frame construction with light covering. The floor is constructed with a 10 cm layer of concrete which is coveredd with ceramic tiles. The building dimensions are 10 m ×10 m × 3 m (Fig. 1). The building meets the Polish regulations for energy-efficient buildings. The roof has a lightweight design packed with 30 cm layer of insulation and covered with a sheet. Inside the building, , there is an open space with no internal partitions. The model does not take into account the equipment and furniture in the office. All other material data are presented in Table 1.

For the first (base) variant, the building wall is constructed with a 30cm thermal insulation (the outside surface was finished with an OSB board, while the inside surface with the a gypsum board). In the next variants, the PCM was built in as a 1cm layer, located on the internal side of the wall (Fig. 2). For the analyses, the application of an organic Phase Change Material was assumed. In simulations available types of PCM were used. They differed regarding the temperature of phase change which was equal to 23°C, 25°C and 27°C respectively (the variants were called PCM 23, PCM 25, PCM 27, accordingly). The dependence of the material enthalpy on the temperature, for the analyzed PCMs was assumed based on the literature [2]. Adopted to calculation, the dependence of the enthalpy on the temperature, for the PCM, is illustrated in Fig. 3.

The glazing covers 40% of the south façade area. The window frames have very good thermal insulation ($U = 0.8$ W/m^{2}K) and are in accordance with the regulations for the total energy transmission factor $g_c = 0.5$. In addition, the windows have shading. It should be noted that, in the analyzed building, all passive solutions to reduce the energy needed for heating and cooling were used.

It is assumed that 5 persons are simultaneously present in the building during working hours and the additional interior lighting is also being used. To consider these, during working hours (i.e. 7 am to 6 pm) heat gains from people (80 W per person) and lighting (3 W/m^2) were added. In the simulations, the weather data for the period between 1st June and 31st August were used. The ventilation rate was assumed as 0.5 air change per hour. All the simulations were performed with the Energy Plus ver. 7.1 software which allows for the modeling of the phase transition of some materials and for considering variable external conditions.
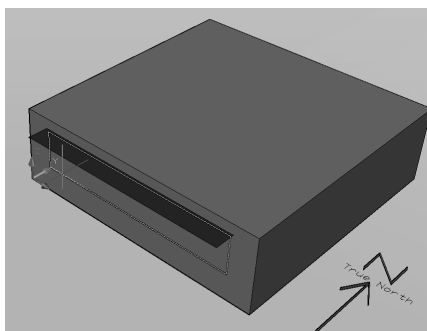
Fig. 1. The schematics of the analyzed building
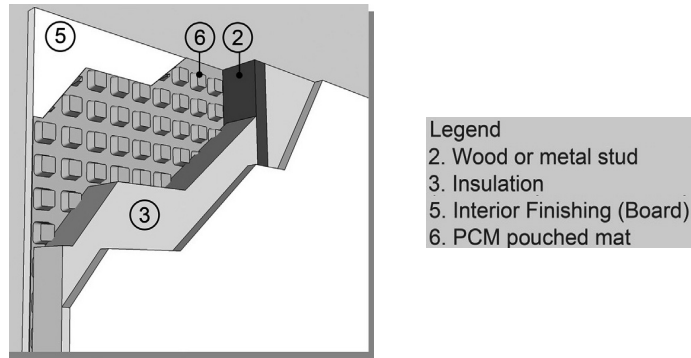
Fig. 2. The location of the PCM layer in the walls of buildings [3]

T a b l e 1

Material data

Material	Thickness, [m]	λ, [W/mK]	Specific heat, [J/kgK]	Thermal absorptance	Solar absorptance
external metal sheet	0.001	58	500	0.9	0.4
termal-insulation	0.3	0.04	1381	0.9	0.5
gypsum board	0.013	0.16	1150	0.9	0.42
PCM	0.01	0.2	c_w (T)	0.9	0.7
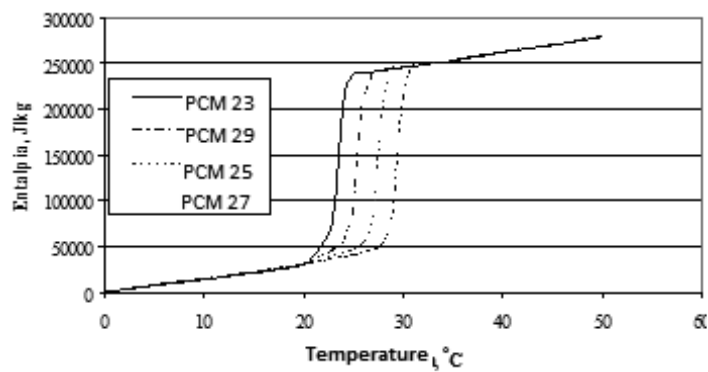
Fig. 3. The relationship between enthalpy and temperature for the analyzed PCM [2]

4. Results

4.1. The influence of the PCM on the overheating risk

Operative temperatures inside the building, for the walls without PCM and with different kinds of PCMs, have been analyzed. Both the interior air temperature and the temperature of internal surfaces have influence on the operative temperature (wind chill).
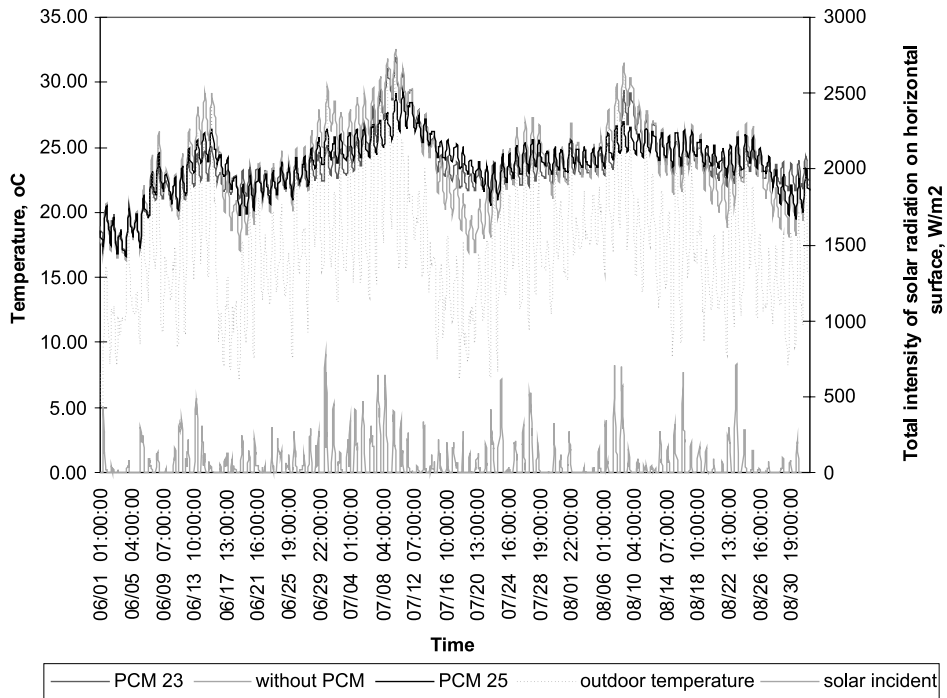
Fig. 4. The operative temperature inside the building in the analyzed period, the cases: without PCM, with 23 PCM and with 25 PCM

Fig. 4 shows the graph of operative temperature inside the building during the analyzed period for different material variants (without PCM and with PCMs of different point of phase change: 23°C and 25°C).

Regardless of the PCM type, it is always visible that the temperature has smaller oscillations in comparison to the base case (without PCM). This demonstrates the much higher thermal stability of the building rooms and the reduced impact of outdoor temperature. The maximum wind chill that occurs for the base variant is at 32.6°C, 32.2°C for PCM 23, and 29.21°C for PCM 25. Thus, the most significant reduction of the maximum temperature can be achieved by using PCM 25.

The largest reduction of the period duration with exceeded temperature of 24°C can be achieved by using PCM 23, but the shortest period with temperature exceeding 27°C can be achieved by using PCM 25 (Fig. 5).
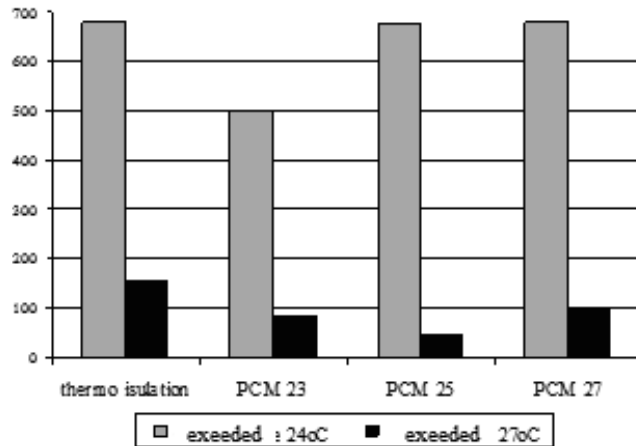
Fig. 5. The amount of hours with exceeded temperature of 24°C and 27°C

4.2. The influence on the cooling energy requirements

It is assumed that, in the building, there are heating and cooling systems. The cooling system works according to the following scheme: from 7:00 to 18:00 it works above 24°C, outside this time period: above 27°C. The ventilation rate was assumed as 0.5 air change per hour. The analysis showed that the best results are achieved for PCM 23. For the base variant, the energy demand for cooling is 1.98 GJ. After the application of the PCM, it decreases to 1.62 GJ.

5. Conclusions

The analyzed building uses all possible passive energy sources in order to minimize its energy demand. The application of PCM inside the building walls causes a risk of interior overheating. The simulation results indicate that the most efficient solution is the application of PCM which has the phase change point at 23°C. This is probably due to the highest frequency of the temperature passing in the phase change point for the material. The application of PCM 23 can potentially reduce 18% of the energy demand for cooling in the analyzed period from 1st June till 30th August. The application of PCM 23 causes the most significant reduction in the total time with the temperature over 24°C. The solutions with PCM 25 and PCM 27 perform effectively only in the case of higher temperature. To determine which option is more comfortable for the people inside a building, it would be required to analyze the thermal comfort, considering the length of the peak temperatures period for each day more precisely. It also seems necessary to carry out an analysis, which takes into account the other parameters of thermal comfort (eg. effect of humidity). The analysis should refer to relevant indicators such as the rate of PPD (Predicted Percentage Dissatisfied). This will be the subject of future research.

R e f e r e n c e s

[1] Wnuk R., *Magazynowanie ciepła, pozyskanego z energii promieniowania słoneczne-go, z wykorzystaniem materiałów fazowo-zmiennych, w budownictwie*, II Konferencja SOLINA 2008, Innowacyjne Rozwiązania. Materiały i Technologie dla Budownictwa, Solina 2008, 521-528.

[2] Muruganantham K., *Application of Phase Change Material in Buildings: Field Data vs. EnergyPlus Simulation*, Arizona State University, 2010.

[3] Rodriguez-Ubinas E., Arranz Arranz B., Vega Sánchez S., González F.J., *Influence of the use of PCM drywall and the fenestration in building retrofitting*, Energy and Buildings 65, 2013, 464-476.

[4] Jaworski M., *Zastosowanie materiałów zmiennofazowych PCM w budownictwie*, Materiały budowlane, 2, 2012, 30-33.

[5] Ostermana E., Tyagib V.V., Butala V., Rahim N.A., Stritih U., *Review of PCM based cooling technologies for buildings*, Energy and Buildings 49, 2012, 37-49.

[6] Rostamizadeha M., Khanlarkhani M., Sadrameli S.M., *Simulation of energy storage system with phase change material (PCM)*, Energy and Buildings 49, 2012, 419-422.

[7] Jaworski M., *Materiały zmiennofazowe (PCM) w budownictwie – właściwości i rodza-je*, Izolacja 02/2009.

[8] Baetensa R., Jelle B.P., Gustavsend A., *Phase change materials for building applica-tions: A state-of-the-art review*, Energy and Buildings 42, 2010, 1361-1368.

[9] Tabares-Velasco P.C., Christensen C., Bianchi M., *Verification and validation of EnergyPlus phase change material model for opaque wall assemblies*, Building and Environment 54, 2012, 186-196.

[10] Evola G., Marletta L., Sicurella F., *A methodology for investigating the effectiveness of PCM wallboards for summer thermal comfort in buildings*, Building and Environment 59, 2013, 517-527.

[11] Soaresa N., Costab J.J., Gasparb A.R., Santosc P., *Review of passive PCM latent heat thermal energy storage systems towards buildings' energy efficiency*, Energy and Buildings 59, 2013, 82-103.

[12] Ibáñez M., An *approach to the simulation of PCMs in building applications using TRN-SYS.*, Appl Therm Eng, 25 (11–12), 1, 2005, 796-807.

[13] Pedersen, CO. *Advanced zone simulation in EnergyPlus: incorporation of variable properties and phase change material (PCM) capability*, Building simulation, Beijing, China 2007.

[14] Heim D, Clarke JA., *Numerical modelling and thermal simulation of PCM gypsum composites with ESP-r.*, Energy Build, 36 (8), 2004, 795-805.

XINGXING ZHANG[*]

SOCIAL-ECONOMIC BENEFITS OF A NOVEL PHOTOVOLTAIC/LOOP-HEAT-PIPE SYSTEM AND ITS ADAPTABILITY IN BUILDING ENERGY PLANT

SPOŁECZNO-EKONOMICZNE KORZYŚCI PŁYNĄCE Z NOWEGO FOTOWOLTAICZNEGO (LOOP-HEAT-PIPE) SYSTEMU ORAZ JEGO ADAPTACJI W BUDYNKU

Abstract

This article describes a novel photovoltaic/thermal (PV/T) water heating system. Through incorporating a loop-heat-pipe (LHP) and a heat pump, the system can essentially maximise the electrical return of PV panel, and simultaneously produce a reasonable amount of heat. This system can therefore harvest larger amount of solar energy and enable enhanced system performance. It is expected that such dedicated technology could become the next generation of solar driven heating system and enable a significant reduction of building's carbon footprint.

Keywords: Social-economic, PV/T, Loop heat pipe, energy envelope

Streszczenie

Artykuł ten opisuje nowe fotowoltaiczno-termiczne (PV/T) systemy ogrzewania wody. Poprzez włączenie do pętli ciepłowodów (LHP) oraz pompy ciepła system może w istocie zmaksymalizować zwrot elektryczny panelu fotowoltaicznego, a jednocześnie produkować wystarczającą ilość ciepła. System ten może więc zebrać większą ilość energii słonecznej i zwiększyć wydajność systemu. Oczekuje się, że takie dedykowane technologie mogą stać się następną generacją instalacji solarnej j i umożliwić znaczną redukcję emisji dwutlenku węgla.

Słowa kluczowe: społeczno-ekonomiczne, PV/T, pętle ciepłowodów

[*] Ph.D. Xingxing Zhang, School of Engineering, Faculty of Science, University of Hull, UK.

Denotations

A_c –   collecting area [m^2]
COP –   coefficient of performance
I –   solar radiation [W/m^2]
Q –   energy rate [W]
W_c –   work of compressor [W]
η   –   energy efficiency [%]
ζ   –   exergy efficiency [%]

1. Introduction

The PV/Thermal (PV/T) technology enables the dual solar collecting functions in one module for output of both electricity and heat. Such synergetic integration of PV and thermal collector not only results in improved PV efficiency [1], but also generates more energy per unit area whilst compared with standard-alone PV panel or solar collector. Additional characteristics of the PV/T technology lie in potential savings in material use, reduction in installation cost and homogeneous facade appearance [1]. It is now becoming a significant solution to yield more electricity and offset heating load freely in contemporary energy environment.

In recent years, the heat-pipe based PV/T technology was proposed due to its specific characteristics, such as large heat-transfer capacity, availability of anti-freezing media, hermetically sealed loop and homogeneous capillary force [2]. Loop heat pipe (LHP), as a special type of heat pipe, has large capacity of remote and passive heat transfer by circulating the working fluid in a closed loop. LHP has the separate configuration of vapour and liquid transportation lines without the entrainment between the two-phase flows, which leads to a large heat flux transported in long distance. Such feature enables the wide applications of LHP in thermal controls of satellites, spacecrafts, electronics, lighting and cooling/heating systems [3]. However, conventional gravitational LHP faces common 'dry-out' phenomena on the top wick surface due to the limited capillary force for liquid elevation [4]. A novel LHP structure with the top-positioned three-way feeder was therefore initiated to overcome the above difficulty. In addition, an aluminium-alloy (Al-alloy) sheet will be utilised as the PV baseboard to accelerate heat dissipation at the back of PV cells [5]. When such LHP integrates with the PV layer, a new PV/LHP module will be developed. The heat pump will be involved to remain a steady-and-low system working temperature. In line with this initiative, a social-economic study of such a PV/LHP heat-pump system will be conducted. The research result will assist the accelerated deployment of the PV/T technologies, resolve the fuel poverty and reduce carbon emission in future energy supply.

2. System Description

Fig. 1 illustrates the PV/LHP heat pump water heating system. The system comprises a modular PV/LHP collector, an electricity control/storage unit, the vapour/liquid transportation lines, a flat-plate heat exchanger, a hot water tank, a compressor, a coil-type condenser embedded into the water tank and an expansion valve.
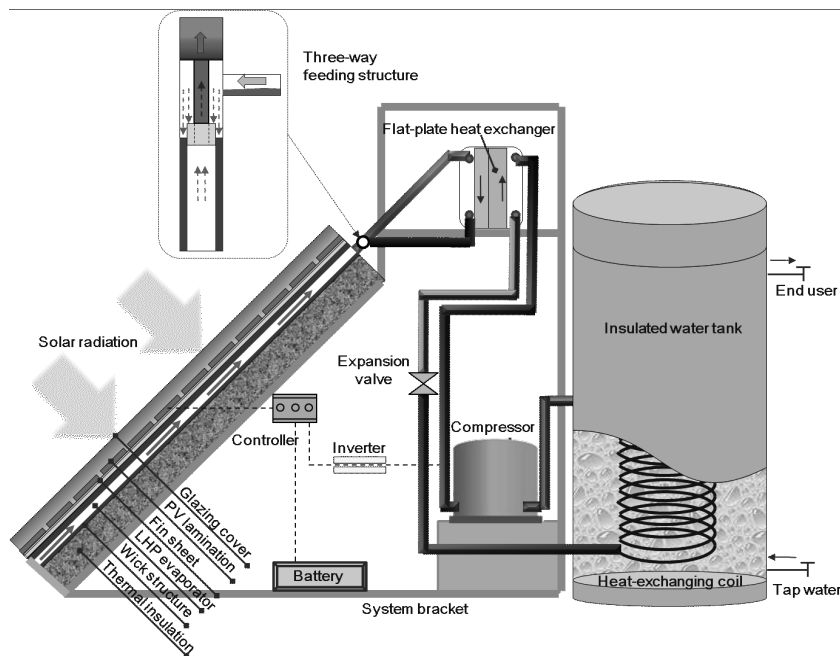
Fig. 1. Schematic of the solar PV/LHP heat pump water heating system

A prototype PV/LHP heat pump system was designed with a total effective absorbing area of 0.612m². The PV/LHP module was fixed to the 30° tilted frame and fitted with the single glazing cover on top. The PV cells, consisting of totally 36 (4 × 9 array) pieces each with sizes of 125 × 125 × 0.3 (mm × mm × mm), took up nearly 90% of the absorbing surface. Table 1 presents the values of the characteristic parameters relating to the PV cells under the standard testing conditions. When making-up the PV layer, a black 5052 aluminum alloy sheet coated with 20μm anodic oxidation film (electrical insulation) was used to replace the conventional TPT (Tedlar-Polyester-Tedlar) base-board for the PV cells. A 5 mm thick aluminum Ω-type fin sheet, embracing a wicked pipe (with 160 × 60 copper meshes), was adhered to the PV base-board using the silicon sealants. This pipe, when being connected to the liquid and vapour transportation lines and condensing heat exchanger, formed up a loop that was evacuated and then filled with 75ml of water/glycol mixture (95%/5%) as the working fluid. The detailed technical data relating to the loop components are given in Table 2. The system employed a 0.735 kW-rating heat pump with the evaporation/condensation temperatures of 10°C/55°C, which was charged with 300g of R134a refrigerant. A 35-liter water tank with a built-in copper heat exchanging coils was also installed and connected to the heat pump to obtain heat and store the heating water. The electrical parts of the system include a 12 V (10A) controller, 500W DC/AC inverter, a 100AH (12 V) battery, and the connection wires.

Photovoltaic characteristics of the PV module under standard testing conditions

At short-circuit current	I_{SC} = 5.54 A, V_{SC} = 0 V
At open-circuit voltage	I_{OC} = 0 A, V_{OC} = 22.32 V
At the maximum power point	I_{mp} = 4.89 A, V_{mp} = 18.23 V (P_{mp} = 89.1 W, η_o = 16.8%)

Design parameters of the LHP operation and heat exchanger

Parameters	Value	Unit
Diameter of heat pipe	0.022/0.0196	[m]
Internal diameter of vapour column (three-way fitting)	0.014	[m]
Operating presssure in heat pipe	1.3×10^{-4}	[Pa]
Heat pipe evaporator length	1.2	[m]
Evaporator-to-condenser height difference	0.3	[m]
Liquid filling level	75	[ml]
Heat pipe transportation line length	1.0/0.9	[m]
Wire diameter (wick layer I/II)	$7.175 \times 10^{-5}/12.23 \times 10^{-5}$	[m]
Layer thickness (wick layer I/II)	3.75×10^{-4}	[m]
Mesh number (wick layer I/II)	6299/2362	[m]
Heat exchanger plate cluster width/ length/ height	0.076/0.055/0.206	[m]

3. Results and Discussion

3.1. Modelling results

The annual operational performance of the prototype system could be predicted by using the established computer model, which has already been proved with a reasonable accuracy [6]. The input weather data of Shanghai (121.8°E, 31.2°N) are derived from the Energy-plus software (583670_IWEC) [7]. It was found the mean electrical, thermal and overall energetic/ exergetic efficiencies of the PV/LHP module were 9.13%, 39.25% and 48.37%/15.02% respectively. The system performance coefficient (COP) was almost 5.51. The available amount of solar radiation in Shanghai was 1516 kWh/m²-yr. As a result, the annual electrical generation, thermal output, heat-pump power consumption, and heat-pump condensation heat production of the system were estimated at 85 kWh/yr, 364kWh/yr, 81 kWh/yr and 445 kWh/ yr respectively. The initial water temperature was assumed at 16°C on average in the 35L tank,

referring to the ground water temperature at depth of 0.5 m while the temperature criteria of hot water supply were set at 45°C. Thus, the annual hot-water demand will be around 432 kWh/yr. It is seen that this system can meet the hot-water load throughout the year by outputting additional electricity of 4kWh/yr while subtracting the electricity consumption of compressor from the PV generation.

3.2. Energy, Economic and Environmental Benefit

Performance of such a novel LHP and associated solar PV/T system presents several remarkable advantages over the existing straight heat pipe and LHPs and associated solar thermal collecting and PV/T systems in Fig. 2 [8–15]: (1) heat transport capacity of the new LHP was 6.75 and 1.55 times that of the straight HP and LHP in gravitational field; (2) solar efficiency of the new LHP based solar thermal collecting system was 18% higher than that for the conventional solar thermal collecting systems; (3) solar exegetic efficiencies of the new LHP based PV/T system was 24% higher than that of the existing PV/T systems; and (4) Coefficient of performance (COP) of the new LHP based solar heat pump system was 1.5 times that of the conventional solar heat pump systems.
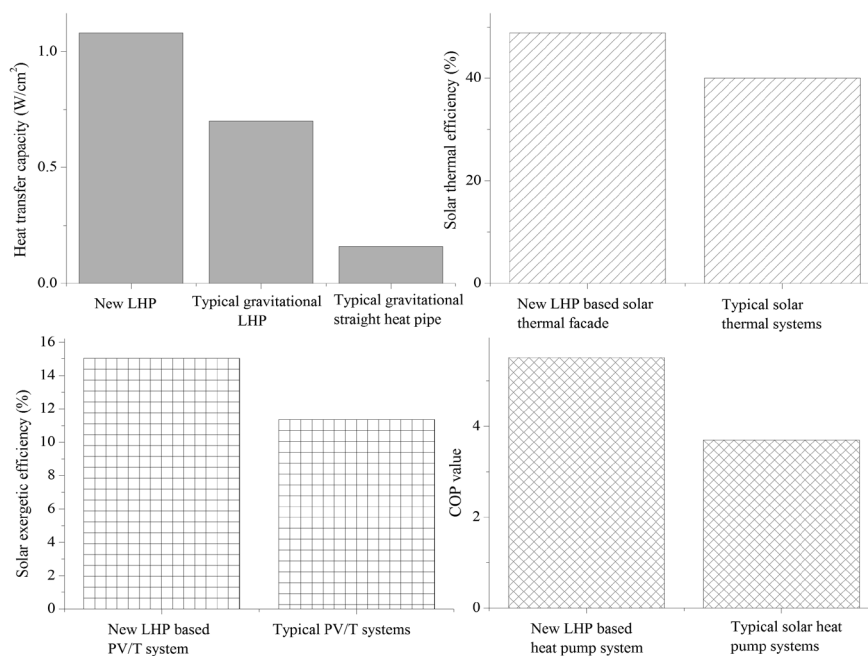
Fig. 2. The new LHP and associated thermal and power systems against the conventional ones

A simple analysis into the economic and environmental benefits of the PV/LHP heat pump water heating system was carried out using the mean values from above simulation results. The electricity price from national grid is CNY￥0.8/kWh [16] and electricity from

the distributed PV panels in Shanghai is CNY￥1.35/kWh [17]. Capital cost of the system is about CNY￥6,050. To replace with a conventional electric water heater of 90% heating efficiency, the system's payback periods were estimated at nearly 16 years in Shanghai. The CO_2 emission reduction was estimated at 12 tons by the electricity-to-CO_2 conversion factor (0.997 kg CO_2/kWh-heat in Shanghai [18]) throughout its life span of 25 years.

3.2. Adaptability to Future Building Energy Plant

The overall concept, as shown in Fig. 3, is to use an LHP device to cool the PV cells, thus enabling improvement in PV efficiency and, meanwhile, make feasible use of the absorbed heat through a heat pump for one or more of the following purposes: space heating, hot water supply, desiccant and evaporative cooling, and natural ventilation in buildings. Electricity generation from the PV cells, either exported to the national grid or stored in batteries, will meet the building electrical load and drive the heat pump compressor. The LHP device can passively transfer a large amount of heat for a long distance using its capillary power, thus eliminating the need for a circulation pump. The combination of these concepts is expected to create a low (zero) carbon heating, ventilation and air conditioning (HVAC) and hot water supply system driven by solar energy.
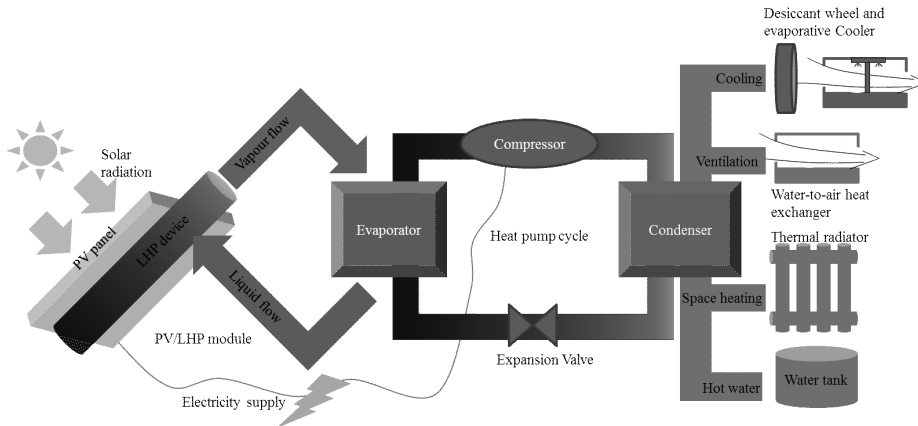
Fig. 3. Schematic of the PV/LHP heat pump micro-generation system for building services

To enable a widespread deployment of such hybrid solar technology, the explicit benefits and challenges for PV/LHP stakeholders have been identified as summarised in Table 3 [1], which need to be elaborated during the coming years. What seems necessary is the establishment of an interdisciplinary working group which can attain sound information exchange of results related to R&D, design specifications, design tools, test methods, installation barriers, market surveys, and policy development. This interdisciplinary cooperation may lead to a clear understanding of various problems over the PV/LHP developments.

Opportunities and challenges for PV/LHP stakeholders

Stakeholders	Opportunities	Challenges
R&D institutes	Quest for new technological solutions	• Performance and reliability standards • Increased system performance
Engineering Consultants	Innovative and high profile technology	• Design tools development • New system concepts development
Architects	New solutuions for integration	• PV/LHP integrated with building design • New building concepts
Installers	Reduced installation effort	• Plug-and-play integration in comfort systems • Combination of two professional specialisms
Building Industry	Increased energy performance	• Integration of module into building facade • Prefabrication possibilities
Manufacturers	Enlarged markets	• Cost-effective production • Plug-and-play systems
Policy makers	More effective path to renewable targets	• Building regulations, market and R&D support

4. Conclusions

This article illustrates a PV/LHP heat-pump water heating operation in Shanghai. Performance of such a novel LHP and associated solar PV/T system presents remarkable advantages over the existing straight heat pipe/LHPs and associated solar thermal and PV/T systems.The analysis of economic and environmental benefits demonstrated this system might be competitive in future energy supply with its payback period of 16 years and life-cycle carbon reduction of 12 tons. Explicit benefits and future challenges were brought forward for PV/LHP stakeholders to accelerate the development of such technology.

R e f e r e n c e s

[1] International Energy Agency. *Photovoltaics/thermal Solar Energy Systems – Status of the technology and roadmap for future develpoment*, Task 7 report to PVPS T7-10, 2002.
[2] Dunn P.D. & Reay D.A., *Heat Pipes* (fourth edition), ELSEVIER science LTD, 1994.
[3] Maydanik Yu.F., *Loop heat pipes*, Applied Thermal Engineering, 25, 2005, 635-657.
[4] Zhang X. et al., *Review of R&D progress and practical application of the solar photovoltaic/thermal (PV/T) technologies*, Renewable and Sustainable Energy Reviews, 16 (01), 2012, 599-617.

312

[5] Liang Z. et al., *The experimental study on backplane material influencing the performance of solar cell module*, Proceeding 10th China solar photovoltaic conference, Changzhou, Jiangsu, China, 19th–21st September 2008, 988-993.

[6] Zhang X. et al., *Characterization of a Solar Photovoltaic/Loop-heat-pipe Heat Pump Water Heating System*, Applied Energy, 102, 2013, 1229-1245.

[7] Energyplus, Weather profile, http://apps1.eere.energy.gov, access: 17.07.2013.

[8] Wei He et al., *Theoretical investigation of the thermal performance of a novel solar loop-heat-pipe façade-based heat pump water heating system*, Energy and Buildings 77, 2014, 180-191.

[9] Zhang X et al.,, *Study of the Heat Transport Capacity of a Novel Gravitational Loop Heat Pipe*, International Journal of Low Carbon Technologies; 8 (3), 2013, 210-223.

[10] Zhang X et al., *Dynamic performance of a novel solar photovoltaic/loop-heat-pipe heat pump system*, Applied Energy, 114, 2014, 335-352.

[11] Zhang X et al., *Design, fabrication and experimental study of a solar photovoltaic/ loop-heat-pipe based heat pump system*, Solar Energy, 97, 2013, 551-568.

[12] Riffat S.B., Zhao X., Doherty P.S., *Analytical and numerical simulation of the thermal performance of 'mini' gravitational and 'micro' gravitational heat pipes*, Applied Thermal Engineering, 22, 2002, 1047-1068.

[13] Solar water heating, http://www.bigginhill.co.uk/solar.htm, access: 12.02.2014.

[14] Sobhnamayan F. et al., *Optimization of a solar photovoltaic thermal (PV/T) water collector based on exergy concept*, Renewable Energy, 68, 2014, 356-365.

[15] Huang B.J., Chyng J.P., *Performance characteristics of integral type solar assisted heat pump*, Solar Energy, 71 (06), 2001, 403-414.

[16] Electricity price, http://www.sh.sgcc.com.cn, access: 21.03.2013.

[17] The standard for distributed photovoltaic award, http://www.sdpc.gov.cn, access: 21.08.2013.

[18] Electricity-to-CO_2 conversion ratio, http://www.china5e.com, access: 21.08.2013.

MATHEMATICAL FORMULAE

Thermal efficiency of a PV/LHP module is the ratio of useful thermal energy (Q_{th}) to incident irradiation (I) striking on the collecting area (A_c):

$$\eta_{th} = Q_{th}/IA_c \qquad \text{* MERGEFORMAT} \qquad (1)$$

Electrical efficiency of a PV/LHP module is the ratio of electricity generated from PV cells (Q_e) to the overall incident irradiation:

$$\eta_e = Q_e/IA_c \qquad \text{* MERGEFORMAT} \qquad (2)$$

The overall efficiency of a PV/LHP module will be the sum of above two efficiencies. The overall exergetic efficiency could be derived as:

$$\xi_o = \eta_c\eta_{th} + \eta_e \qquad \text{* MERGEFORMAT} \qquad (3)$$

where:

η_c – the ideal Carnot efficiency determined by the working fluid and surrounding air.

The performance coefficient (*COP*) of a heat pump system is defined as the ratio of heating or cooling generated (Q_w) to the electrical energy consumed (W_c):

$$COP = Q_w / W_c \qquad \text{\\* MERGEFORMAT} \qquad (4)$$

MAREK ZOZULÁK[*]

COMPARISON OF DETAILED AND SIMPLIFIED WINDOW FRAME MODELLING IN TERMS OF INFLUENCE ON SURFACE TEMPERATURE

PORÓWNANIE MODELOWANIA SZCZEGÓŁOWEGO I UPROSZCZONEGO RAMY OKIENNEJ NA WARUNKACH WPŁYWU NA TEMPERATURY POWIERZCHNI

Abstract

Window frame profile modeling methodology is varied. Simplified and detailed models were considered and results from transient calculation of surface temperature were compared. As is shown, the detailed window frame profile modelling has the influence and whether it is useful or not depends on purpose of modelling.

Keywords: window frame profile, simplified profile, frame cavities, mathematical model, numerical analysis, surface temperature

Streszczenie

Metodologia modelowania profilu ramy okna jest zróżnicowana. Uproszczone i szczegółowe modele zostały przedstawione. Porównano wyniki z obliczeń w warunkach nieustalonych temperatury powierzchni. Jak pokazano, szczegółowe modelowanie profilu ramy okna ma wpływ na wyniki, a to, czy warto go stosować zależy od celu modelowania.

Słowa kluczowe: profil ramy okiennej, uproszczony profil, model matematyczny, analiza numeryczna, temperatura powierzchni

[*] Eng. Marek Zozulák, Institute of Architectural Engineering, Civil Engineering Faculty, Technical University of Kosice, Slovakia.

1. Introduction

The subject of the transient numerical analysis is a construction detail of a window and a brick wall connection in a window sill. The selection of details is determined by their inhomogeneity – changing material properties and geometry of this place. The considered construction is a fragment of an envelope of the outdoor experimental chamber for in situ measurement. The objective is the results comparison of temperature in construction gained by transient numerical calculation with different methodology of window frame modelling – simplified and detailed frame. The influence of geometric and emissivity properties of air cavities on the overall thermal performance of aluminium frames for windows was investigate by Asdrubali et al. [1]. The use of dynamic boundary conditions and transient calculation tools is reasonable and mentioned in many cases, for example Bagoňa, 2011 [2].

2. Theoretical analysis

1.1. Physical analysis of an air cavity – detailed model

The process that determines heat transfer through an air cavity includes both natural convection and radiation. It is influenced by the geometry of the cavity, its position (vertical, horizontal or inclined), the solid surfaces emissivities, and the thermophysical properties of the gas: density, thermal conductivity, specific heat capacity, thermal expansion coefficient and dynamic viscosity [1]. Thus, a simplification is needed. It is useful to introduce an equivalent conductivity of the cavity, so treating the cavity as a solid component with above thermophysical properties calculated in.

The calculation of the equivalent thermal conductivity of unventilated air cavity is based on the European standards EN ISO 10077-2 and EN ISO 6946. The calculation is based on characteristic rectangular dimensions of air cavity. The depth is parallel to the heat flow direction and the width is perpendicular to the heat flow direction (Fig. 1), (1).
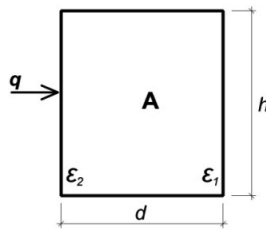
Fig. 1. Characteristic dimensions of air cavity

$$\lambda_{eq} = \frac{d}{R} = (h_c + h_r).d \qquad (1)$$

where:

h_c – convective heat transfer coefficient (W/m²·K),
h_r – radiation heat transfer coefficient (W/m²·K),

d – cavity dept (m);

R – Thermal resistance of the cavity (m².K/W).

1.2. Simplification of window frame – simplified model

According to the aim of the comparison, we also use the window frame without air cavities. If a simplified analysis is present, the entire frame is a solid component, represented by equivalent thermal conductivity gained from thermal transmittance of window frame profile construction. Plastic material specific heat capacity and density are considered in this case.

$$U_f = \frac{1}{R_{si} + R + R_{se}} \rightarrow \lambda_{eq} = \frac{d}{R} \tag{4}$$

where:

R – Thermal resistance (m².K/W),

$R_{si/se}$ – Surface heat transfer resistances (m².K/W),

U_f – Thermal transmittance of a frame system (W/m²·K),

d – Thickness of the window component (glass or frame system) (m).

3. Methodology

3.1. Window sill

Four places (Fig. 2) in the position of a window sill are solved. There is a heat flow deformation and thus, a decrease of inside surface temperature in detail of a window sill. For results analysis, two places in a nook of the brick wall and bottom window frame profile connection and two places in glass system inner surface (Fig. 2) were chosen. The results obtained by the detailed and the simplified (without air cavities – frame is a solid component) model are compared, with the aim of quantifying the differences.
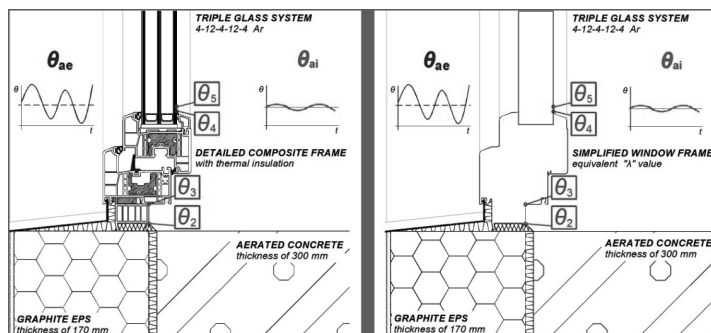
Fig. 2. Solved places in window sill of brick wall construction of the experimental chamber. Left-detailed frame model. Right – simplified frame model, without cavities of frame

3.2. Construction

It is a fragment of the building envelope construction of the experimental chamber wall. Composition of the brick wall construction is presented in Table 1 and Fig. 2. Computed thermal transmittance of the opaque wall parts is $U = 0.12$ W/m²K [3].

List of basic material characteristics. Composition of the construction (from interior)

	Layer definition	d [m]	λ_D [W/mK]	C [J/kgK]	ρ [kg/m³]
1	Autoclaved Aerated Concrete P2-350	0.300	0.104	900.0	350.0
2	Adhesive PUR foam	0.010	0.040	800.0	35.0
3	Graphite Styrofoam	0.170	0.033	920.0	16.0
4	Adhesive mortar	0.002	0.850	900.0	1300.0
5	Primer	–	–	–	1000.0
6	Silicone plaster	0.002	0.700	900.0	1700.0

The window frames construction made by plastic composite material without frame reinforcement ($U_f = 0.9$ W/m²·K). Triple glass system of 4-16-4-16-4 Ar ($U_g = 0.5$ W/m²·K) is applied.

4. Numerical analysis

The numerical calculation of transient two dimensional thermal field of window sill detail is realized to solve the temperature results of the points (θ_2, θ_3, θ_4 and $\theta5$ – Fig. 2). As the boundary conditions measured local climate and indoor data, the indoor air temperature and the outdoor air temperature (Fig. 3) are used. For the results´ analysis a 7 day winter period in one week of January 2013 (01.01–08.01.2013) is chosen.
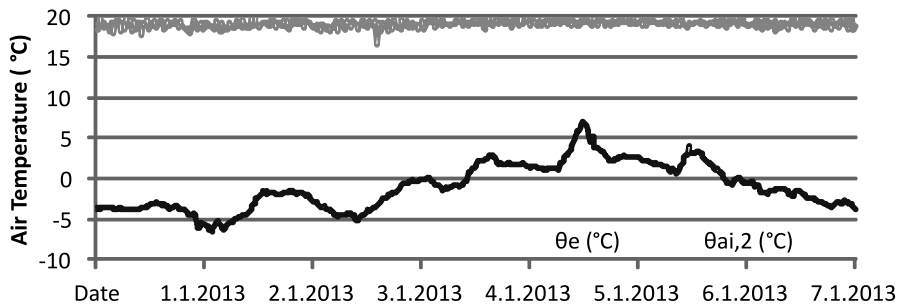
Fig. 3. Boundary temperature conditions

Transient 2D calculation is performed by Physibel software, module BISTRA. The energy balance method is used to set up a system of linear equations. The system is solved using a fast and accurate iteration procedure. Transient simulations are solved using the Crank-Nicolson finite difference method [4]. This method meets the criteria of the standard STN EN ISO 10211 Annex A, for software computing methods.

For the comparison of both simulations modelling procedures, simplified and detailed window frame models are used.

5. Results

The results from the simplified model calculation are marked θ_{xs} and from the detailed one are marked normally θ_x. The dot lines in the Fig. 5 represent results in the points from detailed model and full lines represent the simplified model results.
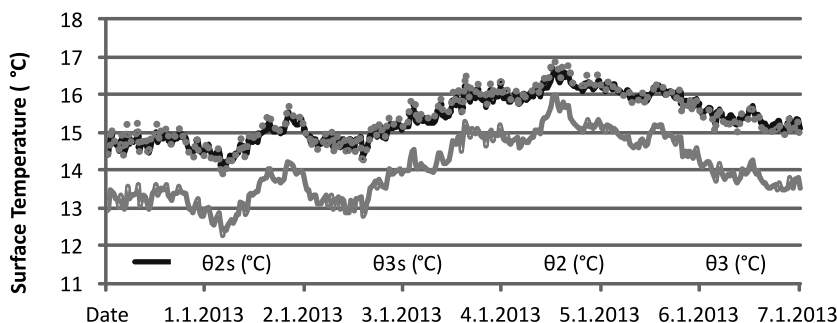
Fig. 4. Results of temperature calculation in points θ_2, θ_{2s}, θ_3, θ_{3s}

The analysis of the results from different models – simplified and detailed shows differences, Fig. 5. When comparing the averages of temperature in bottom profile and frame profile connection, point θ_{3s} has a lower temperature than the temperature in point θ_3. The average temperature in θ_{3s} is only 14.04°C, while in θ_3 it is 15.39°C, so the average difference is 1.35 K.
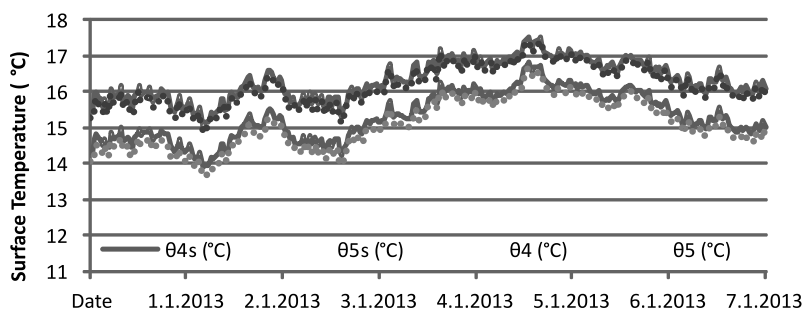
Fig. 5. Results of temperature calculation in points θ_4, θ_{4s}, θ_5, θ_{5s}

The maximum difference is 1.56 K on 2.1.2013, 4:00 am. The minimum difference between them is 0.88 K on 5.1.2013, 12:00. Average difference in the nook of the brick wall and bottom window frame profile connection temperature results, thus between points θ_{2s} and θ_2 is 0.05 K (Fig. 5).

Maximum differences between models in place of glass system and frame system connection θ_4 and θ_{4s}, and on the glass system θ_5 and θ_{5s} do not reach the 0.5 K, Fig. 6. Average difference on the place mentioned first, is 0.23 K and 0.15 K in the place θ_5, θ_{5s}.

6. Conclusions

The subtlety and strictness of modelling frame profiles of windows affect the surface temperature in the surrounding structures. Especially when the window sill detail is analysed, some of the results differ between detailed and simplified models. The most influenced is the bottom profile and the frame profile connection with average difference between values of 1.35 K. It is conspicuous when we look at the model (Fig. 2). Air cavity presence performed different thermal field patterns in the mentioned place. Any other places of window sill (or connection generally) detail are less sensitive to geometry and thermophysical changes caused by air cavities in window frame profile. Material connection of window and opaque wall part is influenced the least where the average difference is only 0.05 K. The points on glass system are also affected by air cavity presence. The further place from frame reaches the lower difference between values calculated in detailed and simplified models. The average values difference is 0.15 K, while in the nearest place to the window frame it is higher, at 0.23 K. As it is shown, detailed window frame profile modelling has influence on the surface temperature. Its use depends on the purpose of modelling, task severity (requested calculation exactness) and the point where we want to measure the surface temperature.

References

[1] Asdrubali F., Baldinelli G., Bianchi F., *Influence of cavities geometric and emissivity properties on the overall thermal performance of aluminum frames for windows*, Energy and Buildings 60, Elsevier B.V., 2013, 298-309.

[2] Bagoňa M., Lopušniak M., Vertaľ M., *Numerical analysis of the hygrothermal performance of selected building structures in Slovak climatic conditions*, 12th Conference of International Building Performance Simulation Association, Sydney 2011, 2263-2268.

[3] Katunský D. et al., *Monitoring in situ and Experimental Laboratory Physical Aspects of Building Skins*, Czasopismo Techniczne, vol. 109, no. 3, 2012, 199-203.

[4] Physibel Software, *User manual for Physibel*, Maldegem, Belgium 2013.

CONTENTS

TREŚĆ

324

Reviewers of Technical Transactions 5-B/2014